Elements

An International Magazine of Mineralogy, Geochemistry, and Petrology

June 2020
Volume 16, Number 3

ISSN 1811-5209

Redox Engine of Earth

ROBERTO MORETTI, MARIA RITA CICCONI, and DANIEL R. NEUVILLE, Guest Editors

Earth's Electrodes

Planetary Accretion

Earth's Interior

Magmas

Volcanic Gases and Geothermal Fluids

Critical Zone Metal Cycling

Earth's Ocean and Atmosphere

CAMECA®
SCIENCE & METROLOGY SOLUTIONS

Elemental & isotopic microanalytical instruments for geo & environmental sciences

EPMA

SXFive-TACTIS

A unique touchscreen **Electron Probe MicroAnalyzer** for high resolution trace element mapping and reproducible quantitative analysis of the most challenging geological samples.
Shown here: quantitative X-ray map from intensely brecciated Howardite meteorite. High spatial resolution is achieved using a focused electron beam (7 keV/30 nA). *Courtesy of B. Moine, J.-L. Devidal and T. Hammouda, Univ. of Clermont-Ferrand, France.*

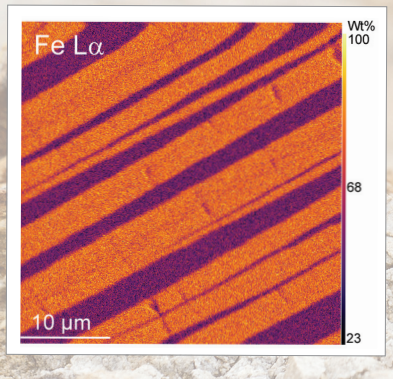

SIMS

IMS 1300-HR³

Large Geometry **Secondary Ion Mass Spectrometer** with unequalled analytical performance for a wide range of geoscience applications: tracking geological processes using stable isotopes, dating minerals, determining the distribution of trace elements...

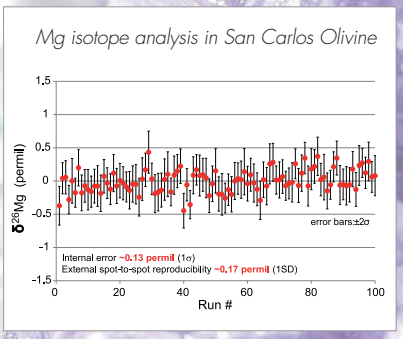

Also in our SIMS product lines:
NanoSIMS 50L: High spatial resolution multicollection SIMS
IMS 7f-GEO: High throughput SIMS for geoscience laboratories

APT

LEAP® 5000

The state-of-the-art **Atom Probe Tomography** system: 3D nanoscale chemical analysis of trace elements in complex mineral systems and extra-terrestrial samples. Shown here: analysis of igneous zircon from Martian meteorite NWA 7475, revealing a complex nano-structure of trace element enrichment within multiple linear features and numerous clusters. *Courtesy of Prof. D. Moser, Univ. of Western Ontario.*

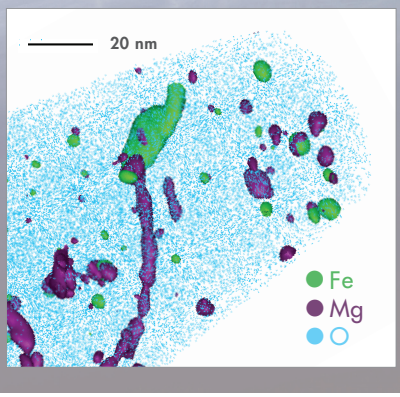

Expand your knowledge with our free guides!

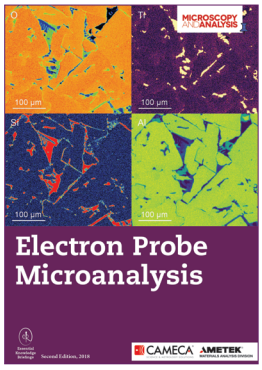

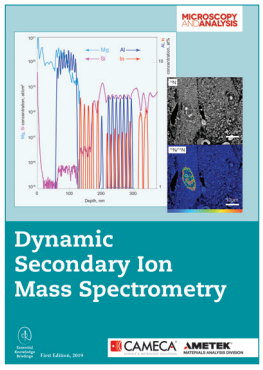

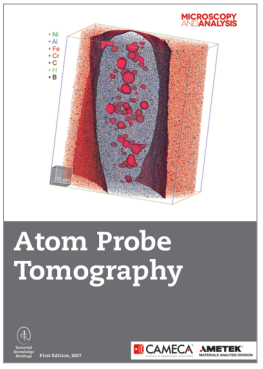

*Co-edited with Wiley, Essential Knowledge Briefs on Electron Probe Microanalysis, Secondary Ion Mass Spectrometry and Atom Probe Tomography are available for **free download** at cameca.com. Each booklet provides a simple introduction to the analytical technique, details some of its specific implementations and explores the developments that are likely to be seen in the future. Case studies provide examples of how each technique is used in the real world by leaders in fields spanning geo- and cosmochemistry, geochronology, and more!*

Scan the QR code to download your free guides
***or visit** www.cameca.com/focus/tuto*

www.cameca.com • cameca.info@ametek.com

AMETEK®
MATERIALS ANALYSIS DIVISION

Elements

An International Magazine of Mineralogy, Geochemistry, and Petrology

Volume 16, Number 3 • June 2020

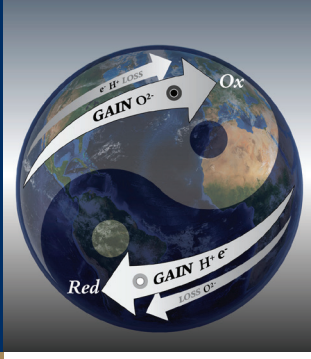

The Redox Engine of Earth

Guest Editors: **Roberto Moretti**, **Maria Rita Cicconi**, and **Daniel R. Neuville**

DEPARTMENTS

Elements is published jointly by the Mineralogical Society of America, the Mineralogical Society of Great Britain and Ireland, the Mineralogical Association of Canada, the Geochemical Society, The Clay Minerals Society, the European Association of Geochemistry, the International Association of GeoChemistry, the Société Française de Minéralogie et de Cristallographie, the Association of Applied Geochemists, the Deutsche Mineralogische Gesellschaft, the Società Italiana di Mineralogia e Petrologia, the International Association of Geoanalysts, the Polskie Towarzystwo Mineralogiczne (Mineralogical Society of Poland), the Sociedad Española de Mineralogía, the Swiss Society of Mineralogy and Petrology, the Meteoritical Society, the Japan Association of Mineralogical Sciences, and the International Association on the Genesis of Ore Deposits. It is provided as a benefit to members of these societies.

Elements is published six times a year. Individuals are encouraged to join any one of the participating societies to receive *Elements*. Institutional subscribers to any of the following journals—*American Mineralogist*, *Clay Minerals*, *Mineralogical Magazine*, and *The Canadian Mineralogist*—also receive one copy of *Elements* as part of their 2020 subscription. Institutional subscriptions are available for US$180 (US$195 non-US addresses) a year in 2020. Contact the executive editor (jrosso.elements@gmail.com) for information.

Publications mail agreement no. 40037944

Printed in USA

ISSN 1811-5209 (print)
ISSN 1811-5217 (online)

elementsmagazine.org
pubs.geoscienceworld.org/elements

GeoScienceWorld
Participating Publisher

MIX
Paper from responsible sources
FSC® C006300

The Mineralogical Society of America is for individuals interested in mineralogy, crystallography, petrology, and geochemistry. Founded in 1919, the society promotes, through research, education, and publications, the understanding and application of mineralogy by industry, universities, government, and the public. Membership benefits include *Elements* magazine, access to the electronic version of the *American Mineralogist*, as well as discounts on journals, Reviews in Mineralogy & Geochemistry series, textbooks, monographs, reduced registration fees for meetings and short courses, and participation in a society that supports the many facets of mineralogy.

WEBSITE: **www.minsocam.org**

CONTACT: **business@minsocam.org**

SOCIETY NEWS EDITOR: Andrea Koziol (akoziol1@udayton.edu)

The Mineralogical Society of Great Britain and Ireland is an international society for all those working in the mineral sciences. The society aims to advance the knowledge of the science of mineralogy and its application to other subjects, including crystallography, geochemistry, petrology, environmental science and economic geology. The society furthers its aims through scientific meetings and the publication of scientific journals, books and monographs. The society publishes *Mineralogical Magazine* and *Clay Minerals*. Students receive the first year of membership free of charge. All members receive *Elements*.

WEBSITE: **www.minersoc.org**

CONTACT: **info@minersoc.org**

SOCIETY NEWS EDITOR: Kevin Murphy (kevin@minersoc.org)

The Mineralogical Association of Canada was incorporated in 1955 to promote and advance the knowledge of mineralogy and the related disciplines of crystallography, petrology, geochemistry, and economic geology. Any person engaged or interested in these fields may become a member of the association. Membership benefits include a subscription to *Elements*, reduced cost for subscribing to *The Canadian Mineralogist*, a 20% discount on Topics in Mineral Sciences, formerly Short Course series volumes, and special publications, and a discount on the registration fee for annual meetings.

WEBSITE: **mineralogicalassociation.ca**

CONTACT: **office@mineralogicalassociation.ca**

SOCIETY NEWS EDITOR: Johanne Caron (johanne.caron@ete.inrs.ca)

The Clay Minerals Society (CMS) began as the Clay Minerals Committee of the US National Academy of Sciences – National Research Council in 1952. In 1962, the CMS was incorporated with the primary purpose of stimulating research and disseminating information relating to all aspects of clay science and technology. The CMS holds annual meetings, workshops, and field trips, and publishes *Clays and Clay Minerals* and the CMS Workshop Lectures series. Membership benefits include reduced registration fees to the annual meeting, discounts on the CMS Workshop Lectures, and *Elements*.

WEBSITE: **www.clays.org**

CONTACT: **cms@clays.org**

SOCIETY NEWS EDITOR: Katerina Dontsova (dontsova@email.arizona.edu)

The Geochemical Society (GS) is an international organization founded in 1955 for students and scientists involved in the practice, study, and teaching of geochemistry. Our programs include cohosting the annual Goldschmidt Conference®, editorial oversight of *Geochimica et Cosmochimica Acta* (*GCA*), supporting geochemical symposia through our Meeting Assistance Program, and supporting student development through our Student Travel Grant Program. GS annually recognizes excellence in geochemistry through its medals, lectures, and awards. Members receive a subscription to *Elements*, special member rates for *GCA* and *G-cubed*, and publication and conference discounts.

WEBSITE: **www.geochemsoc.org**

CONTACT: **gsoffice@geochemsoc.org**

SOCIETY NEWS EDITOR: Kevin Johnson (kjohnson@geochemsoc.org)

Founded in 1985, the **European Association of Geochemistry** is a non-profit organization dedicated to promoting geochemistry internationally. The society is a dynamic association that organizes the Goldschmidt Conference® in Europe, publishes *Geochemical Perspectives* and *Geochemical Perspectives Letters*, recognizes scientific excellence through awards, supports Early Career Scientists, sponsors workshops and conferences in Europe, organizes Distinguished Lecture and Outreach Programs, publishes job opportunities, newsletters and blogs, and partners with other learned societies to strengthen geochemistry internationally.

WEBSITE: **www.eag.eu.com**

CONTACT: **office@eag.eu.com**

SOCIETY NEWS EDITOR: Alice Williams (awilliams@eag.eu.com)

The International Association of GeoChemistry (IAGC) has been a preeminent international geochemical organization for over 40 years. Its principal objectives are to foster cooperation in the advancement of applied geochemistry by sponsoring specialist scientific symposia and the activities organized by its working groups and by supporting its journal, *Applied Geochemistry*. The administration and activities of IAGC are conducted by its council, comprising an executive and ten ordinary members. Day-to-day administration is performed through the IAGC business office.

WEBSITE: **www.iagc-society.org**

CONTACT: **businessoffice@iagc-society.org**

SOCIETY NEWS EDITOR: Chris Gardner (BusinessOffice@IAGC-Society.org)

The Société Française de Minéralogie et de Cristallographie, the French Mineralogy and Crystallography Society, was founded on 21 March 1878. The purpose of the society is to promote mineralogy and crystallography. Membership benefits include the *European Journal of Mineralogy*, *Elements*, and reduced registration fees for SFMC meetings.

WEBSITE: **www.sfmc-fr.org**

CONTACT: **sfmc@ccr.jussieu.fr**

SOCIETY NEWS EDITOR: Mary-Alix Kaczmarek (mary-alix.kaczmarek@get.omp.eu)

The Association of Applied Geochemists is an international organization founded in 1970 that specializes in the field of applied geochemistry. It aims to advance the science of geochemistry as it relates to exploration and the environment, further the common interests of exploration geochemists, facilitate the acquisition and distribution of scientific knowledge, promote the exchange of information, and encourage research and development. AAG membership includes the AAG journal, *Geochemistry: Exploration, Environment, Analysis*; the AAG newsletter, *EXPLORE*; and *Elements*.

WEBSITE: **www.appliedgeochemists.org**

CONTACT: **office@appliedgeochemists.org**

SOCIETY NEWS EDITOR: John Carranza (ejmcarranza@gmail.com)

The Deutsche Mineralogische Gesellschaft (DMG; German Mineralogical Society) was founded in 1908 to "promote mineralogy and all its subdisciplines in teaching and research as well as the personal relationships among all members. Its great tradition in geoscience is reflected in the list of honorary fellows, which include M. v. Laue, G. v. Tschermak, P. Eskola, C.W. Correns, P. Ramdohr, and H. Strunz, to name but a few. Today, the subdisciplines in the DMG are also bridging the gap with other communities such as materials science, solid state chemistry/physics, and environmental sciences. The society especially tries to support young researchers, e.g., to attend conferences and short courses. Membership benefits include the *European Journal of Mineralogy*, *Elements*, and *GMit*.

WEBSITE: **www.dmg-home.org**

CONTACT: **post@dmg-home.org**

SOCIETY NEWS EDITOR: Klaus-Dieter Grevel (klaus-dieter.grevel@rub.de)

The Società Italiana di Mineralogia e Petrologia (Italian Society of Mineralogy and Petrology), established in 1940, is the national body representing all researchers dealing with mineralogy, petrology, and related disciplines. Membership benefits include receiving the *European Journal of Mineralogy*, *Plinius*, and *Elements*, and a reduced registration fee for the annual meeting.

WEBSITE: **www.socminpet.it**

CONTACT: **segreteria@socminpet.it**

SOCIETY NEWS EDITOR: Costanza Bonadiman (bdc@unife.it)

The International Association of Geoanalysts is a worldwide organization supporting the professional interests of those involved in the analysis of geological and environmental materials. Activities include the management of proficiency-testing programmes for bulk-rock and micro-analytical methods, the production and certification of reference materials and the publication of the association's journal, *Geostandards and Geoanalytical Research*.

WEBSITE: **geoanalyst.org**

CONTACT: **jmc@bgs.ac.uk**

SOCIETY NEWS EDITOR: Michael Wiedenbeck (michawi@gfz-potsdam.de)

The Polskie Towarzystwo Mineralogiczne (Mineralogical Society of Poland), founded in 1969, draws together professionals and amateurs interested in mineralogy, crystallography, petrology, geochemistry, and economic geology. The society promotes links between mineralogical science and education and technology through annual conferences, field trips, invited lectures, and publishing. Membership benefits include subscriptions to *Mineralogia* and *Elements*.

WEBSITE: **www.ptmin.pl**

CONTACT: **ptmin@ptmin.pl**

SOCIETY NEWS EDITOR: Zbigniew Sawłowicz (zbigniew.sawlowicz@uj.edu.pl)

The Sociedad Española de Mineralogía (Spanish Mineralogical Society) was founded in 1975 to promote research in mineralogy, petrology, and geochemistry. The society organizes annual conferences and furthers the training of young researchers via seminars and special publications. The *SEM Bulletin* published scientific papers from 1978 to 2003, the year the society joined the *European Journal of Mineralogy* and launched *Macla*, a new journal containing scientific news, abstracts, and reviews. Membership benefits include receiving the *European Journal of Mineralogy*, *Macla*, and *Elements*.

WEBSITE: **www.ehu.es/sem**

CONTACT: **npvsem@lg.ehu.es**

SOCIETY NEWS EDITOR: Encarnación Ruiz-Agudo (encaruiz@ugr.es)

The Swiss Society of Mineralogy and Petrology was founded in 1924 by professionals from academia and industry and amateurs to promote knowledge in the fields of mineralogy, petrology, and geochemistry and to disseminate it to the scientific and public communities. The society coorganizes the annual Swiss Geoscience Meeting and publishes the *Swiss Journal of Geosciences* jointly with the national geological and paleontological societies.

CONTACT: **bernard.grobety@unifr.ch**

SOCIETY NEWS EDITOR: Torsetn Vennemann (torsten.vennemann@unil.ch)

The Meteoritical Society is an international organization founded in 1933 for scientists, collectors, and educators to advance the study of meteorites and other extraterrestrial materials and their parent asteroids, comets, and planets. Members receive our journal, *Meteoritics & Planetary Science*, reduced rates for *Geochimica et Cosmochimica Acta*, which we cosponsor, the *Meteoritical Bulletin*, and *Elements*. We organize annual meetings, workshops, and field trips, and support young planetary scientists worldwide. Through our medals and awards, we recognize excellence in meteoritics and allied fields.

WEBSITE: **meteoriticalsociety.org**

CONTACT: **meteoritical.org/contact**

SOCIETY NEWS EDITOR: Cari Corrigan (corriganc@si.edu)

The Japan Association of Mineralogical Sciences (JAMS) was established in 2007 by merging the Mineralogical Society of Japan, founded in 1955, and the Japanese Association of Mineralogists, Petrologists, and Economic Geologists, established in 1928. JAMS covers the wide field of mineral sciences, geochemistry, and petrology. Membership benefits include receiving the *Journal of Mineralogical and Petrological Sciences* (*JMPS*), the *Ganseki-Koubutsu-Kagaku* (*GKK*), and *Elements*.

WEBSITE: **jams.la.coocan.jp**

CONTACT: **KYL04223@nifty.ne.jp**

SOCIETY NEWS EDITOR: Atsusui Kyono (kyono@geol.tsukuba.ac.jp)

The International Association on the Genesis of Ore Deposits (IAGOD) was established in 1963 to promote international cooperation and increase knowledge in the field of the genesis of ore deposits and is affiliated with the International Union of Geological Sciences (IUGS). The society organizes quadrennial symposiums and cosponsors sessions at the International Geological Congress and SGA Biennial Meetings. The IAGOD working groups and commissions promote ore deposits research and sponsor an international speaker series. Membership includes reduced fees at our meetings, discounted subscriptions to our flagship journal *Ore Geology Reviews* and other publications, and a subscription to *Elements*.

WEBSITE: **www.iagod.org**

CONTACT: **http://iagod.org/node/87**

SOCIETY NEWS EDITOR: Simon Jowitt (simon.jowitt@unlv.edu)

Affiliated Societies

The International Mineralogical Association, the European Mineralogical Union, and the International Association for the Study of Clays are affiliated societies of *Elements*. The affiliated status is reserved for those organizations that serve as an "umbrella" for other groups in the fields of mineralogy, geochemistry, and petrology, but that do not themselves have a membership base.

Elements
An International Magazine of Mineralogy, Geochemistry, and Petrology

EDITORIAL OFFICE
Washington State University Tri-Cities
2710 Crimson Way, Floyd 263
Richland, WA 99354-1671, USA
Tel/Fax: (509) 420-5331 (UTC-8)
Layout: POULIOT GUAY GRAPHISTES
Copy editor: PATRICK ROYCROFT
Proofreader: PATRICK ROYCROFT
Printer: ALLEN PRESS

elementsmagazine.org

A SYMPHONY OF ELECTRONS

DOI: 10.2138/gselements.16.3.151

Jon Blundy

The concept of oxidation as the process that turns iron metal into rust is familiar to all of us. We might be equally familiar with reduction, the "reverse" of oxidation, by which iron metal is produced by heating iron ore with coke in a blast furnace. Rusting and smelting of iron are just two examples of reduction–oxidation ("redox") reactions. As one species (e.g., the iron ore) becomes reduced, so the other (e.g., the coke) becomes oxidised. In redox, there is always something being oxidised and something else being reduced; it's the yin and the yang of geochemistry, as the guest editors of this issue of *Elements* refer to it (cover).

Redox, despite the name, is not just about oxygen: what really matters is the transfer of electrons from one species to another. In this view, the loser of electrons becomes oxidised, and the gainer of electrons becomes reduced. Ultimately, redox is about moving electrons from one place to another. In the solid Earth, over geological time, electrons have flowed from the oxidised surface to the reduced core, but the path that they follow is far from straightforward. Charting the movement of electrons through and between Earth's various geochemical reservoirs is at the heart of this issue of *Elements*. What emerges is a symphony of electrons migrating, stalling, and even changing direction as our planet evolves. In effect Earth's "redox engine" is a kind of geological map: not of strata, but of electrons.

Earth scientists have long been fascinated with maps, the business of making data visual. In that sense, mapping electrons is geological business as usual. It is just over 200 years since that most celebrated of geological maps, *A Delineation of the Strata of England and Wales with part of Scotland*, was published by William Smith, a blacksmith's son from Oxfordshire (UK). Smith, almost entirely self-educated, trained as a surveyor. While overseeing construction of the canal network that underpinned the nascent industrial revolution, Smith recognised that rock strata could be correlated from one canal trench to another and that those strata could, potentially, be extrapolated underground. By this means, he could anticipate the subsurface geology, notably the extent to which seams of coal, and other valuable commodities, might lie at depth. The business of first making and then selling his map broke Smith physically and financially. Just four years after completing his map in 1815, he found himself in a London debtor's prison, overcome by exigent creditors and unable to capitalise on the anticipated demand for his map.

FIGURE 1 Rodney Harris' elemental ("redox") version of William Smith's map. Copyright Rodney Harris. Reproduced with permission.

In a popular retelling of Smith's life, Simon Winchester's 2001 book *The Map that Changed the World* suggests that Smith's nemesis was George Bellas Greenough, then President of the Geological Society of London. Unlike Smith, Greenough was an educated man (Eton College, no less). Greenough's *Geological Map of England and Wales* became available in 1820, just in time to greet Smith on his release from prison. Whether its imminent publication played any part in Smith's demise is a matter of keen debate, but it certainly makes for a good tale. For Smith, at least, there was a redemptive ending. Shortly before his death in 1839, he was recognised by the self-same Geological Society of as the inaugural recipient of the Wollaston Medal, the society's highest honour.

William Smith is one of science's unsung heroes, rarely mentioned in the same breath as those luminaries as Charles Lyell or Charles Darwin, contemporaries in the quest to understand geology, or Michael Faraday, poster-child of the Royal Institution, or Sir Humphrey Davy, a scientific rock star long before Brian May. Yet Smith's achievements, from humble beginnings, are no less remarkable.

To celebrate the bicentenary of Smith's map, Bristol-based sculptor Rodney Harris began work on a contemporary version. He came up with the idea of an elemental geological map, replacing the coloured inks of Smith's original with pigments fashioned from the appropriate ground-up strata. The resulting map (Fig. 1) reveals a landscape stripped bare, denuded of its anthropogenic and biological clutter. And in this, it is the colours that reflect the redox state of the rocks themselves, from the dark grey of reduced coal, to the reddish brown of oxidised red beds and clays. But the overwhelming impression is of a profoundly beige country beneath our "green and pleasant land".

In 2015, Bristol University (UK) held a series of four public lectures on different aspects of geological maps, from the history of William Smith's own effort, to the modern mapping of Mars using the *Curiosity* rover. Almost 1,000 people attended the lectures, testifying to widespread public interest in the Earth sciences, and the enduring power of geological maps. Reading this issue of *Elements*, it occurs to me that an electron map of the Earth would have made a welcome addition to that theme.

Jon Blundy, Principal Editor

ABOUT THIS ISSUE – REDOX

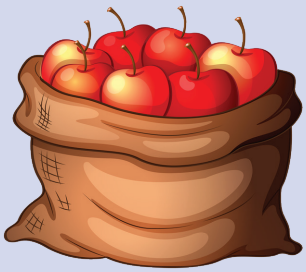

The *Elements* editorial office is located in the middle of a highly productive agricultural region (Washington, USA). Asparagus was harvested a few weeks ago. Cherries are being picked now (and they are delicious). Apples, onions, potatoes will be harvested in late summer/early autumn. When not from this harvest season, most of what is available in our supermarkets will be from last season's harvest. Even in the dead of winter, one can go to a market to buy a bag of apples, or onions, or potatoes. But have you ever thought about how it is that we are able to buy produce, such as apples, when they are out of season? We all know that storing produce on a kitchen counter or in a refrigerator will eventually result in rotten, dehydrated, or mealy fruits and vegetables. So, how can fruits and vegetables be "fresh" when purchased from a market up to a year post-harvest? The answer to that question lies within the topic of this issue of *Elements*: reduction and oxidation reactions, otherwise known as "redox".

Photosynthesis, the big daddy of all redox reactions, is used by plants to convert water and carbon dioxide into oxygen and sugars (the food for plants). In order for a plant to grow, it converts those sugars into energy via respiration (also a redox reaction), which it does as follows:

$$C_6H_{12}O_6 \text{ (sugar)} + 6O_2 \rightarrow 6CO_2 + 6H_2O + 32 \text{ ATP (energy)}$$

It is this respiration process that allows fruits and vegetables to ripen and age. Ingeniously, the food industry has utilized the power of redox to extend the life of the agricultural produce that we enjoy. Controlled atmosphere (CA) storage is probably the most successful technology introduced to the fruit and vegetable industry in the 20th century. The goal behind CA storage is to slow the ripening (aging) process and allow prolonged storage of fruits and vegetables by lowering the temperature and controlling the atmosphere. The lower temperatures and low-O_2 atmospheres of CA storage reduce the rate of respiration, leading to the slowing down of the natural ripening process and, thereby, extending the shelf-life of produce. The addition of CO_2 (the byproduct of respiration) both reduces the rate of respiration and inhibits the development and growth of pests and diseases that would normally damage fruits and vegetables.

There are many controlled-atmosphere facilities located near the farms where fruits and vegetables are grown. If you live in an agriculturally productive area, you may often see large truckloads of onions, apples, and other delicious things being transported from farms to nearby CA facilities. This produce is then later sold en masse locally, nationally, and globally. It is an impressive industry, and one that employs millions of workers worldwide. Yet, none of it would be possible without understanding the power of redox.

CALL FOR PROPOSALS

Every year, *Elements* publishes six thematic issues on subjects related to the broad disciplines of mineralogy, geochemistry, and petrology. Each issue of *Elements* is born from an idea, or point of interest, about a particular area of our science. That idea is then brought to the editorial team who, in turn, discuss it as a potential subject for a future thematic issue.

The successful ideas that get published are those that

- are broadly related to mineralogy, geochemistry, and petrology;
- are interdisciplinary;
- are in established, but progressing, fields;
- are of interest to a broad cross section of readers;
- are not adequately covered by previous issues of *Elements* or that have considerably advanced since that topic was previously covered.

If you have an idea for a future thematic issue of *Elements*, you are most welcome to submit a proposal for consideration. Visit our website to learn more about proposing topics (http://elementsmagazine.org/publish-in-elements-2/).

Please submit proposals by the end of July 25 for consideration at the next editorial meeting.

COVID-19: A COMMENT ON THE ROLE OF SCIENTISTS

When we started finalizing this issue for publication the prospect of a pandemic seemed very distant. In the intervening three months, COVID-19 has come to dominate everything: our conversations, news broadcasts, our working patterns, and our social lives. For many, this has been a tragic time, and we extend our condolences to all those readers of *Elements* who have lost loved ones and colleagues to COVID-19. For scholars, this is an uncertain time, as universities and research organizations take stock of the impact of the pandemic on their activities, and their financial well-being. The dramatic drop in student mobility across the world is already starting to take a toll on university income and may yet pose an existential threat. On a brighter note, it is hard to overlook the benefits of having cleaner air, happier wildlife, and lower global emissions due to our traveling less.

The pandemic has thrown into sharp relief the important role that scientists play in our world, in providing advice, engendering trust, and maintaining hope. COVID-19 has been something of a rollercoaster ride for scientists in this regard. Their myriad advice, often contradictory, has been variously debated, spurned, ridiculed, or uncritically adopted by governments across the world. Public confusion about how science works has been palpable, and increasingly skeptical. Most alarming is the extent to which anyone and everyone can become an "expert". Even respectable news outlets confuse the informed expertise of a researcher in a pandemic-related field with the subjective opinion of an individual whose main credentials are a degree in "science". COVID-19 is not an Earth sciences catastrophe (although some colleagues have redirected their efforts in this direction), but it is not so different from, say, a volcanic eruption, earthquake, or extreme climate event. The pandemic has been a sobering reminder that simply working in a broad field does not qualify us to write opinion pieces in newspapers or on Twitter which criticize public policy, question mitigation measures, or predict consequences of apocalyptic proportion. With knowledge comes some degree of responsibility. Informed criticism is valid; reckless prognostication is not.

Jon Blundy, **John Eiler**, **Richard Harrison**, and **Jodi Rosso**

Meet the Authors

Marc F. Benedetti is a professor of geochemistry at the Université de Paris, Insitut de Physique du Globe de Paris (France). He studies how major and trace elements interact with water and soil. In his studies, he determines the speciation of chemical elements in the environment mainly by experimentally studying processes at interfaces. This allows him to understand the mechanisms that control the speciation and transfer of elements in water and soil, especially the interactions between metal ions and natural organic matter. He also leads field studies on the speciation of chemical elements in the natural environment (water and soil).

Asmaa Boujibar is a postdoctoral fellow at the Carnegie Institution for Science (Washington DC, USA). She received her PhD in Earth and planetary science from Blaise Pascal University (France). She is interested in the origin of the chemical heterogeneities of extraterrestrial material and the formation of terrestrial planets. High-pressure and high-temperature experiments are allied to numerical modeling to replicate the conditions of core segregation, crust formation and magma-ocean crystallization. She also uses machine learning algorithms to evaluate the classification of meteorites and their components.

Maria Rita Cicconi is a senior researcher (Akademischer Rätin) at the Department of Materials Science and Engineering, Institute of Glass and Ceramics, of the Friedrich-Alexander-Universität Erlangen-Nürnberg (Germany). She obtained her PhD in experimental mineralogy in 2010 from the University of Camerino (Italy). She works on redox processes, structure and properties of silicate glasses, and, in particular, on the redox and structural behaviour of rare earth elements. Her research interests include the use of vibrational-, optical-, and synchrotron-based techniques to investigate the relationship between structure, redox, and optical/mechanical properties in natural glasses and melts and in functional glass-ceramics.

Melanie Davranche is a professor of geochemistry at the University of Rennes 1 (France). She researches how organic matter and iron interact and how those interactions affect the behaviour of other, associated, metals at the soil/water interface. She is particularly interested in the mobility of the rare earth elements and arsenic and employs field observation, experimentation, spectroscopic studies, and geochemical modelling to determine their mobility.

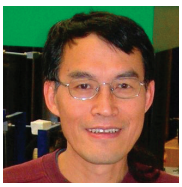

Yingwei Fei is an experimental petrologist at the Earth and Planets Laboratory of the Carnegie Institution for Science (Washington, DC, USA). He is interested in phase transitions, element partitioning, melting relations, chemical reactions, and physical properties of materials at high pressure and temperature, with applications to geophysics, petrology, mineral physics, geochemistry, and planetary sciences. He obtained his BS in geochemistry from Zhejiang University (China) in 1982 and his PhD in geochemistry from the City University of New York (USA) in 1989. Since 1991, he has been a faculty member at the Carnegie Institution for Science.

Alexandre Gélabert is a biogeochemist studying the role exerted by microorganisms on metal(loid) cycles in the critical zone. He focuses on the reactions at mineral/biofilm/solution interfaces; the physico-chemical properties of microenvironments; and the processes of metal(loid) complexation, transformation, and any resultant biomineralization. To do this, he combines experimental studies with field work, thermodynamics with isotopic approaches, and uses synchrotron-based techniques. He is currently an associate professor at the Université de Paris and the Institut de Physique du Globe de Paris (France), where he is head of the geomicrobiology group.

Christopher D. Herd is a professor at the University of Alberta (Canada) who studies the mineralogy, petrology, and geochemistry of meteorites in order to elucidate the conditions of formation and evolution of the terrestrial planets. He obtained a BSc in geological sciences from Queen's University (Canada) and a PhD in Earth and planetary sciences from the University of New Mexico (Albuquerque, USA). His research on meteorites from Mars has provided novel insights into variations in redox state, notably how such states relate to magma-ocean crystallization. He is currently a participating scientist on the returned sample aspect of NASA's Mars 2020 mission.

Charles Le Losq obtained his PhD in 2012 from the Institut de Physique du Globe de Paris (IPGP) (University Paris VII, France) and worked as a postdoctoral fellow from 2013 to 2015 at the Geophysical Laboratory, Carnegie Institution for Science (Washington DC, USA) on the molecular structure of hydrous magmas. Following this, he conducted research on the geochemistry of magmas and minerals as a research fellow at the Research School of Earth Sciences (Australian National University, Australia). In 2019, Charles became Maître de Conférences at IPGP. He is now teaching and leading research activities on magma rheology, petrology, and geochemistry.

Roberto Moretti is a senior geophysicist at the Institut de Physique du Globe de Paris (Université de Paris, France). He received his Laurea VO degree in geological sciences at the Università di Genova (Italy) in 1996 and his PhD in Earth sciences from the Università di Pisa (Italy) in 2002. His research is on the reactive properties of Earth materials, particularly magmas and fluids, and their application to the understanding of volcanic processes and the monitoring of volcanic–hydrothermal unrest. Before moving to France, he was a researcher at the Osservatorio Vesuviano, Istituto Nazionale Geofisica e Vulcanologia (Napoli, Italy) and then an associate professor at the Università della Campania (Italy).

Daniel R. Neuville is a CNRS research director based at the Institut de Physique du Globe de Paris (IPGP), Université de Paris (France). He studies the thermodynamic and rheological properties of glasses, crystals, and melts by linking their structure at high temperature to their macroscopic properties. This has applications in Earth and materials sciences. He is the head of the geomaterials group and of the IPGP's Masters programs in geochemistry, geomaterials, geobiology, and the environment. He is the elected President of the Union pour la Science et la Technologies Verrieres, Chair of the International Commission on Glass's Glass Structure Committee, and Chair of the International Mineralogical Associations' Commission on the Physics of Minerals.

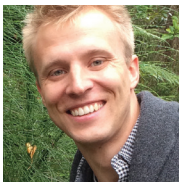

Noah J. Planavsky is an assistant professor in the Department of Geology and Geophysics at Yale University (Connecticut, USA). Prior to taking on a faculty role at Yale, he received his PhD from the University of California, Riverside (USA) and held a postdoctoral fellowship at the California Institute of Technology (USA). He tracks changes in the composition of Earth's atmosphere, understanding the links between the evolution of Earth's surface environments and life, and tries to understand how the atmosphere on Earth and Earth-like exoplanets evolve. His research relies on a combination of petrography, nontraditional isotope geochemistry, and geochemical modeling.

Christopher T. Reinhard is a biogeochemist by training, with an interest in Earth system evolution, modern marine biogeochemistry, and the chemistry of planetary atmospheres. Reinhard's research aims to integrate information from Earth's rock record with theoretical models in an effort to reconstruct, understand, and predict the dynamics of Earth's coupled carbon, oxygen, sulfur, and nutrient cycles, and to leverage this understanding in the search for temperate terrestrial planets beyond the solar system.

Kevin Righter is a planetary scientist and curator for both the Antarctic meteorites and the Origins, Spectral Interpretation, Resource Identification, Security-Regolith Explorer (OSIRIS-REx) asteroid samples within the Astromaterials Research and Exploration Science (ARES) Division at the Johnson Space Center (Texas, USA). Righter applies igneous petrology, experimental petrology, and geochemical analysis to understand core formation, the origin of the Earth and the Moon, as well as differentiated and chondritic meteorites and the role of volatiles in the origin of basaltic magmatism. Righter's research and curation activities help understand the origin and evolution of the solar system and the potential for life elsewhere.

Vincenzo Stagno is an experimental petrologist interested in understanding the role of volatile elements before, during, and after the formation of Earth (and other planets), as well as the mantle redox state, melting processes, magma rheology, diamond formation, and the speciation of Fe in minerals. After obtaining his PhD at the Bayerisches Geoinstitut (Bayreuth, Germany) he worked at the Geophysical Laboratory of the Carnegie Institution for Science (Washington DC, USA) and the Geodynamics Research Center (Ehime University, Japan) to investigate geomaterials at extreme conditions. Since 2015, he has been a professor at the Sapienza University of Rome (Italy) and works in collaboration with Italy's National Institute of Geophysics and Volcanology.

Andri Stefansson is a professor of geochemistry at the University of Iceland. He works on volcanic and geothermal fluid geochemistry, including fluid–rock and redox reactions in the crust, the hydrogeology of volcanic geothermal systems, the sources and cycling of volatile elements, and the thermodynamics of hydrothermal fluids.

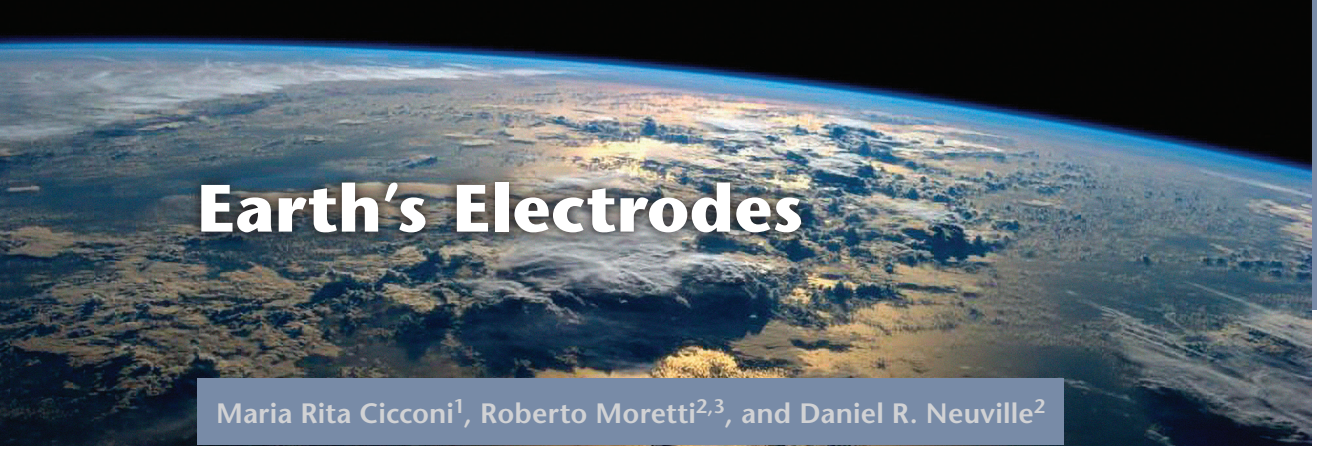

Earth's Electrodes

Maria Rita Cicconi[1], Roberto Moretti[2,3], and Daniel R. Neuville[2]

Sunrise over the ocean. Image Credit: Reid Wiseman (@astro _ reid), NASA

1811-5209/20/0016-0157$2.50 DOI: 10.2138/gselements.16.3.157

The oxidation–reduction ('redox') state is an important intensive property of any geologic system and is typically measured (and reported) as either the redox potential (E_h) or the oxygen fugacity (fO_2). These two concepts cover the whole spectrum of geologic systems: from low-temperature aqueous and sedimentary systems to high-temperature rock-forming environments. The redox state determines the speciation of a fluid phase and exercises fundamental controls on phase relations and geochemical evolution. Here, we review the concepts that underpin the redox state and outline a framework for describing and quantifying the concept of the oxidation state.

Keywords: redox potential, oxygen fugacity, hydrogen and oxygen electrodes, redox buffer, fluid-phase speciation

INTRODUCTION

Oxidation–reduction (or 'redox') reactions are chemical reactions in which the oxidation state of the participating chemical species changes. Many redox reactions are familiar to us, such as combustion, rusting and corrosion, respiration, and photosynthesis. At Earth's surface, nearly all materials tend to be oxidized when exposed to the atmosphere. Chemical weathering, the main exogenous agent of geological evolution, is an ensemble of oxidative processes that operate collectively to consume atmospheric oxygen. This tendency is counterbalanced by life processes by which photosynthesis leads to carbon dioxide reduction and oxygen production, thereby enabling life to flourish on Earth's surface.

In Earth's abiotic and hot interior, oxygen drives the redox reactions that allow abundant elements such as Fe, S, and C to change their oxidation states; redox also controls the distribution of these elements between the different geochemical reservoirs (core, mantle, crust, hydrosphere). The redox state of each reservoir is related to their distinctive mineralogy, itself inherited from a long geologic history, from early core–mantle segregation through differentiation of the primitive magma ocean, to formation of the crust and the onset of plate tectonics. This issue of *Elements* reviews how redox chemistry is used to derive valuable information about the present and the past of our planet.

1 Universität Erlangen-Nürnberg
Department Werkstoffwissenschaften, Lehrstuhl für Glas und Keramik
Martensstraße 5, D-91058 Erlangen, Germany
E-mail maria.rita.cicconi@fau.de

2 Institut de Physique du Globe de Paris
UMR 7154 CNRS
5238 Paris, France
E-mail: moretti@ipgp.fr, neuville@ipgp.fr

3 Observatoire Volcanologique et Sismologique De Guadeloupe
Institut de Physique du Globe de Paris
97113 Gourbeyre, Guadeloupe, French West Indies

OXYGEN, HYDROGEN AND ELECTRON TRANSFER

The term 'oxidation' was first used by Antoine Lavoisier in 1777. He recognized that the discovery of oxygen in 1774 by Joseph Priestley could explain the weight gains that followed the burning of sulfur and phosphorus and the calcination of metals. By the end of the 18th century, Lavoisier's ideas were applied to the more complex processes of respiration and photosynthesis. Reactions in which atmospheric oxygen was consumed (added to a compound) were called *oxidations*, whereas *reductions* were those in which oxygen was lost. During the 19th century, with the development of electrochemistry, it was realized that the oxidized substance loses electrons, whereas other substances in the reaction gain electrons. The latter were termed 'reduced' substances, and the meanings of 'oxidation' and 'reduction' became extended to include any reaction in which electrons were transferred from one substance to another, regardless of whether oxygen itself was involved.

The concept of 'oxidation state' (or 'oxidation number') was introduced as a measure of the degree of oxidation (thus, loss of electrons) of an atom in a substance. The oxidation state corresponds to the (hypothetical) charge that an atom would have if all its bonds to atoms of different elements were 100% ionic. Some elements have a greater affinity for electrons than others: for example, oxygen tends to exist as the O^{2-} species in its ionic compounds, whereas hydrogen tends to behave as H^+. Although it is widely recognized that in molecules and ion complexes other than H_2 and O_2 hydrogen has an 'oxidation number of +1', and oxygen an 'oxidation number of –2', we need to understand how oxidation and reduction can be described apparently without exchanging electrons. This point is quite important, given that the great majority of redox exchanges on Earth are related to chemical transfers involving oxygen and/or hydrogen. For example, in the extraction of iron from its ore, reduction of Fe_2O_3 to Fe is accompanied by oxidation of CO to CO_2:

$$Fe_2O_{3(ore)} + 3CO_{(gas)} \leftrightarrow 2Fe_{(metal)} + 3CO_{2(gas)} \quad (1)$$

Oxidation and reduction occur simultaneously, as summarized in the two half-reactions:

$$Fe_2O_3 \leftrightarrow 2Fe + 3/2O_2 \quad (\textit{reduction}) \quad (2)$$

$$3CO + 3/2O_2 \leftrightarrow 3CO_2 \quad (\textit{oxidation}) \quad (3)$$

The decay of organic matter, the opposite of photosynthesis, is a good example of oxidation:

$$CH_2O + O_2 \leftrightarrow CO_2 + H_2O \quad (4)$$

At present levels of oxygen in the atmosphere (~21%, or log pO_2 = –0.68), combustion of organic matter starts at 234 °C. The tendency of nearly all surface materials to be oxidized by the atmosphere is reversed by the photosynthetic reduction of carbon dioxide, enabling life's complex compounds to exist on Earth's surface.

Oxidation and reduction can also be defined in terms of hydrogen transfer: oxidation and reduction are the loss and gain of hydrogen, respectively. An example is the oxidation of methane to graphite:

$$CH_4 \rightarrow C + 2H_2 \quad (5)$$

Redox, as defined in terms of oxygen and hydrogen transfer, has a parallel in acid–base exchanges that are familiar concepts in aqueous chemistry. In fact, redox and acid–base reactions comprise the yin and the yang of chemistry, related to each other by the Lewis theory, for which an acid is any substance that can *accept* an electron pair (an acceptor), and a base is any substance that can *donate* an electron pair (a donor). Therefore, implicit in the above reactions are the half-reactions that are called the *hydrogen* and *oxygen electrodes*:

$$2H^+ + 2e^- \leftrightarrow H_2 \quad (6)$$

$$½O_2 + 2e^- \leftrightarrow O^{2-} \quad (7)$$

When the hydrogen electrode (Equation 6) is involved (e.g., highly protonated systems, such as aqueous solutions), we can readily see how oxidation corresponds to hydrogen loss. For example, the reaction in Equation (4) can be rewritten as two half-reactions, whereby electron transfer drives changes in the (formal) oxidation numbers:

$$C^{IV}H_4 \rightarrow C^0 + 4H^+ + 4e^- \quad (8a)$$

$$4H^+ + 4e^- \leftrightarrow 2H_2 \quad (8b)$$

When the oxygen electrode is involved (e.g., in systems such as molten rocks and oxygen-bearing gas species), oxidation corresponds to oxygen gain. In this case, the reaction in Equation (3) can be re-written as two different half-reactions involving electron transfer:

$$C^{II}O \rightarrow [C^{IV}O]^{2+} + 2e^- \quad (9a)$$

$$½O_2 + 2e^- \leftrightarrow O^{2-} \quad (9b)$$

Reaction pairs (Equations 8a–8b and Equations 9a–9b) show how every redox reaction comprises the sum of two half-reactions, each corresponding to an electrode and involving entities (molecules or ion complexes) in which Roman numerals denote the formal oxidation numbers. It emerges that redox reactions represent charge transfer processes in which ions and electrons are transferred, depending on the acid–base properties of the system. Bulk chemistry of the system under investigation plays a central role. For instance, in the chalcosphere (Goldschmidt 1929), one could set a reference electrode based on the S^0/S^{2-} pair: in this case, the word 'oxidation' might be better replaced by *sulfidation*.

REDOX POTENTIAL

The equilibrium of a generic redox reaction 'oxidized (Ox) species + ne^- = reduced (Red) species', which involves the exchange of n electrons, can be calculated from the free energy of the species involved. The tendency of a species to gain electrons, and thereby move from an oxidized to a reduced state, can be expressed as electron potential or redox potential, E_h (as volts, V). The change in the standard Gibbs free energy ($\Delta G°$) is then related to the standard reduction potential E^0 (the decrease in Gibbs free energy per coulomb of charge transferred) as follows:

$$\Delta G° = - n \, F \, E^0 \quad (10)$$

where F is the Faraday constant (96,485 C/mol). For any reaction, the more positive is E^0, the greater the tendency to gain electrons; conversely, the more negative is E^0, the greater the tendency to lose electrons. Both E^0 (at standard conditions) and E_h (under non-standard conditions) are related by the Nernst equation:

$$E_h = E^0 - \frac{2.303RT}{n\mathrm{F}} \log_{10} \frac{a_{red}}{a_{ox}} \quad (11)$$

where R is the ideal gas constant (J/ mol K), T is temperature (K), and a denotes the activity of the relevant species. The standard reduction potential, E^0, is characteristic of each redox system and corresponds to the redox potential, E_h, when the activity of the species is unity (a = 1). The standard reduction potential can also be described as a measure of the oxidizing power (affinity to gain electrons) of a particular redox couple. The redox couple with the largest E^0 will dominate the system's redox as a whole.

In order to compare different redox reactions, a common redox potential scale can be set for any solvent (e.g., water) whereby the reduction potential of the standard hydrogen electrode E^0 (Equation 6) is zero at all temperatures and pressures. By using the IUPAC convention (all reactions are written as a reduction), more positive E^0 indicates a stronger oxidizer (i.e., a greater tendency to become reduced). By sorting the different species according to decreasing E^0, it is possible to determine for each species its ability to reduce redox pairs that have lower E^0 values and, conversely, to oxidize those that have higher E^0 values.

Water is a particularly interesting molecule because it can undergo either reduction, leading to the formation of H_2, or oxidation, leading to the formation of O_2. The reduction corresponds to Equation (6), for which $E^0_{(H^+/H_2)}$ = 0 V, whereas the oxidation gives:

$$4H^+ + O_2 + 4e^- \leftrightarrow 2H_2O \qquad E^0_{(O_2/H_2O)} = 1.23 \text{ V} \quad (12)$$

According to the respective Nernst equations, it is possible to derive the trend of the redox potential as a function of pH and to construct the so-called Pourbaix (or E_h–pH) diagram (Pourbaix 1945). This diagram shows the thermodynamic stability fields of the different species in solution. For example, from Equation (6), the redox potential at room temperature (298.15 K) can be expressed as:

$$E_h = E^0_{(H^+/H_2)} - 2.303 \frac{8.314 \text{ J(K·mol)} \times 298.15 \text{ K}}{2 \times 96{,}485 \text{ J/V·mol)}} \log_{10} \frac{a^2_{(H^+)}}{a_{(H_2)}} \quad (13)$$

$$= E^0_{(H^+/H_2)} - 0.059 \text{ pH}$$

This equates to a line of slope –0.059 on an E_h–pH diagram on which can be plotted the thermodynamic stability fields for O_2, H_2, and H_2O species (Figure 1A). The upper and lower stability limits of water correspond, respectively, to Equations (6) and (12). Thus, at standard conditions (P = 1 bar; T = 298.15 K), water is stable only in a well-defined region, above which it undergoes oxidation, to form oxygen, and below which water is reduced, to form hydrogen.

Not all E_h–pH diagrams are quite as straightforward as that for water. If we select other elements/molecules that have multiple stable species, the diagram quickly becomes very complicated depending on pH conditions. A good example is the H–O–S system, in which the introduction of the highly reactive sulfur components leads to many reactions that either involve hydrogen–sulfur dissociation or redox exchanges that involve changes in the sulfur oxidation state from S^{2-} to S^{6+} (see Figure 1B).

Countless measurements of E_h have been carried out in natural aqueous and sedimentary systems by geochemists, soil scientists and biologists. Although not always easy to interpret due to the very different equilibrium kinetics of other redox couples present in natural waters (e.g., Fe^{2+}/Fe^{3+}, $Mn^{2+}/Mn^{3+}/Mn^{4+}$, H_2S/SO_4^{2-}, HS^-/SO_4^{2-}, NO_3^-/N_2, CO_2/CH_4, etc.), E_h measurements, nevertheless, are invaluable in the theoretical assessment of aqueous speciation states.

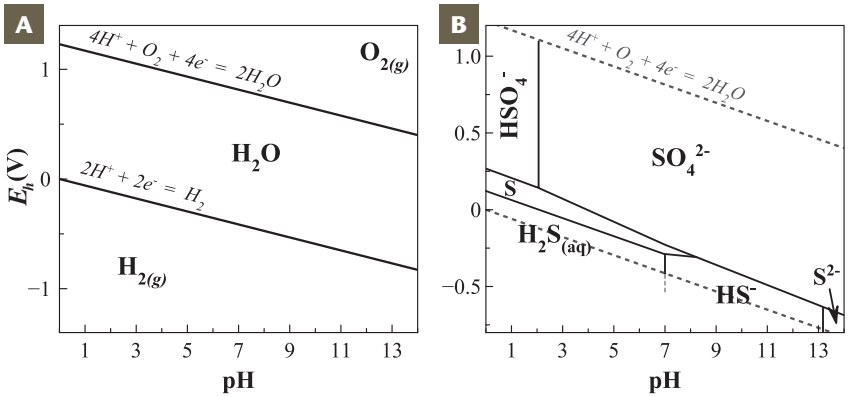

Figure 1 Examples of E_h–pH diagrams at room temperature (298.15 K) and 1 bar pressure. (**A**) E_h–pH diagram for water. Upper and lower stability limits of water are defined by Equation (6) where P_{O_2} = 1 bar and Equation (12) where P_{H_2} = 1 bar. Water, at standard conditions, is thermodynamically stable in a well-defined area. (**B**) E_h–pH diagram for the H–O–S system at 298.15 K. The S^{2-}–SO_4^{2-} limit separates the overall reducing conditions from the moderately oxidizing conditions. Grey lines from Figure 1A. See Biernat and Robins (1969) for the calculation of potential values.

OXYGEN FUGACITY

To measure the chemical potential of redox exchanges in higher temperature geological systems, for which the hydrogen electrode (Equation 6) is no longer a useful reference electrode, geoscientists use oxygen transfer. Without explicitly defining the oxygen electrode (Equation 7), geochemists took inspiration from Ellingham diagrams (Ellingham 1944), which are used in metallurgy to evaluate the ease of reduction of metal oxides and sulfides. The Ellingham diagram is used to predict the equilibrium temperature between oxygen, a metal, and that metal's oxide, and, by extension, the reactions of that metal with sulfur, nitrogen, and other non-metals. Ellingham diagrams are useful in predicting the conditions under which an ore will be reduced to its metal (e.g., Equation 2), particularly with respect to the oxygen partial pressure (pO_2).

In the early 1900s, geoscientists realized the importance of controlling pO_2 when performing high-temperature experiments in closed systems for phases containing redox-sensitive elements (iron, being ubiquitous, was the first element considered). In the pioneering studies of Bowen and Schairer (1932), the authors used iron crucibles in an inert (O_2 free) atmosphere in order to equilibrate the phases with metallic iron at very low pO_2. Darken and Gurry (1945) realized the need to explicitly monitor and control pO_2 at every temperature. Control was achieved by using gas mixtures and exploiting their dissociation at high temperature, and oxygen-bearing gases in the C–O system allowed one to control the pO_2 for a wide range of temperatures. For example, Darken and Gurry (1945) used CO–CO_2 gas mixtures to determine the phase stability limits of wüstite.

Hans Eugster, in his early experiments to determine the phase relations of annite, attempted to prevent oxidation and the formation of magnetite (Eugster 1957, 1959; Eugster and Wones 1962). To this end, he developed the double capsule technique, with a Pt capsule containing the starting material, enclosed in a larger gold capsule. Between the two metal containers he placed a metal–oxide or oxide–oxide pair plus H_2O. At high T and P, the reaction between the solids and H_2O provides a fixed and known hydrogen fugacity (f_{H_2}) (Eugster 1977). Through the dissociation reaction $H_2 + 1/2\ O_2 = H_2O$, and by knowing f_{H_2}, it is possible to derive both f_{O_2} and f_{H_2O} of the internal capsule. Eugster used (among others) iron oxide mixtures (hematite–magnetite) but noted that "any assemblage of solids which has a fixed fugacity of oxygen for a given temperature can be used together with water" (cf. Eugster and Wones 1962). He called such oxide mixtures 'buffers'; this was the birth of the now widely used oxygen buffer assemblages (Eugster 1977). Eugster and Skippen (1967) showed how the composition of the fluid phase in equilibrium with graphite in metamorphosed pelitic rocks depends greatly on f_{O_2} and T, opening up the possibility of evaluating fluid phase speciations and pressures in otherwise inaccessible past and present geologic environments.

Eugster started to use the term 'fugacity' to replace pressure. Indeed, Eugster (1959) was the first to relate the oxidation potential of oxygen (the *oxygen electrode* equilibrium, see Equation 7) to the oxygen partial pressure (pO_2), hence to oxygen fugacity (f_{O_2}), for real gases and to introduce this important variable in igneous and metamorphic geology. Since Eugster's work, several mineral assemblages of pure oxides and minerals that are representative of igneous rocks have been equilibrated under different conditions and the various solid buffer equations calibrated, e.g., data compilation by Frost (1991) and Herd (2008). Many of these buffers consider iron species, and it is noteworthy that iron species equilibria are reported in several contributions in this issue, either when talking about critical zones (Davranche et al. 2020 this issue), Earth's interior (Righter et al. 2020 this issue) or photosynthesis (Reinhard and Planavsky 2020 this issue). Being the most abundant multivalent transition element on Earth, iron is often used to express the general redox state of a system. For instance, when we talk about redox conditions related to systems where metallic iron is present, such as Earth's core or meteorites, a very low f_{O_2} is expected (see Equation 2). At more oxidized conditions, iron will occur mainly as Fe^{2+} and be incorporated in silicate phases; for even higher f_{O_2} conditions, iron will be stabilized as Fe^{3+} (Frost 1991). Consequently, to describe f_{O_2} conditions of different systems, several equilibria can be used:

$$2Fe + O_2 \leftrightarrow 2FeO \quad (14)$$
iron/wüstite (IW)

$$3Fe_2SiO_4 + O_2 \leftrightarrow 2Fe_3O_4 + 3SiO_2 \quad (15)$$
fayalite/magnetite + quartz (FMQ)

$$2Fe_3O_4 + 1/2O_2 \leftrightarrow 3Fe_2O_3 \quad (16)$$
magnetite/hematite (MH)

As these equilibria relate to pure solid phases, their equilibrium constants simply describe the variation of f_{O_2} with temperature. Figure 2 shows these buffers graphically. For instance, the T–f_{O_2} conditions where pure fayalite (F), magnetite (M) and quartz (Q) coexist in equilibrium are represented by the line FMQ. These buffers are, in effect, the high-temperature analogues of the reference electrodes introduced above.

Iron-bearing rock-forming minerals are very useful in petrogenetic studies because their occurrence and chemical composition reflect the f_{O_2} conditions of the environment in which they formed. Several techniques have been established to evaluate the f_{O_2} of rock-forming systems from natural specimens, such as the widely used oxy-thermobarometer of Buddington and Lindsley (1964) which is based on the coexisting iron–titanium oxide solid solutions of titanomagnetite (Fe_3O_4–Fe_2TiO_4) and of hemo-ilmenite (Fe_2O_3–$FeTiO_3$). The T–f_{O_2} conditions at the time of rock crystallization were thereby determined, particularly in the case of rapidly quenched glassy volcanic rocks. Carmichael (1966) and Carmichael and Nicholls (1967) pioneered this approach to bracket the T–f_{O_2} ranges of basaltic and acidic

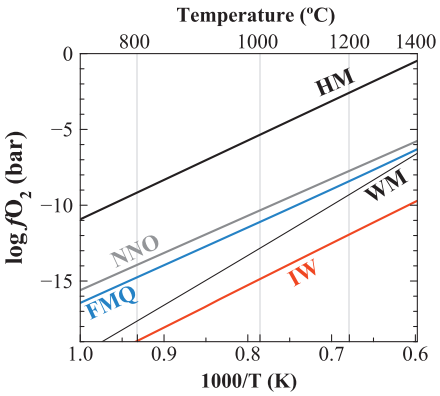

FIGURE 2 Common solid oxygen buffers used in petrology and geochemistry (and used throughout this issue of *Elements*). Lines represent the unique fugacity–temperature conditions where the phases coexist stably. Abbreviations: FMQ = fayalite–magnetite–quartz; NNO = nickel–nickel oxide; IW = iron–wüstite; WM = wüstite–magnetite; HM = magnetite–hematite. Oxygen fugacity values were computed for a total pressure of 1 bar.

volcanic rocks, showing that most glassy rocks lay close to the FMQ buffer. The possibility offered by modern analytical tools to directly measure the oxidation state of redox-sensitive elements in minerals and glasses has led to many empirical and theoretical formulations. Some examples, based on cutting-edge techniques, are reported by Sutton et al. (2020) and references therein.

Even though iron is the most used reference element to express the redox conditions of different shells of the Earth, it is important to remember that magmas are also enriched in other major and minor elements, multivalent or not, that influence and guide mineral stability fields (see Cicconi et al. 2020 this issue; Moretti and Stefansson 2020 this issue; Stagno and Fei 2020 this issue). Among these, special mention goes to the volatile components, whose speciation state can be highly variable in different physico-chemical environments. For instance, carbon can occur as CH_4, CO, and CO_2. Its speciation depends on the bulk composition of the system (e.g., the C:H:O ratio) at a given *P*–*T* condition. Hence, a unique f_{O_2} value characterizes the system. Whereas this is true for a closed system, in real geological environments most systems can be considered open. This is the case, in particular, when highly mobile volatile components are involved (see Moretti and Stefansson 2020 this issue) such that f_{O_2} can be fixed by factors that are external to the system chosen. For Earth's relatively reduced interior, the system C–H–O is described in more detail by Stagno and Fei (2020 this issue), while Moretti and Stefansson (2020 this issue) deal with the importance of C–H–O species at more oxidizing near-surface conditions.

The concept of oxygen fugacity (f_{O_2}) provides a high-temperature alternative to the E_h concept, via the oxygen electrode reaction shown in Equation (7). In solid electrolyte cells, an oxygen standard (of known f_{O_2}) and a sample atmosphere of unknown f_{O_2} are connected to a solid electrolyte (basically, a voltmeter). The whole-cell reaction is simply the subtraction of the oxygen electrode of the sample (Equation 7) from the oxygen electrode of the standard (Equation 7 again), for which E_h is given by:

$$E_h = -\frac{2.303RT}{n\mathrm{F}} \log_{10} \frac{f_{O_{2,\mathrm{std}}}}{f_{O_{2,\mathrm{sample}}}} \qquad (17)$$

Anderson and Crerar (1993) described the similarity and interrelation between f_{O_2} and E_h and show how to draw, for example, logf_{O_2}–pH diagrams in place of E_h–pH diagrams.

Unlike E_h measurements, direct f_{O_2} measurements are often inconvenient or even impossible. The practice, instead, is to measure the concentration ratio of redox couples of multiple valence elements in melts (e.g., Fe^{2+}/Fe^{3+}, S^{2-}/S^{6+}, V^{3+}/V^{5+} etc) or in gases (e.g. H_2/H_2O, CO/CO_2, H_2S/SO_2) and then relate them to f_{O_2} via thermodynamic calculations using appropriate standard state thermochemical data or oxybarometers such as those for gas–solid reactions shown in Equations (14) to (16). Although the approach is relatively straightforward for some gas-phase reactions, many caveats apply for the speciation state of elements in the liquid phase of magmatic systems, as described more fully by Cicconi et al. (2020 this issue). This, ultimately, demands a consistent treatment that unifies the description of redox and acid–base chemistry.

REFERENCES

Anderson GM, Crerar DA (1993) Thermodynamics in Geochemistry: The Equilibrium Model. Oxford University Press, Oxford, 608 pp

Biernat RJ, Robins RG (1969) High temperature potential/pH diagrams for the sulfur-water system. Electrochimica Acta 14: 809-820

Bowen NL, Schairer JF (1932) The system, FeO–SiO_2. American Journal of Science 24: 177-213

Buddington AF, Lindsley DH (1964) Iron-titanium oxide minerals and synthetic equivalents. Journal of Petrology 5: 310-357

Carmichael ISE (1966) The iron-titanium oxides of salic volcanic rocks and their associated ferromagnesian silicates. Contributions to Mineralogy and Petrology 14: 36-64

Carmichael ISE, Nicholls J (1967) Iron-titanium oxides and oxygen fugacities in volcanic rocks. Journal of Geophysical Research 72: 4665-4687

Cicconi MR, Le Losq C, Moretti R, Neuville DR (2020) Magmas are the largest repositories and carriers of Earth's redox processes. Elements 16: 173-178

Darken LS, Gurry RW (1945) The system iron-oxygen. I. The wüstite field and related equilibria. Journal of the American Chemical Society 67: 1398-1412

Davranche M, Gelabert A, Benedetti MF (2020) Electron transfer drives metal cycling in the critical zone. Elements 16: 185-190

Ellingham HJT (1944) Reducibility of oxides and sulphides in metallurgical processes. Journal of the Society of Chemical Industry 63: 125-160

Eugster HP (1957) Heterogeneous reactions involving oxidation and reduction at high pressures and temperatures. Journal of Chemical Physics 26: 1760-1761

Eugster HP (1959) Reduction and oxidation in metamorphism. In: Abelson PH (ed) Researches in Geochemistry. Volume 1. John Wiley & Sons, New York, pp 397-426

Eugster HP (1977) Compositions and thermodynamics of metamorphic solutions. In: Fraser DG (ed). Thermodynamics in Geology. D. Reidel Publishing Company, Dordrecht, pp 183-202

Eugster HP, Skippen GB (1967) Igneous and metamorphic reactions involving gas equilibria. In: Abelson PH (ed) Researches in Geochemistry. Volume 2, John Wiley & Sons, New York, pp 492-520

Eugster HP, Wones DR (1962) Stability relations of the ferruginous biotite, annite. Journal of Petrology 3: 82-125

Frost BR (1991) Introduction to oxygen fugacity and its petrologic importance. Reviews in Mineralogy and Geochemistry 25: 1-9

Goldschmidt VM (1929) The distribution of the chemical elements. Nature 124: 15-17

Herd CDK (2008) Basalts as probes of planetary interior redox state. Reviews in Mineralogy and Geochemistry 68: 527-553

Moretti R, Stefansson A (2020) Volcanic and geothermal redox engines. Elements 16: 179-184

Pourbaix MJN (1945) Thermodynamique des solutions aqueuses diluées: représentation graphique du rôle du pH et du potentiel. Doctoral thesis, Delft University of Technology

Reihard CT, Planavsky NJ (2020) Biogeochemical controls on the redox evolution of Earth's oceans and atmosphere. Elements 16: 191-196

Righter K, Herd CDK, Boujibar A (2020) Redox processes in early Earth accretion and in terrestrial bodies. Elements 16: 161-166

Stagno V, Fei Y (2020) The redox boundaries of Earth's interior. Elements 16: 167-172

Sutton SR, Lanzirotti A, Newville M, Darby Dyar M, Delaney J (2020) Oxybarometry and valence quantification based on microscale X-ray absorption fine structure (XAFS) spectroscopy of multivalent elements. Chemical Geology 531

Redox Processes in Early Earth Accretion and in Terrestrial Bodies

Kevin Righter[1], Christopher D. K. Herd[2] and Asmaa Boujibar[3]

1811-5209/20/0016-0161$2.50 DOI: 10.2138/gselements.16.3.161

The Earth is a unique rocky planet with liquid water at the surface and an oxygen-rich atmosphere, consequences of its particular accretion history. The earliest accreting bodies were small and could be either differentiated and undifferentiated; later larger bodies had formed cores and mantles with distinct properties. In addition, there may have been an overall trend of early reduced and later oxidized material accreting to form the Earth. This paper provides an overview—based on natural materials in our Earthbound sample collections, experimental studies on those samples, and calculations and numerical simulations of differentiation processes—of planetary accretion, core–mantle equilibration, mantle redox processes, and redox variations in Earth, Mars, and other terrestrial bodies.

KEYWORDS: accretion, oxygen fugacity, differentiation, core formation

The current make-up of the inner solar system ranges from airless and dry Mercury to oxygen-rich atmosphere and watery Earth. The ultimate critical controlling factor on this configuration is the early history of inner solar system bodies. Redox processes control the distribution and solubility of the key elements within both metallic and silicate liquids, such elements having the potential to react at depth or be outgassed later at the surface. An understanding of these equilibria and how they change with temperature and pressure affords insight into redox variations in the planets.

Iron provides important information about redox variation. The simple equilibrium Fe + O = FeO constrains the oxygen fugacity (f_{O_2}) within the inner solar system, commonly portrayed on a Prior diagram (e.g., Prior 1916). A Prior diagram can show the variation in the proportions of reduced (Fe metal) and oxidized (FeO and Fe_2O_3) iron that is present in meteorites (FIG. 1A). The range of f_{O_2} documented in planetary materials varies from iron–wustite (IW) from minus 8 to plus 7 (Righter et al. 2016): the IW+7, for example, refers to the oxygen fugacity (f_{O_2}) being 7 log units above that defined by the iron–wüstite (Fe–FeO) buffer. This convenient shorthand notation will be used throughout this paper. The variation of the distribution of Fe and FeO is also seen in terrestrial planets through correlations between FeO content of the mantle and the mass fraction of Fe-rich cores in Vesta (18%), Mars (21%), Earth and Venus (~30%) and Mercury (70%) (FIG. 1B). The causes of the different Fe/FeO distributions include variation in building block materials; redox equilibria that involve H, C, S, O, and Si; and planetary dynamics. Here, we will discuss these three topics and show how they can explain the variations we see in our solar system.

PLANETARY BUILDING BLOCKS

Terrestrial planet formation is thought to occur in three main stages: accretion of gas and dust, formation of planetesimals, merging of larger bodies in a late impact stage (FIG. 2). Because we have samples of materials from each of these stages, we can place f_{O_2} constraints on the building blocks that may have been present during planetary growth by examining mineral, melt, or trace element equilibria that are redox sensitive (Righter et al. 2016).

The first stage is represented by components in chondrites (i.e., the calcium aluminum–rich inclusions, or CAIs; the chondrules themselves; and the matrix) and primitive dust particles. Calcium aluminum–rich inclusions are considered to be the first crystalline materials to have condensed in equilibrium with the gaseous solar nebula at low pressures. They are made of refractory minerals such as spinel, clinopyroxene, melilite, perovskite, and anorthite. All of these first-stage materials exhibit a remarkable range of f_{O_2} from IW–8 (CAI fassaitic pyroxene) and upwards to metal-rich carbonaceous chondrite (CH) metal (IW–5.5), enstatite-rich chondrite (EL3) olivine (IW–6.5 to IW–4.5), the "Inte" Stardust particle (IW–6), inclusions in carbonaceous chondrites (IW–5 to IW–1.5), chondrules in ordinary and carbonaceous chondrites (IW–4 to 0), to Rumuruti-type chondrites (e.g., Righter et al 2016), GEMS (glass with embedded metal and sulfides) and oxidized Stardust particles (IW–3 to IW+1.5). This wide range of values spans ten logf_{O_2} units including solar values near IW–7 (Righter et al. 2016 and references therein) (FIG. 2 TOP).

The second stage is represented by samples of planetesimals such as meteorites from differentiated and undifferentiated bodies. As with the first stage, such materials span a wide f_{O_2} range from aubrites (IW–7 to –5), various iron meteorite groups (IW–4 to –2), acapulcoite/lodranite and winonites

1 NASA Johnson Space Center
2101 NASA Parkway
Houston, TX, 77058, USA
E-mail: kevin.righter-1@nasa.gov

2 University of Alberta
Department of Earth and Atmospheric Sciences
1-26 Earth Sciences Building
Edmonton, AB, T6G 2E9, Canada
E-mail: herd@ualberta.ca

3 Earth and Planets Laboratory
Carnegie Institution for Science
5251 Broad Branch Road NW
Washington DC 20015-1305, USA
E-mail: aboujibar@carnegiescience.edu

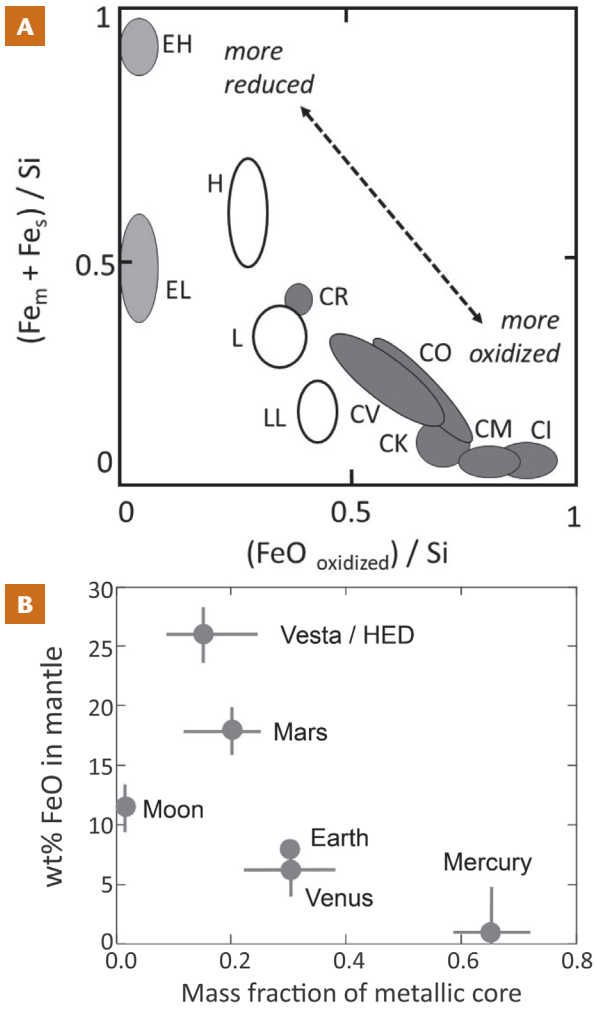

Figure 1 (**A**) A Prior (or Urey–Craig) diagram illustrating the negative correlation between reduced Fe (in metal, Fe_m; and sulfide, Fe_s) and oxidized Fe (as FeO), both normalized to Si. Abbreviations: EH and EL are enstatite chondrites (light grey ellipses); H, L, and LL are ordinary chondrites (white ellipses); CR, CV, CO, CK, CM, and CI are varieties of carbonaceous chondrites (dark grey ellipses). (**B**) Mass fraction of metallic core and mantle FeO are roughly correlated for the terrestrial planets and an asteroid (Vesta). Abbreviation: HED = howardite–eucrite–diogenite meteorite group, as derived from asteroid 4 Vesta. A notable exception is Earth's Moon, which has a very small core, presumably due to its unique origin by impact process. Modified from Righter et al. (2006).

(IW–3 to –1), ureilites (IW–3 to IW), the howardite–eucrite–diogenite clan and pallasites (IW–2 to –0.5), brachinites and related Graves Nunataks 06128/9 achondrites (IW–1 to IW+0.5), angrites (IW+1), to the thermally metamorphosed CK chondrites (IW+2 and higher; not shown in Fig. 2). Samples from Ceres may exhibit similar oxidation states to those of type 2 carbonaceous chondrites, given their similar mineralogy (McSween et al. 2018), and would, thus, fall as low as IW–3 for fayalite formation to as high as IW+3 for formation of smectite, saponite, phyllosilicates and magnetite. Samples from this stage also span an f_{O_2} range similar to that of the first stage materials of nearly 10 log units (Righter et al. 2016 and references therein) (Fig. 2 middle) and are also equilibrated at relatively low pressures.

The third stage is the formation of the planets themselves, in which case we have samples from Earth, Moon, and Mars, and remote spacecraft data for Mercury and Venus. For Earth, a great body of data has defined a wide range of oxygen fugacities that start near IW for continental xenoliths and ocean floor peridotites, extending to higher values for subduction zone mantle and hot spots (Kilauea, Hawaii, USA), to the highest values in magmas derived from metasomatized (oxidized) mantle (IW+4 to IW+8). Samples from Mars include picritic and basaltic rocks (the shergottite meteorites), cumulate clinopyroxenites (nakhlites) and some older crustal lithologies (orthopyroxenite and breccia). These samples collectively span over six logf_{O_2} units from IW–2 to IW+5. Venus has a similar core mass and core-to-mantle proportion to that of Earth, and we have some constraints on Venusian mantle FeO content from analyses of surface basalts. These crude constraints suggest that Venus, without plate tectonics and, thus, without recycling of surface volatiles to oxidize the mantle, may have f_{O_2} near that of Earth's early interior, perhaps IW–2 to IW–1. Mercury on the other hand, has S enrichment and FeO depletion at the surface, and possesses a large metallic core. The combination of these observations, and the fact that high S and low FeO silicate melts are favored at very low f_{O_2}, suggests that Mercury may have experienced f_{O_2} from IW–6 to IW–3 (Righter et al. 2016 and references therein) (Fig. 2 bottom). Finally, Earth's moon exhibits a narrow f_{O_2} range between IW and IW–2, despite having a very small metallic core. However, its formation in a giant impact involving the proto-Earth is somewhat unique.

Some redox variations in planets are caused by processes in relatively shallow crustal rocks, and knowledge of these processes can help to understand how initial planetary redox values can be modified. Thus, variations in redox states can, ultimately, be used to reveal information about planetary interiors. For example, applying multiple oxybarometers to certain shergottites (coexisting oxides, Fe^{3+}/Fe^{2+} in melts, olivine–pyroxene–spinel equilibria) shows that their redox state likely increased by two to three logf_{O_2}units during degassing (e.g., Righter et al. 2016; Castle and Herd 2017). On the other hand, nakhlites may record evidence of a reduction sequence caused by degassing of S_2, which is known to cause reduction in lunar basalts, eucrites, and ordinary chondrites (Righter et al. 2016 and references therein). If gaseous species (e.g., S^0) have different valences to species dissolved in a silicate melt (e.g., S^{2-}), then degassing can lead to a change in redox of the degassed magma. Thus, the difference in these two sequences ultimately lies in the different magmatic volatiles (e.g., Cl, H_2O, S) that may have been dissolved and degassed. This must be kept in mind when interpreting planetary basalt samples, such as those from Mars (and the Moon, Vesta, etc.).

Once degassing effects are recognized and accounted for, the inferred redox conditions of initial crystallization of the shergottite magmas provide insights into the f_{O_2} of Martian mantle sources (Castle and Herd 2017) and yield interesting insights into the interplay between building block composition, planetary size, and redox equilibria when compared with Earth. Correlations between time-integrated incompatible element enrichment and redox conditions strongly suggest the formation of mantle sources with linked geochemical and redox variations during initial fractionation of the silicate portion of Mars, most likely via magma ocean crystallization, over the f_{O_2} range of ~IW–1 to IW+2 (e.g., Castle and Herd 2017). Such sources are then left undisturbed until magma genesis, ascent, and eruption of the shergottites during the latter half of Mars' history (<2,400 Ma). The preservation of

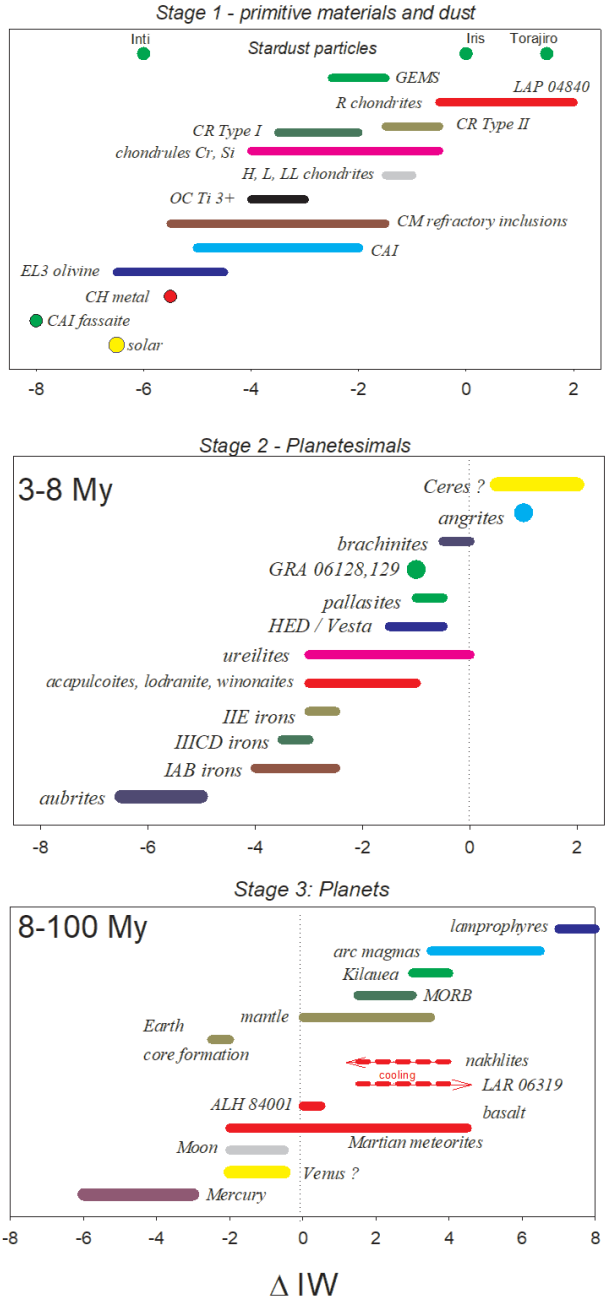

FIGURE 2 Range of oxygen fugacity recorded in planetary materials during the three main stages of accretion and planet building: (**UPPER**) Stage 1 is primitive materials and dust; (**MIDDLE**) Stage 2 is planetesimals; (**LOWER**) Stage 3 is planets. Abbreviations: HED, CH, CK, CM, CR, H, L, LL, and EL refer to the meteorite groups as in FIGURE 1; CAI = calcium aluminum–rich inclusions; OC = ordinary chondrite; Type I and Type II refer to the chondrules types in CR chondrites; GEMS = glass with embedded metal and sulfides; IIE, IIICD, and IAB refer to iron meteorite groups that contains silicate inclusions; MORB = mid ocean ridge basalt. Location abbreviations: GRA = Graves Nunataks; ALH =Allan Hills; LAP = LaPaz Icefield; LAR = Larkman Nunataks. These locations are for the dense collection areas in Antarctica where these meteorites (identified by number) were collected. Vertical sequence is f_{O_2} increasing upwards. ORIGINAL REFERENCES AND DETAILED DESCRIPTIONS OF SAMPLES AND MEASUREMENTS CAN BE FOUND IN RIGHTER ET AL. (2016).

such source characteristics over billion-year timescales is consistent with limited convection and mixing in the Martian mantle relative to Earth. More oxidized lithologies are generally produced through degassing, although early formed (~4,400 Ma) alkali basalt clasts in the Martian breccia have the highest recorded f_{O_2} for a Mars lithology, ~IW+5 (McCubbin et al. 2016). This might reflect conditions during formation of the primitive Martian crust.

In contrast, the much more vigorous convection and mixing within the Earth's mantle has apparently obliterated most early formed geochemical signatures (e.g., ^{142}Nd, ^{182}W) (Mundl et al. 2017). Furthermore, the dominant control on early mantle redox may have been the disproportionation of Fe^{2+} and the loss of metallic iron to the core, thereby oxidizing the lower mantle by several logf_{O_2} units immediately after core formation (e.g., Wood et al. 2006). Such a process would not occur within Mars due to its smaller size, because the disproportionation mechanism typically works only at pressures higher than those in the deep Martian mantle (Wood et al. 2006). For Earth, the progressive mixing of an oxidized lower mantle with a reduced upper mantle may be the cause of secular oxidation from ~IW+3 to IW+4.5 starting at ~3,500 Ma. Such a process may have played a role oxidizing the Earth's atmosphere at ~2,400 Ma (Nicklas et al. 2019). Thus, due to differences in planetary size, dynamics, and conditions of formation, primordial geochemical or redox mantle variations on Mars have been preserved whereas those in the Earth have been largely erased.

An interesting observation of materials from these three planetary formation stages is that they all record nearly the same range of f_{O_2} from IW–7 to IW+2, suggesting that the starting materials for planet growth may have had a direct influence on the end products. However, samples from Earth and Mars record the highest f_{O_2} values, which may mean that oxidation in the Earth may have been caused by later processes such as aqueous alteration, metasomatism, and recycling, whereas Mars may have had an oxidized early crust through degassing.

HIGH *P–T* REDOX EQUILIBRIA (METAL–SILICATE)

Planetary Fe-rich cores can contain significant amounts of light elements, including Si, S, O, C, and H. The presence of light elements is required to explain the density deficit of the Earth's core (Poirier et al. 1994). For Mars' core, the presence of S was proposed to explain geophysical data such as its moment of inertia (Sanloup et al. 1999). Experiments at high pressure and temperature that can replicate the chemical equilibria that occurs during core segregation confirm that light elements can be incorporated into core-forming Fe alloys in substantial concentrations (Poirier 1994). Reaction and equilibration of and between a silicate mantle and a metal core can be visualized through simple equilibria, such as:

$$Fe_{(metal)} + \tfrac{1}{2}O_2 = FeO_{(silicate)} \quad (1)$$

$$SiO_{2(silicate)} = Si_{(metal)} + O_2 \quad (2)$$

$$FeO_{(silicate)} = Fe_{(metal} + O_{(metal)} \quad (3)$$

$$FeO_{(silicate)} + \tfrac{1}{2}S_2 = FeS_{(metal)} + \tfrac{1}{2}O_2 \quad (4)$$

$$C_{(metal)} + O_2 = CO_{2(silicate)} \quad (5)$$

None of these equilibria alone are dominant: all are important when considering multicomponent equilibria that can be understood through appropriate experimental studies. These equilibria control the composition and size of the core and the composition and volatile content of

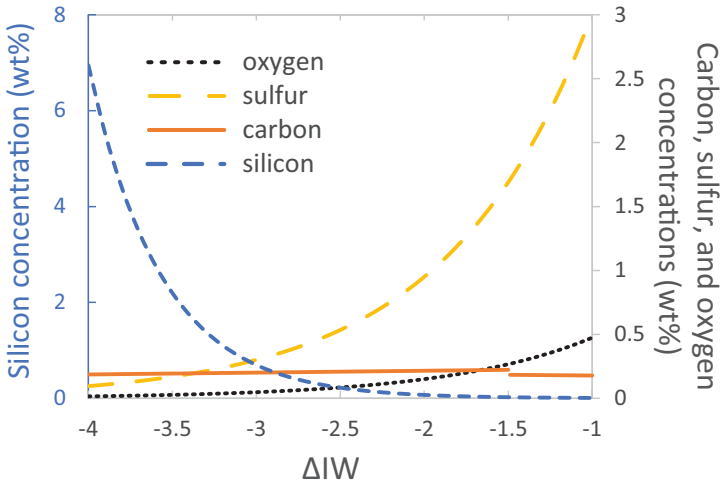

Figure 3 Role of oxygen fugacity (f_{O_2}) on the abundances of four light elements (C, S, O, Si) in an Fe alloy equilibrated with silicate at 5 GPa and 2,000 K on a graph of element concentrations versus change in the iron–wüstite buffer (ΔIW). The Si concentration (blue curve and left axis) decreases with the f_{O_2}; the concentrations of O and S (black and yellow curves, right axis) are correlated with the f_{O_2}. The abundance of C in Fe alloy is relatively weakly correlated with the oxygen fugacity. The degree of melt polymerization (as measured by the nonbridging oxygen per tetrahedrally coordinated cation parameter) and sulfide capacity (log C_S) were fixed at 2.56 and −5.324, respectively, as expected for the chemical composition of the Earth's mantle. Sulfur partitioning depends on the FeO concentration in the silicate melt (Boujibar et al. 2019), which was calculated at each f_{O_2} using Reactions (1) and (4) (see text). We used γ_{FeO}^{sil} = 1.7 and calculated γ_{Fe}^{met} using the online metal activity calculator (https://norris.org.au/expet/metalact/). Elements S, O, and Si were calculated using expressions presented by Boujibar et al. (2019), and C was calculated according to Li et al. (2016), all of which are based on data acquired on samples from a wide range of P–T–f_{O_2} conditions. The slight discontinuity in the C curve is due to the use of two expressions from Li et al. (2016): one for low f_{O_2} (<IW–1.5), and one for high f_{O_2} (>IW–1.5). To calculate S, C, and Si concentrations in metals from partition coefficients, we considered Earth's mantle values for S (200 ppm, from Palme and O'Neill 2014), C (765 ppm, from Marty et al. 2012), Si (45 wt%, from Palme and O'Neill 2014) and H_2O (300 ppm, from Cabral et al. 2014).

the mantle. Indeed, as a planet grows and a magma ocean deepens, the accreting material may contain H_2O or CO_2 that can oxidize the core-forming metal to FeO:

$$Fe + H_2O = FeO + H_2 \quad (6)$$

$$2Fe + CO_2 = 2FeO + C \quad (7)$$

In this way, core size and composition can change considerably compared to the original building blocks (Righter et al. 2006). This approach has been used to model the building blocks of Mars, whilst also matching core size, mean density, mean moment of inertia, and tidal response (Liebske and Khan 2019).

The S, C, Si, and O content of a planetary core can change dramatically with changes in f_{O_2}. These elements exhibit a trade-off in their solubility in Fe metal at the high pressures and temperatures relevant to planetary accretion. We illustrate this point with calculations of the core concentrations of S, C, Si, and O for the P–T conditions and composition of a planetesimal, but at variable f_{O_2}. Over the last few decades, the scientific community has constructed a significant body of high-P–T experimental data on metal–silicate equilibria. These data can be used to predict light element incorporation into Fe alloys across a wide range of pressure, temperature, oxygen fugacity, and chemical composition.

Partitioning of Si, O, S, and C between metal and silicate is described by the reactions shown in Equations (2), (3), (4), and (5), where the partition coefficient (via the equilibrium constant of each reaction) can be related to T, P, and oxygen fugacity (f_{O_2}); the activities of these elements in the metal and silicate can be calculated using semi-empirical expressions derived by Boujibar et al. (2019) and Li et al. (2016). To illustrate the effect of variable f_{O_2} on the corresponding core composition (in terms of Si, O, S and C), concentrations in liquid metal equilibrated with peridotitic silicate melt at f_{O_2} from IW–4 to IW–1 and constant P–T conditions (5 GPa, 2,000 K) were calculated using expressions from these two studies (Fig. 3). The resulting calculations show that oxygen fugacity has a strong effect on the solution of Si, O, S, and C in Fe metal alloys (Fig. 3). Carbon partitioning is less sensitive to f_{O_2} and its abundance in the metal remains relatively constant within each f_{O_2} range below and above IW–1.5. Conversely, whereas Si concentration in the metal is negatively correlated with f_{O_2}, S and O abundances increase with the f_{O_2}. At a low f_{O_2}, such as IW–4, metals contain 7 wt% Si, and less than 0.2 wt% S, C, or O. For oxidized conditions, such as IW–1, Si in metal is very low (< 0.007 wt%), whereas the concentrations of S and O can reach 3 wt% and 0.5 wt%, respectively. It is important to note that the abundance of each light element is calculated assuming that no other light element is in the Fe alloy, in order to isolate the effect of f_{O_2} and investigate evolutionary trends independently from chemical composition. However, because the partitioning of all four considered elements depends on the abundance of at least one other light element (Boujibar et al. 2019), the cumulative effect of f_{O_2} is more complex and requires iterative calculations. Moreover, core segregation is a continuous process

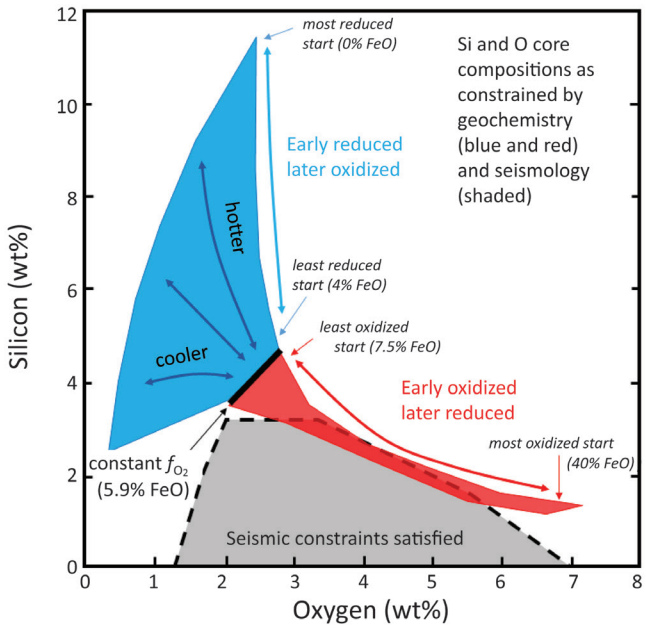

Figure 4 Light-element (Si and O) compositions for Earth's core that satisfies both geochemistry (colored bands) and seismology (black dashed line and gray background). The geochemically consistent cores are generated from multistage core-formation models, for various thermal conditions, and for increasing or decreasing magma ocean FeO contents (see Badro et al. 2015). The seismologically consistent composition space consists of the area delimited by the black dashed line. Models that start with more reduced low FeO magma oceans and that become more oxidizing during accretion result in relatively Si-rich cores, whereas models that start with more oxidized high-FeO magma oceans and that become more reduced during accretion (low FeO magma ocean) result in a relatively O-rich core. Redrawn after Badro et al. (2015).

where pressure and temperature increase over the course of accretion. These parameters are important to consider when addressing the chemistry of planetary cores.

An example of core formation at more extreme conditions is represented by the Earth. Because Si and O dissolve into Fe alloy at higher *P*–*T* conditions, and Si at more reduced conditions, these two elements have been used to show that Earth's density deficit (or solubility of a light element in the core) might be satisfied by some combination of Si and O, which covers a wide range of conditions (Fig. 4). This could also be true for S and C, but their availability is limited by cosmochemical constraints. Thus, Si and O—both major elements—provide the main constraints on Earth's core composition.

Another aspect of core-forming equilibria involving light elements, such as H and C, is the speciation of the associated volatile phase. For example, H_2O is very low in reduced systems even near the IW buffer, whereas H_2O is predominant in the H–O system at more oxidized conditions near the hematite–magnetite (HM) buffer (e.g., Behrens and Gaillard 2006). Similarly, CO_2 solubility in peridotite melt is strongly dependent on f_{O_2} and is <1 ppm at IW–2 but rises to >1,000 ppm at IW+1 (Dasgupta et al. 2013). These speciation effects and dependence upon f_{O_2} show that the dissolved and potentially degassed volatiles, and, thus, the composition of planetary atmospheres, are also strongly dependent on f_{O_2}.

PLANETARY ACCRETION MODELS

The first quantitative accretion models for Earth involved two components (Wänke 1981): an early reduced (metal-rich) component A, and a late oxidized (oxide-bearing) component B. The two-component mixture satisfied the overall chemical traits of the Earth. Such scenarios received some support from planetary dynamics where "feeding zones" extended outwards from Earth's local portion of the solar system to include more material from a larger heliocentric distance (Wetherill 1990). This shift from reduced state to oxidized state as *P* and *T* increased during accretion is also seen in the work of Fischer et al. (2017), who tested models of accretion with various starting compositions and degrees of mixing. Fischer et al. (2017) demonstrated that if starting materials are more reduced then there is more Si in the final core, whereas if they are more oxidized, the Si content is lowered (and O content raised) (Fig. 5). Additionally, accretion models for the solar system such as the Grand Tack (where giant planet dynamics control the sources of materials available for inner solar system planet growth) see a larger input of oxidized material from the outer solar system as accretion proceeds (Walsh et al. 2012). However, heterogeneous accretion models are not the only variety to produce gradual oxidation with increasing distance from the Sun. The nebular condensation calculations of Saxena and Hrubiak (2014) also predict that a Mercury-like metal-rich body forms closest to the Sun, followed by intermediate Earth- and Venus-like planets with ~30% cores, and finally Mars-like bodies with more FeS and FeO that form further out from the Sun. It is clear that both planetary dynamics simulations and nebular condensation calculations produce redox gradients that resemble our inner solar system.

Given these constraints, we can look more generally at ideas for the accretion of planets. Due to the large core and the FeO-poor and S-rich surface materials characterized first by remote spectroscopy (e.g., Sprague et al. 1995) and then by *MESSENGER* (Izenberg et al. 2014), it is clear that Mercury is a reduced body that might have accreted from enstatite chondrite–like material, or some metal-rich building blocks

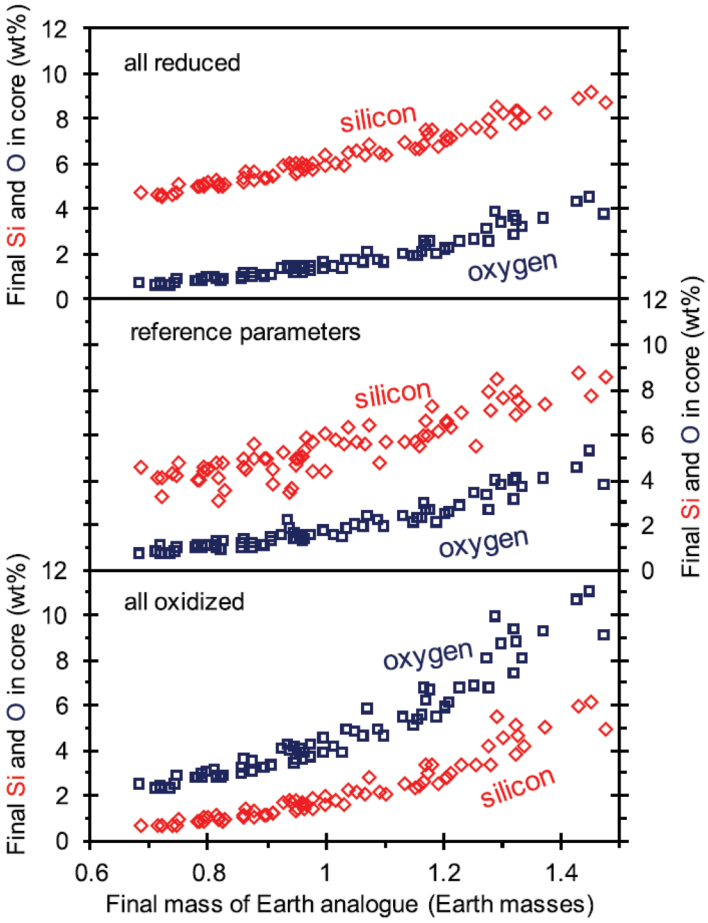

Figure 5 Final Si and O composition of the core as a function of Earth analogue mass for different oxidation states of the accreted material. Initial oxidation state of accreted material is the only core-formation model parameter varied between cases (panels); all other parameters were held fixed at their reference values. (**Upper panel**) All reduced starting materials; IW–3.5. (**Middle panel**) Reference set of model parameters (step function in oxidation state of starting materials). (**Lower panel**) All oxidized starting materials (IW–1.5). Navy blue squares: oxygen. Red diamonds: sillicon. The size of a planet largely controls its core Si and O contents, but accretion history also exerts an influence. Figure reprinted from Fischer et al. (2017), with permission from Earth and Planetary Science Letters.

such as the CH or CB chondrites (e.g., Brown et al. 2009). The metal enrichment may have also been caused, to some extent, by impact erosion of the Mercurian crust, leaving a metal-enriched body (Brown et al. 2009).

Earth must be made of material that will allow the 32% core but still leave a moderate amount of FeO in the mantle. Although two-component or heterogeneous accretion models can explain Earth's chemistry by variable f_{O_2} during accretion (e.g., Wänke 1981; Badro et al. 2015) (Fig. 5), several models have proposed that Earth is enstatite chondrite–like with FeO forming by oxidation of Fe metal as growth occurred (Javoy et al. 2010; Liebske and Khan 2019). That there are several processes and starting materials that can make Earth seems safe to say. Earth's formation is still an open topic without a clear paradigm. By analogy we can extend this argument to Venus, because we have so little detailed information about the Venusian interior.

Finally, Mars contrasts with Earth in that even 35 years ago geochemists realized it was easier to explain Mars' more oxidized and volatile-rich composition compared to Earth (Dreibus and Wänke 1985). Lodders and Fegley (1997) argued for 85% H chondrite along with 11% CV and 4% CI chondrite material. Sanloup et al. (1999) also argued for dominantly H chondrite but with the balance made up of EH chondrites. The most recent look at Mars' bulk composition, which also draws on extensive isotopic data that is now available for chondritic and other building blocks, shows that Mars could be accreted from a mixture of chondrites and an oxidized differentiated body. The chondritic material could have come from as many as 12 different meteorite groups contributing to the overall bulk composition (Liebske and Khan 2019).

The contrast between Earth, which could have formed mostly from material like enstatite chondrites, and Mars, which apparently formed from a mixture of diverse materials (including an important role for oxidized differentiated material), indicates that the redox properties of the planets really were controlled by all three processes highlighted above: their building blocks, high *P*–*T* redox equilibria, and the degree of mixing and accretion dynamics that affected the relevant portion of the inner solar system.

SUMMARY

Great strides have been made in understanding the role of redox equilibria and redox variation during planetary accretion. Although experimental studies have provided fundamental constraints on accretion and differentiation in planetary interiors, much work remains to be done to understand the phase equilibria of planetary cores and mantles at high pressures and temperatures, especially those containing volatiles such as H, C, S, and N. Additional understanding will come from new sample materials, such as meteorites and sample return missions, especially from Venus for which we currently have no samples and for which our knowledge of its exterior and interior is poor. Models and numerical calculations of the accretion process and a refined knowledge of the sources of materials that become accreted onto a planet will undoubtedly lead to new insights into redox variation within the inner solar system.

REFERENCES

Badro J, Brodholt JP, Piet H, Siebert J, Ryerson FJ (2015) Core formation and core composition from coupled geochemical and geophysical constraints. Proceedings of the National Academy of Sciences of the United States of America 112: 12310-12314

Behrens H, Gaillard F (2006) Geochemical aspects of melts: volatiles and redox behavior. Elements 2: 275-280

Boujibar A and 7 coauthors (2019) U, Th, and K partitioning between metal, silicate, and sulfide and implications for Mercury's structure, volatile content, and radioactive heat production. American Mineralogist 104: 1221-1237

Brown SM, Elkins-Tanton LT (2009) Compositions of Mercury's earliest crust from magma ocean models. Earth and Planetary Science Letters 286: 446-455

Cabral RA and 9 coauthors (2014) Volatile cycling of H_2O, CO_2, F, and Cl in the HIMU mantle: a new window provided by melt inclusions from oceanic hot spot lavas at Mangaia, Cook Islands. Geochemistry, Geophysics, Geosystems 15: 4445-4467

Castle N, Herd CD (2017) Experimental petrology of the Tissint meteorite: redox estimates, crystallization curves, and evaluation of petrogenetic models. Meteoritics & Planetary Science 52: 125-146

Dasgupta R (2013) Ingassing, storage, and outgassing of terrestrial carbon through geologic time. Reviews in Mineralogy and Geochemistry 75: 183-229

Dreibus G, Wänke H (1985) Mars, a volatile-rich planet. Meteoritics 20: 367-381

Fischer RA, Campbell AJ, Ciesla FJ (2017) Sensitivities of Earth's core and mantle compositions to accretion and differentiation processes. Earth and Planetary Science Letters 458: 252-262

Izenberg NR and 16 coauthors (2014) The low-iron, reduced surface of Mercury as seen in spectral reflectance by MESSENGER. Icarus 228: 364-374

Javoy M and 10 coauthors (2010) The chemical composition of the Earth: enstatite chondrite models. Earth and Planetary Science Letters 293: 259-268

Li Y, Dasgupta R, Tsuno K, Monteleone B, Shimizu N (2016) Carbon and sulfur budget of the silicate Earth explained by accretion of differentiated planetary embryos. Nature Geoscience 9: 781-785

Liebske C, Khan A (2019) On the principal building blocks of Mars and Earth. Icarus 322: 121-134

Lodders K, Fegley B Jr (1997) An oxygen isotope model for the composition of Mars. Icarus 126: 373-394

Marty B (2012) The origins and concentrations of water, carbon, nitrogen and noble gases on Earth. Earth and Planetary Science Letters 313-314: 56-66

McSween HY Jr. and 9 coauthors (2018) Carbonaceous chondrites as analogs for the composition and alteration of Ceres. Meteoritics & Planetary Science 53: 1793-1804

Mundl A and 7 coauthors (2017) Tungsten-182 heterogeneity in modern ocean island basalts. Science 356: 66-69

Nicklas RW and 8 coauthors (2019) Secular mantle oxidation across the Archean-Proterozoic boundary: evidence from V partitioning in komatiites and picrites. Geochimica et Cosmochimica Acta 250: 49-75

Palme H, O'Neill H (2014) Cosmochemical estimates of mantle composition. In: Carlson RW (ed) The Mantle and Core. Treatise on Geochemistry, Volume 3, 2nd edition, Elsevier Press, pp 1-39

Poirier J-P (1994) Light elements in the Earth's outer core: a critical review. Physics of the Earth and Planetary Interiors 85: 319-337

Prior GT (1916) On the genetic relationship and classification of meteorites. Mineralogical Magazine and Journal of the Mineralogical Society 18: 26-44

Righter K, Drake MJ, Scott ERD (2006) Compositional relationships between meteorites and terrestrial planets. In: Lauretta DS, McSween HY Jr (eds) Meteorites and the Early Solar System II. University of Arizona Press, pp 803-828

Righter K, Sutton SR, Danielson L, Pando K, Newville M (2016) Redox variations in the inner solar system with new constraints from vanadium XANES in spinels. American Mineralogist 101: 1928-1942

Sanloup C, Jambon A, Gillet P (1999) A simple chondritic model of Mars. Physics of the Earth and Planetary Interiors 112: 43-54

Saxena SK, Hrubiak R (2014) Mapping the nebular condensates and the chemical composition of the terrestrial planets. Earth and Planetary Science Letters 393: 113-119

Sprague AL, Hunten DM, Lodders K (1995) Sulfur at Mercury, elemental at the poles and sulfides in the regolith. Icarus 118: 211-215

Walsh KJ, Morbidelli A, Raymond SN, O'Brien DP, Mandell AM (2012) Populating the asteroid belt from two parent source regions due to the migration of giant planets—"The Grand Tack". Meteoritics & Planetary Science 47: 1941-1947

Wänke H (1981) Constitution of terrestrial planets. Philosophical Transactions of the Royal Society of London, Series A: Mathematical, Physical and Engineering Sciences 303: 287-302

Wetherill GW (1990) Formation of the Earth. Annual Review of Earth and Planetary Sciences 18: 205-256

Wood BJ, Walter MJ, Wade J (2006) Accretion of the Earth and segregation of its core. Nature 441: 825-833

The Redox Boundaries of Earth's Interior

Vincenzo Stagno[1] and Yingwei Fei[2]

An octahedral (7 mm edge) diamond on kimberlite (Kimberley mine, South Africa). Image: Michele Macrì, courtesy of University Museum of Earth Sciences of Sapienza University of Rome (Italy).

1811-5209/20/0016-0167$2.50 DOI: 10.2138/gselements.16.3.167

The interior of the Earth is an important reservoir for elements that are chemically bound in minerals, melts, and gases. Analyses of the proportions of redox-sensitive elements in ancient and contemporary natural rocks provide information on the temporal redox evolution of our planet. Natural inclusions trapped in diamonds, xenoliths, and erupted magmas provide unique windows into the redox conditions of the deep Earth, and reveal evidence for heterogeneities in the mantle's oxidation state. By examining the natural rock record, we assess how redox boundaries in the deep Earth have controlled elemental cycling and what effects these boundaries have had on the temporal and chemical evolution of oxygen fugacity in the Earth's interior and atmosphere.

Keywords: redox state, mantle xenoliths, diamond inclusions, oxygen fugacity, volatile cycle

INTRODUCTION

The Earth's interior represents the largest reservoir of volatile elements (e.g., carbon, hydrogen, sulfur, nitrogen, oxygen) in the planet. The migration of volatiles to the shallow portions of the planet and, eventually, out into the atmosphere, plays an important role in planetary evolution. This process is strongly controlled by physical and chemical conditions at depth. Oxygen fugacity (f_{O_2}), or the partial pressure of oxygen (pO_2) in the case of gaseous mixtures in the atmosphere or volcanic gases, is a critical thermodynamic variable that controls the presence and proportions of multiple oxidation states of an element in minerals, liquids, and gases.

The differentiation of metal and silicate that occurred in the interior of the proto-Earth following its accretion from the solar nebula (Righter et al. 2020 this issue) led to oxygen redistribution, resulting in a stratification of oxidation state by sinking of reduced iron (Fe^0) metal into the core and bonding of O^{2-} to mantle silicates, followed by outgassing of H_2O-vapor, CO_2, and CO into the atmosphere (Fig. 1). The Earth's early atmosphere contained almost no free oxygen (Fig. 2), and its composition was probably more similar to that of extremely reduced volcanic gases (pO_2 of 10^{-6} atm). The atmosphere has become increasingly oxidized over time, a phenomenon that has been plausibly linked to the dynamic changes undergone by Earth, including the initiation of plate tectonics, the formation of continents, and the appearance of life (Fig. 2) (see Reinhard and Planavsky 2020 this issue). A possible link between the redox state of the Earth's interior and its atmospheric composition has been a matter of investigation over the last few decades through laboratory experiments and geochemical analysis of natural rocks. The evolution of the mantle's oxidation state, at least locally, is strongly influenced by recycling of surface materials via subduction. We can investigate the mantle's redox state by determining the mineralogy and chemical compositions of the mantle rocks, as well as understanding the effect of pressure and temperature on element partitioning among the coexisting phases. The observed mineralogy and chemistry of planetary interiors represent the final integration of numerous geodynamic

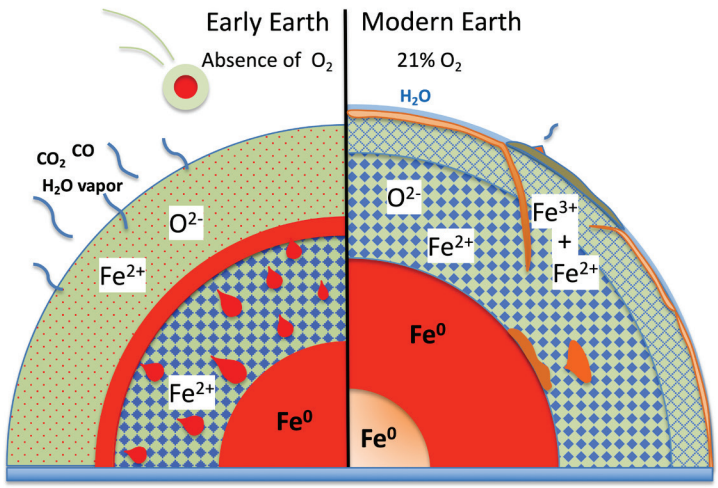

Figure 1 Schematic of the evolution of redox boundaries of the Earth's interior. (**Left**) Differentiation of the early Earth. Reduced metal (red teardrop shapes) sinks through the molten silicate to the core to establish oxidation state stratification between the mantle and the core at about 2 log units below the iron–wüstite, IW, buffer. (**Right**) The oxidation state of modern Earth's mantle has been significantly modified by subduction: heterogeneous f_{O_2} is expected in subduction zones. Layers shown are the inner core, outer core, lower mantle, upper mantle, and crust; oceanic crust (light orange) can subduct down to lower mantle depths. Note development of mantle plumes (orange) at the bottom of the lower mantle.

1 Sapienza University of Rome
Department of Earth Sciences
Rome, Italy
E-mail: vincenzo.stagno@uniroma1.it

2 Earth and Planets Laboratory
Carnegie Institution for Science
Washington DC, USA
E-mail: yfei@carnegiescience.edu

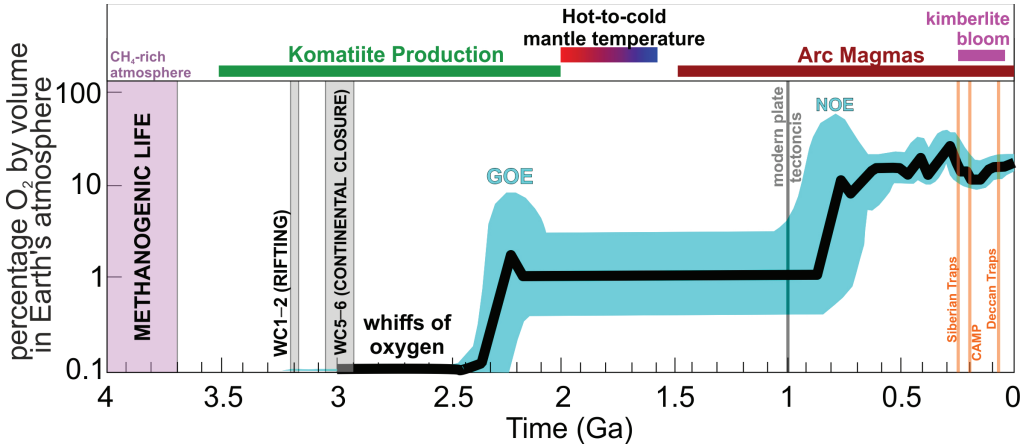

Figure 2 Variations in atmospheric oxygen partial pressure (pO_2) over the Earth's history. The maximum values are represented by the Great Oxidation Event (GOE) at 2.5–2.0 Ga and the Neoproterozoic Oxygenation Event (NOE) at 1.0–0.8 Ga. These two events are shown in relation to high-impact geological events such as the onset of plate tectonics through the Wilson Cycle (WC): WC1 and 2 for rifting, WC5–6 for continental collision (Shirey and Richardson 2011). These cycles are accompanied by the production of large volumes of magmas formed at hot mantle temperatures (producing komatiites) and cold mantle temperatures (as for arc magmas and kimberlites) (Tappe et al. 2018), plus the development of three large igneous provinces (LIPs): the Siberian Traps (predominantly Russia), the Central Atlantic Magmatic Province (CAMP), and the Deccan Traps of India. These LIPs likely caused mass extinctions (orange bars). The width of the blue band denotes uncertainty. The onset of modern plate tectonics is according to current continental growth models (Tappe et al. 2018). The timing of 'whiffs of oxygen' is marked by the enrichment of metals, such as Mo and Re, in the ocean resulting from their weathering-promoted mobilization from shallow sediments (after Lyons et al. 2014; see also Reinhard and Planavsky 2020 this issue).

processes dating back to the formation of the solar system: these processes involve planetary accretion, core–mantle separation, and plate tectonics. In order to address the nature of redox boundaries in the interior of a planet, we summarize the oxidation state recorded in natural mantle rocks, ancient and contemporary lavas, and preserved mineral inclusions in sublithospheric diamonds. These natural observations are combined with experimental studies aimed at simulating the Earth's interior to understand how the redox state has evolved over geological time.

Peridotites and eclogites are mantle-derived rocks whose minerals (chiefly olivine, orthopyroxene, clinopyroxene, spinel, and garnet) contain multivalent elements, such as iron, chromium, and vanadium. The ratios of the oxidized and reduced forms of these elements are sensitive to the redox conditions at which they formed. Incorporation of these elements in their oxidized or reduced form can be used to determine the f_{O_2}, which is taken as representative of the redox state of the mantle from which these rocks are derived. Mantle rocks from ancient Archaean cratons often host diamondiferous deposits, such as those in South Africa and Canada. Because carbon may exist either as oxidized carbonate (CO_3^{2-}) or reduced graphite/diamond (C^0), the presence of diamonds suggests that these mantle rocks equilibrated under reducing conditions. Two important goals in experimental geochemistry have been 1) to investigate how the behavior of relevant elements has been influenced by f_{O_2} and to develop interpretative models to understand the change of redox conditions in the Earth's interior, and 2) to explore how this might have controlled atmospheric composition though space and time. Because mantle rocks exposed at the surface are only those equilibrated up to, at most, depths of 200–250 km, information on the redox state of the upper mantle transition zone (410–660 km) and lower mantle (660–2,890 km) relies on the discovery and study of mineral inclusions in sublithospheric diamonds. In order to use inclusions composition to understand the redox conditions of the deep mantle, it is necessary to carry out experimental syntheses of phase equilibria and determine element partitioning under appropriate conditions. Analyses of data from natural rocks and laboratory experiments have allowed us to understand the extent to which the Earth's interior can be considered stratified, having either gradual or sharp redox boundaries. Here, we summarize our understanding of redox conditions and evolution in Earth's deep interior.

MANTLE OXIDATION STATE FROM THE STUDY OF NATURAL ROCKS AND ERUPTED LAVAS

The oxidation state of Earth's interior controls the speciation of multivalent elements, such as carbon (C^0 or C^{4+}) and iron (Fe^0, Fe^{2+}, or Fe^{3+}) in minerals and melts. The transformation from reduced phases such as carbide, graphite, and diamond, to oxidized carbonate minerals and melts provides an important indicator of mantle oxidation state. It also affects mantle processes due to changes in physicochemical properties, such as the melting of mantle rocks at lower temperatures by the addition of CO_2 (i.e., redox melting) (Stagno et al. 2013 and references therein). On the other hand, carbonate minerals and melts can be deprived of oxygen as a consequence of redox conditions buffered locally by the oxidation of Fe^{2+} to Fe^{3+} in minerals to form elemental carbon (Rohrbach and Schmidt 2011). The change of redox state of the mantle may play an important role in the recycling and mobilization of deep carbon and the production of a large spectrum of magmas at different depths over time (Stagno 2019).

The redox state of the continental lithospheric mantle has been investigated extensively through the analyses of natural rocks and the application of oxy-thermobarometers that use mineral equilibria to estimate their redox state through the correlation between the $Fe^{3+}/\sum Fe$ ratio of minerals and f_{O_2} (Frost and McCammon 2008). The $Fe^{3+}/\sum Fe$ ratio is typically measured by Mössbauer spectroscopy or is estimated on the basis of charge balance calculations. Thermodynamic calculations supported by experiments have facilitated the use of three important mineral equilibria as oxy-thermobarometers for spinel- and garnet-peridotites and for eclogites (Stagno 2019). Figure 3 plots the measured f_{O_2} of natural mantle rocks, normalized to a common reference buffer, in this case fayalite–magnetite–quartz (FMQ). The results show a heterogeneous mantle oxidation state, varying by 7 log units over 250 km depth. The general trend becomes more reduced with depth as result of the positive pressure effect on the incorporation of Fe^{3+} in garnet's crystal structure. Deep mantle eclogites (>175 km) can extend to the reduced conditions required to stabilise metallic Fe and methane-rich fluids, as indicated by the dot-dashed and dotted lines in Figure 3.

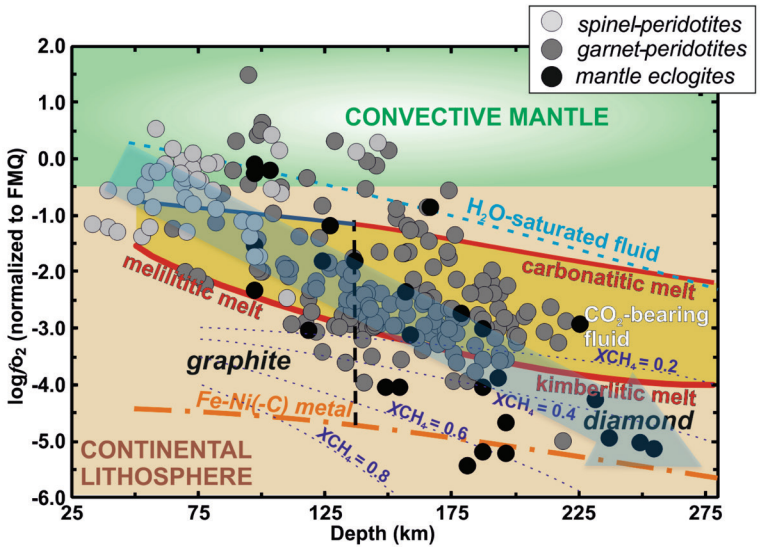

Figure 3 Plot of logf_{O_2} (relative to the fayalite–magnetite–quartz, FMQ, buffer) as a function of depth. Grey/black circles represent the calculated values for mantle peridotite and eclogite xenoliths using spinel and garnet oxy-thermobarometers (Stagno 2019). The thick light-blue arrow (going upper left to lower right) indicates the general trend of upper mantle redox state. The red lines are oxygen fugacities calculated along a cratonic geotherm of 44 mW·m^{-2} that define the stability field for diamond (or graphite) coexisting with solid (liquid) carbonate and kimberlitic magmas, respectively. The vertical dashed line represents the graphite–diamond boundary. The orange line is the Fe–Ni precipitation curve (Frost and McCammon 2008). In addition, the light and dark blue lines represent the calculated f_{O_2} at which C–O–H fluids in equilibrium with graphite/diamond consist of pure water (H_2O maximum) or the mole fractions of methane (XCH_4 = 0.2, 0.4, 0.6, and 0.8) according to Luth et al. (2014). The green and brown boxes mark the convective mantle and continental lithosphere, respectively.

Figure 3 also shows the calculated f_{O_2} as a function of depth for C–O–H fluids of different compositions that are in equilibrium with graphite/diamond, marked by the mole fractions of methane (XCH_4) (dark blue lines). The observations show that peridotites and eclogites can coexist with C–O–H fluids along cratonic *P*–*T* conditions. Under more oxidized conditions, H_2O-saturated fluids coexist with mantle rocks (blue dashed line), the fluids then becoming progressively richer in C as f_{O_2} decreases. The formation of rare carbonate-rich magmas, such as carbonatites and kimberlites, is the consequence of the oxidation of elemental carbon to CO_2 (yellow area) that, in turn, lowers the melting temperatures of peridotite (or eclogite) rocks at depth (Hammouda and Keshav 2015). Under more reducing conditions, partial melting of peridotite is inhibited by the presence of coexisting (nonreactive) methane-bearing fluids. Interestingly, most mantle rocks fall in the diamond and graphite stability fields, while thermodynamic models predict the potential coexistence of small volumes of water, CO_2(–H_2O)-rich magmas (and/or fluids), and methane, probably involving the following redox equilibria:

$$2Fe_2O_{3(solid)} + C = 4FeO_{(solid)} + CO_{2(vapor/melt)} \quad (1)$$

$$Fe_2O_{3(solid)} + H_2 = 2FeO_{(solid)} + H_2O_{(vapor/melt)} \quad (2)$$

$$2Fe_2O_{3(solid)} + CH_4 = 4FeO_{(solid)} + C + 2H_2O_{(vapor/melt)} \quad (3)$$

For these reactions, $Fe_2O_{3(solid)}$ and $FeO_{(solid)}$ refer to ferric and ferrous iron incorporated in upper mantle minerals, predominantly spinel and garnet. Importantly, the reactions shown in Equations (1) and (3) are those causing mantle redox melting to produce a wide range of CO_2- and H_2O-bearing magmas until all volatiles are exhausted, whereupon f_{O_2} is solely buffered by the coexisting minerals. Such magmas are rarely observed in nature. On the other hand, the reaction in Equation (2) is likely to have occurred in the interior of Earth after core formation where the release of H_2 brought about rapid oxygenation of the residual early formed mantle and an enrichment in water. Conversely, in subduction-related environments, the reactions in Equations (1)–(3) are probably controlled by locally released decarbonation and/or dehydration reactions in the subducted slab (Frost and McCammon 2008; Debret and Sverjensky 2017).

Because most of the rocks plotted in Figure 3 are of Archaean age, knowledge of their f_{O_2} permits understanding of how mantle redox state has changed over time. Three main points remain a matter of debate. (1) Does the f_{O_2} gradient observed in peridotites from the continental lithosphere hold for the convective (asthenospheric) mantle? (2) Do erupted magmas inherit the oxidation state of their mantle source rocks? (3) Has mantle redox state changed gradually over time? Answers to these questions are related to the redox boundaries in the interior of Earth. The most fertile garnet peridotite rocks [e.g., peridotite xenolith sample PHN1611 from Lesotho, see McCammon and Frost (2008)] have a bulk chemistry that coincides with that inferred for bulk silicate Earth (BSE) on cosmochemical grounds. For this reason, it is a suitable analogue for the asthenospheric mantle. By assuming an $Fe^{3+}/\sum Fe$ equal to that found in abyssal peridotites (1%–3%), thermodynamic models (Stagno et al. 2013; Stagno 2019) predict a similar redox profile to that observed for the continental lithosphere (Fig. 3) with f_{O_2} as low as –5 log units (ΔFMQ) at depths greater than 175 km.

Geochemical data (CO_2 vs Nb and CO_2 vs Ba) in oceanic basalts have been recently used (Eguchi and Dasgupta 2018) to argue that more oxidizing conditions, between –0.5 and +2 log units (ΔFMQ), must exist in the mid- to deep-oceanic mantle down to ~150 km in depth. This is due to the requirement that carbon must be mobilized from the subducted slab in the form of CO_2, thereby producing the observed enrichments in erupted lavas. Interestingly, the chemical composition (SiO_2/CO_2 ratio) of small-degree partial melts is determined by the depth, mantle temperature, and local mantle f_{O_2} at which elemental carbon is oxidized to carbonate by the redox reaction shown in Equation (1). These magmas undergo devolatilization, changes in melt polymerization, crustal assimilation, fractional crystallization, and net oxidation during their ascent toward the surface. Once the magmas are exposed at the surface, alteration processes can mask their initial redox state and make it difficult to link them to the f_{O_2} of the source. The effect of devolatilization on the residual melt has been attested to by the change in oxidation state of iron and sulfur in droplets of basaltic magmas (as melt inclusions) trapped in olivine from Kilauea volcano (Hawaii, USA) (Moussallam et al. 2016) and Laki volcano (Iceland) (Hartley et al. 2017) relative to their respective host magmas. The loss of volatile elements (e.g., sulfur and H_2O) would lead to a reduction of the erupted lavas compared to the preserved un-degassed magmas through the following reaction:

$$H_2S_{(melt)} + 3Fe_2O_{3(melt)} = SO_{2(vapor)} + 6FeO_{(melt)} + H_2O_{(vapor)} \quad (4)$$

Birner et al. (2018) showed agreement between the f_{O_2} of mid-ocean ridge (MOR) basalts and that of the corresponding MOR peridotites when both are back-calculated to source *P*–*T* conditions. However, the spread in f_{O_2} values in MOR basalts and peridotites have distinct standard deviations, with MOR basalts being more homogeneous than the peridotites. Indeed, heterogeneities are observed even at the hand-specimen scale. These discrepancies were also reported in experimental studies aimed at reproducing melting conditions of a fertile spinel peridotite (Sorbadere et al. 2018). Further studies are needed to better understand how the signature of mantle redox state is physically transferred from rocks to partial melts and, in turn, to magmatic gases that ultimately are released to the atmosphere.

REDOX STATE OF THE TRANSITION ZONE AND LOWER MANTLE FROM INCLUSIONS IN SUPERDEEP DIAMONDS

Mantle xenoliths provide a unique window on the redox state of the upper mantle down to ~250 km. We have a reasonably good understanding of redox variations with depth and the key factors that control those variations, as illustrated in Figure 3. However, information on even deeper portions of the upper mantle, the transition zone (410–660 km) and the lower mantle (down to ~2,890 km), is limited because only a few, rare diamond inclusions have been found from those depths. These sublithospheric (or superdeep) diamonds are witness to geological processes occurring in the hidden deep mantle (Kaminsky 2012). Minerals found in superdeep diamonds include majoritic garnet, carbonates, ringwoodite, $CaSiO_3$ walstromite, ferropericlase, Fe–Ni alloys, and carbides. Analyses of those inclusions, supported by experimental petrology studies, allows inferences to be made as to the possible deep mantle *P*–*T*–f_{O_2} conditions at which the inclusions formed. Such information is particularly valuable in the case of minerals formed prior to entrapment by the growing diamonds (i.e., protogenetic inclusions). To date, the redox state of the deep mantle has been determined for a suite of diamonds from Jagersfontein (South Africa) using the Fe^{3+} content of majoritic garnet inclusions that equilibrated at depths of 220–550 km (Kiseeva et al. 2018). In addition, some 53 Type II diamonds contained metallic inclusions along with H_2 fluids. These diamonds are interpreted to have formed in the transition zone by precipitation from an Fe–Ni liquid metal (Smith et al. 2016). However, some deep diamonds show inclusions of solid carbonates (Kaminsky 2012 and references therein), suggesting some portions of the lower mantle might be oxidized to similar levels as the upper mantle.

Figure 4 shows the estimated f_{O_2} from different deep diamond inclusions and provides a snapshot of the different oxygenation levels of the mantle at different depths. Experimental measurements of the f_{O_2} at which diamonds and solid carbonate can coexist along with silicate minerals of the transition zone and lower mantle (see Stagno 2019 and references therein) suggest a general trend of decreasing f_{O_2} with depth in the deep mantle (the dark blue line on Fig. 4). The relationship can be applied as oxybarometers for carbonate inclusions trapped in superdeep diamonds. For comparison, the upper mantle redox state (gray shaded region below 10 GPa on Fig. 4) recorded by mantle xenoliths has a much steeper pressure dependence (cf. Fig. 3); the likely f_{O_2} of the transition zone and lower mantle (the horizonal gray shaded region on Fig. 4) would be close to the iron–wüstite (IW) buffer. The estimated f_{O_2} of mantle-derived rocks and diamond inclusions provides a more complex picture of the deep mantle. Majoritic garnet inclusions from Jagersfontein (red diamond symbol) show

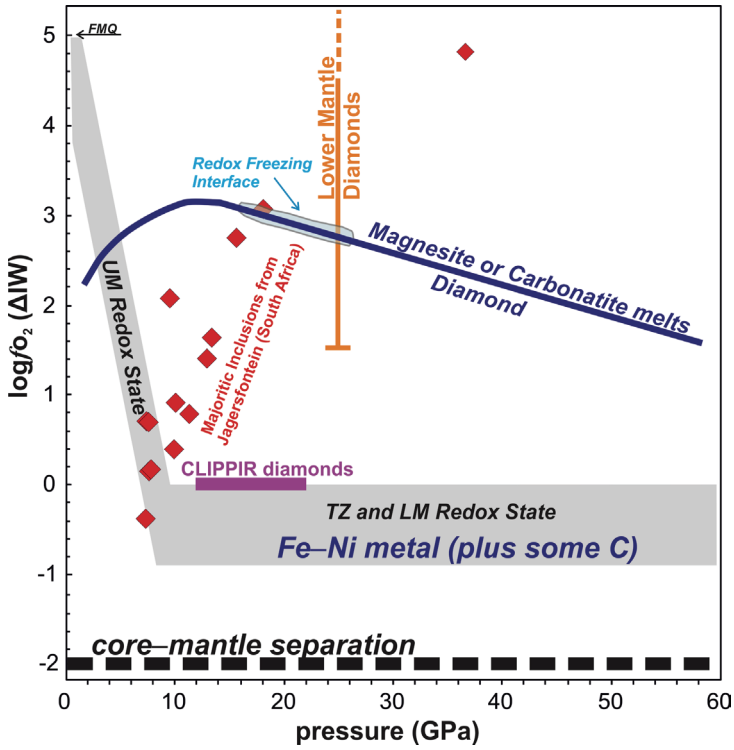

Figure 4 Plot of logf_{O_2} (relative to changes in the iron–wüstite, IW, buffer) as a function of pressure in the deep mantle. The red diamond symbols show the estimated f_{O_2} from majorite inclusions in diamonds (Kiseeva et al. 2018); the thick purple line shows the estimated f_{O_2} from metal-bearing "CLIPPIR" (Cullinan-like, large, inclusion-poor, pure, irregular, resorbed) diamonds (Smith et al. 2016); the vertical orange line shows the estimated f_{O_2} from ferropericlase inclusions in diamonds (Kaminsky et al. 2015). The dark blue line indicates the f_{O_2} at which diamonds and carbonate (magnesite) are in equilibrium with a mantle mineral assemblage (Stagno 2019). The gray shaded region indicates the upper mantle (UM) redox state recorded by mantle xenoliths (cf. Fig. 3) and the likely f_{O_2} of the transition zone (TZ) and lower mantle (LM), if it is reduced enough to allow Fe–Ni alloy (± dissolved carbon) to be stable (Frost and McCammon 2008). Most of the superdeep diamonds are thought to have originated at the interface between the oxidized subducting slab and the reduced asthenospheric mantle (shaded blue) where CO_2-rich fluids have been proposed to "freeze" (Rohrbach and Schmidt 2011).

a large range of f_{O_2}, whereas CLIPPIR (Cullinan-like, large, inclusion-poor, pure, irregular and resorbed) diamonds (purple line) indicate very reducing conditions to help produce Fe–Ni metal alloy inclusions (Fig. 4). Indeed, the recovered inclusions and their redox conditions may reflect only local environments and may not be applicable to the whole mantle. The chemical compositions of natural mantle-derived rocks attest to the fact that the mantle's physical evolution through time has created chemical and f_{O_2} heterogeneities. The dichotomy between *sharp* versus *gradual* redox boundaries in Earth's interior is a result of mantle evolution and material exchange between the surface and deep mantle over time.

TEMPORAL VARIATIONS IN MANTLE f_{O_2}: GRADUAL VS SHARP BOUNDARIES

Whether mantle oxidation state has changed gradually or suddenly over time has long been debated. The temporal evolution of mantle redox state and that of melts and volcanic gases derived therefrom may have played a key role in the volatile cycle, greenhouse effects, plate tectonics, and life on Earth. To answer this question, geologists have been looking at potential geochemical markers in ancient rocks

and minerals. Redox-sensitive geochemical signatures, such as the cerium (Ce) concentration of Hadaean zircons and the vanadium/scandium (V/Sc) ratio of erupted basalts, have been used to claim the constancy of the mantle redox state over the last 3.8 billion years to values where carbon is stable as C^{4+} (i.e., CO_2 in solids, melts, and gases). In particular, the higher solubility of Ce^{4+} compared to Ce^{3+} in zircons equilibrated with melts allows an estimation of the oxidation state of Hadean melts with respect to MOR lavas (Trail et al. 2011). In addition, the V/Sc ratio in basaltic melts is a function of redox conditions during melting processes, with V^{5+} being more incompatible than Sc^{3+} at high f_{O_2} (Li and Lee 2004).

The investigation and quantification of mantle redox state over time requires the integration of f_{O_2} values, as estimated by oxy-thermobarometry, with radiometric dating of mantle rocks, inclusions in diamonds, and mantle-derived lavas. FIGURE 5 shows the temporal evolution of mantle f_{O_2} from the value set by core–mantle separation (IW–2, corresponding to FMQ–6) soon after Earth's accretion, to the ~IW+3.5 (FMQ–0.5) recorded by present-day mantle rocks. FIGURE 5 also shows a schematic model that takes into account gradual mantle self-oxidation (up to IW+2) caused by disproportionation of FeO to metallic Fe and Fe_2O_3 in the magma ocean (Armstrong et al. 2019). The model is constrained by f_{O_2} estimates of eclogitic, picritic, and komatiitic rocks of Archaean age, along with a determination of the mantle's oxidation state through Ce in Hadean zircons and oxy-thermobarometry of mantle rocks. For comparison, the redox state of present-day volcanic gases is also shown on FIGURE 5 (Moussallam et al. 2019). When these data are compared with modern MOR lavas, a gradual increase in f_{O_2} of the Earth's mantle can be seen in both komatiites (Nicklas et al. 2019) and eclogites (Aulbach and Stagno 2016). This conclusion contrasts with that of a previous geochemical model in which mantle oxygenation was inferred to have occurred suddenly based on f_{O_2} recorded by Hadean zircons (Li and Lee 2004; Trail et al. 2011). It is currently uncertain whether the scattered Hadean zircon data might refer to either local evidence of an already oxidized shallow mantle or the input of reduced chondritic material delivered during the Late Heavy Bombardment (about 4.1–3.8 Ga). The low redox state of Archean magmas implies low $Fe^{3+}/\sum Fe$ of the mantle source they were equilibrated with. Oxidized mantle sources are likely to turn elemental carbon and methane into the CO_2 and H_2O that are responsible for the formation of low degree partial melts (see Equations 1–3). For reduced mantle rocks, such as those in the hot Paleoarchaean, volatiles were likely stored in their elemental state or dissolved in metallic phases. If any volcanic outgassing occurred, this must have been characterized by a redox state 2–3 orders of magnitude lower than present.

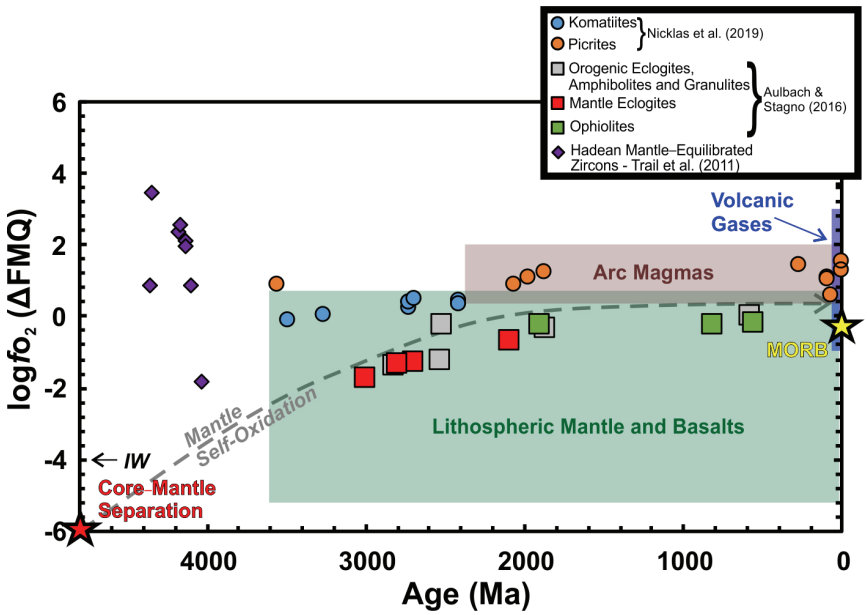

FIGURE 5 Temporal variation of $\log f_{O_2}$ (relative to changes in the fayalite–magnetite–quartz, FMQ, buffer) from the Earth's formation to the present-day; the iron–wüstite, IW, buffer is indicated at –4. The f_{O_2} values were estimated from the chemical reconstruction of V/Sc ratios of Archean metabasalts (Aulbach and Stagno 2016), V partitioning between olivine and melt for picritic and komatiitic rocks of Archaean age (Nicklas et al. 2019), and Ce concentration in Hadean zircons (Trail et al. 2011). The f_{O_2} of present mid ocean ridge basalt (MORB) is after Berry et al. (2018). The dashed line is the idealized trend if self-oxidation occurred during magma ocean crystallization gradually through time due to secular cooling. The estimated uncertainties in the calculated f_{O_2} values are generally within ±0.5 log units. The f_{O_2} interval recorded by natural rocks and gases is shown, for comparison, by the shaded areas.

THE REDOX STATE OF THE SUBDUCTED SLAB AND VOLATILE SPECIATION

The subducted slab, as the main carrier of oxidized fluids such as water and CO_2, is generally believed to be responsible for oxygenation of the mantle. The slab's diverse mineral assemblages, developed from the many metamorphic reactions at the different depth and temperature regimes experienced by the downgoing slab, have resulted in gross changes in the mantle from it being oxidized (FMQ+2) to being reduced f_{O_2} (FMQ–1) (Frost and McCammon 2008). This, in turn, influences the transport and oxidation state of the volatile elements at depth, such as H, C, and S, which are the dominant gases released from arc volcanoes upon eruption. A key role is played by the subduction of hydrous phases in the subducted lithospheric mantle, such as serpentinites. Subducted serpentinites show f_{O_2} varying between FMQ–2 and FMQ–1 (Deschamps et al. 2013). Observations from natural rocks, such as those exposed in the Cerro del Almirez Massif (Spain) and which are representative of serpentinized oceanic lithosphere, show, however, that the redox state of serpentinites might be more heterogeneous depending on the initial bulk composition. In particular, the presence of either sulfide or Fe–Ni metal alloys is able to buffer the local f_{O_2} at reduced values of –5 log units below FMQ (Debret and Sverjensky 2017), thereby stabilizing H_2 and CH_4 in equilibrium with serpentinites. In the absence of reduced phases, on the other hand, and as prograde metamorphism increases, the buffering capacity diminishes from abyssal serpentinites to chlorite harzburgites as a consequence of decreasing the bulk $Fe^{3+}/\sum Fe$ in the rock from ~70% to ~35% due to antigorite breakdown (at a depth of ~50 km and ~650 °C). As a breakdown product, Fe^{2+}-rich minerals such as olivine and orthopyroxene form along with less Fe^{3+}-rich chlorite plus water according to the reaction shown in Equation (2) (Debret and Sverjensky 2017 and references therein). This, in turn, favors the circulation of oxidized fluids, such as H_2O, and sulfates at f_{O_2} values between –1 and +5 log units below FMQ.

In contrast with the subducted ultramafic, serpentine-bearing portion of the slab, metamorphism of the subducted oceanic crust gives rise to a mineral assemblage containing Fe-bearing eclogitic phases, such as omphacitic clinopyroxene and garnet. Both minerals have a large capacity for incorporating Fe^{3+}. With increasing depth, the silicates could incorporate increasing amounts of Fe^{3+} while simultaneously reducing the volatile species. This form of oxygen sequestration by minerals would cause the reduced portions of the subducted slab to host diamond as the stable form of carbon (cf. FIG. 3) (Stagno 2019). Reduced C–O–H fluids with methane and light hydrocarbons would form at the expense of subducted carbonates at depths of 200–400 km. Recently, the interface between subducted slab and asthenospheric mantle has been described as favorable for the formation of diamonds due to the presence of chemical and f_{O_2} gradients (Thompson et al. 2016). Only when portions of the slab enter the convective mantle, can the Fe^{3+} of silicates be reduced back to Fe^{2+} due to the effect of pressure on the reaction in Equation (1), providing enough oxygen to reconvert C to CO_2 and then lower the melting temperature of the surrounding rocks to produce CO_2- and H_2O-bearing magmas and metasomatic fluids.

In summary, the current redox state of the Earth's interior results from initial differentiation on a global scale, modified subsequently by exchange of materials between the interior and the surface at plate boundaries through time. By experimental simulations and analysis of natural samples, we can derive information on the mantle's redox state at different depths and its temporal evolution. Experimental studies, supported by observations, suggest that the redox boundaries in the Earth's interior are gradual rather than sharp because of mineral–mineral and mineral–fluid chemical interactions. The general trend is that the mantle has become progressively more oxidized through time, although the mantle's oxidation state remains spatially heterogeneous.

ACKNOWLEDGMENTS

VS acknowledges financial support from Sapienza University of Rome through "Bandi di Ateneo 2016–2018". YF acknowledges supports from NASA, NSF, and Carnegie Science. We thank Paolo Sossi and an anonymous reviewer for constructive suggestions.

REFERENCES

Armstrong K, Frost DJ, McCammon CA, Rubie DC, Boffa Ballaran T (2019) Deep magma ocean formation set the oxidation state of Earth's mantle. Science 365: 903-906

Aulbach S, Stagno V (2016) Evidence for a reducing Archean ambient mantle and its effects on the carbon cycle. Geology 44: 751-754

Berry AJ, Stewart GA, O'Neill HS, Mallmann GF, Mosselmans JF (2018) A re-assessment of the oxidation state of iron in MORB glasses. Earth and Planetary Science Letters 483: 114-123

Birner SK, Cottrell E, Warren JM, Kelley KA, Davis FA (2018) Peridotites and basalts reveal broad congruence between two independent records of mantle f_{O_2} despite local redox heterogeneity. Earth and Planetary Science Letters 494: 172-189

Debret B, Sverjensky DA (2017) Highly oxidising fluids generated during serpentinite breakdown in subduction zones. Scientific Reports 7, doi: 10.1038/s41598-017-09626-y

Deschamps F, Godard M, Guillot S, Hattori K (2013) Geochemistry of subduction zone serpentinites: a review. Lithos 178: 96-127

Eguchi J, Dasgupta R (2018) Redox state of the convective mantle from CO_2-trace element systematics of oceanic basalts. Geochemical Perspective Letter 8: 17-21

Frost DJ, McCammon CA (2008) The redox state of the Earth's mantle. Annual Review of Earth and Planetary Sciences 36: 389-420

Hammouda T, Keshav S (2015) Melting in the mantle in the presence of carbon: review of experiments and discussion on the origin of carbonatites. Chemical Geology 418: 171-188

Hartley ME, Shorttle O, Maclennan J, Moussallam Y, Edmonds M (2017) Olivine-hosted melt inclusions as an archive of redox heterogeneity in magmatic systems. Earth and Planetary Science Letters 479: 192-205

Kaminsky F (2012) Mineralogy of the lower mantle: a review of 'super-deep' mineral inclusions in diamond. Earth-Science Reviews 110: 127-147

Kaminsky FV and 6 coauthors (2015) Oxidation potential in the Earth's lower mantle as recorded from ferropericlase inclusions in diamond. Earth and Planetary Science Letters 417: 49-56

Kiseeva ES and 10 coauthors (2018) Oxidized iron in garnets from the mantle transition zone. Nature Geoscience 11: 144-147

Li Z-XA, Lee C-TA (2004) The constancy of upper mantle f_{O_2} through time inferred from V/Sc ratios in basalts. Earth Planetary Science Letters 228: 483-493

Luth RW, Stachel T (2014) The buffering capacity of lithospheric mantle: implications for diamond formation. Contributions to Mineralogy and Petrology 168, doi: 10.1007/s00410-014-1083-6

Lyons TW, Reinhard CT, Planavsky NJ (2014) The rise of oxygen in Earth's early ocean and atmosphere. Nature 506: 307-315

Moussallam Y and 6 coauthors (2016) The impact of degassing on the oxidation state of basaltic magmas: a case study of Kīlauea volcano. Earth and Planetary Science Letters 450: 317-325

Moussallam Y, Oppenheimer C, Scaillet B (2019) On the relationship between oxidation state and temperature of volcanic gas emissions. Earth and Planetary Science Letters 520: 260-267

Nicklas RW and 8 coauthors (2019) Secular mantle oxidation across the Archean-Proterozoic boundary: evidence from V partitioning in komatiites and picrites. Geochimica et Cosmochimica Acta 250: 49-75

Reinhard CT, Planavsky NJ (2020) Biogeochemical controls on the redox evolution of Earth's oceans and atmosphere. Elements 16: 191-196

Righter K, Herd CD, Boujibar A (2020) Redox processes in early Earth accretion and in terrestrial bodies. Elements 16: 161-166

Rohrbach A, Schmidt MW (2011) Redox freezing and melting in the Earth's deep mantle resulting from carbon–iron redox coupling. Nature 472: 209-212

Shirey SB, Richardson SH (2011) Start of the Wilson Cycle at 3 Ga shown by diamonds from subcontinental mantle. Science 333: 434-436

Smith EM and 6 coauthors (2016) Large gem diamonds from metallic liquid in Earth's deep mantle. Science 354: 1403-1405

Sorbadere F and 6 coauthors (2018) The behaviour of ferric iron during partial melting of peridotite. Geochimica et Cosmochimica Acta 239: 235-254

Stagno V (2019) Carbon, carbides, carbonates and carbonatitic melts in the Earth's interior. Journal of the Geological Society 176: 375-387

Stagno V, Ojwang DO, McCammon CA, Frost DJ (2013) The oxidation state of the mantle and the extraction of carbon from Earth's interior. Nature 493: 84-88

Tappe S, Smart K, Torsvik T, Massuyeau M, de Wit M (2018) Geodynamics of kimberlites on a cooling Earth: clues to plate tectonic evolution and deep volatile cycles. Earth and Planetary Science Letters 484: 1-14

Thomson AR, Walter MJ, Kohn SC, Brooker RA (2016) Slab melting as a barrier to deep carbon subduction. Nature 529: 76-79

Trail D, Watson EB, Tailby ND (2011) The oxidation state of Hadean magmas and implications for early Earth's atmosphere. Nature 480: 79-82

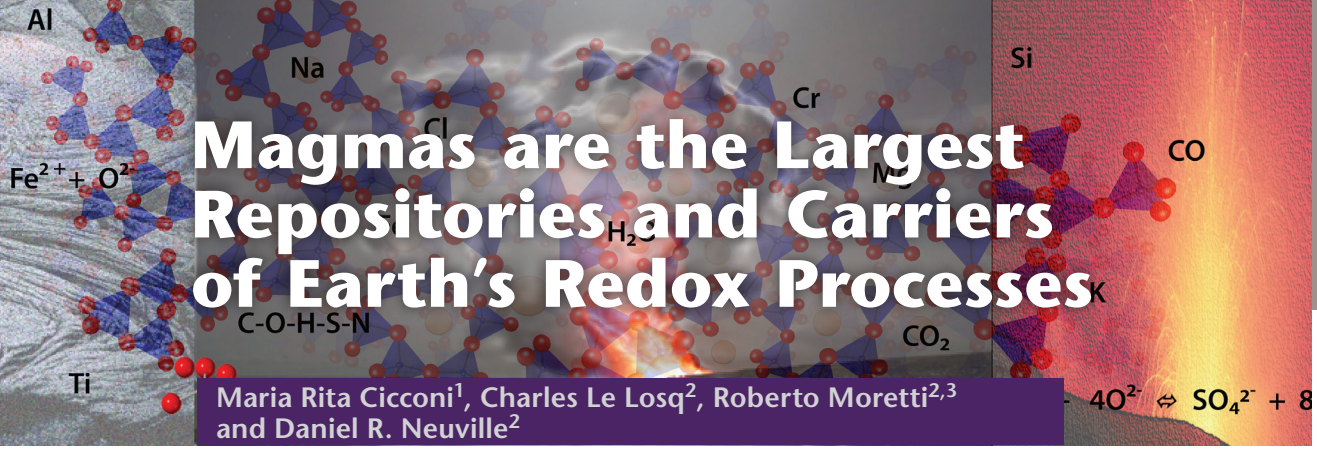

Magmas are the Largest Repositories and Carriers of Earth's Redox Processes

Maria Rita Cicconi[1], Charles Le Losq[2], Roberto Moretti[2,3] and Daniel R. Neuville[2]

1811-5209/20/0016-0173$2.50 DOI: 10.2138/gselements.16.3.173

Magma is the most important chemical transport agent throughout our planet. This paper provides an overview of the interplay between magma redox, major element chemistry, and crystal and volatile content, and of the influence of redox on the factors that drive igneous system dynamics. Given the almost infinite combinations of temperature, pressure, and chemical compositions relevant to igneous petrology, we focus on the concepts and methods that redox geochemistry provides to understand magma formation, ascent, evolution and crystallization. Particular attention is paid to the strong and complex interplay between melt structure and chemistry, and to the influence that redox conditions have on melt properties, crystallization mechanisms and the solubility of volatile components.

KEYWORDS: melt structure, magma properties, iron, crystallization, volatiles

INTRODUCTION

Magma is an intricate, multicomponent, multiphase system, comprising a silicate melt, with or without suspended gas bubbles, and crystals. Each second, approximately 1,200 tons of magma arrives at the surface of the Earth at mid-ocean ridges. This magma builds the oceanic floor and makes up 90% of all volcanism on Earth. Besides shaping Earth's geology and geography, magma is the main carrier, from depth to surface, of all the most important chemical elements, particularly oxygen. Because the chemistry of Earth's rocks and minerals is, at a fundamental level, related to how oxygen atoms complex around metals, understanding how magma transfers and redistributes oxygen through the Earth remains one of the main goals in geochemistry, petrology and mineralogy.

The amount of oxygen available to react with elements in any thermodynamic system can be conveniently described by its fugacity, f_{O_2} (see Cicconi et al. 2020 this issue). Estimating and understanding the oxygen fugacity conditions of a multicomponent silicate liquid at any temperature is complicated by the non-linear dependence of f_{O_2} on bulk composition. Indeed, the physical and thermochemical properties of natural silicate melts depend strongly on the silicate network structure that is, in turn, controlled by melt composition. For this reason, many models of silicate melts tend to (over)simplify the structural role of certain elements, and sometimes even neglect differences between the different cations that build the network structure.

1 Université Erlangen-Nürnberg
Department of Materials Science and Engineering WW3
Martensstraße 5, D-91058 Erlangen, Germany.
E-mail: maria.rita.cicconi@fau.de

2 Université de Paris, Institut de physique du globe de Paris, CNRS
1, Rue Jussieu
F-75005 Paris, France

3 Observatoire Volcanologique et Sismologique De Guadeloupe
Institut de Physique du Globe de Paris
97113 Gourbeyre, Guadeloupe, French West Indies

In the following sections, we will try to rationalize the interplay between melt structure and bulk chemistry by using Fe as the archetype for redox exchanges in melts. Iron is, by far, the most common multivalent transition element on Earth (32%) and is the fourth most abundant element in the Earth's silicate mantle (the average elemental abundance is 6.3%). Because iron is orders of magnitude more abundant than other transition elements, it is intuitive that the proportion of ferric (Fe^{3+}) and ferrous (Fe^{2+}) iron will control (buffer) the overall oxygen fugacity conditions of silicate melts. Ergo, the evaluation of iron redox equilibria and structural environments in melts and mineral assemblages is critical for determining a magma's thermodynamic and transport properties. However, it should be noted that other multivalent elements also play a crucial role in Earth systems in terms of exchanged electrons or oxygens. For instance, sulfur species deserve a special mention because the oxidation of sulfide to sulfate involves 8 electrons, and for any increment of the Fe^{3+}/Fe^{2+} redox ratio, there is an eight-fold increment for sulfur species (S^{6+}/S^{2-}) (see Cicconi et al. 2020 this issue; Moretti and Stefansson 2020 this issue). Despite this large electron transfer, the effectiveness of the sulfide to sulfate ratio as a buffer of the redox potential is limited by the abundance of sulfur in a melt, which is significantly lower than iron in most commonly encountered natural magmas.

COMPOSITION AND STRUCTURE: WHO CONTROLS WHAT?

The effect of melt composition/structure upon properties is a hot topic in the geosciences and in the technological world. Understanding the structural role of cations allows us to predict melt redox conditions based on the physical, thermal, and rheological properties of melts, as well as the capacity of magmas to carry oxygen through the influence of melt composition on redox conditions.

To understand the link between magma structure and bulk composition, we need to revisit a few concepts regarding the structural role of elements in silicate melts. The main cation that builds the silicate network is silicon, which is bonded to four oxygens to form SiO_4 tetrahedral units. A three-dimensional network is formed when each tetrahedron connects to other SiO_4 units via apical oxygens (so-called bridging oxygens, BO). All other cations play one of two structural roles: (i) *network formers*, such as Si^{4+}, Ti^{4+}, P^{5+}, and Al^{3+}, which help to build the network; (ii) *network modifiers,* such as the metal cations Na^+, K^+,

Mg^{2+}, Ca^{2+}, which disrupt the network by breaking inter-tetrahedral bonds to form non-bridging oxygens (NBO) and even non-network and free oxygens (Fincham and Richardson 1954; Mysen and Richet 2005; Le Losq et al. 2019 and references therein). Network modifiers have low cation field strengths (i.e., the ratio of the cation valence to the squared cation–oxygen distance), whereas network formers have high cation field strengths. Unfortunately, this simple picture is too good to be true: metal cations also serve to charge-balance tetrahedral units within an overall charge deficit, such as for AlO_4 where Al^{3+} replaces Si^{4+}. Thus, in aluminosilicate melts, the overall role of metal cations depends on aluminium concentration in the network. From the redox perspective, Fe plays different roles depending on its oxidation state (Mysen and Richet 2005; Cicconi et al. 2015 and references therein): Fe^{2+} acts as a network modifier, whereas Fe^{3+} plays a more complex role that will be discussed later. Given the abundance of iron in melts, the various exchanges between Fe^{3+} and Fe^{2+} can have dramatic effects on melt structure and properties.

Bulk Chemistry, Silicate Melt Structure, Oxygen Transport

The statement that magmas can be considered as oxygen transporters may appear, at first sight, to be rather surprising. The key to this claim lies in the many multivalent elements present in magmas, e.g., Fe, Ti, V, Cr, Eu, and Ce. These elements have different structural roles in silicate melts, and they present distinct oxidation states and coordination numbers, some of which are uncommon even in minerals (e.g., five-fold coordinated $^{[5]}Ni^{2+}$) (Galoisy and Calas 1993). There exists a plethora of redox reactions involving these elements. The equilibrium constant of each redox couple depends on temperature, pressure, bulk chemical composition (*T*–*P*–*X*), and the interplay of these variables in closed systems, all of which also determines the oxygen fugacity of the system. Conversely, in open systems, what controls f_{O_2} arises through the exchange of mobile components between the magmatic system and the surrounding environment. For instance, the proportions of ferrous and ferric iron can be described by equilibria expressed either as oxide components (Equation 1a) or as ionic species (Equation 1b)

$$2FeO + 1/2\ O_2 \leftrightarrow Fe_2O_3 \quad (1a)$$

$$4Fe^{2+} + O_2 \leftrightarrow 4Fe^{3+} + 2O^{2-} \quad (1b)$$

A lot of experimental work has been carried out to rationalise the impact of temperature, pressure, composition and f_{O_2} on the equilibrium oxidation state of Fe in magmas, and several simple, empirical models have been proposed, (e.g., Kress and Carmichael 1991; Borisov et al. 2018). But complications arise from the complex relationships between *real* ionic species (e.g., ionic complexes of iron, which in turn depend on how they are measured) and their components (the corresponding oxides). This distinction between ionic species and oxide components is critical in understanding redox behaviour. Of particular importance is how the activity of oxide components varies with the distribution of the three kinds of oxygens described above (BO, NBO and free), which in turn depends on the melt structure at the *P*–*T*–*X* conditions of interest. Fortunately, geoscientists have a set of concepts that help them to rationalize the links between melt structure, chemical composition and redox species. At the scale of short-range ordering (e.g., coordination polyhedra), redox processes reflect how the charge is distributed (or transferred) between the central cation and the surrounding oxygens (the ligand field). In other words, redox exchanges are related to the mean electronic polarization state of the oxygen ligand, which, in turn, is determined by the proportions of the three kinds of oxygen in the melt (BO, NBO and free). Consequently, atomistic properties (electronegativity, electronic polarizability, optical basicity) of complexing cations can be related to the equilibrium disproportionation of the BO, NBO and free oxygens that make up the melt's structural framework. This also strongly relates to the activity of the free/non-network oxygens (aO^{2-}). The latter represents the basicity of the melt and measures the polarization state of the ligand. It should be seen as analogous to pH, and, as such, is the key to solving the compositional dependence of redox equilibria in melt species (e.g., Duffy 1993; Ottonello et al. 2001; Moretti 2005; Dimitrov and Komatsu 2010 and references therein). Thus, in a similar fashion to aqueous solutions, the effect of silicate melt composition results in the intimate connection between redox exchanges and the melt's acid–base character, as reflected in its structure.

Most multivalent element equilibria follow the general rule of redox controlled by melt basicity, with the oxidation–reduction equilibrium shifting toward more oxidized species with increasing basicity of the melt (i.e., by increasing the amount of modifier oxides). Network modifier cations form ionic bonds with surrounding oxygen ions, whereas network formers form covalent bonds. Thus, glass covalence is inversely correlated to basicity. Because greater network-modifying ion activity results in an increase in melt depolymerization, this ion activity parameter can broadly be related to the ratio of non-bridging oxygens (NBO) per tetrahedral cations (T) in glasses and melts: NBO/T.

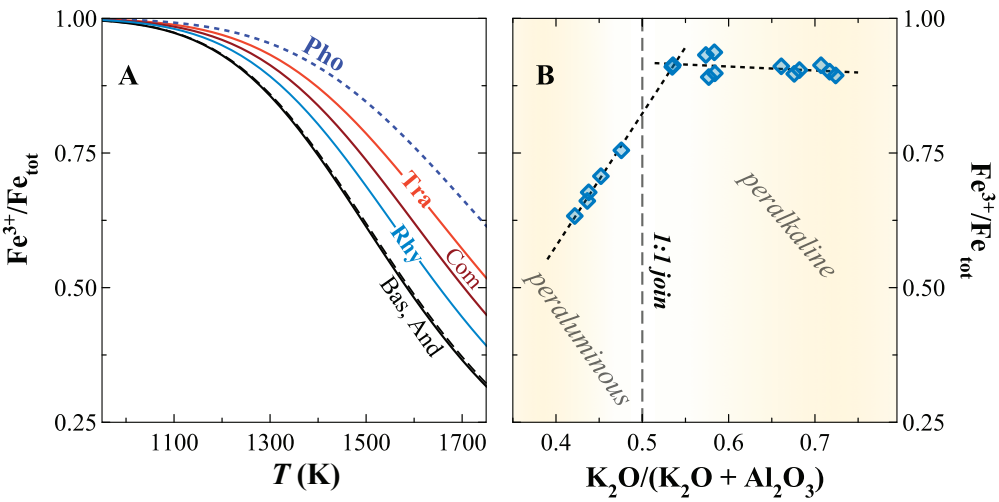

Figure 1 (**A**) Evolution of the Fe^{3+}/Fe_{tot} ratio with temperature for different melt compositions in air. Abbreviations: Rhy = rhyolite; Tra = trachyte; Com = comendite; And = andesite; Bas = basalt. Compositions with higher alkali contents (Pho, Tra, Com) are more oxidized than alkali-poor ones (Bas, And, Rhy), which follows the basicity of the melt. Data estimated from the algorithm of Kress and Carmichael (1991). (**B**) The Fe^{3+}/Fe_{tot} redox fraction versus the $K_2O/(K_2O + Al_2O_3)$ molar ratio. At constant temperature, depending on the alkali/Al ratio, the Fe redox ratio shows contrasting behaviour. Data from Dickenson and Hess (1982).

Armed with this set of conceptual tools, we turn again to iron. The Fe^{3+}/Fe^{2+} ratio in a rock provides information about the amount of oxygen available in the system and its changes upon magma migration, for example to a different *P* or *T*. Iron exhibits variable oxidation states and coordination geometries, and experimental studies have shown that several Fe species are stable in silicate melts, including $^{[4]}Fe^{3+}$, $^{[5]}Fe^{3+}$, $^{[5]}Fe^{2+}$, and also 6-fold coordinated ferrous and ferric ions $^{[6]}Fe^{2+}$, $^{[6]}Fe^{3+}$ (e.g., Dingwell and Virgo 1987; Wilke et al. 2004; Cicconi et al. 2015 and references therein). Thus, while Fe^{2+} is predominantly considered as a network modifier, Fe^{3+} displays amphoteric behaviour within the silicate network. Indeed, depending on temperature, bulk chemistry, the identity of the predominant network modifier cations, and Al concentration and coordination, Fe^{3+} can act both as a network former and as a network modifier. Generally speaking, oxidized species, such as Fe^{3+}, are stabilized by larger proportions of modifier cations, which increases melt basicity. This trend can be better visualized when calculating the Fe redox ratio using the Kress and Carmichael (1991) algorithm (Fig. 1A). When a magma composition changes from phonolite to rhyolite to andesite/basalt, the alkali content decreases strongly. Alkalis have basicity values much higher than network-forming cations, so they contribute strongly to increasing the overall basicity of the melt, and thereby influence the equilibrium constant of Equation (1) that determines the Fe redox ratio. In addition to alkali content, the Fe redox ratio also depends on the alkali/Al_2O_3 molar ratio. In natural and synthetic peralkaline systems (alkalis > Al), increasing the molar alkali content induces a stabilization of Fe^{2+}, whereas in metaluminous systems (alkalis = Al) or peraluminous systems (alkalis < Al), increasing the molar alkali content drives a strong stabilization of Fe^{3+} (Dickenson and Hess 1982) (Fig. 1B). At constant alkali/Al (or silica) ratios, the cation field strength (CFS) will influence the Fe^{3+}/Fe^{2+} ratio, with higher Fe^{3+}/Fe^{2+} ratios for K than for Li (CFS K < CFS Na < CFS Li). This can be explained by considering oxygen activities around cations (larger cations will induce larger negative charge on the oxygen ion; i.e., higher electronic polarizability), and the ability of K^+ ions to be more efficient in stabilizing Fe^{3+} in tetrahedral sites (Cicconi et al. 2015 and references therein).

Assessment of the average Fe valence and coordination environment is very important in understanding the influence of Fe on magma properties. The technique of X-ray absorption spectroscopy (XAS) is an element-selective tool used to study Fe speciation in melts and glasses. The spectra acquired on divalent and trivalent iron-bearing minerals show clear differences in absorbed energy positions, as well as in spectra shape, with the spectrum related to oxidized species shifted toward higher energies (e.g., Wilke et al. 2004 and references therein). The detailed study of some features (e.g., Fe K-edge pre-edge peak) can provide further insights into Fe speciation (and local symmetry): for example, many experimental data show that Fe^{2+} ions have a higher average coordination number. This can be appreciated in studies of the Fe K-edge pre-edge peak in minerals and glasses, when the pre-edge centroid energy is plotted against its integrated intensity. Upon iron reduction, the pre-edge centroid energy shifts toward lower values, and the overall intensity of the pre-edge decreases (Fig. 2). Because the area under the pre-edge peak is related to the structural environment surrounding the Fe ions (their coordination and symmetry), this peak provides remarkable insights into the variations in iron's geochemical role in melts and glasses (Wilke et al. 2004 and references therein).

MAGMA REDOX AND MOBILITY: VISCOSITY AND PARTIAL MOLAR VOLUME EFFECTS

The significant effect of redox state on a melt's physical properties has long been demonstrated. The first study to clarify the effects of iron valence state on viscous flow behaviour in a multicomponent system involved Fe-rich (~19 mol% FeO) lunar material analogues (Cukierman and Uhlmann 1974). Several experimental studies followed, confirming the effect of the Fe redox ratio on viscous flow and the effect of bulk composition and iron content on the redox ratio itself. These studies attempted to explain the observed correlation between Fe redox state and a magma's physical properties by taking into account structural changes (in terms of oxygen coordination), suggesting that while Fe^{2+}, similar to alkaline earth cations, acts as a network modifier, Fe^{3+} partially behaves as a structural analogue of Al^{3+} (Fig. 2). Dingwell and Virgo (1987) demonstrated the correlation between viscosity, Fe redox state, Fe^{3+} coordination environment(s), and the degree of polymerization of the melt (NBO/T) (Fig. 3). Their data suggest that the f_{O_2} effect on viscosity is related to the different oxygen coordination of the Fe species and that there is an intermediate Fe^{3+}/Fe_{tot} ratio where Fe^{3+} species are stabilized as complexes with 4-fold and 6-fold coordination (Dingwell and Virgo 1987 and references therein).

In addition to the influence on melt viscosity, the occurrence of ferrous and ferric species with different coordinations (which have different structural roles) has consequences for melt density and compressibility. The dependence of partial molar volume of the two Fe oxides on bulk composition was extensively debated in the 1980s (e.g., Mo et al. 1982; Lange and Carmichael 1987 and references therein) in order to calculate the dependence of the Fe^{3+}/Fe_{tot} redox fraction on pressure. To calculate the density and compressibility of magmatic liquids at one bar, there are well-known

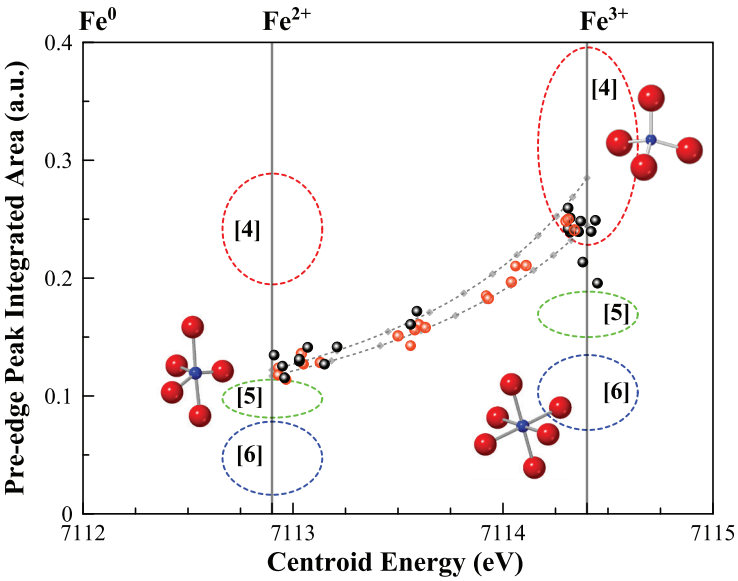

Figure 2 Iron pre-edge peak centroid energy (in electron volts, eV) plotted against its integrated area (in arbitrary units, a.u.). This variogram is based on the study of the Fe pre-edge peak of several minerals (modified after Giuli et al. 2012 and references therein). Example 4-, 5- and 6-coordinated Fe species are shown. The energy of metallic Fe is 7,112 eV, and the dashed ovals represent different Fe coordination environments. Red and black circles are data for glasses [from Wilke et al. (2004) and Cicconi et al. (2015)] (± 0.05 eV). Grey lines and diamond symbols are mixing lines between ferrous and ferric end-members. Iron reduction is accompanied by an increase in its average oxygen coordination.

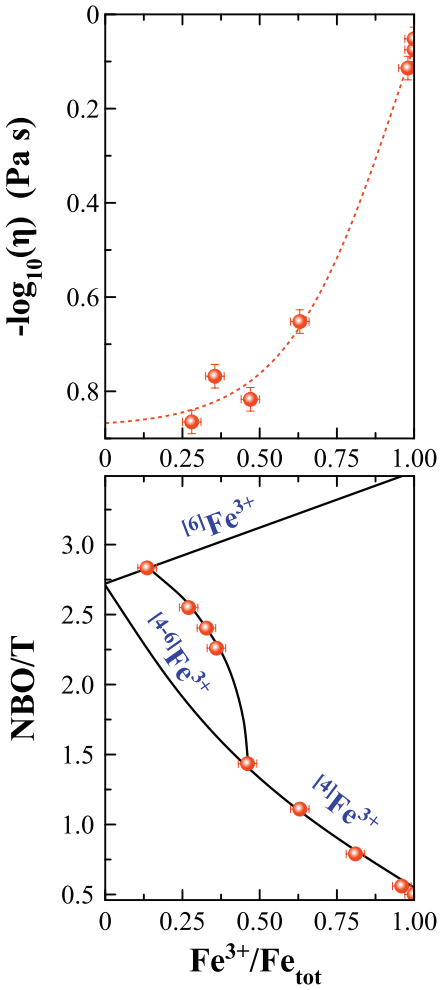

Figure 3 (**Upper graph**) Non-linear relationship between viscosity (η) and Fe redox fraction (T = 1,200 °C). There is an increase in melt viscosity with increasing Fe^{3+}/Fe_{tot} redox fractions, particularly important at Fe^{3+}/Fe_{tot} values higher than 0.5. This is related to the transformation of ferrous network-modifier species to ferric ones that behave as network formers ($^{[4]}Fe^{3+}$). (**Lower graph**) Non-linear relationship between Fe^{3+} coordination with NBO/T in the melt and Fe redox. At low Fe^{3+}/Fe_{tot} fractions, ferric ions stabilize with higher coordination(s), causing only small variations in the NBO/T parameter and melt viscosity. Numbers in square brackets beside Fe symbols are the coordination numbers. Data from Dingwell and Virgo (1987).

models e.g., Lange and Carmichael (1987) and Kress and Carmichael (1991). However, to derive the partial molar volume of FeO, these models rely on data from simplified systems that do not take into account the complexity of the Fe^{2+} structural environment. Early studies (Mo et al. 1982) and more recent studies (Guo et al. 2013) indicated that Fe^{2+} species have partial molar volume values ranging between 12 and 17 cm^3/mol, with a strong composition dependence that suggests changes in Fe^{2+} coordination with magma chemistry. The partial molar volume of Fe_2O_3 ranges between 40.7 ± 0.8 and 42.1 ± 0.3 cm^3/mol, at 1,400 °C (Mysen and Richet 2005; Liu and Lange 2006 and references therein). From high-temperature experiments in peralkaline silicate liquids, Liu and Lange (2006) reported a temperature- and composition-independent partial molar volume of 41.5 ± 0.3 cm^3/mol.

Evidently, the redox of aluminosilicate melts affects melt viscosity and density, which represent their resistance to, and potential for, movement in the Earth. However, despite variations of the aluminosilicate melt properties being important for geological processes, an even more important phenomenon is influenced by redox processes within the melt. Crystallization.

CRYSTALLIZATION OF SILICATE MELTS

It is mandatory to consider the appropriate f_{O_2} conditions when determining magma phase equilibria relationships and chemistry. Different f_{O_2} conditions will control the Fe^{3+}/Fe_{tot} redox fraction in the melt, the composition of the Fe-bearing phases nucleating and crystallizing, and the composition of the residual melt (which will typically be enriched in silica and depleted in iron). Redox conditions of the system are also responsible for shifts of phase equilibria: they can influence the differentiation history and magma rheological evolution and also the crystallization of the Fe-bearing phases that will control the oxygen fugacity conditions of the melt (see Cicconi et al. 2020 this issue). Hill and Roeder (1974) studied basaltic compositions and showed that, depending on the imposed f_{O_2}, the crystallization of chromite is hampered in favour of clinopyroxene phases at higher temperatures, and in favour of Ti-magnetite + pyroxene + plagioclase at lower temperatures. Equilibrium crystallization experiments have been performed to constrain phase relations and the stability of Fe–Ti oxides, for example by Toplis and Carroll (1995) on synthetic anhydrous Fe-rich basalts in a range of f_{O_2} covering 4 log units (Fig. 4A). Their data show that the appearance temperature of magnetite–ulvöspinel (Fe_3O_4–Fe_2TiO_4) and ilmenite–hematite ($FeTiO_3$–Fe_2O_3) solid solutions depend strongly on the f_{O_2} conditions of the magma. Moreover, depending on redox conditions, the onset of clinopyroxene crystallization varies between ~1,385 K and 1,413 K. When water was added, the differentiation history of hydrous ferrobasalt was significantly modified: there was i) a strong decrease of the liquidus temperatures of the mineral phases, ii) changes in the crystallization sequence, iii) variations in Ca/Fe and Mg/Fe partitioning between clinopyroxene and melts, and in the forsterite content in olivine (Botcharnikov et al. 2008).

In addition to phase stability, the prevailing f_{O_2} conditions of a magma will influence the abundance, shape and size of the crystals, which in turn will affect the overall rheology of the magma. Figure 4B shows that crystallization kinetics depend on f_{O_2}, with higher crystal nucleation/growth rates for oxidized than for reduced melts. To explore the effect of f_{O_2} on lava rheology, dynamic undercooling experiments, and high-temperature viscosity measurements of a trachybasalt from Etna volcano (Italy), were performed in air and under reducing conditions (close to the FMQ buffer) by Kolzengurg (2018). The onset of crystallization was shifted to much lower temperatures under the reducing conditions, whereas oxidized magmas had a lower crystallization tendency. The crystallization of small nano- and microcrystal phases (nanolites or microlites) may be particularly effective in influencing magma viscosity. In recent years, the influence of particle size and shape on the rheology of magmas has been extensively investigated. Liebske et al. (2003) reported that although the Fe^{3+}/Fe_{tot} redox fractions largely affected the viscosity of andesitic melts, the occurrence of Fe crystals exercised a decisive influence over magma rheology. Recently, it has been proposed that the crystallization of sub-micron Fe crystals (nanolites), and the consequent relative enrichment in silica and depletion in iron of the residual melt, could be an important mechanism to drive changes in magma rheology and volatile exsolution. This then can profoundly affect the dynamics of volcanic eruptions (Di Genova et al. 2017).

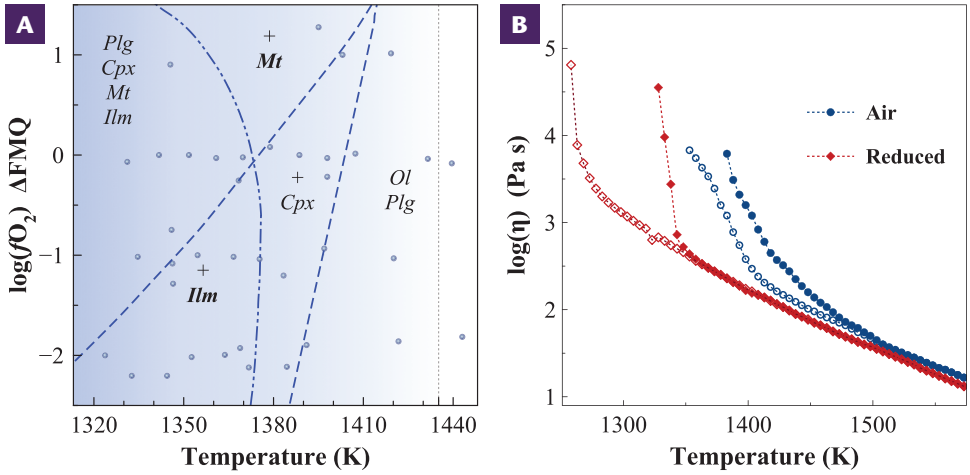

Figure 4 **(A)** Phase equilibria for anhydrous Fe-rich basalt as a function of temperature and redox conditions. The range of f_{O_2} covers 4 log units, from >2 log units below to 1.5 log units above the fayalite–magnetite–quartz (FMQ) buffer. Lines outline the stability fields of mineral phases. Abbreviations: Ol = olivine; Plg = plagioclase; Cpx = Ca-rich clinopyroxene; Mt = magnetite–ulvöspinel solid solution; Ilm = ilmenite–hematite solid solution. Plagioclase and liquid phases are always present below the liquidus (vertical solid line ~1,430 K). The appearance of Ilm or Mt strongly depends on the f_{O_2} conditions of the magma. Small circles indicate the experimental data of Toplis and Carroll (1995). **(B)** Evolution of apparent viscosity (Pascal second) of crystallizing trachybasalt melts at varying cooling rates (empty symbols = 3 °C/min; solid symbols = 0.5 °C/min) performed in air (blue) or under reducing (red) conditions. Dynamic undercooling experiments are representative of non-equilibrium conditions typical of the ascent of magmas in conduits. Modified after Kolzenburg et al. (2018).

VOLATILES IN MAGMA AND f_{O_2} CONDITIONS

The amount of volatiles dissolved in melts, their speciation (i.e., the form they take when incorporated in the liquid), and the mechanisms of their exsolution and diffusion are key parameters in driving volcanic eruptions. The most abundant gas species in magmatic systems are H_2O and CO_2, followed by sulfur species (H_2S and SO_2), halogens, nitrogen, and the noble gases. The dissolution/exsolution behaviour of these volatiles is strongly dependent on the stability of the different gaseous molecular species. For example, carbon can be stable as CH_4, CO, CO_2, depending on P–T–X–f_{O_2}. Consequently, there is a link between magma redox and the speciation of the dissolved volatile elements, and a consequent feedback between degassing and magma f_{O_2} (see Moretti and Stefansson 2020 this issue, and references therein).

In addition to C–H–O species, sulfur may also be abundant in magmatic gases. In magmas, dissolved sulfur can be stable both as sulfide and sulfate (Fincham and Richardson 1954), depending on the f_{O_2} conditions. The proportion of the different species greatly affects sulfur solubility (Moretti and Ottonello 2005; Baker and Moretti 2011 and references therein). A rapid change in sulfur oxidation state occurs within about 2.0–2.5 orders of magnitude of the oxygen fugacity as defined by the nickel–nickel oxide (NNO) oxygen buffer (Fig. 5) such that sulfur solubility is governed by two concomitant equilibria:

$$SO_2 + O^{2-}_{(melt)} \leftrightarrow 3/2O_2 + S^{2-}_{(melt)} \quad (2)$$

$$SO_2 + 1/2O_2 + O^{2-}_{(melt)} \leftrightarrow SO_4{}^{2-}_{(melt)} \quad (3)$$

The total amount of sulfur solubilized in a melt is given by the sum of the oxidized (sulfate) and the reduced (sulfide) species (Fig. 5A). When the total amount of dissolved sulfur in the melt (S wt%) is normalized to the fugacity of SO_2 in the gas, the theoretical slopes of 3/2 and 1/2 (*t.s.* in Fig. 5B) are observed for the equilibria in Equations (2) and (3), respectively. Equation (3) dominates at higher f_{O_2} conditions, whereas under progressively reducing conditions, Equation (2) becomes important. The absolute value of f_{O_2} at which one equilibrium predominates over the other (which determines the relative predominance of sulfate or sulfide species) changes by 2 orders of magnitude depending on P, T and magma composition (including dissolved volatile content, particularly H_2O) (see Figure 3 in Moretti and Stefansson 2020 this issue). The compositional dependence reflects the shift in melt structure, and, hence, solvent properties (Moretti and Ottonello 2005; Baker and Moretti 2011 and references therein).

At first glance, it would appear difficult to incorporate the oxide components and their activities into the redox equilibrium reactions for sulfur species in addition to iron species. However, the complexity fades when it becomes clear that redox equilibrium reactions, such as those given in Equations (1) to (3), make use of the *oxygen electrode*: $½O_2 + 2e^- \leftrightarrow O^{2-}$ (see Cicconi et al. 2020 this issue; Moretti

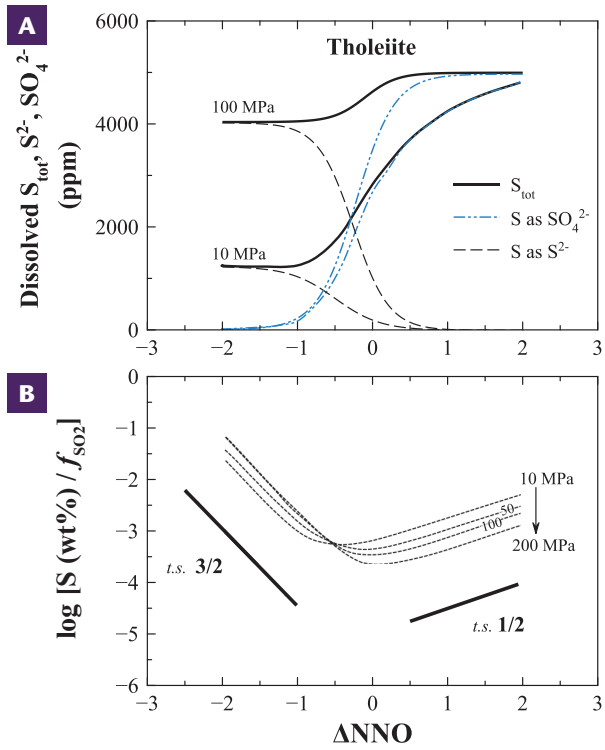

Figure 5 **(A)** The total amount of sulfur solubilized in a melt (here a tholeiitic melt equilibrated with a CO_2–H_2O–SO_2–H_2S gas phase at 1,400 K, between 10 and 100 MPa) is given by the sum of oxidized (sulfate) and reduced (sulfide) species. **(B)** Sulfur solubilized in a tholeiitic melt plotted against logf_{O_2} (expressed as a change in the nickel–nickel oxide buffer, or ΔNNO); note that we cannot appreciate the stoichiometric constraints imposed by Equations (2) and (3). These constraints can be visualised, however, when the total amount of dissolved sulfur in the melt (S wt%) is normalized to the fugacity of SO_2 (f_{SO_2}) in the gas. Abbreviation: *t.s.* = theoretical slope. Data from Moretti's model (see Baker and Moretti 2011 and references therein).

and Stefannson 2020 this issue). This half-reaction is an aspect of redox that is all too often overlooked, yet one that provides the link between redox and acid–base chemistry in melts. It is essentially related to the exchanges that occur between the bridging, non-bridging, and (non-network) free oxygens.

SUMMARY

Magmas are composed of a silicate melt, with or without suspended crystals and gas bubbles. The silicate melt network is built from bonding between anions and cations having different size, valence, coordination environments, bonding strength, and preferred associations. Variations in the relative proportions of those ionic species, and the activity of the different kinds of oxygen that bond to the redox species, strongly influences melt properties and controls magma crystallization behaviour and differentiation. This ionic composition when allied to volatile solubilities plays a key role in magma transport and exercises a direct influence on the dynamics of volcanic eruptions.

In aluminosilicate melts, the *oxygen electrode* links f_{O_2} directly to the acid–base character of the melt, a connection expressed via the aO^{2-}. This activity measure has the same role as pH in aqueous solutions and provides a robust way to relate redox and acid–base chemistry in melts, and, in turn, to predict physico-chemical properties by including an all-important compositional parameter into redox reactions that involve silicate melts.

REFERENCES

Baker DR, Moretti R (2011) Modeling the solubility of sulfur in magmas: a 50-year old geochemical challenge. Reviews in Mineralogy and Geochemistry 73: 167-213

Borisov A, Behrens H, Holtz F (2018) Ferric/ferrous ratio in silicate melts: a new model for 1 atm data with special emphasis on the effects of melt composition. Contributions to Mineralogy and Petrology 173, doi: 10.1007/s00410-018-1524-8

Botcharnikov RE, Almeev RR, Koepke J, Holtz F (2008) Phase relations and liquid lines of descent in hydrous ferrobasalt—implications for the Skaergaard Intrusion and Columbia River flood basalts. Journal of Petrology 49: 1687-1727

Cicconi MR, Giuli G, Ertel-Ingrisch W, Paris E, Dingwell DB (2015) The effect of the [Na/(Na+K)] ratio on Fe speciation in phonolitic glasses. American Mineralogist 100: 1610-1619

Cicconi MR, Moretti R, Neuville DR (2020) Earth's electrodes. Elements 16: 173-178

Cukierman M, Uhlmann DR (1974) Effects of iron oxidation state on viscosity, lunar composition 15555. Journal of Geophysical Research 79: 1594-1598

Di Genova D and 6 coauthors (2017) A compositional tipping point governing the mobilization and eruption style of rhyolitic magma. Nature 552: 235-238

Dickenson MP, Hess PC (1982) Redox equilibria and the structural role of iron in alumino-silicate melts. Contributions to Mineralogy and Petrology 78: 352-357

Dimitrov V, Komatsu T (2010) An interpretation of optical properties of oxides and oxide glasses in terms of the electronic ion polarizability and average single bond strength. Journal of the University of Chemical Technology and Metallurgy 45: 219-250

Dingwell DB, Virgo D (1987) The effect of oxidation state on the viscosity of melts in the system Na_2O-FeO-Fe_2O_3-SiO_2. Geochimica et Cosmochimica Acta 51: 195-205

Duffy JA (1993) A review of optical basicity and its applications to oxidic systems. Geochimica et Cosmochimica Acta 57: 3961-3970

Fincham CJB, Richardson FD (1954) The behaviour of sulfur in silicate and aluminate melts. Proceedings of the Royal Society of London Series A: Mathematical, Physical and Engineering Sciences 223: 40-62

Galoisy L, Calas G (1993) Structural environment of nickel in silicate glass/melt systems: Part 1. Spectroscopic determination of coordination states. Geochimica et Cosmochimica Acta 57: 3613-3626

Giuli G and 6 coauthors (2012) Effect of alkalis on the Fe oxidation state and local environment in peralkaline rhyolitic glasses. American Mineralogist 97: 468-475

Guo X, Lange RA, Ai Y (2013) The density and compressibility of CaO–FeO–SiO_2 liquids at one bar: evidence for four-coordinated Fe^{2+} in the $CaFeO_2$ component. Geochimica et Cosmochimica Acta 120: 206-219

Hill R, Roeder P (1974) The crystallization of spinel from basaltic liquid as a function of oxygen fugacity. Journal of Geology 82: 709-729

Kolzenburg S, Di Genova D, Giordano D, Hess KU, Dingwell DB (2018) The effect of oxygen fugacity on the rheological evolution of crystallizing basaltic melts. Earth and Planetary Science Letters 487: 21-32

Kress VC, Carmichael ISE (1991) The compressibility of silicate liquids containing Fe_2O_3 and the effect of composition, temperature, oxygen fugacity and pressure on their redox states. Contributions to Mineralogy and Petrology 108: 82-92

Lange RA, Carmichael ISE (1987) Densities of Na_2O-K_2O-CaO-MgO-FeO-Fe_2O_3-Al_2O_3-TiO_2-SiO_2 liquids: new measurements and derived partial molar properties. Geochimica et Cosmochimica Acta 51: 2931-2946

Le Losq C, Cicconi MR, Greaves GN, Neuville DR (2019) Silicate glasses. In: Musgraves JD, Hu J, CAlvez L (eds) Springer Handbook of Glass. Springer, Cham, pp 441-503

Liebske C, Behrens H, Holtz F, Lange RA (2003) The influence of pressure and composition on the viscosity of andesitic melts. Geochimica et Cosmochimica Acta 67: 473-485

Liu Q, Lange RA (2006) The partial molar volume of Fe_2O_3 in alkali silicate melts: evidence for an average Fe^{3+} coordination number near five. American Mineralogist 91: 385-393

Mo X, Carmichael ISE, Rivers M, Stebbins J (1982) The partial molar volume of Fe_2O_3 in multicomponent silicate liquids and the pressure dependence of oxygen fugacity in magmas. Mineralogical Magazine 45: 237-245

Moretti R (2005) Polymerisation, basicity, oxidation state and their role in ionic modelling of silicate melts. Annals of Geophysics 48: 583-608

Moretti R, Ottonello G (2005) Solubility and speciation of sulfur in silicate melts: the conjugated Toop-Samis-Flood-Grjotheim (CTSFG) model. Geochimica et Cosmochimica Acta 69: 801-823

Moretti R, Stefansson A (2020) Volcanic and geothermal redox engines. Elements 16: 179-184

Mysen BO, Richet P (2005) Silicate Glasses and Melts: Properties and Structure. 1st edition. Elsevier, 560 pp

Ottonello G, Moretti R, Marini L, Vetuschi Zuccolini M (2001) Oxidation state of iron in silicate glasses and melts: a thermochemical model. Chemical Geology 174: 157-179

Toplis MJ, Carroll MR (1995) An experimental study of the influence of oxygen fugacity on Fe–Ti oxide stability, phase relations, and mineral–melt equilibria in ferro-basaltic systems. Journal of Petrology 36: 1137-1170

Wilke M, Partzsch GM, Bernhardt R, Lattard D (2004) Determination of the iron oxidation state in basaltic glasses using XANES at the K-edge. Chemical Geology 220: 143-161

Volcanic and Geothermal Redox Engines

Roberto Moretti[1,2] and Andri Stefánsson[3]

1811-5209/20/0016-0179$2.50 DOI: 10.2138/gselements.16.3.179

Direct sampling of fumaroles at La Soufrière de Guadeloupe (French West Indies) andesitic volcano. The collection of major and minor gaseous species provides the full chemical information to calculate pressure, temperature and redox conditions of the hydrothermal reservoir.

The redox (reduction–oxidation) potential is an essential variable that controls the chemical reactions of fluids in magmatic and associated geothermal systems. However, the evolution of the redox potential is difficult to trace from a magma's source at depth to the surface. The key is knowing that electron transfer is the twin face of the acid–base exchanges that drive charge transfer in the many reactions that occur in multiphase and chemically complex systems. The deduced redox reactivity can reveal many features about the evolution of a system's composition and the external factors that control it. As such, redox potential analysis is an important geochemical tool by which to monitor volcanoes and to explore geothermal systems.

KEYWORDS: oxygen fugacity, degassing, melt and magma, geothermal system

INTRODUCTION

Volcanic systems possess extremes in terms of thermal and physicochemical shifts: they evolve from deep regions of magma storage up to near surface eruptions, at which point associated shallow geothermal systems often develop (FIG. 1). Over the range of temperatures for geothermal and magmatic systems (~100 °C to ~1,200 °C), typical reactions that fix oxygen fugacity can vary over tens of orders of magnitude (FIG. 2A). Relative to a particular equilibrium mineral assemblage (e.g., fayalite–magnetite–quartz, FMQ) (see Cicconi et al. 2020 this issue), the ensemble of observed terrestrial magmatic redox states ranges over ~6 orders of magnitude (e.g., Behrens and Gaillard 2006), and extends to ~10 orders if we consider geothermal systems (FIG. 1B). Even more reducing conditions, down to ~FMQ–2.5 can be inferred by extrapolating the relative redox state ($\log f_{O_2}$) field of volcanic gases ($T > 500$ °C) to the temperature range of Archaean komatiite magmas (FIG. 2B) (see Moussallam et al. 2019), suggesting that a change in the buffering capacity of the early deep Earth could have contributed to the subsequent change in the f_{O_2} of volcanic gases, leading to a rise in atmospheric O_2.

In open-conduit volcanic settings characteristic of 'basaltic' (sensu lato) magmatism, redox is controlled by both iron- and sulfur-components, with the silicate melt possibly representing a continuous medium from depth to surface. However, compositional changes due to crystallization, as well as degassing, can significantly modify the redox state *en route* (FIG. 3), given the fundamental role of compositional variables in controlling redox couples and f_{O_2}. Conversely, at 'andesitic' (sensu lato) volcanoes during both quiescent and pre-eruptive unrest, closed-conduit conditions help to stabilize magma-induced thermal, baric and chemical anomalies in the form of homogenizing the convective geothermal systems that act to disperse perturbations in pressure and density. [Geothermal systems related to mid-oceanic ridge magma chambers will not be discussed here. The interested reader is referred to Petersen et. al. (2018).]

In both basaltic and andesitic cases, non-eruptive activity is characterised by passive degassing, a process that carries direct information about the chemical variations of the magma source, including its redox state. At open-conduit and generally basaltic volcanoes, redox processes are determined by continuous chemical exchanges that occur in the multiphase, melt-rich magma (FIG. 1A). At closed-conduit and generally andesitic volcanoes, we observe a strong physico-chemical change toward low-temperature and low-pressure environments that are characterized by brines (or hypersaline liquids) and hot water rather than melts (FIG. 1C) (see also Giggenbach 1987, 1996). In both cases, it is the higher relative mobility and volume ratio of the fugitive exsolved fluid phase compared to the relatively immobile melt and rock matrix that dominates ongoing exchanges, particularly the redox state of the environments where gases evolve. These factors can be recorded by taking samples of surface emissions, such as plumes, fumaroles and solfataras.

Geothermal systems are complicated by the strong role played by the advective and convective transport of heat and mass within permeable and fractured reservoirs. Unless full equilibrium conditions are reached (rare for natural open systems), the resulting redox state will be the product of the competition between the rock's mineral assemblage and the pressure, temperature and fluid composition, these latter being determined by the arrhythmic injection of deep, hot and acid magmatic gases. The large spectrum of redox conditions results from the superposition of these factors and the chemical state of the entire fluid–rock system (FIGS. 1B, C and FIG. 4) (Giggenbach 1987, 1996; Stefánsson 2017).

1 Université de Paris, Institut de Physique du Globe de Pairs
CNRS UMR 7154
F-75238 Paris, France
E-mail: moretti@ipgp.fr

2 Observatoire Volcanologique et Sismologique de Guadeloupe
Institutde Physique de Globe de Paris
Gourbeyre, France

3 Institute of Earth Sciences, University of Iceland
Reykjavík, Iceland
E-mail: as@hi.is

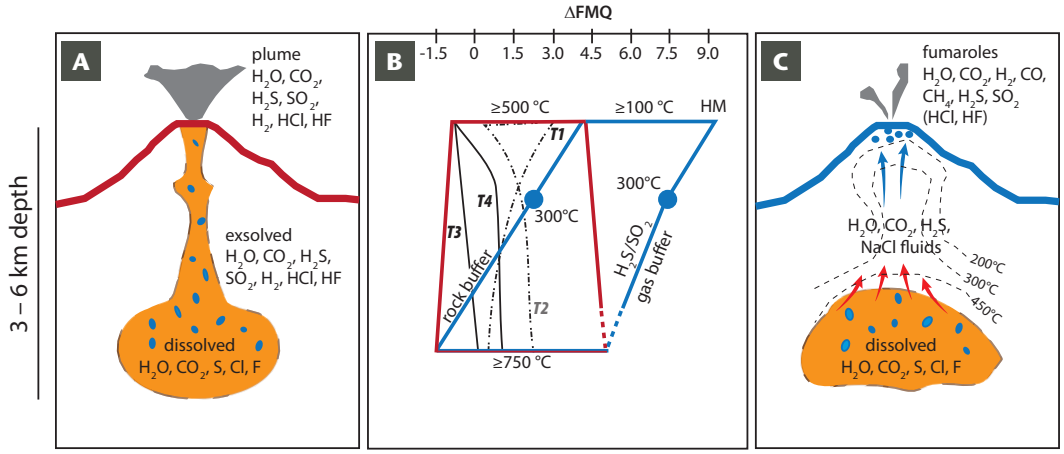

FIGURE 1 (**A**) Ideal profile for an open-conduit volcano. The depth range applies to FIGURES 1B and 1C also and was arbitrarily set at 3–6 km to enhance the redox overlaps and departures in 1B and to better compare the systems 1A and 1C. The open-conduit volcano can be one of two types: (a) basaltic, with less viscous magma being characterized by decoupled transport of the gas with respect to the melt; (b) andesitic/explosive, with viscous magma carrying its gas phase. (**B**) Relative oxygen fugacity variations (in terms of changes in the fayalite–magnetite–quartz buffer, ΔFMQ) for magmatic and geothermal systems. Relative excursions in deeper magma bodies are nearly the same for both basaltic and andesitic models (–1.5 ≤ ΔFMQ ≤ 5) (Behrens and Gaillard 2006). The upper range for a basaltic volcano comes from the volcanic gas compilation in FIGURE 2B, whereas for the andesitic volcano it embraces high- and low-*T* fumaroles from geothermal systems developed from either immature magmatic-geothermal systems or mature geothermal ones (see FIG. 4 and text). The high oxidation limits are provided by the hematite–magnetite (HM) and H_2S/SO_2 buffers at 1 bar, whereas the low-oxidation limits are fixed by the FeO–$FeO_{1.5}$ 'rock' buffer at 1 bar (FIG. 2A). The isothermal on-axis trends labelled T1, T2, T3, and T4 (T1 and T2: 825 °C; T3 and T4: 1,150 °C) show typical patterns of redox evolution modelled in the literature for silicic (T1, T2) and basaltic (T3, T4) systems. (**C**) Ideal profile of a closed-conduit volcano for which isotherms are drawn to better appreciate the zoning of a developing geothermal system.

It is not straightforward to say whether magmatic systems are more oxidized than geothermal ones. In terms of redox potential, evolved magmatic and post-magmatic environments show higher f_{O_2} values than typical geothermal ones and are, thus, more oxidized (FIG. 4). However, we are here comparing chemically and thermally different environments. When using the same reference buffer (e.g., FMQ) to embody temperature-induced variations, geothermal systems show relative f_{O_2} values that are generally higher than magmatic systems (FIG. 1B). Such comparisons between different systems do not account for the important role of compositional change during cooling and that result from chemical interactions with the surroundings. Both these compositional factors generate a series of progressive and irreversible redox exchanges through a chain of intermediate equilibrium steps.

REDOX, MAGMATIC DIFFERENTIATION AND DEGASSING

Volcanic and geothermal environments are open, multiphase (solid–liquid–gas) systems with species abundances and redox reactions and conditions that are controlled by sources and processes that may not be at equilibrium. Nonetheless, f_{O_2} is often assumed to be controlled by a given redox buffer at equilibrium (e.g., FIG. 2A), but even then, it is difficult and unnecessary to ask, "what controls what?". Does differentiation by crystallization and/or degassing dictate redox evolution, or is the oxidation state fixed by factors external to the system? This dichotomy is a perennial source of confusion in igneous petrology. The question of what controls f_{O_2} is relevant in laboratory experiments, but in the polybaric and continuously evolving volcanic environment the "efficiency" of available geochemical buffers to reach equilibrium depends on the abundance and mobility of given elements and their speciation and occurrence over two (and sometimes more) oxidation states. It follows that in a magma the predominant redox species that control electron transfer involve major or, in any case, abundant elements and their redox couples, such as Fe^{II} and Fe^{III} or S^{-II} and S^{VI} (Giggenbach 1987; Moretti 2005; Cicconi et al. 2020 this issue and references therein). By convention, Roman numerals are used when we cannot distinguish between the element in a complex and the element making up a single ion species, whereas Arabic numerals are used when a formal charge can be attributed to a given ion species. For the reasons stated above, we cannot expect that redox couples for trace elements, such as Ni^0/Ni^{II}, to be an effective electron transfer–controlling reaction in a magmatic system. Therefore, the so-called nickel–nickel oxide (NNO) buffer, relating oxygen fugacity (f_{O_2}) via the reaction

$$Ni_{(s)} + ½\ O_2 \leftrightarrow NiO_{(s)} \qquad (1)$$

(with the subscript 's' referring to solid phases) is not representative of a controlling or influencing buffering redox exchange, even though its f_{O_2} variation with temperature overlaps that observed in many magmatic–volcanic environments (FIG. 2A). Nevertheless, in igneous petrology and volcanology, the oxidation state is conveniently expressed as f_{O_2} relative to gas–solid redox exchanges that involve mainly ferromagnesian minerals in the silicate (rock, melt) matrix via simple oxybarometers of the type $\log f_{O_2} = a + b/T$ (FIG. 2A). However, in multiphase (melt + crystals + gas) magma, the thermal and chemical carrier is represented by the melt phase, which is not a simple reservoir inert from a redox chemistry perspective, but it is the actual solvent that provides the redox buffer via iron and sulfur species (see also Moretti and Ottonello 2003; Nash et al. 2019; Cicconi et al. 2020 this issue). In terms of macroscopic oxide component, the basic reaction is best expressed as

$$2FeO_{(m)} + ½O_2 \leftrightarrow Fe_2O_{3(m)}$$
$$\text{or} \quad FeO_{(m)} + ¼O_2 \leftrightarrow FeO_{1.5(m)} \qquad (2)$$

with the subscript 'm' referring to the melt phase (Lange and Navrotsky 1992; Cicconi et al. 2020 this issue). This highlights how, together with temperature, both the oxidation state and f_{O_2} help control a magma's crystallization sequence and differentiation, and how these factors also control volatile partitioning between gas and melt (e.g., Fudali 1965; Carmichael and Ghiorso 1986; Moretti and Papale 2004).

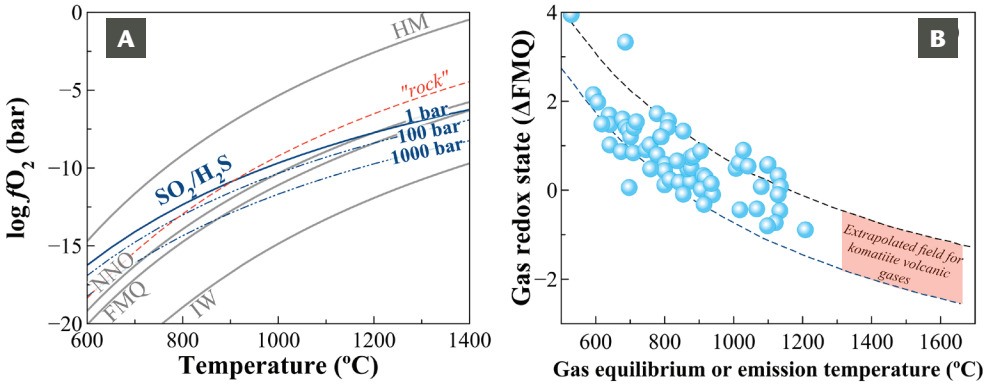

Figure 2 (**A**) Plot of the commonly used redox buffers to fix f_{O_2} versus temperature (°C). Curves are computed for 1 bar total pressure; the three blue lines for the S buffer are for pressures of 1 bar, 100 bar and 1,000 bar. Abbreviations: FMQ = fayalite–magnetite–quartz; HM = hematite–magnetite; IW = iron–wüstite; NNO = nickel–nickel oxide. The red 'rock' line represents the equimolar FeO–$FeO_{1.5}$ buffer of Giggenbach (1987). (**B**) Changes in gas redox state (ΔFMQ) versus emission temperature. Values are for measured volcanic gases worldwide at either emission or equilibration temperatures. Modified after Moussallam et al. (2019).

Reactions such as Equations (1) and (2) are based on the adoption of oxide *components* because they represent the heritage of the gravimetric analytical practice from old-fashioned mineral chemistry. However, such oxide components are not necessarily representative of the actual chemical *species* that take part in redox reactions. Oxide components are useful to show the thermodynamic concept of f_{O_2} for pure single-phase melts that are undersaturated in volatiles and, consequently, un-degassed. The strong effect of melt composition on activity–composition relations makes a direct relationship between $\log f_{O_2}$ and $\log Fe^{II}/Fe^{III}$ difficult to formulate. Several useful efforts have been made to deal with compositional variables, from truly empirical ones (e.g., Kress and Carmichael 1991) to those based on the thermochemical modelling of melt mixing properties (Moretti 2005 and references therein): this latter recognizes ionic entities involving iron in either its divalent or trivalent oxidation state. In particular, ionic-polymeric approaches (see Cicconi et al. 2020 this issue and references therein) have shown that electron exchange may involve variable couple combinations of Fe^{2+}/Fe^{3+} (both modifiers) and Fe^{2+}/FeO_2^- via:

$$Fe^{3+}_{(m)} + \tfrac{1}{2}O^{2-}_{(m)} \leftrightarrow Fe^{2+}_{(m)} + \tfrac{1}{4}O_{2(m)} \quad (3)$$

$$FeO_2^-{}_{(m)} \leftrightarrow Fe^{2+}_{(m)} + 3/2O^{2-}_{(m)} + \tfrac{1}{4}O_{2(m)} \quad (4)$$

Compositional dependence, and, thus, the role of magmatic differentiation, is most easily understood if we fix oxygen fugacity. Applying Le Chatelier's principle to reaction (3) with an alkali addition (i.e., increase in O^{2-} concentration, or *basicity*) leads to iron reduction, whereas oxidation occurs through reaction (4). The same approach can be extended to the ionic species of sulfur (sulfide, S^{2-}; sulfate, SO_4^{2-}) (see also Cicconi et al. 2020 this issue) and requires solving the strong compositional dependencies that affect their solubilities at equilibrium with a gas phase as well as their redox state (Fig. 3A) (see Moretti and Ottonello 2003; Baker and Moretti 2011; Nash et al. 2019). The basicity-based assessment of the role of composition in a large database that includes natural and industrial compositions allows us to overcome the composition-independent predictions of simple empirical treatments (e.g., Wallace and Carmichael 1994; Jugo 2010). In fact, even redox equilibrium between sulfide and sulfate in melts, such as:

$$S^{2-}_{(m)} + 2O_2 \leftrightarrow SO_4^{2-}{}_{(m)} \quad (5)$$

shows a strong dependence on composition, in addition to temperature, because the chemistry of the *solvent* (the silicate matrix) greatly affects the activity–composition of both sulfide and sulfate (Moretti and Ottonello 2003; Baker and Moretti 2011 and references therein; Nash et al. 2019). The apparent difficulty of composition-based treatments of iron and sulfur disappears when it becomes clear that Equations (3), (4) and (5), and similar, make use of the half-reaction known as the *oxygen electrode*: $\frac{1}{2}O_2 + 2e^- \leftrightarrow O^{2-}$ (see Cicconi et al. 2020 this issue), which can be combined with the iron and sulfur *electrodes* ($Fe^{3+} + e^- \leftrightarrow Fe^{2+}$; $FeO_2^- + e^- \leftrightarrow Fe^{2+} + O^{2-}$; $SO_4^{2-} + 8e^- \leftrightarrow S^{2-} + 4O^{2-}$). It is useful to combine Equation (5) with either Equation (3) or (4) to obtain two overlapping reaction mechanisms (see Moretti and Ottonello 2003 and Nash et al. 2019) for

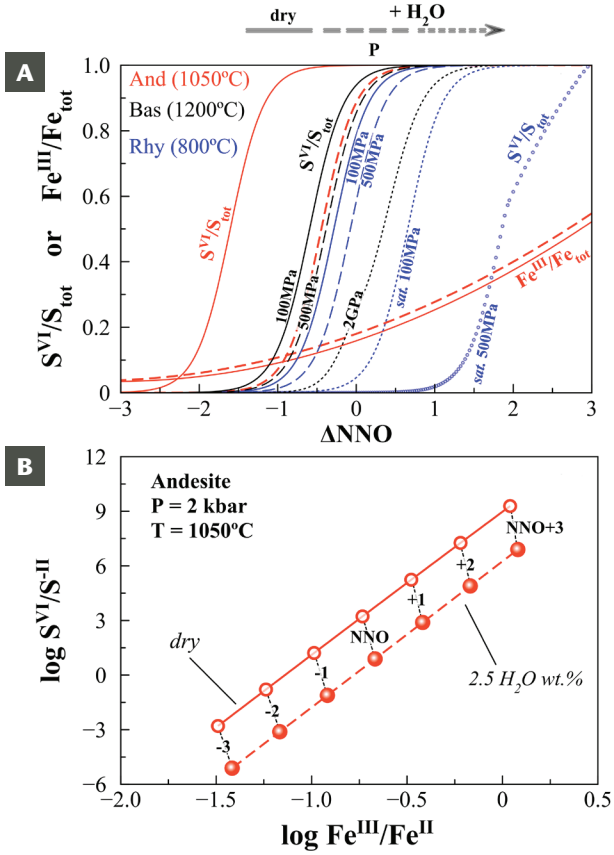

Figure 3 (**A**) Graph showing how the sulfur redox couple in the melt phase (S^{VI}/S^{-II}) shifts for various f_{O_2} values, as computed isothermally for a basalt (Bas) (0.5 wt% H_2O), a rhyolite (Rhy) (0.5 wt% H_2O; or H_2O-saturated, labelled '*sat.*') and an andesite (And) that is at 1,050 °C and 200 MPa, under conditions that are either dry (solid line) or with 2.5 wt% H_2O (dashed line). Also shown is the Fe^{III}/Fe^{II} redox fraction of dry and hydrous andesitic composition. Note the much smaller variation of the iron redox fraction, which, contrary to the sulfur redox, does not attain its extreme values (0 and 1) in the considered f_{O_2} field. All data are computed via ionic-polymer modelling of silicate melts (Moretti 2005; Baker and Moretti 2011 and references therein; Cicconi et al. 2020 this issue) to account for the non-linear interplay of temperature, pressure and composition. (**B**) Isothermal plot of sulfur versus Fe oxidation states as applied to two andesitic compositions and over a range in f_{O_2}. From this graph, it is possible to verify that stoichiometry-driven mutual redox interactions are established between iron and sulfur species (Moretti and Ottonello 2003; Nash et al. 2019).

the mutual interaction of Fe and S species in melts whose stoichiometry fixes the slope of $\log(S^{VI}/S^{-II})$ vs $\log(Fe^{III}/Fe^{II})$ at 8 for any given temperature and composition (Fig. 3B).

We can make an appropriate use of f_{O_2} even if molecular oxygen in melts is absent. The amount of O_2 in volcanic gases is vanishingly small (molar fraction of $\leq 10^{-8}$) (Fig. 2A). Likewise, in the exsolved gas or fluid phase accompanying magma evolution, there are orders of magnitude difference between the concentration of O_2 and that of the other species which dominate the volcanic gas or fluid phase. In the C–H–O–S system, oxygen is, in fact, carried by species such as H_2O, CO_2 and SO_2, which represent the 'oxidized' counterparts to the 'non oxidized' species, such as H_2, CH_4 and H_2S, or the 'partly oxidized' species, such as CO. All these species are released during decompression and the subsequent crystallization of volatile-saturated magma (a process sometimes referred to as 'second boiling'). Thus, their speciation is expected to be governed by the same oxygen fugacity as the coexisting melt. Exsolution of the gas/fluid mixture is a form of magmatic differentiation that depends on the melt–volatile saturation state (or mixed-volatile solubility), which is related to speciation and, hence, f_{O_2}. Again, the composition of the whole system is key. At equilibrium, it is futile to discriminate 'what controls what'. Certainly, the interplay of compositional variables, plus pressure and temperature regimes, makes every volcano unique. In its entirety, the redox potential of each volcanic system is then determined by coexisting gas–solid–melt phases via iron in its two oxidation states and/or via sulfur, which in the gas phase appears as SO_2 and H_2S. Conversely, and similarly to the Ni–NiO pair in the rock/melt matrix, CO and CH_4 are present only as minor or negligible components, making them unsuitable to set as a redox buffer because the dominant C-bearing species is CO_2, at least for typical volcanic conditions.

Both hydrogen and sulfur may occur as various species in magmatic gases. Thus, their study in gases discharged by active volcanoes offers indirect, but still highly valuable, insights into the redox properties of magmatic systems, particularly f_{O_2}. A very useful redox reaction that can be directly applied to volcanic plume measurements is the oxidation of H_2S to SO_2 and the reduction of O_2 to H_2O:

$$H_2S + 3/2O_2 \leftrightarrow SO_2 + H_2O \quad (6)$$

The equilibrium constant for reaction (6) can be expressed using thermodynamic data from Stull et al. (1969):

$$\log(SO_2/H_2S) = 27{,}377/T - 3.986 + 3/2\log f_{O_2} - \log f_{H_2O} \quad (7)$$

It follows that, at a given temperature and f_{O_2}, SO_2/H_2S depends on the partial pressure of water, which is related to magma via water solubility. For example, at 1,100 °C and $f_{O_2} = -9.1$ corresponding to FMQ, H_2S/SO_2 varies from 200 at P_{H_2O} = 1 bar to 0.2 at P_{H_2O} = 1,000 bar.

As O_2 gas is, to all intents and purposes, a virtual species and f_{O_2} itself is largely a thermodynamic construct useful for making calculations, there is virtue in adopting H_2 as a proxy for magmatic gas redox conditions. In addition, given its low molecular weight and low solubility in groundwater and geothermal fluids (all conferring an overall high mobility), H_2 is a potentially excellent tracer of processes operating deep in magmatic systems. Attempts have been made to measure H_2 in a variety of high-temperature magmatic gases (e.g., Giggenbach 1996; Aiuppa et al. 2011 and references therein). However, the potential control of H_2 behaviour by processes other than magma degassing dynamics (such as H_2 production by fluid–rock interaction in geothermal systems) (Stefánsson 2017) has diverted attention from making measurements of H_2. Only recently have volcanic gas plumes been targeted for their H_2 content (e.g., Aiuppa et al. 2011). A better indicator for redox potential is given by the variable R_H (Giggenbach 1987):

$$R_H = \log fH_2/fH_2O \approx \log XH_2/XH_2O \quad (8)$$

This has the advantage of being measurable directly at many volcanic vents. The R_H value relates to f_{O_2} via water dissociation ($H_2O \leftrightarrow H_2 + \frac{1}{2}O_2$). The value of $R_H = -2.82$ corresponds to the $FeO–FeO_{1.5}$ 'rock' buffer (Fig. 2A) and is almost independent of temperature. It follows that Equation (6) is more correctly expressed in terms of H_2 rather than O_2 to give:

$$H_2S + 2H_2O \leftrightarrow SO_2 + 3H_2 \quad (9)$$

The SO_2 component dominates the gaseous sulfur species at magmatic temperatures and is favoured by decreasing pressure via the positive volume change of Equation (9) (four moles of gas on the right-hand side, but only three on the left). In andesitic volcanism, this reaction is the redox buffer that drives the early chemical evolution of the steam-rich fluids that carry the S species upward, after separation from magmas ponding at depth (Fig. 4).

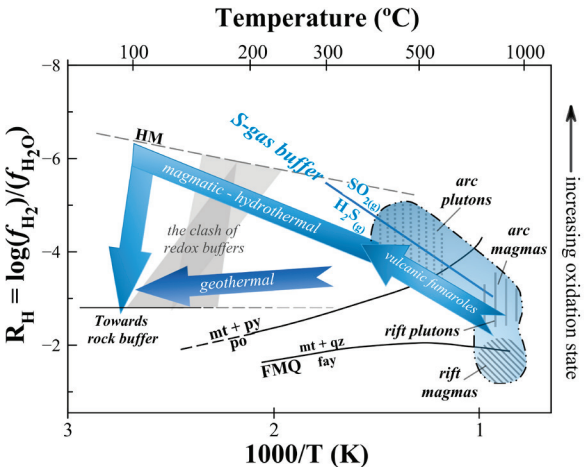

Figure 4 Schematic R_H (Equation 8) versus temperature diagram illustrating the theoretical variation imposed by well-established redox buffers on magmas and geothermal fluids, including magmatic-geothermal gases discharged by arc volcanoes (modified after Einaudi et al. 2003). Limits are consistent with Figure 1B. The lower limit of the redox conditions for mature geothermal fluids is given by the line above the label 'towards rock buffer' (Giggenbach 1987) (reported at 1-bar only for clarity) and, at higher temperatures, by the pyrrhotite–pyrite–magnetite buffer that fixes the fugacity of sulfur species. Abbreviations: fay = fayalite; FMQ = fayalite–magnetite–quartz; HM = hematite–magnetite; mt = magnetite; po = pyrrhotite; py = pyrite; qtz = quartz.

REDOX SIGNATURE AND MAGMATIC ACTIVITY: FROM SOURCE TO SURFACE

Modelling and observations demonstrate that the oxygen fugacity of mantle-derived melts can be strongly affected by volatile degassing during magma ascent. The f_{O_2} values in volcanic gases discharged at crater vents result from the non-linear interplay of source characteristics, composition, chemical differentiation and degassing style.

Burgisser and Scaillet (2007) modelled an ascending iron-poor rhyolitic magma under completely closed-system conditions (no exchange with the surroundings) and without crystallization. Under these conditions, Burgisser and Scaillet (2007) showed that in sulfur-free systems there can only be oxidation as the magma rises and the pressure decreases (T1 in Fig. 1B). This is because H_2O exsolution favours an increase in f_{O_2} to maintain an equilibrium of water dissociation ($H_2O \leftrightarrow H_2 + 1/2O_2$) in the gas. Different trends arise when sulfur is introduced, with a general tendency of decreasing f_{O_2} in the low-P region (< 100 bar). In the presence of sulfur species, pressure decrease favours conversion of H_2S to SO_2 (see Equation 9), and f_{O_2} in a closed system must decrease because oxygen is picked-up

by SO_2. For an Fe-poor rhyolitic system, this effect is larger than in an Fe-rich basaltic one, because there is too little iron accommodating oxygen in the rhyolitic melt through $FeO–Fe_2O_3$ exchange (Equation 2).

Apart from the case of rapidly rising rhyolitic magmas prior to fragmentation and explosive eruption, it is not realistic to consider a magmatic system as 'closed' to oxygen, which can then be picked up by H_2O, SO_2 and CO_2 in the gas and by $FeO–Fe_2O_3$ and sulfur species in the melt, without any oxygen exchange between liquid and crystals. Besides, melt speciation of volatile components affects mass balances, hence fluid phase equilibria, such as in case of water exsolution from the melt, which requires conversion of dissolved OH species to H_2O in the gas via hydrogen consumption. Ghiorso and Kelemen (1987) instead defined oxygen as a perfectly mobile component to be continuously added to or removed from the system, and state the necessity of modelling phase equilibria in magmatic systems that are selectively open to oxygen exchange by modifying the Gibbs energy potential. This necessity reflects a current lack of knowledge regarding relevant redox couples that buffer ferric/ferrous ratios in a crystallizing magma. For this reason, Moretti and Papale (2004) eschewed mass conservation of oxygen in favour of the joint redox-degassing evolution constrained by typical f_{O_2} 'buffers' of proven validity (e.g., $H_2S/SO_2 = 1$) (see T2 in Fig. 1B). This suggests that natural cases should be evaluated individually on the basis of available data: for example, the composition of volcanic gases, and backtracking of f_{O_2} values at different pressure and temperature from redox states of Fe and S derived from melt inclusions and/or mineral assemblages.

Precise tracking of Fe and S redox states during degassing are now possible using modern microbeam instrumentation on a set of melt inclusions, in conjunction with measurement of volcanic plume gas compositions. When applied to the same series of melt inclusions and related plume gas measurements from the phonolitic Erebus Volcano (Antarctica) and its lava lake, decreasing trends of $\log f_{O_2}$ characterize magma evolution from depth to surface, either from the modelling of continuous sulfide saturation (Oppenheimer et al. 2011) (T3 line in Fig. 1B) or by tracking of Fe and S redox states using X-ray absorption near-edge structure measurements (Moussallam et al. 2014) (T4 line in Fig. 1B).

At many volcanoes, plume emissions result from both residual degassing of a shallow (and volatile-depleted) conduit magma and the ascent of deep-reservoir (CO_2-rich) fluids carrying a redox signature akin to that of the source. During the rise of magma and fluid, local magma equilibrium conditions will be established depending on gas flux through the melt phase. At the andesitic Soufrière Hills Volcano (Montserrat, Lesser Antilles), plume gases with $SO_2/H_2S \approx 1$, although compatible with shallow closed-system degassing of the shallow and volatile-depleted dome-forming rhyolite, can instead be modelled only in terms of mixing between 1) a deep gas from a vesiculating hydrous (8 wt% H_2O), oxidized (NNO) and S-rich underplating basaltic andesite, and 2) the shallower degassing of S-depleted rhyolitic magma (Edmonds et al. 2010). At the basaltic Etna Volcano (Italy), a deep-sourced relatively H_2-rich magmatic gas ($\log f_{O_2}$ = NNO; $XSO_2/XH_2S \approx 0.5$) (Aiuppa et al. 2011) mixes with a shallow CO_2- and H_2-depleted gas that became further oxidized upon cooling to 550 °C. This 'oxidation upon cooling' effect was further investigated for basaltic volcanoes by Oppenheimer et al. (2018), illustrating that caution is required when using f_{O_2} from lava chemistry to infer the composition of associated volcanic gases. Consequently, variability in gas speciation may mask the variety in speciation that results from the ascent of deeper and oxidized gases and their associated magmas.

COLD AND STEAMY: REDOX IN POST-MAGMATIC STAGES AND WITHIN GEOTHERMAL SYSTEMS

Fluids produced by the degassing of a magma consist mainly of water vapour (>90 mol%), together with CO_2, SO_2 and/or H_2S, HCl, and HF (e.g., Giggenbach 1996) (Fig. 1C). A geothermal system above a cooling magma may be open to the upward transfer of such magmatic gases or can react with sequestered gases. Magma-derived fluids (gases and NaCl-rich brines) may also act as important carriers of metals and trace organic compounds that can complex with major gas species, such as sulfur and chlorine (Wahrenberger et al. 2002; Schwander et al. 2004).

Variations in the relative concentrations of gas species depend mainly on differences in magmatic volatile solubility and the degree of degassing of a magma. Condensation (or 'scrubbing') of exsolved magmatic gases into deep circulating groundwater, which might be of meteoric or seawater origin, results in the formation of acid, relatively oxidized, and reactive solutions. These are later reduced and neutralized through interactions with wall rocks and upon mixing into groundwater (Fig. 1). The primary minerals of igneous rocks are unstable when in contact with high-temperature fluids and tend to react to form more stable secondary minerals. Volcanic gases participate in fluid–rock reactions and may be sequestered into geothermal mineral phases, such as CO_2 into calcite and H_2S into pyrite. The processes of converting primary minerals to secondary minerals by meteoric and/or seawater and magmatic gases are irreversible. At shallow depths within geothermal systems, boiling commonly liberates dissolved gases into the vapour phase, which ascends to the surface and discharges in fumaroles (Fig. 1C). Condensation of these vapours into shallow ground- and surface waters may generate steam-heated acid-sulfate waters through atmospheric oxidation of H_2S. The boiled geothermal liquid can also flow toward the surface in the form of hot springs or mix with non-thermal waters.

Most volcanic-geothermal systems occur in fractured volcanic rock, and it appears logical to conclude that they tend to develop where permeability anomalies exist above the heat source. Fluxes of gases from the magma are likely to be concentrated along these permeable channels from which they will diffuse into microfractures and pores in the wall rock. Geothermal fluids that are relatively close to major conduits of magmatic gas flow may be characterized by more oxidized phases, such as alunite or anhydrite, whereas fluids in pores and microfractures may reflect progressive fluid–rock interaction.

Common redox-sensitive species in volcanic-geothermal systems include carbon (CO_2, CH_4, CO), sulfur (H_2S, SO_4), hydrogen (H_2, H_2O) and iron (Fe^{II}, Fe^{III}). Commonly, redox conditions are considered to approach local equilibrium for various redox reactions, such as the gas–gas and mineral–gas reactions:

$$CH_{4(g)} + 2H_2O_{(g)} \leftrightarrow CO_{2(g)} + 4H_{2(g)} \quad (10)$$

$$4FeO_{1.5(s)} + 4H_{2(g)} \leftrightarrow 4FeO_{(s)} + 2H_2O_{(g)} \quad (11)$$

Such conclusions are based on closely comparing gas ratios in natural volcanic-geothermal emissions to those predicted thermodynamically (e.g., Giggenbach 1987). However, observed mineral–gas and gas–gas equilibria may not hold for open volcanic-geothermal systems. Instead, the redox conditions of these systems are likely to be controlled by the sources of redox species and by gas–gas and fluid–rock reactions. The sources of redox species are mainly from magma gases and fluid–rock interactions, whereas gas–gas and fluid–rock reactions themselves are controlled by metastable equilibria that depend on temperature, pressure, composition and the progress (extent) of the reaction. For example, fugacity of H_2 may closely reflect

mineral–fluid equilibria in geothermal fluids because the magmatic H_2 flux is relatively small and there is a reduction of H_2O to form H_2 by the oxidation of Fe^{II} to Fe^{III}, which occurs faster than the residence time of its host geothermal reservoir. In contrast, CO_2 concentrations are likely to be controlled by a high input of magmatic gas flux, which requires very large fluid–rock mass transfer to reach equilibrium, and by sluggish reaction kinetics between CH_4 and CO_2 at geothermal temperatures. As the various redox components are probably not in overall equilibrium, geothermal fluids cannot be characterised by a unique f_{H_2}, f_{O_2} or redox potential at a given temperature and pressure (e.g., Stefánsson 2017). This is shown schematically by the 'clash of redox buffers' fields in FIGURE 4, marking the transition from immature magmatic-geothermal to mature geothermal (sensu stricto) fluids.

OUTLOOK

The redox behaviour of magmas that evolve from depth to surface is strongly affected by compositional variables. Compared to hydrothermal systems, the magmatic case suffers from poor parameterization of redox properties of the melt phase, which are intimately related to the melt ion speciation, and, hence, how we define and treat the acid–base character of melts. An important next step would be to create a unified model for acid–base melt solvent properties and redox descriptions of reactive species, in a manner similar to that for aqueous solutions. Only by moving forward on the physico-chemical front will we be able to define precise phase stability diagrams as a function of f_{O_2} and the indicators of the acid–base character of the melt (e.g., the activity of O^{2-}). This will further reveal the horizons for 1) solving many local-scale problems, which we refer to qualitatively as system heterogeneities; 2) improving our knowledge on trace metal and on organic transport and deposition by magmatic-geothermal fluids; 3) interpreting the chemical variations observed during pre-eruptive volcanic unrest, and in low-temperature (down to 100 °C) geothermal systems fed by deep fluid input of magmatic origin.

ACKNOWLEDGMENTS

The manuscript greatly benefited from reviews by Alessandro Aiuppa (University of Palermo), Franco Tassi (University of Firenze) and Jake Lowenstern (USGS), as well as from comments and suggestions by Principal Editor Jon Blundy.

REFERENCES

Aiuppa A and 5 coauthors (2011) Hydrogen in the gas plume of an open-vent volcano, Mount Etna, Italy. Journal of Geophysical Research: Solid Earth 116, doi: 10.1029/2011JB008461

Baker DR, Moretti R (2011) Modeling the solubility of sulfur in magmas: a 50-year old geochemical challenge. Reviews in Mineralogy and Geochemistry 73: 167-213

Behrens H, Gaillard F (2006) Geochemical aspects of melts: volatiles and redox behavior. Elements 2: 275-280

Burgisser A, Scaillet B (2007) Redox evolution of a degassing magma rising to the surface. Nature 445: 194-197

Carmichael ISE, Ghiorso MS (1986) Oxidation-reduction relations in basic magma: a case for homogeneous equilibria. Earth and Planetary Science Letters 78: 200-210

Cicconi MR, Le Losq C, Moretti R, Neuville DR (2020) Magma, the largest repository and carrier of Earth's redox processes. Elements 16: 173-178

Edmonds M and 7 authors (2010) Excess volatiles supplied by mingling of mafic magma at an andesite arc volcano. Geochemistry, Geophysics, Geosystems 11, doi 10.1029/2009GC002781

Einaudi MT, Hedenquist JW, Inan EE (2003) Sulfidation state of fluids in active and extinct hydrothermal systems: transitions from porphyry to epithermal environments. In: Simmons SF, Graham I (eds) Volcanic, Geothermal, and Ore-Forming Fluids: Rulers and Witnesses of Processes within the Earth. Society of Economic Geologists Special Publication 10, pp 285-314

Fudali RF (1965) Oxygen fugacities of basaltic and andesitic magmas. Geochimica et Cosmochimica Acta 29: 1063-1075

Giggenbach WF (1987) Redox processes governing the chemistry of fumarolic gas discharges from White Island, New Zealand. Applied Geochemistry 2: 143-161

Giggenbach WF (1996) Chemical composition of volcanic gases. In: Scarpa R, Tilling RI (eds) Monitoring and Mitigation of Volcano Hazards. Springer, Berlin, Heidelberg, pp 221-256

Ghiorso MS, Kelemen PB (1987) Evaluating reaction stoichiometry in magmatic systems evolving under generalized thermodynamic constraints: examples comparing isothermal and isenthalpic assimilation. In: Mysen BO (ed) Magmatic Processes: Physicochemical Principles. Geochemical Society Special Publication 1, pp 319-336

Jugo PJ, Wilke M, Botcharnikov RE (2010) Sulfur K-edge XANES analysis of natural and synthetic basaltic glasses: implications for S speciation and S content as function of oxygen fugacity. Geochimica et Cosmochimica Acta 74: 5926-5938

Kress VC, Carmichael ISE (1991) The compressibility of silicate liquids containing Fe_2O_3 and the effect of composition, temperature, oxygen fugacity and pressure on their redox states. Contributions to Mineralogy and Petrology 108: 82-92

Lange RA, Navrotsky A (1992) Heat capacities of Fe_2O_3-bearing silicate liquids. Contributions to Mineralogy and Petrology 110: 311-320

Moretti R (2005) Polymerisation, basicity, oxidation state and their role in ionic modelling of silicate melts. Annals of Geophysics 48: 583-608

Moretti R, Ottonello G (2003) Polymerization and disproportionation of iron and sulfur in silicate melts: insights from an optical basicity-based approach. Journal of Non-Crystalline Solids 323: 111-119

Moretti R, Papale P (2004) On the oxidation state and volatile behavior in multicomponent gas–melt equilibria. Chemical Geology 213: 265-280

Moussallam Y and 8 coauthors (2014) Tracking the changing oxidation state of Erebus magmas, from mantle to surface, driven by magma ascent and degassing. Earth and Planetary Science Letters 393: 200-209

Moussallam Y, Oppenheimer C, Scaillet B (2019) On the relationship between oxidation state and temperature of volcanic gas emissions. Earth and Planetary Science Letters 520: 260-267

Nash WM, Smythe DJ, Wood BJ (2019) Compositional and temperature effects on sulfur speciation and solubility in silicate melts. Earth and Planetary Science Letters 507: 187-198

Oppenheimer C and 6 coauthors (2011) Mantle to surface degassing of alkalic magmas at Erebus volcano, Antarctica. Earth and Planetary Science Letters 306: 261-271

Oppenheimer C and 5 coauthors (2018) Influence of eruptive style on volcanic gas emission chemistry and temperature. Nature Geoscience 11: 678-681

Petersen S, Lehrmann B, Murton BJ (2018) Modern seafloor hydrothermal systems: new perspectives on ancient ore-forming processes. Elements 14: 307-312

Schwandner FM, Seward TM, Gize AP, Hall PA, Dietrich VJ (2004) Diffuse emission of organic trace gases from the flank and crater of a quiescent active volcano (Vulcano, Aeolian Islands, Italy). Journal of Geophysical Research: Atmospheres 109, doi: 10.1029/2003JD003890

Stefánsson A (2017) Gas chemistry of Icelandic thermal fluids. Journal of Volcanology and Geothermal Research 346: 81-94

Stull DR, Westrum EF Jr, Sinke GC (1969) The Chemical Thermodynamics of Organic Compounds. John Wiley, New York, 865 pp

Wahrenberger C, Seward TM, Dietrich V (2002) Volatile trace-element transport in high-temperature gases from Kudriavy volcano (Iturup, Kurile Islands, Russia). In: Hellman R, Wood SA (eds) Water-Rock Interactions, Ore Deposits, and Environmental Geochemistry. Geochemical Society Special Publication 7, pp 307-327

Wallace PJ, Carmichael ISE (1994) S speciation in submarine basaltic glasses as determined by measurements of SK_α X-ray wavelength shifts. American Mineralogist 79: 161-167

Electron Transfer Drives Metal Cycling in the Critical Zone

Melanie Davranche[1], Alexandre Gélabert[2], and Marc F. Benedetti[2]

1811-5209/20/0016-0185$2.50 DOI: 10.2138/gselements.16.3.185

Electron transfer in the critical zone is driven by biotic and abiotic mechanisms and controls the fate of inorganic and organic contaminants, whether redox-sensitive or not. In these environments, Fe- and Mn-bearing minerals, as well as organic matter, are key compounds. They interact with each other and constitute important electron shuttles. As a result, not only their solubility but also their structure controls the mobility of many essential and toxic elements. In addition, microorganisms that form hot spots and are widespread in environmental systems are also primordial players in electron transfer processes by acting as a catalyst between an electron donor and an acceptor, and through their contaminant detoxification metabolism.

KEYWORDS: redox, oxides, organic matter, bacteria, trace elements

INTRODUCTION

The biogeochemical cycling of major and trace elements is powered by reactions that involve abiotic and biotic electron transfer (FIG. 1). Redox processes, therefore, control the fate and toxicity of these major and trace elements in the critical zone, as well as the persistence of numerous organic pollutants. The transport properties of most metals (and metalloids) in the critical zone are strongly related to metal(oid) redox state: reduced As(III) is normally much more mobile and toxic than the oxidized form As(V); Cr(VI) is more soluble and toxic than Cr(III).

Ordinarily, air penetrates easily into the upper parts of highly drained soils. But deep horizons and long-term waterlogged systems quickly become depleted in dissolved O_2 from biomass consumption (for respiration), and, as a result, redox gradients develop. Among the different redox-active critical zone constituents, Fe- and Mn-bearing minerals are of particular interest. They are found in significant amounts in soils, their Fe and Mn contents can have multiple redox states, and such minerals can function as both electron donors and acceptors (Melton et al. 2014). Even the fate of non-redox-sensitive species (e.g., Cd or phosphate) can be indirectly impacted by redox changes in Mn and Fe (FIG. 1). Both Mn and Fe can precipitate (or dissolve) as a consequence of redox reactions, thereby providing (or removing) reactive sorption surfaces, or they can trigger co-precipitation processes in the critical zone. In addition, natural organic matter (NOM) plays a key role by exhibiting functional moieties able to promote abiotic electron transfer with mineral surfaces, thereby catalyzing redox transformations.

As a consequence, electron transfer gradients develop in soils which can impact the redox state and bioavailability of nutrients, such as N, S, Fe or Mn. In turn, these redox changes shape multiple microbial communities that differ by their ability to use these nutrients under specific redox states (FIG. 1). As a result, microbes actively contribute to the biotic redox properties of the critical zone. Micro-organisms are found in micro-habitats spread within soils, and they usually form biofilms that are gel-like structures composed of cells embedded in an exopolymer matrix. In these structures, the diffusion of chemical elements is limited, so preventing their loss by transport away from the cells. This generates, in addition to the cells' metabolic activities, micro-environments of specific physico-chemical properties (pH, pO_2) that strongly impact the local redox properties at the biofilm scale and form redox hotspots in the critical zone.

In this article, we focus on a subset of the wide range of redox processes that occur in the critical zone. The abiotic and biotic electron transfers controlled by minerals, NOM and micro-organisms in soils are discussed, as well as the effect of electron transfer on the fate of redox and non-redox-sensitive metallic contaminants.

MINERAL PHASES PLAY A KEY ROLE

Usually, the cycling of redox-sensitive elements in soils is dependent on the presence of redox-active minerals, particularly in environments subjected to changes in redox condition. Among these redox-active minerals, Mn(IV) oxides play a key role by being among the strongest oxidants in nature. They are able to control the redox state of elements hardly oxidizable otherwise, such as Cr, and are frequently invoked for the dramatic release of toxic Cr(VI) in natural systems (Tebo et al. 2004). Iron-bearing minerals can also be highly reactive, with, for instance, Fe(II) being a powerful reductant in various abiotic redox processes, particularly in the presence of Fe(III) (oxyhydr)oxides which enhance Fe-bearing minerals' reduction kinetics (Stewart et al. 2018). Mixed-valence Fe minerals carrying both Fe(II) and Fe(III) – green rusts (layered double Fe hydroxides), and magnetite (a ferromagnetic member of the spinel mineral group) – are of major interest because they exhibit strong redox properties. They are extremely reactive, particularly in redox transition zones within the critical zone, and are reported in numerous studies

1 Univ. Rennes, CNRS
Géosciences Rennes, UMR 6118
F-35000 Rennes, France
E-mail: melanie.davranche@univ-rennes1.fr

2 Université de Paris, Institut de physique du globe de Paris, CNRS, IGN
F-75238 Paris, France
E-mail: gelabert@ipgp.fr, benedetti@ipgp.fr

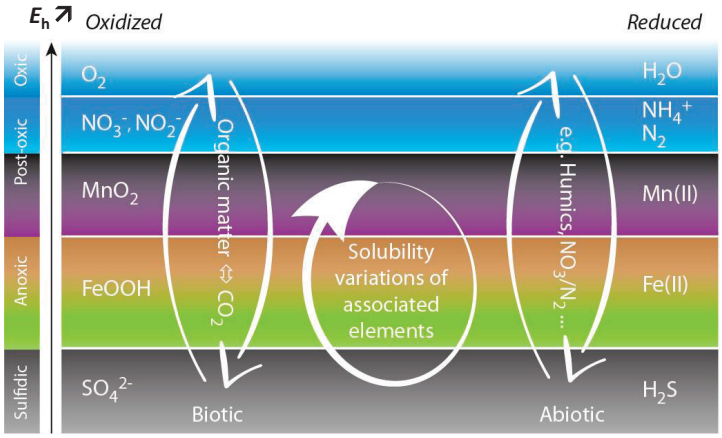

Figure 1 Reduction and oxidation sequence in the critical zone. The redox state can be catalyzed either by heterotrophic bacteria (biotic) or produced by chemical elements/compounds (abiotic). The electron donor substrate is generally soil (natural organic matter) for the biotic reactions. Humics = humic organic matter.

to act as strong reducing agents for nitrite, chlorinated and nitroaromatic compounds, as well as elements such as Cr(VI), Se(VI) or U(VI) (Alowitz and Scherer 2002).

In addition, the production of reactive oxygen species, such as the hydroxyl radical (OH•), by soil minerals under aphotic conditions remain mostly overlooked. Nevertheless, recent evidence for aphotic production of reactive oxygen species and the degradation of organic pollutants by nanomagnetite suggests that such reactions may have important environmental applications (Ardo et al. 2015).

During periods of prolonged waterlogging, soils become enriched in NOM, Fe(II/III), and trace elements. Under such conditions, Fe(II) and Fe(III) are bound to dissolved organic matter (DOM). However, in response to precipitation decrease and evapo-transpiration, O_2 re-enters the soil porosity, resulting in a progressive oxidation of soil constituents and solutions, as well as the oxidation of Fe(II) bound to NOM in presence of various major and trace elements.

Soil solution oxidation by-products are complex, heterogeneous and composed of different Fe-bearing phases embedded in an organic matrix. In organic soil, Guénet et al. (2016), using X-ray absorption spectroscopy (XAS) and small angle X-ray scattering (SAXS), demonstrated that these phases are composed of Fe monomers and clusters bound to organic matter (OM) and of nano-lepidocrocite embedded in the NOM matrix (Fig. 2). Under laboratory conditions, Fe monomers, oligomers and nano-ferrihydrite are formed rather than nano-lepidocrocite (Guénet et al. 2017a). This difference can be explained by the kinetics of oxidation/hydrolysis: lepidocrocite forms from slow kinetics. Moreover, Thomas-Arrigo et al. (2017) demonstrated that in environmental systems where solid–solution equilibria are rapidly attained, NOM stabilizes poorly crystalline Fe-oxyhydroxide minerals such as ferrihydrite.

For low Fe/NOM ratios, Vilgé-Ritter et al. (1999) showed that NOM is strongly complexed to Fe, thus limiting Fe hydrolysis because it occupies growth sites and controls aggregate structuration. Iron nano-oxyhydroxides are organized in fractal networks (Guénet et al. 2017b) (Fig. 3) and are larger than the compact and spherical NOM aggregates. Gentile et al. (2018) showed that NOM forms fractal-like nanoparticles, with molecular NOM constraining Fe nanoparticle size and ensuring cohesion between them. Such Fe–OM nano-aggregates are considered as carriers of many contaminants (Fig. 2). Iron oxyhydroxides and NOM are indeed known to be strong sorbents of metals and metalloids due to their high density of binding sites. When associated as nano-aggregates, they are the main phases that carry trace metals.

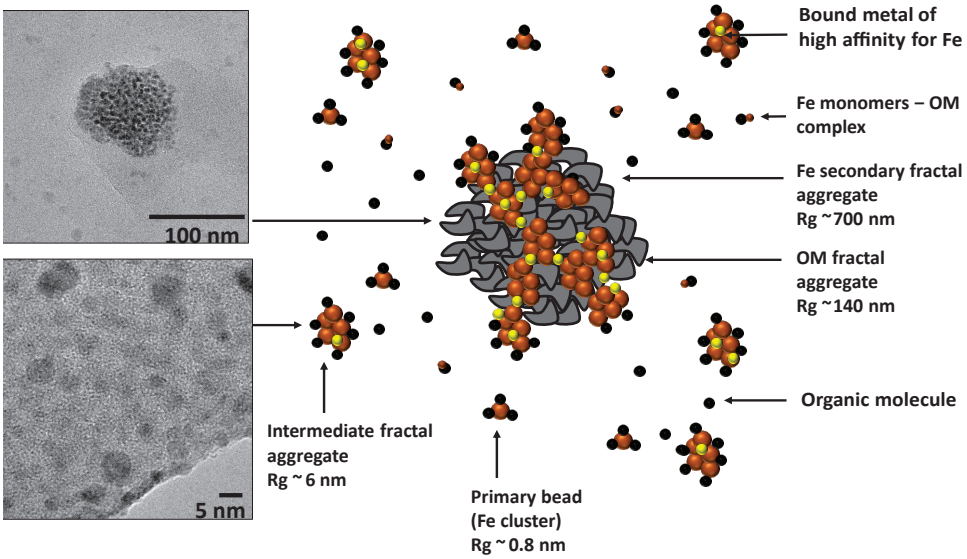

Figure 2 Two transmission electron microscopy (TEM) images (left) of different levels (scales) of iron–organic matter (Fe–OM) aggregates and their corresponding graphic representations (right). Symbols: black dots = organic molecules; brown dots = iron clusters; yellow dots = metals that can be associated with iron; grey crescents = organic matter (OM). The lower TEM image and its graphic is for the smaller intermediary aggregate formed by primary Fe beads and organic molecules. The upper TEM image and its graphic includes the larger secondary Fe/OM aggregate [Fe/OM ratio = 0.4 (wt/wt)]. All are fractal in shape. Symbol: Rg = radius of gyration. Modified from Guenet et al. (2017b) and Gentile et al. (2018).

NATURAL ORGANIC MATTER AND ELECTRON TRANSFER

Studying the reactivity of NOM in the environment has to overcome the challenge of the intimate association of NOM with minerals, and the variations in NOM concentration. A procedure developed to extract OM, based on its solubility in alkaline/acidic solutions, led to the definition of a 'humic substance' (HS), often used as NOM proxies in laboratory studies. Humic substances encompass fulvic acids (FAs) (soluble in both bases and acids), humic acids (HAs) (soluble in bases, insoluble in acids), and humins (insoluble). It has long been believed that the gradient in OM solubility should parallel that of their stability (Quénéa et al. 2019). Electron transfer activities of dissolved and solid-phase HSs are generally attributed to quinone–hydroquinone moieties (Fig. 3) and to the presence of bound metals ions, such as Fe(II) or Fe(III). In reduced environments, HSs dissolved or adsorbed on solid phases can serve as redox buffers by receiving electrons from respiring microbes and transferring electrons from poorly accessible minerals, and mediating electron transfer

between microbes and other electron acceptors (Macalady and Walton-Day 2011). Moreover, semiquinone radicals produced during chemical reduction of a HS model quinone are strong oxidants capable of oxidizing arsenite to arsenate (Jian et al. 2009).

It is, therefore, crucial to characterize the electron acceptor capacity (EAC) and electron donor capacity (EDC) of a given HS. These capacities are defined as the mole of electrons transferred from a HS at a fixed redox potential value (E_h). The HS EAC was initially quantified by following the oxidation products ($S_2O_3^{2-}$ and Zn^{2+}) of known reductants such as H_2S and Zn^0. Their EDC was then estimated by measuring the Fe(II) quantity obtained by the reduction of Fe(III) complexes in presence of a HS. This latter protocol can be used to estimate the HS redox state in environmental samples, but it has two major drawbacks (Aeschbacher et al. 2010). The first is that electron transfer is obtained indirectly; the second is that those determinations are pH dependent, thus preventing a comparison between the different electron transfer properties of HSs (i.e., HA vs FA) when determined at different pHs. Also, EDC kinetics are generally slow, which prevents the quantification of true equilibrium EDC values. Newer electrochemical methods were developed to circumvent those issues and to prevent the addition of reductants involved in side reactions (Aeschbacher et al. 2010).

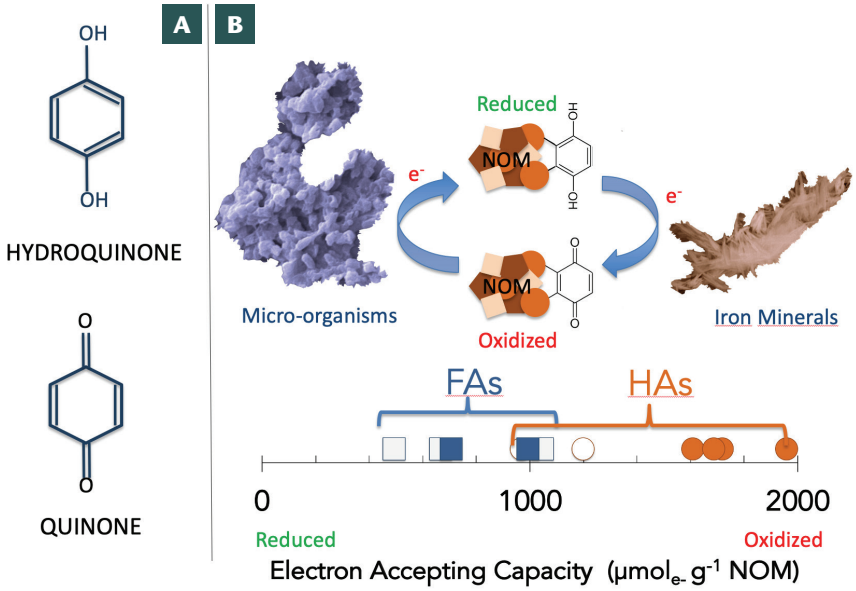

Figure 3 (**A**) Structures of the quinone and hydroquinone functional groups, which are mainly responsible for the redox activity of humic substances. (**B**) The role of natural organic matter (NOM) – in relation to the key molecules in Figure 3A – in the electron transfer capacity (as electron accepting capacity, EAC) between minerals and micro-organisms. Orange symbols correspond to natural humic acids (HAs); blue symbols correspond to natural fulvic acids (FAs). Data on 13 humic substances from Aeschbacher et al. (2010).

Electron acceptor capacities of different HSs were measured and ranged from 493 ± 10 to 1,961 ± 15 $\mu mol_{e^-} g_{HS}^{-1}$. It was shown that humic acids have higher EACs than fulvic acids when derived from the same source material. Aquatic humic acids exhibit lower EACs compared to terrestrial ones (Fig. 3). Fulvic acids of microbial origin have the lowest EAC, probably because they lack lignin-derived moieties. Similarly, the reasonable trends obtained with C/H ratios and the aromaticity data obtained from ^{13}C nuclear magnetic resonance (NMR) data suggest that the high EAC of HSs of terrestrial origin, compared to the low EAC of aquatic fulvics, is related to quinone groups originating from phenolic moieties in lignin (Aeschbacher et al. 2010; Tan et al. 2017).

Humic substances strongly complex trace elements in the biogeosphere (Benedetti et al. 1996), and the resulting complexes can, thus, influence electron transfer during redox processes in the critical zone. Zhou et al. (2015) studied the impact of Fe(III), Cu(II) and Al(III) on the electron shuttling capacities of HAs. Their results showed that HA–Fe and HA–Cu had higher EAC than the original HA, while HA–Al exhibited lower EAC. The increase or decrease in EAC is believed to be related to the nature of the metal ion that binds the HA reactive moieties. The resulting complex makes the electrons more available in the case of redox-sensitive elements (Fe and Cu), and less available for non-redox elements (Al) that could block electron transfer, as confirmed by density functional theory calculations (Zhou et al. 2015). These findings allow a better understanding of the role played by electron transfer in biogeochemical cycles, because HA–metal ion complexes are ubiquitous in the critical zone. These complexes can also be oxidized by Fe(II)-oxidizing microbes and reduced by Fe(III)-reducing microbes. Moreover, the promotion of extracellular electron transfer by HA–metal complexes opens new potential ways to improve soil bioremediation.

Much less is known regarding the role of NOM during its interaction with redox-reactive species, such as sulfide. Abiotic re-oxidation of sulfide to S^0 and $S_2O_3^{2-}$ would explain sustainable organic matter biodegradation by bacteria under conditions where sulphate concentrations are low (i.e., wetlands, paddy soils, sediments). Answering this question will help to better understand the sulfur geochemistry in anoxic conditions, as well as to construct an electron budget of sulfide oxidation upon reaction with NOM or NOM proxies such as HSs (i.e., HAs or FAs) and the formation of NOM–S compounds. Resolving the organic sulfur redox speciation is the key step. Yu et al. (2015) studied the abiotic transformation of sulfide exposed to reduced and non-reduced HAs under anoxic conditions. They showed that HAs could abiotically transform sulfides by incorporating sulfur (i.e., 22% to 37% of initial sulfide content) in addition to the production of elemental sulfur and thiosulfates ($S_2O_3^{2-}$). Yu et al. (2015) reported EACs in a range similar to that given by Aeschbacher et al. (2010). This kinetic study by Yu et al. (2015) showed that electron transfer occurred at rates that are competitive to sulfide oxidation by iron(III) (oxyhydr)oxides or molecular oxygen (i.e., 2.3 $\mu mol_{e^-}\ cm^{-3}\ day^{-1}$). Such rates could, therefore, explain the sulfide turnover under anoxic conditions. However, NOM proxies (HS) must be regenerated into an oxidized state in order to overcome their finite electron transfer capacity; this could potentially limit the importance of such a process (Yu et al. 2015). The input of oxidized HSs or the flow of oxygenated water could sustain this restoration and provide a sulfur sink in the form of organic sulfur incorporated into a HS. The role of redox impurities in the HS (i.e., redox-active and non-redox-active metal ions) used by Yu et al. (2015) was not quantified and future work should definitely focus on ternary systems (S, metal ions, NOM).

As mentioned above, EAC and EDC are characteristics of a given HS and are strongly dependent on its chemical nature (Aeschbacher et al. 2010). However, changing climate conditions may in turn affect HS electron transfer capacities because redox processes are temperature dependent. Moreover, temperature not only directly changes redox processes by changing kinetics, it influences the precipitation and hydration status of soils (i.e., permafrost vs wetlands vs agricultural soils, and so on) so inducing waterlogged (and more reducing) conditions or more aerated (and more oxic) conditions. As a result, the nature of NOM can vary in soils along a climate gradient, or during episodes of glaciation/deglaciation, or become accelerated during the thawing of soils at higher latitudes. Tan et al. (2017) showed that EDC and EAC decreased and increased, respectively, with increasing soil temperature. They demonstrated that EAC was higher for HAs than for FAs extracted from the same original soils (i.e., from 200 to 800 $\mu mol_{e^-} g^{-1}$ FA and only from 500 to 1,500 $\mu mol_{e^-} g^{-1}$ HA). Looking at a wide range of chemical parameters representing structural changes in the selected HS, they concluded, as Aeschbacher et al. (2010) did, that the correlation between electron transfer capacities and different physico-chemical parameters are not HS-source dependent. However, they pointed out the potential strong role of microbial necromass contribution to the NOM extracted in alkaline conditions for soils with longer turnover (Tan et al. 2017). Consequently, the use of the EAC to EDC ratio as a proxy for the magnitude of NOM degradation and transformation in soils is reinforced by these studies.

MICROBIALLY MEDIATED REDOX REACTIONS IN SOILS

In soils, the diversity of prokaryote metabolisms originates partly from the energy source these organisms need. Chemo-organotrophs oxidize a variety of organic compounds; chemo-lithotrophs oxidize inorganic compounds [such as H_2, H_2S, NH_4^+, or Fe(II) and Mn(II), As(III)]; phototrophs are able to convert light energy into chemical energy in locations where light is available. In anoxic environments (deep soil or waterlogged soils), respiration processes require terminal electron acceptors other than O_2. In this case, micro-organisms called either facultative aerobes or obligate anaerobes will be able to conduct anaerobic respiration using oxidized manganese ions (Mn^{4+}), nitrate ion (NO_3^-), ferric ion (Fe^{3+}), sulfate ion (SO_4^{2-}), carbon dioxide (CO_2), and a variety of HSs (e.g., chlorobenzoate or fumarate) as terminal electron acceptors. The use of oxidized metal species such as As(V), Se(VI), Cr(VI) and U(VI) as final electron acceptors has significant implications for the mobility and toxicity of these inorganic pollutants. Dissolved and particulate HSs can be reduced and have been shown to act as electron shuttles for the indirect reduction of Fe(III)-bearing minerals by micro-organisms (Roden et al. 2010). Given their associated redox potential, the energy released from oxidation using O_2 is greater than the use of any other terminal electron acceptors. In addition to respiration, some inorganic compounds (NO_3^-, SO_4^{2-}, and CO_2) can be reduced and used in biosynthesis as sources of cellular nitrogen, sulfur and carbon. This reduction process is called assimilative metabolism, in opposition to a dissimilative metabolism for which an electron acceptor is reduced and the reduced product is excreted into the environment. Finally, many detoxification processes involve redox processes that convert toxic forms of an element into less harmful species. Thus, microbes participate in a great number of element cycles in soils by modifying an elements redox status.

As an example, oxidation of Fe(II) by O_2 can be biotically or chemically catalyzed (Melton et al. 2014). Bacteria belonging to the phylum Proteobacteria, which include *Leptothrix*, *Gallionella* and *Sideroxydans* and which are micro-aerophilic Fe(II)-oxidizers. *Leptothrix* and *Gallionella* growth is slowed down under anoxic conditions and actually stops under high redox variations. The conditions by which Fe(II) oxidation is biotically catalyzed are, thus, drastic: little oxidation occurs in wetlands subjected to recurrent redox cycles. In these systems, and particularly at circumneutral pH, Fe(II) oxidation is mainly driven by a three-step abiotic reaction: first, a rate-limiting oxidation of Fe(II) by O_2; second, oxidation by secondary oxidants (reactive oxygen species); third, the reaction is surface-catalyzed by the previously produced Fe(III) oxyhydroxides (auto-oxidation). However, under O_2-limiting conditions, microbial Fe(II) oxidation can outcompete abiotic Fe(II) oxidation at temperatures higher than 20°C, which corresponds to, for example, the optimum growth temperature of *Gallionella ferruginea* (Melton et al. 2014).

Many abiotic redox reactions are catalyzed by micro-organisms. At low pH, Fe(II) microbial oxidation dominates because chemical oxidation of Fe(II) is kinetically limited. It is only at near-neutral pH that competition occurs between microbial (micro-aerophilic Fe(II)-oxidizing bacteria) and chemical Fe(II) oxidation (Borch et al. 2009). Abiotic Mn(II) and Mn(III) oxidation, while being possible, is usually kinetically limited, and biological Mn oxidation is, thus, dominant in the environment, with reported oxidation rates up to five orders of magnitude higher. As a result, most Mn(IV) oxides in the environment are believed to derive from biogenic Mn(II) oxidation (Tebo 2004). It seems as if Mn bio-oxidation indirectly controls the redox state of elements such as Cr or U, as well as their mobility and toxicity.

An important process associated with redox processes is the release of poorly soluble metabolic by-products by micro-organisms, resulting in the formation of biologically induced minerals. Precipitation of oxidized iron (Melton et al. 2014), the formation of manganese oxides nanoparticles, or the reduced forms of chromium or uranium are but a few examples. Also, micro-environments within biofilms and cell surfaces function as nucleation sites which can enhance local oversaturation relative to mineral phases, and, consequently, favour metal immobilization. There is also evidence for microbial communities exerting a major control on mineral weathering that involves bio-oxidation processes, with strong increases in dissolution rates for soil bacteria and up to two orders of magnitude for groundwater bacteria.

A wide range of micro-organisms can produce the extracellular superoxide anion $O_2^{\bullet-}$ and a variety of reactive oxygen species (Diaz 2013). These molecules initiate strong reduction and oxidation reactions, with $OH^\bullet$ being among the strongest oxidants in the environment. These processes have long been overlooked despite their potentially great importance for the cycling of metal(loid)s in environments not exposed to light.

REDOX CONTROL ON THE FATE OF METAL CONTAMINANTS

Redox-Sensitive Elements

Arsenic Redox Behaviour in Peatlands and Wetlands

Arsenic is oxidized/reduced by biotic and abiotic oxidants [such as Mn(IV), HS radicals, reactive Fe minerals, etc.]. In wetlands and peatlands, arsenic speciation is mainly

controlled by Fe redox reactions and the carbon cycle. Under oxidizing conditions, As(V) is bound as ternary complexes between As(V), Fe(III) and OM are bound onto Fe–OM nano-aggregates (Guenet et al. 2016), and small amounts of As(III) can be detected (Guénet et al. 2016). The presence of Fe as a monomer or as clusters bound to NOM and nano-sized Fe(III) oxyhydroxides limits As(III) binding as bi-dendate, corner-sharing complexes, which have been suggested to catalyze As(III) oxidation (Auffan et al. 2008). This results in As(III) preservation in wetland, even under prolonged oxidizing periods (Guénet et al. 2016).

Under reducing conditions, As speciation depends on the stability of the phases it is a part of, and its solubilization is indirectly controlled by NOM (Davranche et al. 2013). When As is bound to Fe(III)-oxyhydroxides, its solubilization depends on the rates and extent of reductive dissolution of these minerals, and, thus, on the NOM's ability to bind the solubilized Fe(II) and to act as an electron shuttle. In organic rich environments, NOM binds the released Fe(II), preventing its re-adsorption and its subsequent precipitation as secondary minerals. This results in a high extent of Fe(III) oxyhydroxide dissolution and the release of associated elements such as As. Combining wetland soil reducing experiments and a genomic study, Dia et al. (2015) suggested that arsenic is released as As(V) in the reduced solution, and is then biotically reduced through detoxification mechanisms involving micro-organisms such as *Geobacter*. Dissimilatory reduction of As(V) by metal-reducing bacteria can also occur. By contrast, in peatland, where reducing conditions are more intense, Fe(III) oxyhydroxides are absent. Without them, arsenic present as As(III) is bound to NOM via sulfhydryl reactive sites, as mono-dentate complexes, and/or forms nano-crystalline As sulfides (Langner et al. 2011).

Copper and Silver Interaction with Reduced NOM

Metal binding to NOM affects its electron transfer capacities. In turn, redox processes mediated by NOM will affect the metal redox state for elements such as Cu or Ag. For copper, the redox state is related to the stability of complexes formed by NOM and the different Cu redox states: Cu(II), Cu(I) and Cu(0). Fulda et al. (2013) showed that reduced NOM stabilizes Cu(I) complexes when Cu(II) or Cu(I) were added at low loadings. At higher loadings, the formation of Cu(0) nanoparticles was detected and could represent up to 65% of the total copper. The formation of nano-Ag(0) was also observed when Ag(I) was exposed to reduced NOM (Maurer et al. 2012). These results demonstrate that reduced NOM will prevent the disproportionation of redox-sensitive elements (e.g., Cu) in NOM-rich systems, where N and S functional groups account for redox-sensitive element stabilization (Fulda et al.2013).

Non-Redox-Sensitive Elements: Redox Oscillations and Rare Earth Element Mobility

Rare earth elements (REEs) are now considered as emerging pollutants. They are used in many high-technology products and no efficient recycling technologies exist. Several disruptions in their biogeochemical cycle have been observed (e.g., for Gd and La). Redox variations can indirectly influence the speciation of non-redox-sensitive elements, such as REEs, except for Ce(III) which can be oxidized to Ce(IV). Under reducing conditions, in water-logged soils, Fe(III) oxyhydroxides are reductively dissolved and there can be a concomitant release of REEs, Fe(II), and NOM (either dissolved or colloidal). This has been observed in experimental and field studies regardless of soil type (e.g., Cao et al. 2001). The REEs are solubilized as colloids and dissolved organic complexes (Guénet et al. 2018). Natural OM is released by desorption from soil minerals in response to the pH increase involved by the H^+ consumption of reducing reactions (Grybos et al. 2009). Under reducing conditions, REE solubilization is, therefore, driven by pH increase, involving desorption of the colloidal NOM onto which they are bound.

Once conditions become oxidizing, Fe and NOM precipitate as nano-aggregates, as previously described. However, in the field, no drastic modifications to REE patterns and speciation occurs between reducing and oxidizing periods (Fig. 4). More recently, Guénet et al. (2018) demonstrated through redox alternating experiments that REE patterns varied between redox cycles and were distributed in various size fractions of the oxidation by-products. Using REE pattern evolution and concentrations, Guénet et al. (2018) determined that REEs are concentrated in particulate and colloidal fractions. The REEs are bound to humic substances and NOM of bacterial origin embedding Fe(III) nano-oxyhydroxides aggregates in the particulate fraction, whereas REEs are bound to Fe–NOM nano-aggregates in the colloidal fraction. These results show that soil re-oxidation involves the scavenging and immobilization of large amounts of REEs.

Interestingly, reducing and oxidizing REE patterns are different for field and experimental conditions (Fig. 4). This is a consequence of underestimating Fe control, even under reducing conditions. However, reduction in a riparian wetland is insufficient to allow total Fe–NOM

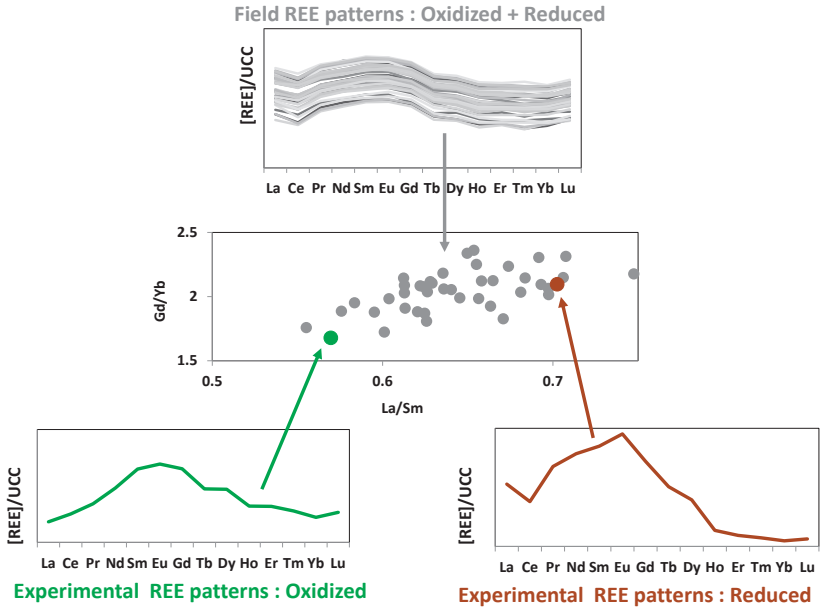

Figure 4 Rare earth element (REE) patterns of field of the Mercy wetland (France) collected during the hydrological years (under both reducing and oxidizing periods) as compared to experimental soil solutions produced from the Mercy wetland soil incubations under reducing and oxidizing conditions, and the corresponding La/Sm and Gd/Yb ratios. The REEs are normalized relative to the REE content of the upper continental crust (UCC) (logarithmic scale). Field REE patterns are different and varied from the REE pattern obtained under experimental oxidizing conditions (REE bound to Fe–OM aggregates) and from the REE pattern obtained under experimental reducing conditions (REE bound to OM), suggesting that REE speciation in the field is controlled by both OM and Fe aggregates and, therefore, that Fe aggregates are not totally dissolved even under the reducing period.

nano-aggregate dissolution. Speciation of the REEs is, thus, controlled by both NOM (major) and Fe (minor) under environmental conditions.

PERSPECTIVES

Electron transfer processes are needed to fully understand and predict environmental perturbations. For instance, few studies address the potential impact of climate changes on redox cycles. What are the consequences of increasing the precipitation and the subsequent flooding in soil redox conditions? What is its impact on ecosystem micro-biodiversity and activity-controlling biotic redox changes? More data are needed regarding electron transfer rates during direct transfer. More work is needed on cable bacteria and microbial nanowires. More work is needed on ligand-mediated transfer between microbes and minerals. Also, the kinetic processes that govern electron buffering capacity of dissolved and particulate NOM need further investigations. What is the role of sulfur moieties in metal ion speciation? What are the reactive oxygen species produced under aphotic conditions by biotic and abiotic processes?

We have, in this review, focused on the molecular-scale processes that control trace element and contaminant cycling at larger scales. However, an open question remains regarding the incorporation of such knowledge in quantitative models that describe the fate of these elements in the critical zone.

ACKNOWLEDGMENTS

We thank Dr. Anne-Catherine Pierson-Wickmann for her construction of FIGURE 1. The authors thank Dr. A. Kappler and two anonymous reviewers. We appreciate their thoughtful suggestions. We also thank Dr. Maria Rita Cicconi for additional inputs as well as editorial handling. This work was supported by the Projects ANR- 12-IS06-0001, MAMBA ANR-18-CE01-0001 and ARSENORG ANR-11- JS56-0010.

REFERENCES

Aeschbacher M, Sander M, Schwarzenbach RP (2010) Novel electrochemical approach to assess the redox properties of humic substances. Environmental Science & Technology 44: 87-93

Alowitz MJ, Scherer MM (2002) Kinetics of nitrate, nitrite, and Cr(VI) reduction by iron metal. Environmental Science & Technology 36: 299-306

Ardo SG and 6 coauthors (2015) Oxidative degradation of nalidixic acid by nano-magnetite via Fe^{2+}/O_2-mediated reactions. Environmental Science & Technology 49: 4506-4514

Auffan M and 11 coauthors (2008) Enhanced adsorption of arsenic onto maghemites nanoparticles: As(III) as a probe of the surface structure and heterogeneity. Langmuir 24: 3215-3222

Benedetti MF and 5 coauthors (1996) Metal ion binding by natural organic matter: from the model to the field. Geochimica et Cosmochimica Acta 60: 2503-2513

Borch T and 6 coauthors (2009) Biogeochemical redox processes and their impact on contaminant dynamics. Environmental Science & Technology 44: 15-23

Cao X, Chen Y, Wang X, Deng X (2001) Effects of redox potential and pH value on the release of rare earth elements from soil. Chemosphere 44: 655-661

Davranche M and 8 coauthors (2013) Organic matter control on the reactivity of Fe(III)-oxyhydroxides and associated As in wetland soils: a kinetic modeling study. Chemical Geology 335: 24-35

Dia A and 10 coauthors (2015) Bacteria-mediated reduction of As(V)-doped lepidocrocite in a flooded soil sample. Chemical Geology 406: 34-44

Diaz JM and 5 coauthors (2013) Widespread production of extracellular superoxide by heterotrophic bacteria. Science 340: 1223-1226

Fulda B, Voegelin A, Maurer F, Christl I, Kretzschmar R (2013) Copper redox transformation and complexation by reduced and oxidized soil humic acid. 1. X-ray absorption spectroscopy study. Environmental Science & Technology 47: 10903-10911

Gentile L, Wang T, Tunlid A, Olsson U, Persson P (2018) Ferrihydrite nanoparticle aggregation induced by dissolved organic matter. Journal of Physical Chemistry A 122: 7730-7738

Guénet H and 7 coauthors (2017a) Highlighting the wide variability in arsenic speciation in wetlands: a new insight into the control of the behavior of arsenic. Geochimica et Cosmochimica Acta 203: 284-302

Guénet H and 10 coauthors (2017b) Characterization of iron–organic matter nano-aggregate networks through a combination of SAXS/SANS and XAS analyses: impact on As binding. Environmental Science: Nano 4: 938-954

Guénet H and 6 coauthors (2016) Evidence of organic matter control on As oxidation by iron oxides in riparian wetlands. Chemical Geology 439: 161-172

Guénet H and 9 coauthors (2018) Experimental evidence of REE size fraction redistribution during redox variation in wetland soil. Science of the Total Environment 631-632: 580-588

Jiang J, Bauer I, Paul A, Kappler A (2009) Arsenic redox changes by microbially and chemically formed semiquinone radicals and hydroquinones in a humic substance model quinone. Environmental Science & Technology 43: 3639-3645

Langner P, Mikutta C, Kretzschmar R (2012) Arsenic sequestration by organic sulphur in peat. Nature Geoscience 5: 66-73

Macalady DL, Walton-Day K (2011) Redox chemistry and natural organic matter (NOM): geochemists' dream, analytical chemists' nightmare. In: Tratnyek PG, Grundl TJ, Haderlein SB (eds) Aquatic Redox Chemistry. American Chemical Society, pp 85-111

Maurer F, Christl I, Hoffmann M, Kretzschmar R (2012) Reduction and reoxidation of humic acid: influence on speciation of cadmium and silver. Environmental Science & Technology 46: 8808-8816

Melton ED, Swanner ED, Behrens S, Schmidt C, Kappler A (2014) The interplay of microbially mediated and abiotic reactions in the biogeochemical Fe cycle. Nature Reviews Microbiology 12: 797-808

Quénéa K, Derenne S, Benedetti MF (In Press) Insight into continental organic matter: a chemist's view. In: Horváth IT, Malacria M (eds) Advanced Green Chemistry, Part 2. World Scientific Publishing Company

Roden EE and 7 coauthors (2010) Extracellular electron transfer through microbial reduction of solid-phase humic substances. Nature Geoscience 3: 417-421

Stewart SM, Hofstetter TB, Joshi P, Gorski CA (2018) Linking thermodynamics to pollutant reduction kinetics by Fe^{2+} bound to iron oxides. Environmental Science & Technology 52: 5600-5609

Tan W and 12 coauthors (2017) Increased electron-accepting and decreased electron-donating capacities of soil humic substances in response to increasing temperature. Environmental Science & Technology 51: 3176-3186

Tebo BM and 7 coauthors (2004) Biogenic manganese oxides: properties and mechanisms of formation. Annual Review in Earth Planetary Sciences 32: 287-328

Thomas-Arrigo LK, Mikutta C, Byrne J, Kappler A, Kretzschmar R (2017) Iron(II)-catalyzed iron atom exchange and mineralogical changes in iron-rich organic freshwater flocs: an iron isotope tracer study. Environmental Science & Technology 51: 6897-6907

Vilgé-Ritter A, Rose J, Masion A, Bottero J-Y, Lainé J-M (1999) Chemistry and structure of aggregates formed with Fe-salts and natural organic matter. Colloids and Surfaces A: Physicochemical and Engineering Aspects 147: 297-308.

Yu Z-G, Peiffer S, Göttlicher J, Knorr K-H (2015) Electron transfer budgets and kinetics of abiotic oxidation and incorporation of aqueous sulfide by dissolved organic matter. Environmental Science & Technology 49: 5441-5449

Zhou S, Chen S, Yuan Y, Lu Q (2015) Influence of humic acid complexation with metal ions on extracellular electron transfer activity. Scientific Reports 5, doi: 10.1038/srep17067

Biogeochemical Controls on the Redox Evolution of Earth's Oceans and Atmosphere

Christopher T. Reinhard[1,2,3] and Noah J. Planavsky[2,4]

1811-5209/20/0016-0191$2.50 DOI: 10.2138/gselements.16.3.191

The redox state of Earth's atmosphere has undergone a dramatic shift over geologic time from reducing to strongly oxidizing, and this shift has been coupled with changes in ocean redox structure and the size and activity of Earth's biosphere. Delineating this evolutionary trajectory remains a major problem in Earth system science. Significant insights have emerged through the application of redox-sensitive geochemical systems. Existing and emerging biogeochemical modeling tools are pushing the limits of the quantitative constraints on ocean–atmosphere redox that can be extracted from geochemical tracers. This work is honing our understanding of the central role of Earth's biosphere in shaping the long-term redox evolution of the ocean–atmosphere system.

KEYWORDS: biogeochemistry, oxygenation, biosphere, redox, evolution

REDOX ON A PLANETARY SCALE

Earth's Modern Oxygen Cycle

On the modern Earth, molecular oxygen (O_2) is produced through photosynthesis in sunlit surface environments in which cyanobacteria, algae, and plants use energy from the Sun to transfer electrons from water to biomass. Much of the biomass produced by the photosynthetic biosphere is consumed rapidly through aerobic respiration, which gains energy by transferring electrons from biomass back to O_2. These coupled processes can be denoted as:

$$CO_2 + H_2O \leftrightarrow CH_2O + O_2 \quad (1)$$

Any photosynthetic biomass removed from the surface system via burial in marine or terrestrial sediments leads to a net accumulation of O_2 in the ocean–atmosphere system (moving from left to right in Equation 1). On geologic timescales, this organic matter can be consumed through exhumation and oxidation in terrestrial weathering environments and through thermal breakdown of organic carbon during metamorphism. Both of these processes lead, ultimately, to a net consumption of O_2 from the ocean–atmosphere system (moving from right to left in Equation 1). Thus, Equation (1) can be thought of conceptually as showing a "fast" O_2 cycle (photosynthesis/respiration), responding on timescales of less than ~10^3 years, and a "slow" O_2 cycle (organic carbon burial and weathering/thermal breakdown), responding on timescales of ~10^6 years.

There is an additional long-term cycle that links O_2 to the cycling of sulfur (S) and iron (Fe) at Earth's surface:

$$2Fe_2O_3 + 8SO_4^{2-} + 16H^+ \leftrightarrow 15O_2 + 4FeS_2 + 8H_2O \quad (2)$$

Moving from left to right in Equation (2) denotes the sum of three processes: (1) photosynthesis; (2) consumption of biomass through microbial sulfate (SO_4^{2-}) reduction, producing reduced sulfur (S^{2-}); (3) formation of pyrite (FeS_2) via reaction between reduced sulfur and reactive iron in the environment (shown here as hematite, Fe_2O_3). In essence, the overall effect of this process is to transfer reducing power from water to pyrite via organic biomass, causing a net release of O_2. The subsequent uplift/weathering and/or volatilization of reduced sulfur species in the crust balances this release of O_2 on geologic timescales (moving from right to left in Equation 2).

Oxygen can also be consumed via reaction with reduced volcanic volatiles that originate from Earth's crust and mantle and during the oxidation of reduced minerals in seafloor basalt as oxygen-rich seawater percolates through the oceanic lithosphere. In addition, the escape of hydrogen to space allows oxygen atoms produced by photochemistry to recombine as O_2, irreversibly oxidizing Earth surface environments. Similarly, oxidized or reduced species can be subducted into Earth's mantle, leading to secular net oxidation/reduction of Earth's surface environments that is not necessarily irreversible but that can persist on timescales of mantle overturn (that is, on the order of ~10^9 years). For example, organic carbon deposited in deep-sea sediments can potentially be preserved as graphite during subduction, leading to a net export of reducing power from Earth's surface (FIG. 1).

Nutrients as a Driver of Earth's Redox Balance

The global oxygen cycle is fundamentally a story of the redox cycling of carbon, sulfur, and iron through the Earth system. However, O_2 cycling is also fundamentally controlled by the availability of bio-essential elements ("nutrients") in oceanic and terrestrial ecosystems. All organisms require a range of major and trace nutrients to produce biomass, which can be seen by elaborating on Equation (1) to include the major nutrients involved in oxygenic photosynthesis:

1 School of Earth and Atmospheric Sciences
Georgia Institute of Technology
Atlanta, GA, USA
E-mail: chris.reinhard@eas.gatech.edu

2 NASA Astrobiology Institute, Alternative Earths Team

3 NASA Nexus for Exoplanet System Science (NExSS)

4 Department of Geology and Geophysics
Yale University
New Haven, CT, USA
E-mail: noah.planavsky@yale.edu

$$106CO_2 + 16HNO_3 + H_3PO_4 + 122H_2O \leftrightarrow (CH_2O)_{106}(NH_3)_{16}(H_3PO_4) + 138O_2 \quad (3)$$

The stoichiometric coefficients in Equation (3) denote the bulk stoichiometry of photosynthetic biomass (the classical "Redfield ratio", initially observed by US oceanographer Alfred Redfield in 1934), which can vary significantly as a function of taxonomic identity and organism growth status. A variety of trace elements—for example, Fe and Zn—are also incorporated into biomass, but for simplicity are neglected here. An important result is that every 138 moles of O_2 produced by the photosynthetic biosphere requires a mole of bioavailable phosphorus (P, shown here as phosphate) and 16 moles of bioavailable nitrogen (N, shown here as nitrate). These nutrient elements can then either be recycled by respiration back to inorganic, bioavailable forms ("remineralized") or buried in sediments. In the ocean, nutrients are generally taken up in sunlit surface waters and exported to depth with organic matter, leading to a vertical "biological pump" of organic carbon and nutrients into the ocean interior, with a corresponding demand for O_2.

There are strong stabilizing feedbacks that link the oceanic inventories of bioavailable nitrogen and phosphorus (Tyrrell 1999) and that draw together the long-term cycling of nutrients and O_2 (Fig. 2). For instance, a transient increase in the size of the marine phosphorus reservoir is expected to catalyze increased rates of biological nitrogen fixation, increasing oceanic nitrogen content and bringing the mean ocean N and P budgets back to a "set point" specified by the growth requirements of phytoplankton (the "Redfield ratio"). Conversely, a transient decrease in the size of the marine phosphorus reservoir should inhibit growth of less competitive biological nitrogen fixers, such that

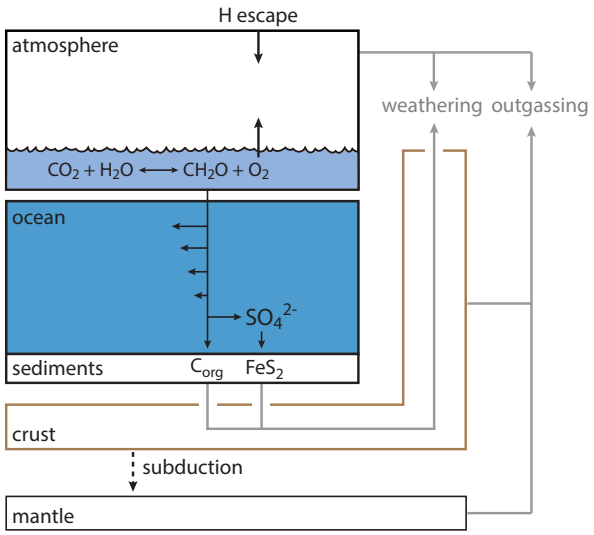

Figure 1 Schematic of Earth's global oxygen cycle. Black arrows = oxygen sources; grey arrows = oxygen sinks. Oxygenic photosynthesis produces O_2 in the surface ocean, and some of this is released to the atmosphere. A corresponding amount of organic matter (CH_2O) is exported from the sunlit surface ocean, creating a respiratory demand for O_2 in the ocean's interior (the 'biological carbon pump'). A fraction of the reducing power contained in this organic matter is deposited in marine sediments, either directly as organic carbon or through burial of reduced sulfur. This burial represents a net release of O_2. On geologic timescales, this reducing power is reintroduced to the surface system via uplift, and consumed via weathering or through metamorphic production of reducing gases. Additional long-term fluxes include the escape of hydrogen to space, subduction of oxidized or reduced species into the deep Earth, and the degassing of primitive reducing volatiles from Earth's mantle.

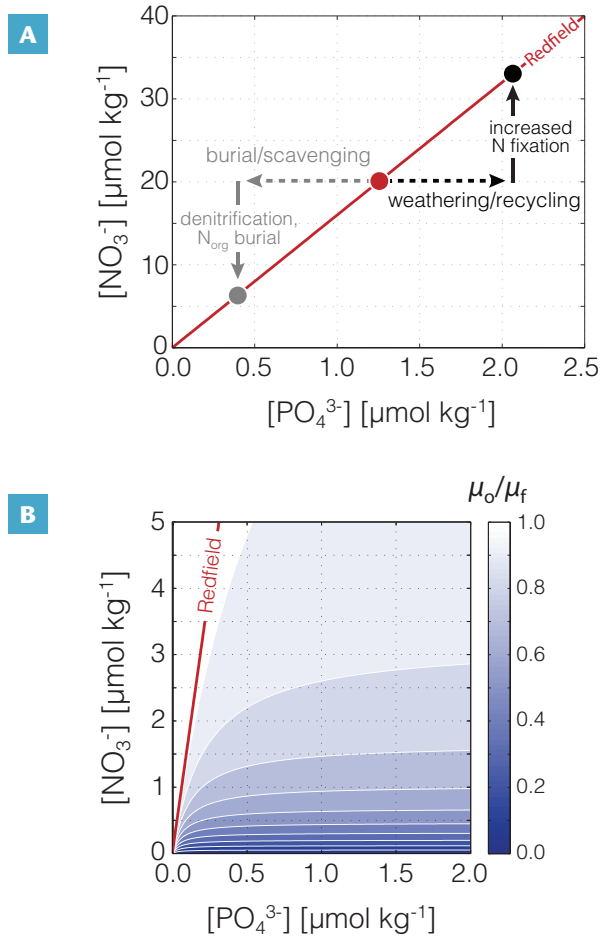

Figure 2 Processes that regulate the mean ocean nutrient budgets. (**A**) The Redfield line (in red) is the ratio of N to P in marine phytoplankton and in the deep oceans. A point on the line (red circle) is taken as an example of what happens under two scenarios: enhanced weathering/recycling of P and elevated burial/scavenging of P. Dashed and solid arrows denote adjustments following the perturbations to the ocean phosphate (PO_4^{3-}) budget from an initial state. (**B**) Long-term regulation of the mean ocean N and P budgets is driven by competition between N fixing (μ_f) and nonfixing phytoplankton (μ_o) (Tyrrell 1999). When P is in excess relative to N, the N fixers outcompete other phytoplankton (low μ_o/μ_f) and push the ocean N/P ratio back toward that required for the growth of nonfixing plankton (the Redfield ratio).

continued loss of nitrogen from the ocean interior through microbial denitrification and the sedimentary burial of organic nitrogen will draw the nitrogen reservoir down until the N/P set point is reached (Fig. 2). This simple thermostatic behavior can be modulated by the taxonomically diverse nutrient requirements of plankton and ocean circulation, but requires only that nitrogen fixation incur an energetic cost due to the difficulty of enzymatically breaking down N_2 (Tyrrell 1999). In this framework, the long-term fertility of the biosphere (and, thus, the capacity of Earth's biosphere to produce O_2) is controlled most directly by the availability of P in Earth's oceans. Earth's surface O_2 cycle must, therefore, be considered in the context of the processes that regulate oceanic P cycling.

The Importance of Ocean Redox Structure for Oxygen and Nutrient Cycling

The impacts of atmospheric chemistry and planetary nutrient cycling on Earth's surface O_2 are tightly linked through ocean redox structure. First, it is the abundance of O_2 in the atmosphere and the cycling of nutrients through the biological pump that structure the ocean

redox landscape. At the same time, this redox landscape feeds back on marine nutrient cycling through a range of mechanisms that can, ultimately, act as either positive or negative feedbacks on long-term biospheric O_2 production.

Deep ocean O_2 is governed by the balance between O_2 supply through gas exchange at the ocean surface and through downward mixing of O_2-rich waters, and by O_2 demand through aerobic respiration once a water mass is no longer in communication with the atmosphere. Thus, under a constant ocean circulation regime, O_2 supply is controlled principally by atmospheric O_2 abundance, whereas O_2 demand is controlled principally by the intensity of the biological carbon pump (and, hence, nutrient abundance). This relationship can be understood heuristically by considering a simple three-box ocean model of oxygen and nutrient biogeochemistry (Fig. 3). In this model, we can derive a simple expression for the global average O_2 concentration in the ocean interior at steady state ($[O_2]_{int}$):

$$[O_2]_{int} = [O_2]_{vent} - \lambda([PO_4^{3-}]_{int} - [PO_4^{3-}]_{vent}) \quad (4)$$

where $[O_2]_{vent}$ and $[PO_4^{3-}]_{vent}$ denote the oxygen and phosphate concentrations of cold, high-latitude waters ventilating the ocean interior, $[PO_4^{3-}]_{int}$ denotes the phosphate abundance of the ocean interior, and λ denotes the stoichiometric relationship between the amount of phosphate released during consumption of O_2 during aerobic respiration (see Equation 3). The term in parentheses describes the fraction of nutrients mixed into the high-latitude surface ocean that is consumed during photosynthesis (currently with a value of ~1 µmol kg^{-1}) and can be thought of as depicting the efficiency of the biological pump.

Using this approach, one can estimate the steady state concentration of O_2 in the deep ocean as a function of both atmospheric O_2 abundance and biological pump efficiency (Fig. 3). This analysis shows that the ocean interior can be driven to the point of pervasive anoxia by either dropping atmospheric O_2 abundance or by increasing the strength/efficiency of the biological pump. For example, with a modern biological pump this model predicts that the ocean interior would become pervasively anoxic at an atmospheric O_2 abundance ~40% that of the modern Earth. Alternatively, with an atmospheric O_2 abundance of 10% of the modern Earth even a relatively weak biological pump operating at ~20% of modern intensity would provide sufficient O_2 demand in the ocean interior to drive the ocean toward extensive anoxia. Despite being incapable of capturing the impact of differences in ocean circulation, remineralization length scale of organic carbon in the water column, or spatial variability in deep O_2, this model illustrates an important principle—it is the combination of atmospheric O_2 abundance and the activity level of the ocean biosphere (as governed by ocean nutrient inventory) that fundamentally dictates the marine redox landscape.

There is, however, an important caveat to this analysis. It implicitly assumes that the abundance of O_2 in the ocean–atmosphere system and the marine inventory of bioavailable phosphorus can be varied independently of one another. In reality, the throughput of bioavailable phosphorus fundamentally controls the ocean–atmosphere O_2 abundance at steady state (Lenton and Watson 2000), while ocean redox state controls the recycling and bioavailability of phosphorus in marine systems (Van Cappellen and Ingall 1994; Reinhard et al. 2017). To gain intuition for this, one can consider the dynamics regulating the most significant O_2 production and removal fluxes on the modern Earth—the burial and oxidation of organic carbon (Fig. 1). The efficiency of organic carbon burial in marine sediments, and, thus, the amount of O_2 released by the biosphere at a given nutrient abundance, increases as O_2 decreases. At the same time, all of the processes that consume O_2, including oxidation of organic carbon in the crust, slow down as O_2 drops. This combination provides strong negative feedback against decreasing atmospheric O_2—as atmospheric O_2 drops, the sources of O_2 tend to increase while the sinks tend to decrease, pushing atmospheric O_2 back up. Lowering atmospheric O_2 beyond a certain level requires either a decrease in the inputs of bioavailable P to the marine system or an increase in the inorganic sinks of P from the oceans (e.g., less efficient use of bioavailable P by the marine biosphere).

At the same time, ocean redox plays an important role in controlling the recycling and bioavailability of phosphorus, which, in turn, impacts long-term biospheric O_2 production. When the ocean interior is pervasively oxygenated, as on the modern Earth, bioavailable phosphorus is removed primarily through burial in marine sediments either as an authigenic mineral phase, or as a sorbed species on sedimentary Fe-oxides, or as a constituent of organic matter, with the remainder removed largely in association with Fe-oxide minerals in deep-sea hydrothermal systems (Ruttenberg 2014). In contrast, anoxic conditions can lead to a range of recycling processes that can dramatically impact phosphorus bioavailability. Anoxic and sulfidic

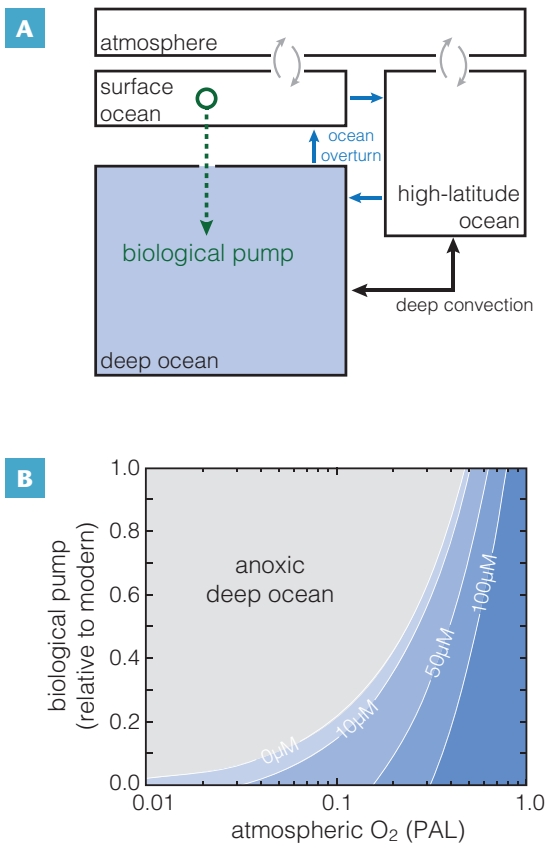

Figure 3 (**A**) Schematic depiction of a three-box model for oxygen and phosphorus distributions within the ocean. Oxygen is introduced through gas exchange at the ocean surface and then mixed throughout the ocean via overturning circulation and deep convection. Organic matter produced by photosynthesis sinks into the ocean interior (the ocean "biological pump"), and creates respiratory O_2 demand. (**B**) Steady state dissolved O_2 concentrations in the deep ocean as a function of both atmospheric O_2 level and the strength of the biological pump relative to that of the modern ocean. Contours are labeled according to dissolved O_2 concentration; the grey shaded region denotes conditions under which the deep ocean is expected to become anoxic. PAL = present atmospheric level.

conditions, either in the water column ("euxinia") or in surface marine sediments, result in remobilization of Fe-oxide–bound phosphorus and can change the style of organic phosphorus recycling, both of which can potentially lead to more effective recycling of bioavailable phosphorus under sulfidic anoxia (Van Cappellen and Ingall 1994). In contrast, anoxic but iron-rich ("ferruginous") conditions can lead to effective scavenging and removal of bioavailable phosphorus through two principal mechanisms: the formation of Fe-phosphate mineral phases and coprecipitation of P with other Fe-bearing minerals (see Reinhard et al. 2017 and references therein).

THE EVOLUTION OF OCEAN–ATMOSPHERE REDOX ON EARTH

Earth's modern atmosphere is strongly oxidizing, being composed of ~21% O_2 by volume, with reducing gases generally present at trace abundance. Indeed, this abundance of O_2 (and its photochemical by-product, ozone, O_3) gives rise to a series of compelling "biosignatures" in the atmosphere that are, in principle, detectable from remote distances through atmospheric spectroscopy (Meadows et al. 2018). An important consequence of this high O_2 level in the atmosphere is that the oceans are generally very well-oxygenated, despite a large and robust biosphere and attendant respiratory demand in the ocean's interior. However, atmospheric O_2 has changed by many orders of magnitude throughout Earth's history, in concert with dramatic shifts in biogeochemical cycling, tectonic events, perturbations to global climate, and biological innovations, all of which have impacted ocean redox structure.

Prior to the evolution of oxygenic photosynthesis, the abundance of O_2 in Earth's atmosphere would have been extremely low, with production largely through CO_2 photolysis, yielding ground-level O_2 abundances of ~10^{-12} times the present atmospheric level (PAL) (Kasting et al. 1979). This means that the redox state of the atmosphere would once have been dominated by some combination of H_2 and CH_4; O_2 would have been virtually absent from oceanic environments. Following the emergence of oxygenic photosynthesis, the potential for locally nontrivial dissolved O_2 abundances in the shallowest marine systems would have emerged (so-called "oxygen oases"). This conceptual framework finds support from both theoretical models (Olson et al. 2013) and geochemical observations (e.g., Planavsky et al. 2014). Nevertheless, the preservation of significant sulfur mass-independent fractionation (S-MIF) isotope signals in marine sediments deposited prior to ~2.3 Ga indicates a pervasively anoxic atmosphere (Farquhar et al. 2000), likely on the order of ~10^{-7} PAL (Zahnle et al. 2006). Such low atmospheric O_2 abundances are consistent with a wide range of independent geologic evidence (Holland 1984). Atmospheric O_2 would be regulated in this Earth system state via consumption by reduced volcanic gasses and reaction with reduced Fe and S in the Earth's crust, with localized regions of elevated O_2 in shallow seas (Fig. 4). An important wrinkle to this framework comes in the form of transient "whiffs" of atmospheric O_2 during the Neoarchean, as deduced from trace element, isotopic, and mineralogical records (see Lyons et al. 2014).

Although it seems clear that O_2 was present at trace abundance for most, if not all, of Hadean and Archean time (at levels of ~10^{-12} – 10^{-7} PAL), the abundances of the most important reducing gases, H_2 and CH_4, are not well-constrained. Photochemical models predict that a nontrivial abundance of reducing atmospheric gas (either H_2 or CH_4) must be present in order to preserve distinct exit channels for photolytic sulfur from the atmosphere and, thus, support the preservation of S-MIF signals. But the precise quantitative requirements are unclear. More recently, it has been suggested that the apparent mass fractionation of xenon isotopes in the Archean atmosphere requires a total hydrogen mixing ratio in the atmosphere above ~1% (corresponding to an atmospheric CH_4 abundance of ~0.5%) in order to support the requisite atmospheric escape rates (Zahnle et al. 2019). This is broadly consistent with photochemical and coupled biosphere–atmosphere models for the Archean Earth system (Kharecha et al. 2005; Ozaki et al. 2018).

A variety of geochemical and geologic observations, including the disappearance of S-MIF signals from the rock record, indicate that the initial accumulation of O_2 in Earth's atmosphere occurred at ~2.4–2.3 Ga. This is often referred to as the Great Oxidation Event (GOE). How "great" this event was, however, remains an open question. The disappearance of S-MIF signals from the sedimentary record only requires a relatively small change in the overall size of the atmospheric O_2 reservoir. For example, a shift in atmospheric pO_2 from 10^{-7} to 10^{-4} PAL, more than sufficient to shut down S-MIF signals, would require the net accumulation of only ~0.01% of the modern atmospheric O_2 inventory. Nevertheless, it is manifestly evident in a range of sedimentological and geochemical records that this geologically brief interval marks an important shift in the background redox state of Earth's atmosphere (Holland 1984).

More recently, it has been suggested that there was a protracted—but ultimately transient—period of elevated atmospheric O_2 abundance between ~2.2 Ga and 2.0 Ga (Fig. 4). This period coincides with a striking perturbation to Earth's carbon cycle, evident in an extended period of ^{13}C-enriched carbonates deposited worldwide—the so-called "Lomagundi Event" (Schidlowski et al. 1976). Early estimates suggested that this carbon cycle perturbation represented a long-term pulse of organic matter

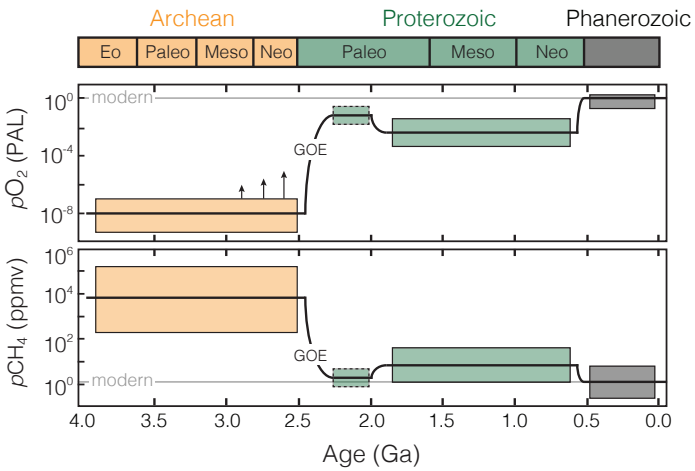

Figure 4 Evolving redox state of Earth's atmosphere in terms of the two major redox-active species in Earth's atmosphere: 1) partial pressures of oxygen (pO_2) relative to the present atmospheric level (PAL); 2) partial pressures of methane (pCH_4) in parts per million by volume (ppmv). Shaded boxes (Archean in orange; Proterozoic in green; Phanerozoic in grey) show ranges derived from the geologic record and theoretical models, while the black line on each of the two graphs shows one plausible trajectory through these models. Upward arrows denote possible Meso- to Neoarchean "whiffs" of atmospheric O_2, though their timing, duration, and magnitude are not fully known. A putative transient high-O_2 interval is also shown with the dashed shaded box (in the Paleoproterozoic), though the atmospheric composition during this period is not well-constrained. Values for the modern atmosphere are shown as grey lines. GOE = Great Oxidation Event.

deposition corresponding to the release of ~10–20 times the current atmospheric O_2 inventory (Karhu and Holland 1996). This is consistent with a number of geochemical records that suggest a transient elevation in atmospheric pO_2 during this interval (Blättler et al. 2018). However, the quantitative scaling between ^{13}C enrichment and O_2 release during this period is somewhat obscure, and it is not yet clear how this O_2 release would have partitioned itself within the ocean–atmosphere–crust system. For example, isotope-enabled biogeochemical models are capable of producing "Lomagundi-type" carbon isotope excursions under conditions of relatively modest atmospheric pO_2 (Miyazaki et al. 2018), but this requires a net transfer of oxidizing power to the crustal sulfate reservoir. In any case, it seems reasonable that between ~2.2 Ga and 2.0 Ga the ocean redox landscape would have featured a pervasively well-oxygenated mixed layer with dissolved O_2 concentrations controlled largely by gas exchange with the atmosphere, and possibly widespread oxygenation of the ocean interior. Fully elucidating these features of the Earth system during this period awaits more precise quantitative constraints on atmospheric O_2 abundance (Fig. 4).

Though it is apparent that atmospheric O_2 increased after ~2.5 Ga, atmospheric abundances of O_2 over the ensuing ~2 Gy are uncertain. A lack of significant stable chromium (Cr) isotope fractionation in some ironstones, marine shales, and ancient soil horizons (paleosols) has been interpreted to reflect very low atmospheric pO_2, perhaps as low as ~10^{-3} PAL, for much of the period between ~1.8 Ga and 0.8 Ga. This is consistent with the observed mobilization behavior of iron (Fe) and manganese (Mn) in paleosols, records of rare earth element (REE) behavior in marine carbonates, and the stable oxygen isotope composition of Proterozoic evaporite minerals (summarized in Planavsky et al. 2018). Some workers have suggested much higher levels of atmospheric pO_2 during this period (Zhang et al. 2016), raising the possibility of significant time-dependent variability in atmospheric redox during the Mesoproterozoic (cf. Planavsky et al. 2016). In any case, the paradigmatic view is that atmospheric pO_2 was significantly lower than that of the modern Earth prior to ~600–800 Ma, somewhere between ~0.1% PAL and 10% PAL (Fig. 4). Regulation of atmospheric O_2 in this state is still unclear, but it is likely to have been controlled by incomplete oxidation of reduced C, Fe, and S in Earth's crust together with muted biospheric O_2 production as a result of P scavenging from pervasively anoxic oceans.

Atmospheric CH_4 during Earth's middle history is less well-constrained, because there are currently no available geologic proxies for the quantitative abundance of CH_4 in Earth's atmosphere at intermediate redox states. Indeed, even under a mildly reducing atmosphere, proxy constraints are indirect and plagued by significant uncertainty. Photochemical models predict that once atmospheric O_2 is high enough to support significant ozone, CH_4 can be shielded from photochemical destruction and tends to "rebound" to relatively high values following an initial drop during the Great Oxidation Event (Claire et al. 2006), perhaps to as high as ~100 ppm. However, models of ocean biogeochemistry that take into account the potential for effective microbial sinks for CH_4 in marine environments tend to predict steady-state atmospheric CH_4 abundances that are much lower than ~100 ppm under Proterozoic conditions, more on the order of ~1–10 ppm (Olson et al. 2016), unless CH_4 abundances had been supplemented by significant fluxes from nascent terrestrial ecosystems (Zhao et al. 2018).

In any case, evidence from the rock record indicates a dramatic reorganization of Earth surface biogeochemistry and ocean–atmosphere redox state at some point in the late Proterozoic, perhaps as early as ~800 Ma (Lyons et al. 2014). This period may have marked a pervasive—though perhaps episodic—oxygenation of Earth's deepest oceans, broadly in step with major shifts in biospheric complexity and perturbations to global climate. Earth's ocean–atmosphere system has been largely oxidizing subsequent to this tumultuous interval. There have been very occasional excursions to more pervasively reducing environments in the ocean interior, but against a backdrop of strongly oxidizing atmospheric chemistry (Fig. 4). Regulation of atmospheric O_2 in this state has been principally through the incomplete oxidation of organic carbon in Earth's crust and the increased efficiency of organic carbon burial when oxygenation of the ocean interior decreases (Daines et al. 2017).

MAJOR REMAINING FRONTIERS

The history of ocean–atmosphere redox on Earth has been understood in broad strokes for many decades (Holland 1962), and this long-term evolutionary texture is very likely robust. However, placing quantitative constraints on ancient atmospheric composition and ocean chemistry is challenging, and many fascinating questions remain. In particular, the coming years will witness many exciting advances in efforts to place more precise constraints on background atmospheric O_2 during the Paleo- and Mesoproterozoic, to constrain the overall size and scope of Earth's photosynthetic biosphere through time, better understand the mechanisms regulating the amount of atmospheric O_2 during different periods of Earth's history and the transitions between them, and to develop a better mechanistic understanding of the processes that link major nutrient cycles to evolving ocean–atmosphere O_2.

Many of the geochemical proxies for the abundance of O_2 in surface environments that have been the most useful in recent years are still being developed, and more direct coupling of proxy records with quantitative models will be central to the further refinement of quantitative estimates for atmospheric pO_2. Issues of particular interest include constraining the duration, causes, and magnitude of Neoarchean "whiffs" of O_2; estimating atmospheric pO_2 during the putative "oxygen overshoot" in the Paleoproterozoic; and more definitively constraining O_2 levels in surface environments during the Mesoproterozoic in the lead up to the rise of complex life. In some cases, proxy reconstructions for atmospheric O_2 will rely on independent constraints on other atmospheric properties, such that the development of better estimates for other atmospheric gases (such as CO_2) will also be crucial for constraining O_2.

Much the same can be said for attempts to constrain the productivity of Earth's biosphere through time, a critical component of the O_2 cycle. A particularly exciting development in this regard is the exploration of the triple oxygen isotope composition of marine and lacustrine sediments during Earth's history, which can potentially be used to constrain global photosynthetic productivity (Crockford et al. 2018) or be inverted to estimate atmospheric pO_2 (Planavsky et al. 2018). However, a number of challenges remain, including the potentially sporadic stratigraphic distribution of the sedimentary archives for the rare oxygen isotope signal, the need for more mechanistic models that couple surface isotope signals to atmospheric production and downstream recycling, and limits of precision that may ultimately be controlled by the need for independent constraints on atmospheric CO_2.

Further development of empirical constraints from Earth's rock record will provide crucial tie points for theoretical models aimed at understanding the basic processes that regulate Earth's oxygen cycle, and the processes that link the surface redox landscape to nutrient recycling and the productivity of the biosphere. A striking example is the Earth system during mid-Proterozoic time, ~1.8–0.8 Ga. Models and existing geochemical data suggest that atmospheric O_2 was well below that of the modern Earth, but how such 'weakly oxygenated' conditions at Earth's surface would be regulated on long timescales is a major outstanding question. This is due in part to uncertainties in empirical reconstructions of atmospheric O_2, but it is also related to the fact that Earth's O_2 cycle at intermediate redox states is likely to be strongly controlled by a range of processes not currently well represented in biogeochemical models. Foremost, parameterizations of nutrient scavenging under reducing conditions; the competitive dynamics between oxygenic and anoxygenic photosynthetic organisms; and the redox cycling of reduced C, S, and Fe in Earth's crust under low O_2 conditions all need to be improved. Some of these improvements will only be possible with new kinetic data.

Interesting questions remain even deeper into Earth's past. For example, it is still not definitively known whether the reducing capacity of Earth's mantle (as described in Stagno and Fei 2020 this issue) has changed over time, with potentially dramatic implications for processes controlling atmospheric abundances of O_2, CH_4, H_2, and a range of other redox-active species. As a result, our understanding of the background redox state of Earth's atmosphere during Hadean/Archean time would benefit significantly from better empirical constraints on mantle redox state during Earth's early history and better empirical and/or theoretical constraints on degassing fluxes throughout Earth's evolution. In addition, it remains unclear when oxygenic photosynthesis first emerged and began to influence the redox structure of Earth's surface oceans. Constraining the timing of this foundational biological novelty with confidence will ultimately require the leveraging of new geochemical redox proxies, the combination of new observations with existing and well-established approaches, and better quantitative models for evaluating "false positives" for the presence of O_2 in Earth's surface environments when Earth's atmosphere was reducing.

ACKNOWLEDGMENTS

We are grateful to the NASA Astrobiology Institute, the NASA Nexus for Exoplanet System Science (NExSS), the Alfred P. Sloan Foundation, and the NSF Earth-Life Transitions Program for financial support. We are also particularly indebted to Giada Arney, Devon Cole, Sean Crowe, Kurt Konhauser, Stefan Lalonde, Timothy Lyons, Stephanie Olson, Kazumi Ozaki, and Edward Schwieterman for the discussions and collaborations that underpin much of what is discussed here.

REFERENCES

Blättler CL and 16 coauthors (2018) Two-billion-year-old evaporites capture Earth's great oxidation. Science 360: 320-323

Claire MW, Catling DC, Zahnle KJ (2006) Biogeochemical modelling of the rise in atmospheric oxygen. Geobiology 4: 239-269

Crockford PW and 9 coauthors (2018) Triple oxygen isotope evidence for limited mid-Proterozoic primary productivity. Nature 559: 613-616

Daines SJ, Mills BJW, Lenton TM (2017) Atmospheric oxygen regulation at low Proterozoic levels by incomplete oxidative weathering of sedimentary organic carbon. Nature Communications, doi:10.1038/ncomms14379

Farquhar J, Bao H, Thiemens M (2000) Atmospheric influence of Earth's earliest sulfur cycle. Science 289:756-758

Holland HD (1962) Model for the evolution of the Earth's atmosphere. In: Engel AEJ, James HL, Leonard BF (eds) Petrologic Studies: A Volume in Honor of A. F. Buddington. Geological Society of America, New York, pp 447-477

Holland HD (1984) The Chemical Evolution of the Atmosphere and Oceans. Princeton University Press, Princeton, 598 pp

Karhu JA, Holland HD (1996) Carbon isotopes and the rise of atmospheric oxygen. Geology 24: 867-870

Kasting JF, Liu SC, Donahue TM (1979) Oxygen levels in the prebiological atmosphere. Journal of Geophysical Research: Oceans 84: 3097-3107

Kharecha P, Kasting J, Siefert J (2005) A coupled atmosphere-ecosystem model of the early Archean Earth. Geobiology 3: 53-76

Lenton TM, Watson AJ (2000) Redfield revisited 2. What regulates the oxygen content of the atmosphere? Global Biogeochemical Cycles 14: 249-268

Lyons TW, Reinhard CT, Planavsky NJ (2014) The rise of oxygen in Earth's early ocean and atmosphere. Nature 506: 307-315

Meadows VS and 16 coauthors (2018) Exoplanet biosignatures: understanding oxygen as a biosignature in the context of its environment. Astrobiology 18: 630-662

Miyazaki Y, Planavsky NJ, Bolton EW, Reinhard CT (2018) Making sense of massive carbon isotope excursions with an inverse carbon cycle model. Journal of Geophysical Research: Biogeosciences, 123: 2485-2496

Olson SL, Kump LR, Kasting JF (2013) Quantifying the areal extent and dissolved oxygen concentrations of Archean oxygen oases. Chemical Geology 362: 35-43

Olson SL, Reinhard CT, Lyons TW (2016) Limited role for methane in the mid-Proterozoic greenhouse. Proceedings of the National Academy of Sciences of the United States of America 113: 11447-11452

Ozaki K, Tajika E, Hong PK, Nakagawa Y, Reinhard CT (2018) Effects of primitive photosynthesis on Earth's early climate system. Nature Geoscience 11: 55-59

Planavsky NJ and 15 coauthors (2014) Evidence for oxygenic photosynthesis half a billion years before the Great Oxidation Event. Nature Geoscience 7: 283-286

Planavsky NJ and 6 coauthors (2018) A case for low atmospheric oxygen levels during Earth's middle history. Emerging Topics in Life Sciences 2: 149-159

Planavsky NJ and 8 coauthors (2016) No evidence for high atmospheric oxygen levels 1,400 million years ago. Proceedings of the National Academy of Sciences of the United States of America 113: E2550-E2551

Reinhard CT and 9 coauthors (2017) Evolution of the global phosphorus cycle. Nature 541: 386-389

Ruttenberg KC (2014) The global phosphorus cycle. In: Karl DM, Schlesinger WH (eds) Treatise on Geochemistry, Volume 10, 2nd Edition. Elsevier, pp 499-558

Schidlowski M, Eichmann R, Junge CE (1976) Carbon isotope geochemistry of the Precambrian Lomagundi carbonate province, Rhodesia. Geochimica et Cosmochimica Acta 40: 449-455

Stagno V, Fei Y (2020) The redox boundary of Earth's interior. Elements 16: 167-172

Tyrrell T (1999) The relative influences of nitrogen and phosphorus on oceanic primary production. Nature 400: 525-531

Van Cappellen P, Ingall ED (1994) Benthic phosphorus regeneration, net primary production, and ocean anoxia: a model of the coupled marine biogeochemical cycles of carbon and phosphorus. Paleoceanography and Paleoclimatology 9: 677-692

Zahnle K, Claire M, Catling D (2006) The loss of mass-independent fractionation in sulfur due to a Palaeoproterozoic collapse of atmospheric methane. Geobiology 4: 271-283

Zahnle KJ, Gacesa M, Catling DC (2019) Strange messenger: a new history of hydrogen on Earth, as told by xenon. Geochimica et Cosmochimica Acta 244: 56-85

Zhang S and 9 coauthors (2016) Sufficient oxygen for animal respiration 1,400 million years ago. Proceedings of the National Academy of Sciences of the United States of America 113: 1731-1736

Zhao M, Reinhard CT, Planavsky N (2018) Terrestrial methane fluxes and Proterozoic climate. Geology 46: 139-142

Association of Applied Geochemists

www.appliedgeochemists.org

OBITUARY FOR VALE DAVID JOHN GRAY (1961–2019)

The exploration geochemical community recently lost one of its most energetic members, Dr David Gray. He died following a battle with brain cancer on 21 November 2019 at his home in Australia surrounded by his family.

David was a senior principal geochemist in the Commonwealth Scientific Industrial Research Organisation (CSIRO) and one of the international leaders in exploration hydrogeochemistry. David would be more widely recognised had he not been such a selfless researcher. He always put the team, project, and organisation ahead of his own personal gain. David was a mentor for many, and he would engage with students and senior colleagues in the same manner: always constructive, supportive and considered. David formally supervised a number of students, including three PhD students, not to mention the many more, like me, he unofficially mentored as undergraduates, postgraduates or colleagues.

David was a Fellow of the Association of Applied Geochemists (AAG), a member and former President of the Australian Regolith Geoscientists Association, and served on the Editorial Board for *Geochemistry: Exploration, Environment, Analysis*.

David's early years were spent in Sydney (Australia) before moving to Perth with his job at CSIRO. He completed his BSc (Honours) in inorganic chemistry at the University of Sydney in 1982 before completing his PhD in soil science from the same institution in 1986, researching the geochemistry of uranium and thorium during weathering. David joined CSIRO in 1987 where he remained until his early retirement due to failing health in 2017. David helped establish hydrogeochemistry as an exploration tool, a tool now widely implemented by Australian state geological surveys and mineral explorers.

David remained an active Honorary Fellow of CSIRO. He was still passing on his ideas of simplifying exploration transition metal indices for groundwater by scaling with pH until the last weeks before his death. He was always positive. Except for his last few days, David's quality of life had been good, something I would attribute to David's positive personality. David's optimism is something that those that spent time in the field with him would know all too well. He was always convinced you could collect another few samples, even as darkness was descending, and he would literally bounce in and out of vehicles all day, every day, to ensure he got as much done as possible in the field.

His dedication to his science in the office was also admirable: he spent years trawling through pdf versions of water reports and pulling out data, doing quality assurance–quality control checks. This work resulted in the Australian continental-scale hydrogeochemistry data that was summarised in a recent news article: see https://www.csiro.au/en/Research/MRF/Areas/Resourceful-magazine/Issue-19/The-groundwater-explorer. The 320,000 quality groundwater data points are all thanks to David's tenacious nature for collecting and curating results and being certain that "true backgrounds" and major element data would show patterns for application in mineral exploration and other fields if we just had enough samples (there was always more David would look for).

David was 58 and is survived by his wife, Celia, and children Ahren, Alex, Bec, Adam and Nathan.

I wrote this article while taking a break from interpreting groundwater data, the methodology of which I learned from David over the last 15 years. I will raise a glass of wine (preferably David's preferred sauvignon blanc) to his memory after I submit this memorial and continue to work on the data and so further David's legacy. I am forever grateful for David's many years of mentorship and for hiring me. A terrific boss, teacher, scientist, colleague and friend. He will be missed.

For those who wish to make a donation in David's honour, see the AAG's Distinguished Geochemists Fund. https://www.appliedgeochemists.org/association/distinguished-applied-geochemists-

Ryan Noble

RECENT ARTICLES PUBLISHED IN *EXPLORE*

The following abstract is for an article that appeared in issue 184 (September 2019) of the *Explore* newsletter.

"Rapid Hydrogeochemistry: A Summary of Two Field Studies from Central and Southern Interior British Columbia, Canada using a Photometer and Voltammeter to Measure Trace Elements in Water"

Ron Yehia[1], David R. Heberlein[2], Ray E. Lett[3]

Two Geoscience BC–funded studies in the central and southern interior of British Columbia (BC) (Canada) have been carried out to test the feasibility of using portable photometer and voltammeter instruments in the field to detect trace element and anion anomalies in stream waters that drain known mineral occurrences. Two-hundred-and-fifty water samples in total were collected and analyzed: 79 at Poison Mountain in 2014, and 171 west of Nazko in 2016. The samples were analyzed in the field by a photometer for Al, Ca, Cl, Cu, Fe, Mg, Mn, Mo, Ni, K, Si, SO_4 and Zn and by a voltammeter (Nazko area only) for As, Cu, Cd and Pb. Anomalous Cu and SO_4 levels measured by photometer in stream water reflect the Cu-sulfide mineralization at the Poison Mountain porphyry Cu–Mo deposit. In the Nazko area, there were elevated Cu and As levels as detected by the voltammeter in stream water near two known mineral occurrences. Sixty-three water samples were also sent to a commercial laboratory for cation and anion analysis to compare values obtained by the photometer and voltammeter. Results revealed an acceptable correlation between the field measurements and the laboratory analysis for most analytes. The Poison Mountain and Nazko surveys show that the photometer and voltammeter are fast and cost effective instruments for rapid trace element analyses in the field.

1 MYAR Consulting, Vancouver BC, myar@telus.net
2 Heberlein Geoconsulting, North Vancouver BC, dave@Hebgeoconsulting.com
3 Geochemist, Victoria BC, raylett@shaw.ca

German Mineralogical Society

www.dmg-home.org

JOINT DMG–MSA SHORT COURSE

Application of Diffusion Studies to the Determination of Timescales in Geochemistry and Petrology

Institute for Geology, Mineralogy and Geophysics, Bochum (Germany)
late 2020 – early 2021 (to be decided)

This is a joint Deutsche Mineralogische Gesellschaft (DMG, the German Mineralogical Society) short course and a Mineralogical Society of America (MSA) workshop. Further details will be provided via both the DMG and MSA mailing lists.

Bochum is located at the heart of Europe. It is, therefore, conveniently accessed by road, train and air. The surrounding region, which includes Cologne and Dusseldorf, is densely settled and boasts a world-renowned cultural infrastructure. Having said this, there is also a real possibility that the course will be moved online and be held virtually. This will depend on how the global covid19 health crisis evolves.

Content: The course is directed at petrologists, geochemists, volcanologists and planetary scientists interested in retrieving timescale information on processes that affected their rocks. Such information might include magma residence time in a reservoir; the cooling- or exhumation rates of rocks; the duration of terrestrial metamorphism; the duration of extra-terrestrial metamorphism (e.g., that which affected the parent bodies of meteorites); the duration of fluid flow (e.g., metasomatism by fluids/melts in the crust or mantle); or the evaluation and application of closure temperatures. Our focus will be high-temperature processes. Therefore "high-temperature thermochronometry" or "geospeedometry" are keywords that may describe the contents of this course.

Goals and expected profile of participants: Previous experience with numerical modeling or programming is not required, but an interest in learning the rudiments of these tools is. One of the objectives of the course is to demonstrate how much it is possible to accomplish without any, or with very little, programming. The basic information on diffusion that is required for carrying out such calculations will be provided, because this is not a course designed to cover all aspects of diffusion in minerals and melts. In addition to instruction via lectures, a major component of the course will be hands-on training to enable participants to "do your own" modeling. All instruction and exercises will be in English. The course material will be designed for graduate students or postdocs starting off in the fields mentioned above, but participants at any level of experience and expertise are, of course, welcome. Student members of DMG and MSA will be given priority for registration if demand for a slot becomes a concern.

Watch this website for updated information: http://www.gmg.ruhr-uni-bochum.de/petrologie/aktuelles/index.html.de.

General enquiries: Sumit Chakraborty (Sumit.Chakraborty@rub.de) or Ralf Dohmen (Ralf.Dohmen@ rub.de). Information on non-technical matters can also be obtained from the departmental secretary's office: Agnes Otto (office-mineralogie@rub.de).

SHORT COURSE REPORT

High Pressure Experimental Techniques and Applications to the Earth's Interior

Bavarian Geoinstitute, Bayreuth, 17–21 February 2020

The short course entitled High Pressure Experimental Techniques and Applications to the Earth's Interior took place 17–21 February 2020 for the 22nd time at the Bavarian Geoinstitute in Bayreuth (Germany). Again, with 31 participants from all over the world, it was very well received by the young scientists this year. The experimental and analytical possibilities at the Bavarian Geoinstitute were impressively illustrated to the young researchers examining the physical and chemical properties of the Earth.

Participants of the Bavarian Geoinstitute short course 2020. PHOTO: F. HEIDELBACH

Attendees could see how to determine the crystal structure of minerals by transmission electron microscopy in the nanometer range or when using the diamond anvil cell, which can generate pressures up to 600 GPa, exceeding the pressure in the Earth's core. The broad range of the high-pressure–high-temperature (HP–HT) techniques, as well as the analytical methods, were taught in a theoretical lesson and then applied practically in the laboratory. During the morning lectures, the theoretical foundations of the methodology and structure of the experimental facility were explained. After lunch in the canteen, workshops concentrated on practical and interactive training.

Experiments specifically prepared by the lecturers helped the students to understand more fully the applications. The young scientists were divided into small groups, which made it possible to work independently on the corresponding systems. For example, all the preparatory steps for the multi-anvil press, which are necessary to carry out an experiment under Earth mantle conditions, were carried out by the participants. Each student had the opportunity to process cubes themselves, to weld thermocouples and to prepare a precious metal capsule. It was made particularly clear which research questions could be best addressed using which method.

Sample processing could be accomplished using the focused ion beam on the scanning electron microscope, and measurements were made using laser ablation inductively coupled plasma mass spectrometry, Fourier transform infra-red spectroscopy and both Raman and Mössbauer spectroscopy. All this illustrated the diverse applications of the high-pressure investigation field and, once again, clarified the need to carry out experimental studies to understand the structure and composition of our planet.

The short course at the Bavarian Geoinstitute gave the young scientists a deep insight into the experimental HP–HT methods, and allowed them to exchange ideas, to discuss and to establish new contacts. A special highlight, and another excellent opportunity for discussion, was the social dinner with typical Bavarian cuisine in a restaurant in downtown Bayreuth.

Our sincere gratitude goes to the organizers, lecturers and everyone who made the course possible. The short course at the Bavarian Geoinstitute was an instructive and rewarding experience for all participants and, in the future, should be considered a must for every young scientist working in the experimental high-pressure field.

Patricia Petri (Tübingen), Sonja Frölich (Freiberg) & Debora Faller (Heidelberg)

STUDY AND TEACHING DURING THE CORONA CRISIS

Concerning the corona crisis, the umbrella organization of geoscientists in Germany, the Dachverband Geowissenschaften (DVGeo), started a survey on whether it would be possible to teach geoscience using only digital tools. More than 600 geoscientists and students took part in the survey; the shared opinion was that digital teaching is possible.

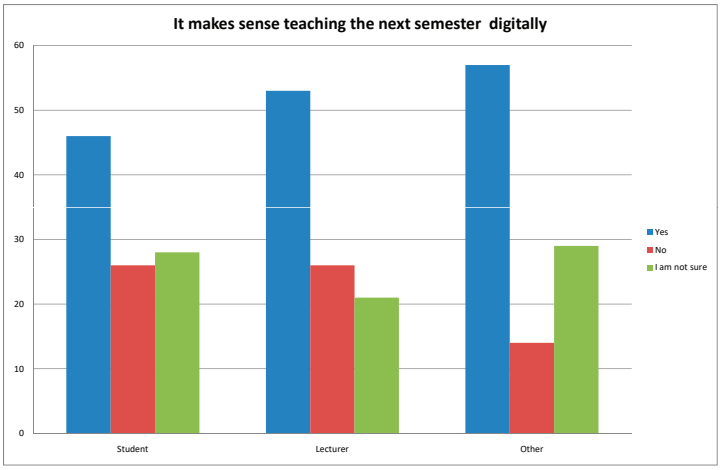

To implement digital teaching, we have the options of online tools such as Cisco WebEx, Skype/Teams, Zoom, BigBlueButton, Adobe Connect or Collaborate Ultra, plus some learning and management platforms. Some lecturers reported using blogs, wikis and podcasts. One potential problem is the capacity of a given university's servers and their supportive IT departments. Nevertheless, students are looking forward to this new development and to increasingly apply digital tools.

A problematic issue is the examinations. There are no standardized regulations. Students and lecturers agree that excursions and practical exercises are essential to learn geoscience and are not replaceable by virtual sessions.

The two graphs below illustrate what German lecturers are planning to master:

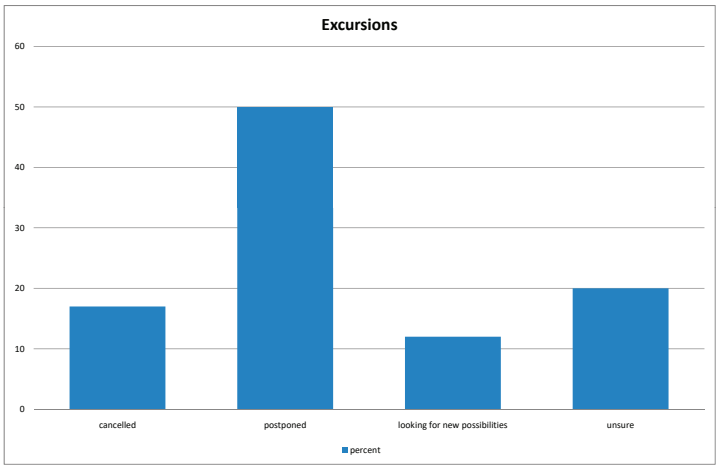

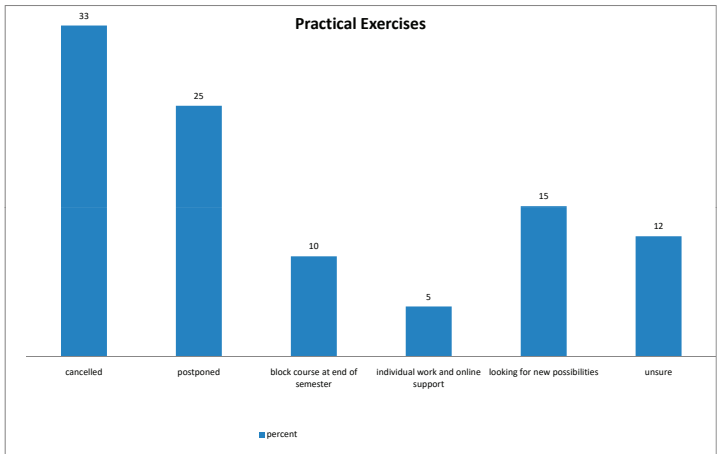

Overall, it seems possible to teach many subjects completely digitally – even if not all options are known and fully developed at present. In practice-oriented subjects, such as the geosciences, most of the theoretical part can be taught digitally in the current situation. But the remaining practical part will have to be made up for at a later date.

Tamara Fahry-Seelig (DVGeo, Berlin)

https://emc2020.ptmin.eu/

It is with deep regret that, due to the current global situation with coronavirus COVID-19, the Scientific and Organizing Committees of the European Mineralogical Conference (EMC) have taken the difficult decision to **postpone emc^{2020} to 2021**. The new proposed date is **29 August – 2 September 2021**. The location of the conference remains unchanged.

This is a tremendous disappointment for the mineralogical community in general, for the emc, and for the emc^{2020} Conference Organizing Committee in particular. We were very much looking forward to welcoming hundreds of you to emc^{2020}: all the participants, exhibitors, and sponsors. However, our primary aim is to keep our delegates, speakers, exhibitors, and staff as safe as possible.

We apologize to all those who will be impacted by this decision but we would request your understanding.

With the best wishes of health, perseverance, and human solidarity in the fight for a secure future.

Yours faithfully,

Tomasz Bajda, **Justyna Topolska** (for the Conference Organizing Committee of emc^{2020})

European Association of Geochemistry

www.eag.eu.com

KAREN HUDSON-EDWARDS' 2019 EAG DISTINGUISHED LECTURER TOUR

Audience for the first lecture at Babes-Bolyai University, Cluj-Napoca (Romania).

Audience at the Geological Survey of Slovenia.

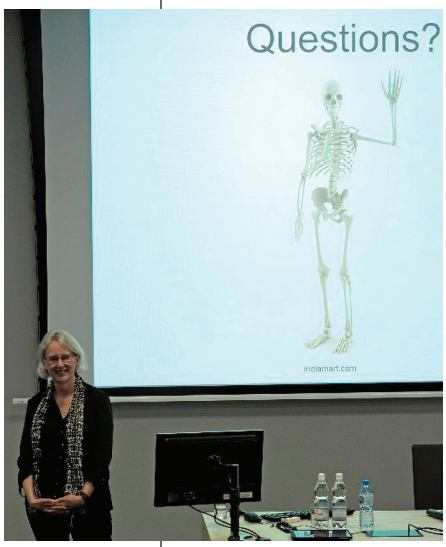

Last slide of the "Environmental Minerals" lecture at the Institute of Geological Sciences, Jagiellonian University, Kraków (Poland).

I was surprised, and very honoured, to receive notification that I had been named the EAG's Distinguished Lecturer for 2019. I am a geologist by training and worked as an exploration geologist for five years between my MSc and PhD before moving on to study the environmental impacts of mining. For over 25 years, I have worked in this field, collaborating with excellent colleagues, post-docs and students. Together, we have explored many facets of this field, including the environmental minerals of mine wastes, the medium- and long-term impacts of tailings dam spills, the influence of mining on global geochemical cycles and human health, the management and remediation of mine wastes and the promotion of sustainable mining practices. I was very excited to be able to communicate this science to geochemical audiences in central and eastern Europe. I proposed three lectures that interested groups could choose from: (1) "The What, Where, How and Why of Mine Tailings", (2) "The Global Biogeochemical and Health Impacts of Mining" and (3) "Environmental Minerals: Bacteria, Fungi, Worms, Toxins and the Human Body".

Shortly before embarking on my tour I broke my ankle in a freak accident, just as last year's EAG Distinguished Lecturer, Jim McQuaid, did! Hopefully, this isn't a new trend for the EAG and that the 2020 recipient will be fine. I had to move what was to be my first lecture, at Charles University in Prague (Czech Republic), to January 2020 while I got literally back on my feet. My first lecture was, therefore, at Babes-Bolyai University in Cluj-Napoca (Romania) in the last week of November 2019. I had an extra day in Cluj, so my host, Calin Baciu, showed me around the city and took me on a tour of the Salina Turda former salt mine, advertised as "A Gate to Transylvania's Heart". I had never been underground in a salt mine before, so it was fascinating to see the beautiful flow structures and delicate stalactites. The following day I gave Lectures (1) and (2) to an audience of students and staff. It was great to speak to students afterwards and hear about the mining-related, and other, research that they were involved in. I received good questions on tailings, the future of sustainable mining, and whether or not acid mine drainage could ever be completely stopped.

My next stop was the Geological Survey of Slovenia in Ljubljana. My host, Mateja Gosar, picked me up from the airport, and we had a delicious lunch and discussed all things geochemistry. In the afternoon, Mateja had arranged for her group to give presentations on their research projects, many of which focused on aspects of legacy mining in Slovenia. I was also able to hear about the group's many years of work on the geochemistry of the area around the former Idrija mercury mine in the west part of the country. The next morning I gave all three of my lectures to an enthusiastic audience, followed by a lively lunch with Mateja's group and colleagues at a restaurant that served traditional Slovenian food. That evening, Mateja showed me around the city, mainly along both banks of the Ljubljanica River, and we enjoyed some excellent Slovenian red wine with further discussions on mining, geochemistry and life.

The next day I moved on to Kraków (Poland) to visit the Institute of Geological Sciences at the Jagiellonian University. That evening, my host, Marek Michalik, and his wife Anna, took me for an excellent dinner at the Barka restaurant, a moored barge serving Polish cuisine on the Vistula River. The next day, I gave Lectures (2) and (3) to students and staff and was given a tour of the institute. It was good to get an overview of the geology from the roof of the building, and to learn about the importance of coal mining in Silesia. In the afternoon, Marek and Anna took me for lunch in a wonderful underground 'cave' restaurant in the middle of Kraków, after which I was able to tour the city and view the stunning Renaissance Cloth Hall and other buildings around the main market square.

The tour began again in early January 2020 with my postponed trip to Charles University in Prague. My host, Vojtěch Ettler, who has similar research interests to me on the environmental behaviour of mineral wastes, picked me up at the airport and took me into town. After a tour of the department and introductions to staff and students, I delivered Lecture (3) on environmental minerals. Subsequently, we had a good discussion about the role of minerals in mining systems and the human body. That night, Vojtěch, his colleagues and I went for Czech roast duck and Pilsner beer, and had a very jolly evening discussing minerals, universities and humorous incidents.

I am very grateful to the EAG, especially to Marie-Aude Hulshoff who helped organise my trip, to my hosts and to all the people who attended the lectures. This was a fantastic experience for me, and I hope also for those who came to listen and to those who I spoke with afterwards. I felt we had good opportunities for exchange of information and experiences in mining and geochemistry, and we have formed collaborations that will go forward into the future.

Karen Hudson-Edwards (University of Exeter, UK)

View the lectures from the 2019 Distinguished lecture tour at http://eag.eu.com/outreach/dlp/.

Invite the 2020 Distinguished Lecturer to Your Institute

Dr Juan Diego Rodriguez-Blanco (Trinity College Dublin, Ireland) has been selected as the 2020 Distinguished Lecturer. He will deliver a series of lectures on the theme of environmental mineralogy and crystallisation on his tour this autumn. If you are based in central or eastern Europe and would like to invite Juan Diego to talk at your institute, please contact the EAG Office (office@eag.eu.com).

CHANGES TO THE *GEOCHEMICAL PERSPECTIVES LETTERS* EDITORIAL BOARD

The *Geochemical Perspectives Letters* editorial board are very pleased to welcome two new prestigious scientists to the team.

Anat Shahar is a staff scientist at the Geophysical Laboratory at the Carnegie Institution for Science (Washington DC, USA). Her research focuses on understanding how stable isotopes can inform our understanding of the processes that brought about the origin of the solar system and the processes that govern planetary formation, differentiation, and evolution.

Gavin Foster is Professor of Isotope Geochemistry within the Ocean and Earth Science, National Oceanography Centre Southampton at the University of Southampton (UK). He uses boron and other elements to reconstruct past climates so as to better understand our future climate.

The board would also like to take this opportunity to thank departing editors **Ariel Anbar** and **Wendy Mao** for their hard work and their immense contributions to the success of the journal.

'LAB CORNER': REPURPOSING EVERYDAY ITEMS FOR GEOCHEMISTRY

For the EAG's new 'Lab Corner' section, we asked the community: "What everyday item or household tool have you repurposed for science?" Read our first contributions below, and if you have any tips or tricks of your own that you'd like to share here in *Elements* or on the EAG Blogosphere, send them to us at office@eag.eu.com!

Making It Up With Make-Up

Fluorphlogopite powder. Photo credit: Filippo Formoso

"A few months ago, we found ourselves in dire need of a standard material for referencing our solid-state nuclear magnetic spectroscopy data. In short, we needed a mineral with defined magnesium–fluorine bonds, and it turned out that the perfect compound for this task was fluorphlogopite, a fluorine-endmember mica. However, the price from some well-known chemical companies was more than £1,000 per gram. We then discovered, after a simple session on the internet, that fluorphlogopite is used in beauty products, such as skin foundation power, because it provides a supreme gloss (it's a really shiny mineral). Fortuitously, some companies sell fluorphlogopite powder as a raw material with a price of roughly £2 for 25 grams. So far, this material is a wonderful standard compared with analytical-grade reference materials, and, as a bonus, our hands look amazing after handling it."

Filippo Formoso, PhD student, University of St Andrews (UK)

Culinary Tricks in The Cryosphere?

Cryoconite hole. Photo credit: Klemens Weisleitner

"Many biologists who have prepared microscope slides for imaging will know that a little nail varnish is a cheap and effective sealant to preserve your specimen underneath the cover glass. However, perhaps few people outside of the relatively niche glacier microbiology community know the secret culinary trick to sampling a cryoconite hole (surface melt-holes on a glacier). Amongst the pipettes and crampons in our packs, you'll often find a turkey baster – which turns out to be a very effective tool for extracting liquid and sediment from these small icy melt pools that are refugia for microorganisms."

James Bradley, Queen Mary University of London (UK)

Geochemical Society

www.geochemsoc.org

GS BOARD OF DIRECTORS OPEN POSITIONS

The Nominations Committee of the Geochemical Society (GS) is seeking nominees for open board seats with terms beginning in January 2021. The potential nominees should have established reputations of leadership in geochemistry and be willing to devote considerable time and effort to the work of the society. Suggestions should be communicated by 15 July 2020 to any member of the Nominations Committee or to the GS business office at gsoffice@geochemsoc.org. More information regarding the duties and responsibilities of board positions can be found at www.geochemsoc.org/about/governance.

2020 GEOCHEMICAL SOCIETY AWARDS

This year's award recipients were invited to give lectures at the virtual Goldschmidt Conference and will also be recognized in person next year.

V.M. Goldschmidt Award

Richard W. Carlson, Director of the Earth & Planets Laboratory of the Carnegie Institution for Science (Washington DC, USA) received the 2020 V.M. Goldschmidt Award. The Goldschmidt Award recognizes major achievements in geochemistry or cosmochemistry consisting of either a single outstanding contribution or a series of publications that have had great influence on the field. Dr. Carlson is recognized for fundamental contributions establishing the age of the lunar crust, the difference in Nd isotopic abundances between chondrites and Earth, and the unravelling of Earth's earliest history.

Victor Moritz Goldschmidt (1888–1947) was a chemist considered to be the founder of modern geochemistry and crystal chemistry. He developed the Goldschmidt classification of elements and worked for many years at the University of Oslo (Norway). The society has presented a medal in his honor since 1972.

Claire C. Patterson Award

Naohiro Yoshida, Professor of Geochemistry and Principal Investigator of Earth-Life Science Institute at Tokyo Institute of Technology (Japan), received the 2020 Clair C. Patterson Award. This award recognizes an innovative breakthrough of fundamental significance in environmental geochemistry, particularly in service of society, consisting of either a single outstanding contribution or a short series of papers published within the last decade. Prof. Yoshida is recognized for the development and application of isotopomeric isotope measurements for biogeochemical studies of oceans, atmospheres, and bio-element cycling. He has developed many new techniques and has been a leader in developing global collaborations on environmental measurements.

Clair C. Patterson (1922–1995) developed the uranium–lead dating method. Using lead and uranium isotopic data from the Canyon Diablo meteorite, he calculated an age for the Earth of 4.55 billion years. This figure was far more accurate than those that existed at the time, and it has remained unchanged for over 50 years. Patterson also made enormous contributions to the understanding of lead's role as an environmental contaminant and to its subsequent elimination from many products.

F.W. Clarke Award

Daniel Stolper, Assistant Professor at the University of California, Berkeley (USA), received the 2020 F.W. Clarke Award, which recognizes an early career scientist for a single outstanding contribution to geochemistry or cosmochemistry published either as a single paper or a series of papers on a single topic. Dr. Stolper is recognized for his work on the use of clumped isotopes of carbon and hydrogen to determine the formation temperature of natural methane, and for insights into the geologic history of atmospheric and marine oxygen content.

Frank Wigglesworth Clarke (1847–1931) was a chemist who determined the composition of the Earth's crust. He taught chemistry and physics at the University of Cincinnati (Ohio, USA) and served in the U.S. Geological Survey for many years. He also collaborated with the Smithsonian Institution on atomic weight research. The society established the award in his name in 1972.

Distinguished Service Award

Sam Savin, the retired Provost of the New College of Florida (USA) will receive the Geochemical Society's Distinguished Service Award for 2020. Dr. Savin is recognized for his service as treasurer of the society from 2011 to 2019. During his tenure, the society increased its reserve fund, moved to a fully electronic accounting system, and consistently received clean audit opinions. Dr. Savin also oversaw a shift toward socially responsible investing for the society's reserves. Before his election as treasurer, he served for three years as a director.

The Distinguished Service Award recognizes outstanding service to the GS and/or the geochemical community that greatly exceeds the normal expectations of voluntary service.

COLLABORATION IN A TIME OF QUARANTINE

The GS exists to foster communication and cooperation among geochemists in every part of the world. Much of this work takes place via conferences, workshops, and other physical gatherings of our members. With the global shutdown on travel and large gatherings, all of us have to think differently about how we collaborate at a distance.

The society's largest program, the Goldschmidt Conference (organized jointly with the European Association of Geochemistry) has shifted to an entirely online meeting. This required creativity and adaptability on the part of the organizing committees, session conveners, conference staff, and participants. Additionally, there are several other ways to keep in touch during these challenging times:

- Read *Elements*! Members have access to the entire back catalog of the magazine online. Past issues are great teaching resources as you plan your curriculum for the next term.
- Read *Geochemical News*. The weekly e-mail newsletter gives you a quick snapshot of exciting discoveries, job openings, and more.
- Nominate a colleague for an award. Celebrating the achievements of colleagues and mentors is more important than ever. The GS has awards for scientists at all stages of their careers.

Find more information at www.geochemsoc.org/about/membership/online-resources.

International Association on the Genesis of Ore Deposits

www.iagod.org

16th SGA BIENNIAL MEETING

Conference venue beside Lake Rotorua, which is within walking distance of the Rotorua central business district.

The 16th Biennial Meeting of the Society for Geology Applied to Mineral Deposits (SGA) will be held 15–18 November 2021 in Rotorua (New Zealand) (www.sga2021.org), and the International Association on the Genesis of Ore Deposits (IAGOD) are among the co-sponsors of the meeting. The SGA biennial meetings typically attract 550–800 delegates from universities, research organisations, the minerals industry, and government and consulting organisations.

Rotorua city and Lake Rotorua within the ~240 ka Rotorua caldera.

The world famous Pōhutu geyser at Te Puia, Rotorua.

Champagne Pool, at Waiotapu thermal area, rimmed by orange Au–Ag-bearing As–Sb precipitates.

The conference host city, Rotorua, is located in the Taupō Volcanic Zone and provides spectacular volcanic scenery and geothermal areas where delegates can view epithermal Au–Ag depositional processes in action. The city, with its 75,000 inhabitants, lies on the margin of Lake Rotorua, within the ~240 ka Rotorua Caldera, and above the Rotorua geothermal system which generates the hot bubbling mud, mineral pools, and spectacular geysers that were the basis for the development of New Zealand's tourism industry from the 1870s. Rotorua continues to be one of New Zealand's main tourism destinations, having spas and a wide variety of other attractions and activities, including adventure tourism. Rotorua is also the heartland of indigenous Māori culture, and conference delegates will have the opportunity to experience the warm spirit of Māori culture and hospitality with a traditional pōwhiri (welcome) at the conference opening, as well as a concert and hangi (food cooked in an earth oven) during one of the evening social functions.

The 2021 SGA Biennial Meeting will feature four days of technical sessions, a trade exhibition, pre- and post-conference workshops, short courses, and field trips. Each day of the conference will also include tours for accompanying persons, partners, and families to enjoy, and there will be evening social functions for networking. The conference has the title "The Critical Role of Minerals in the Carbon-Neutral Future" and the programme will feature oral and poster presentations on topics related to mineral deposit research, exploration, sustainable development, and environmental and social aspects related to mineral deposits.

New Zealand's location at the boundary of the Pacific and the Australian–Indian tectonic plates makes it a geologically active country. Its tectonically dynamic past has endowed it with spectacular geology and scenery and a wide variety of mineral deposit types. This diversity is reflected in the variety of conference field excursions, which include the local volcanic geology, the epithermal and geothermal systems of the central North Island, and the orogenic gold and placer gold deposits of the South Island. During travel to or from New Zealand, overseas visitors will also have the option of field trips to visit arc- and orogenic-associated mineral systems in Victoria (Australia); volcanic massive sulfide and porphyry Sn deposits of Tasmania (Australia); Au and Ni deposits in Western Australia; porphyry and epithermal systems of the Sunda-Banda Arc (Indonesia); and Ni and Cr deposits in the overseas French territory of New Caledonia.

The conference organisers are calling for proposals for technical session themes, workshops, short courses, and field trips. See www.sga2021.org for details, or contact sga2021@confer.co.nz. Participation by IAGOD includes an exhibition booth, a technical session, a keynote speaker and student support. The IAGOD Council encourages IAGOD members to attend this prestigious conference where they may register at the discounted member's rate.

Mineralogical Society of America

www.minsocam.org

MSA PRESIDENT'S LETTER

MSA Members Contribute Online Mineralogy and Petrology Teaching Resources

Carol Frost

Who would have guessed that in March 2020 universities around the world would move from in-person classes to online teaching? The unexpectedness of this change, caused by concerns over public health and welfare, were disruptive enough. Recording lectures or migrating classes to video-conferencing took extra hours in our schedules. For those of us who teach mineralogy and petrology laboratory courses, there was the added challenge of transforming the in-person laboratory exercises that make use of physical materials—rocks and minerals, hand lenses, microscopes, and various other equipment—into effective virtual lessons.

Almost immediately, MSA members came to the rescue. All of us on the MSA-Talk forum enjoyed a vibrant exchange of ideas and approaches to modify lab courses and recommend useful online resources and technologies. People shared their own resources and their favorite websites. They acknowledged the challenges, but offered moral support. One of my favorite comments pointed out that if the *Mars Rover* could identify minerals without handling a rock, surely the rest of us could figure out how do so, too!

The MSA has compiled all the suggested teaching resources contributed to the MSA-Talk discussion on their website under the Education and Outreach tab at http://www.minsocam.org/msa/Teaching_Resources.html. They are now available to everyone. The materials include many 3D models of rocks and minerals (and fossils, too!) that can be examined from all angles and help take the place of physical hand samples. Teaching resources for optical mineralogy, scans of thin sections, and videos of minerals in thin section help to convey the information that we are accustomed to presenting in lab. Links are provided to the online illustrations for MSA's *Mineralogy and Optical Mineralogy* textbook by Dyar, Gunter, and Tasa, and MSA member John Brady has provided access to his online interactive petrology text. Many of the lecture videos from our Centennial Symposium are appropriate for classes: they can be viewed at http://www.minsocam.org/msa/Centennial/MSA_Centennial_Symposium.html.

By the time you read this letter, the spring semester will be over and, hopefully, the coronavirus will be on the wane. But the pandemic may accelerate innovation in teaching and learning. Our familiar model of lecture- and lab-based classes may be replaced with new and creative approaches that integrate learning more seamlessly into our daily lives. We may see continued sharing among faculty members, and more collaboration between faculty, education professionals, and organizations that provide digital platforms. I also hope that a positive outcome of the pandemic will be renewed confidence in the value of science and the problem-solving skills of scientists.

For all these reasons, I'd like to encourage you to continue to share your mineralogy and petrology teaching resources and suggestions with MSA, either on MSA-Talk or via the "Contact Us" button on the MSA homepage at www.minsocam.org. We'll continue to add them to the Teaching Resources page. Please check that page periodically to see what's new!

Carol Frost
2020 MSA President

NOTES FROM CHANTILLY

- **Membership:** All 2018 and 2019 MSA members have been contacted by mail, electronically, or both about renewing their memberships for 2020. If you have not renewed your MSA membership, please do so today. You can renew online anytime.
- **MSA Elections:** MSA will have electronic balloting for the 2020 election of 2021 MSA officers and councilors. The slate of candidates – President: Mark Ghiorso (OFM Research Inc.); Vice President (one to be selected): Pamela Burnley (University of Nevada, Los Vegas) and Craig Manning (University of California, Los Angeles); Treasurer (one to be selected): Glenn Gaetani (Woods Hole Oceanographic Institution, Massachusetts) and Paul Tomascak (State University of New York at Oswego); Councilor position 1 (one to be selected): Robert Bodnar (Virginia Polytechnic Institute) and Michael Williams (University of Massachusetts); and Councilor position 2 (one to be selected): Darrell Henry (Louisiana State University) and Jennifer Jackson (California Institute of Technology).

CALENDAR

The 2020 sixteen-month calendar features the minerals of Colorado. The calendar is published by Lithographie, LLC in cooperation with the Mineralogical Society of America, Fine Mineral Shows, Tucson Gem and Mineral Society, Rocky Mountain Gems & Minerals Promotions, and LLD Productions, Inc. The 2020 calendar, as well as limited numbers from previous years, are available on the MSA website at www.minsocam.org.

RESEARCH GRANTS

The Mineralogical Society of America

2021 Grants for

RESEARCH IN CRYSTALLOGRAPHY

from the Edward H. Kraus Crystallographic Research Fund
with contributions from MSA membership and friends

STUDENT RESEARCH IN MINERALOGY AND PETROLOGY

From an endowment created by MSA members

Selection is based on the qualifications of the applicant; the quality, innovativeness, and scientific significance of the research of a written proposal; and the likelihood of success of the project. There will be up to three US $5,000.00 grants, with the restriction that the money be used in support of research. Application instructions and online submission are available on the MSA website, http://www.minsocam.org. Completed applications must be submitted by 1 March 2021.

VOTE

2020 MSA ELECTIONS

Japan Association of Mineralogical Sciences
http://jams.la.coocan.jp

DID YOU KNOW...?

The MSA has available on its website a collection of fully open access publications. These include *Teaching Mineralogy* (Brady, Mogk, and Perkins 2011); *Mineralogy and Optical Mineralogy Laboratory Manual* (McNamee and Gunter 2014); *Guide to Thin Section Microscopy* (Raith, Raase, and Reinhardt 2012), *Carbon in Earth* (edited by Hazen, Jones, and Baross 2013, RiMG volume 75), and many more. Full-text articles from *American Mineralogist* from 1916 through 1999 are also a part of this collection. The Open Access publications are under the **Publications** pull-down menu on the www.minsocam.org home page.

A MINERAL PUBLICATION FOR CHILDREN

***A Quest for Shiny Purple Crystals: Johnny and Max's Rock Hunting Adventure*, by Monica Rakovan, 2018, 32 pp, softcover, ISBN 978-0-9863349-1-7**

The MSA is pleased to be able to offer this exciting publication for children. In this illustrated book, Johnny and his best (furry) friend, Max, become fascinated by the rocks they are finding. To learn more, they visit a nearby rock shop, where the owner, Sal, answers many of their questions. Johnny and Max are invited to go rock collecting with Sal at a farm where the chickens are digging up purple crystals! The hunt begins for more shiny purple rocks and learning about an unusual amethyst find.

Written by Dr. Monica Rakovan, *A Quest for Shiny Purple Crystals* is a great way to teach children about collecting rocks and encourage enthusiasm for the sciences. A helpful glossary in the back helps introduce children to new words, and the colorful illustrations bring the story alive.

Description and ordering online at www.minsocam.org or contact Mineralogical Society of America, 3635 Concorde Pkwy Ste 500, Chantilly, VA 20151-1110 USA phone: +1 (703)652- 9950 fax: +1 (703) 652-9951 e-mail: business@minsocam.org. Cost is $10.

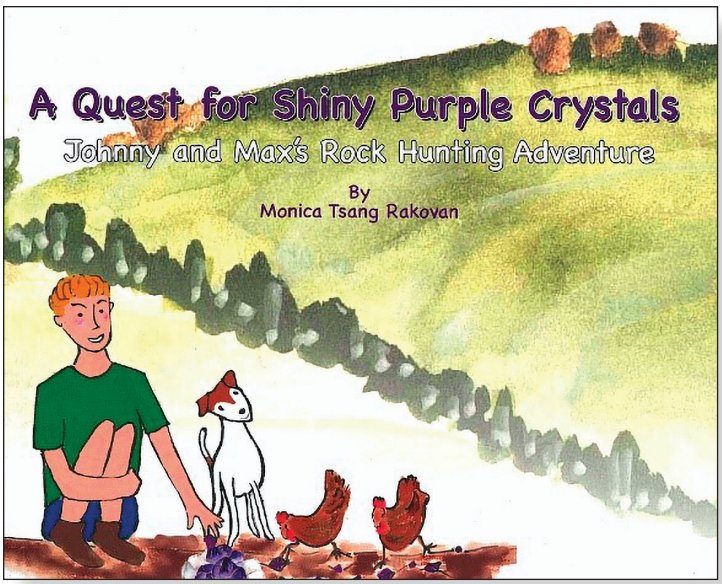

HUNTING MINERAL-CENTERED LIFE FROM THE DEEP ROCKY BIOSPHERE

The emergence of life is generally considered to have been assisted by the power of minerals (Hazen 2012). Modern organisms are equipped with biochemical machineries that might have replaced more primitive mineral parts a long time ago. Given the high energetic costs to operate such sophisticated biochemical machineries, it is speculated that mineral-centered life might have been evolutionarily preserved on modern Earth where the primordial geochemistry prevails with extreme energy starvation. One of the ideal places to hunt possible primitive life is in the deep subsurface because of its restricted supply of energy-rich photosynthetic products. Granite and basalt are geologic giants that have been representative of the continental and oceanic crusts, respectively, since ~4.0 Ga. Energy-starved deep biospheres in granitic and basaltic crusts have been potentially hosting primitive life that is not in competition with biochemically sophisticated microbes.

To explore the granite biosphere, a 69 Ma granite was drilled horizontally from a 300 m deep underground tunnel at the Mizunami Underground Research Laboratory (Tono, central Japan). Pristine groundwater samples were taken and subjected to genome-resolved metagenomic analyses in combination with geochemical and microbiological site characterizations. It was revealed that anaerobic methane-oxidizing archaea were harvesting energy from magmatic methane under energy-starved conditions (Ino et al. 2018). In addition, a diverse phylum within the candidate phyla radiation (CPR), called Parcubacteria, appears to be dominant in the deep granite biosphere. All CPR members are represented by small genomes and cell sizes with restricted metabolic capacities, which might have been inherited from an early metabolic platform for life (Hug et al. 2016).

For the oceanic crust biosphere, the *JOIDES Resolution* research vessel was used to drill into basalts of the following ages: 13 Ma, 33.5 Ma and 104 Ma. This drilling was done during Integrated Ocean Drilling Program (IODP) Expedition 329, which targeted life beneath the seafloor of the South Pacific Gyre (SPG). The South Pacific Gyre is known as an oceanic province where surface photosynthetic activity is exceedingly low (D'Hondt et al. 2015) and which might favor microbes living independent of photosynthesis in the underlying basalt.

Unlike land-based subsurface investigations, it is technically difficult to collect pristine crustal fluid from a borehole drilled from a scientific vessel. Without geochemical information from the crustal fluid, the habitability of the rocky environment remains largely unknown. To understand the nature of the rocky biosphere in oceanic crust, a new life-detection technique was successfully developed for drilled rock cores and used in combination with nanoscale mineralogical characterizations (see Yamashita et al. 2019 and Sueoka et al. 2019). Basalt fractures filled with clay minerals and calcium carbonate were associated with the formation of Fe–Mg-smectite that is compositionally and structurally similar to saponite and/or nontronite, both being indicators of low-temperature basalt–water interactions. Unexpectedly, the dense colonization of microbial cells was directly imaged to exceed ~10^{10} cells/cm^3, a range of cell density typically found in a human gut (Fig. 1) (Suzuki et al. 2020). More surprisingly, there was a dominance of heterotrophic bacteria, as demonstrated by DNA sequences and lipids, from which one can conclude that there is organic matter in the form of carbon and an energy source(s) in subseafloor basalt.

Cont'd on page 206

Cont'd from page 205

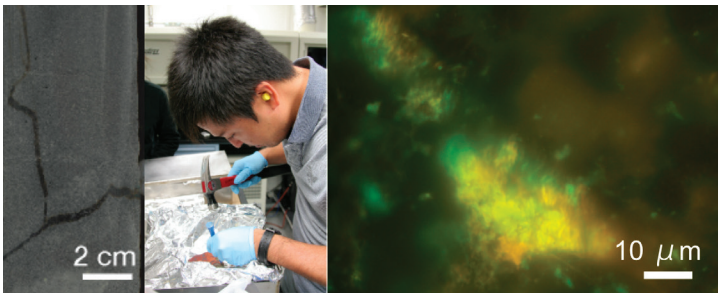

FIGURE 1 (**LEFT**) Picture of a basaltic core sample with fractures. (**CENTER**) A scientist subsampling a part of a rock core. (**RIGHT**) Fluorescence microscopy image of SYBR Green I–stained microbial cells associated with nontronite. Green and orange colors indicate the presence of microbial cells and nontronite; the yellow color indicates the enrollment of microbial cells within nontronite aggregates.

These findings change our view of the rocky biosphere where inorganic energy sources derived from rock–water interactions are generally regarded as of primary ecological importance. Given the prominence of basaltic lava and/or magmatic methane on Earth and Mars, microbial life could exist where subsurface igneous rocks interact with liquid water. It is also important to note that the presence or absence of microbial life and associated metabolic repertories will clarify poorly characterized physicochemical properties in deep igneous rocks, such as permeability and fluid and energy fluxes. Finally, the technology to hunt mineral-centered life in the deep subsurface is now ready – we are on the verge of unveiling life's story from the very beginning.

Yohey Suzuki (The University of Tokyo)

REFERENCES

D'Hondt S and 34 coauthors (2015) Presence of oxygen and aerobic communities from seafloor to basement in deep-sea sediment. Nature Geoscience 8: 299-304

Hazen RM, Papineau D (2012) Mineralogical co-evolution of the geosphere and biosphere. In: Knoll AH, Canfield DE, Konhauser KO (eds) Fundamentals of Geobiology. Blackwell Publishing Ltd., pp 333-350

Hug L and 16 coauthors (2016) A new view of the tree and life's diversity. Nature Microbiology 1, doi: 10.1038/nmicrobiol.2016.48

Ino K and 19 coauthors (2018) Ecological and genomic profiling of anaerobic methane-oxidizing archaea in a deep granitic environment. ISME Journal 12: 31-47

Sueoka Y, Yamashita S, Kouduka M, Suzuki Y (2019) Deep microbial colonization in saponite-bearing fractures in aged basaltic crust: implications for subsurface life on Mars. Frontiers in Microbiology, doi: 10.3389/fmicb.2019.02793

Suzuki Y and 12 coauthors (2020) Deep microbial proliferation at the basalt interface in 33.5–104 million-year-old oceanic crust. Communications Biology, doi: 10.1038/s42003-020-0860-1

Yamashita S, Mukai H, Tomioka N, Kagi H, Suzuki Y (2019) Iron-rich smectite formation in subseafloor basaltic lava in aged oceanic crust. Scientific Reports 9, doi: 10.1038/s41598-019-47887-x

JOURNAL OF MINERALOGICAL AND PETROLOGICAL SCIENCES

Vol. 115, No. 2, April 2020
Special Issue: Indian Continent

Preface of the Special Issue on 'Indian Continent'

Tracking plate tectonics and related events in the Indian continent from Archean to recent times – Kaushik DAS, Jun–ichi ANDO, Toru INOUE

Continental Crustal Dynamics – Old to Recent Tectonic Activities

Deformation and metamorphic history of the Singhbhum Craton vis-à-vis peripheral mobile belts, eastern India: implications on Precambrian crustal processes – Gautam GHOSH, Sankar BOSE

Geological evolution of the northern and northwestern Eastern Ghats Belt, India from metamorphic, structural, and geochronological records: an appraisal – Proloy GANGULY, Amitava CHATTERJEE

Structural architecture and geological relationships in the southern part of Chitradurga Schist Belt, Dharwar craton, South India – Lakshmanan SREEHARI, Tsuyoshi TOYOSHIMA

The Indo–Eurasia convergent margin and earthquakes in and around Tibetan Plateau – Yanbin WANG, Yangfan DENG, Feng SHI, Zhigang PENG

Neotectonic fault movement and intraplate seismicity in the central Indian shield: A review and reappraisal – Anupam CHATTOPADHYAY, Dipanjan BHATTACHARJEE, Srijan SRIVASTAVA

Zirconium in rutile thermometry from garnet granulites of the Jijal complex of Kohistan arc, NW Himalaya – Chihiro NAKAZAWA, Hafiz Ur REHMAN, Hiroshi YAMAMOTO, Tehseen ZAFAR

Interaction Between Life, Sediment and Water, and Evolution of the Early Atmosphere

A review of biotic signatures within the Precambrian Vindhyan Supergroup: Implications on evolution of microbial and metazoan life on Earth – Adrita CHOUDHURI, Santanu BANERJEE, Subir SARKAR

Clue on ocean redox condition from trace element and rare earth element (REE) composition of iron formation and carbonate rocks from the late Paleoproterozoic Morar Formation, Gwalior Group, central India – Pritam P. PAUL, Partha Pratim CHAKRABORTY, Fumito SHIRAISHI, Kaushik DAS, Atsushi KAMEI, Sourabh BHATTACHARYA

Formation of intracratonic Gondwana basins: Prelude of Gondwana fragmentation? – Prabir DASGUPTA

Mantle–Crust Interaction: Geochemical and Rheological Appraisals

Mineralogy and petrology of shoshonitic lamprophyre dykes from the Sivarampeta area, diamondiferous Wajrakarur kimberlite field, Eastern Dharwar craton, southern India – Praveer PANKAJ, Rohit Kumar GIRI, N.V. CHALAPATHI RAO, Ramananda CHAKRABARTI, Sneha RAGHUVANSHI

Serpentinite enigma of the Rakhabdev lineament in western India: Origin, deformation characterization and tectonic implications – Dyuti Prakash SARKAR, Jun–ichi ANDO, Kaushik DAS, Anupam CHATTOPADHYAY, Gautam GHOSH, Kenji SHIMIZU, Hiroaki OHFUJI

Mineralogical Society of Great Britain and Ireland

www.minersoc.org

NEWS FROM LONDON

In the April 2020 issue of *Elements*, we asked from members, and others, for help in terms of outreach. This was with a view to helping those not directly involved in our science to understand a little of what it is that we do. There is now an even wider need that makes the request from the previous issue more relevant than ever: "And, in the spirit of 'ask not what your society can do for you....', what skills and talents could you bring to the society?" We would especially appreciate input in terms of technical offerings, e.g., podcasts, webinars, video editing, etc. *What can you do for **your** society*?

Please contact Kevin Murphy (kevin@minersoc.org) if you have something to share.

MEETING – NEW TOPICS IN MINERAL SCIENCES 1. DIFFUSION IN MINERALS, ROCKS AND MELTS: POTENTIAL AND PITFALLS

Date: 23 October 2020
Location: Burlington House, London (UK)

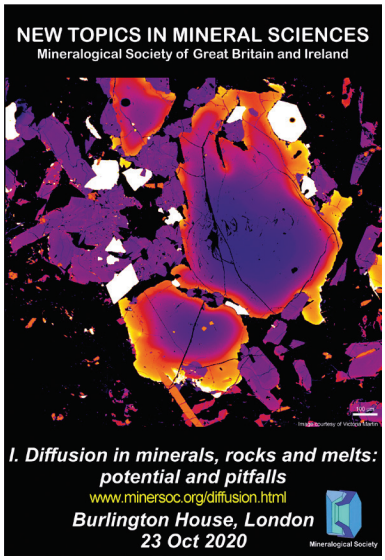

IMAGE COURTESY OF VICTORIA MARTIN

The meeting will appeal to those interested in applying diffusion modelling across a wide range of mineralogical contexts to problems of rates, timing, and thermal history.

The meeting will be led by invited speakers who will address the fundamentals of diffusion theory, apply that theory to modelling of geological processes, and provide examples of state-of-the-art research on diffusion in different geological contexts. The invited speakers and their general topics are as follows:

- Sumit Chakraborty – Diffusion Theory
- Dan Morgan – Modelling and Theory
- John MacLennan – Timescales of Magmatic Processes
- Thomas Müller – Diffusion and Thermobarometry in Metamorphism
- Tina Marquardt – Grain Boundary Diffusion
- Clare Warren – Diffusion and Thermochronometry

These will be followed by a poster session, primarily for student poster presentations, with 90 second 'nano-introductions' to each. The proceedings will conclude with a panel discussion.

Short Course

The MinSoc will hold a one-day short course on diffusion modelling on October 22 at the Natural History Museum, London (UK). Details will be made available shortly.

Note: We currently plan to run this as an in-person meeting. If this changes we will provide appropriate information on our website (https://www.minersoc.org/diffusion.html).

MINERALOGICAL MAGAZINE

Papers from the 3rd International Critical Metals Meeting, Edinburgh (UK) in May 2019

"Critical Metal Mineralogy and Ore Genesis Revisited: Thematic Set Arising from the Third International Critical Metals Meeting, Edinburgh"
Eimear Deady, Sam Broom-Fendley

"Challenges to the European Automotive Industry in Securing Critical Raw Materials for Electric Mobility: The Case of Rare Earths"
Marc Schmid

"Structural State of Rare Earth Elements in Eudialyte-Group Minerals"
Anouk M. Borst, Adrian A. Finch, Henrik Friis, Nicola J. Horsburgh, Platon N. Gamaletsos, Joerg Goettlicher, Ralph Steininger, Kalotina Geraki

"Sulfur-bearing Monazite-(Ce) from the Eureka Carbonatite, Namibia: Oxidation State, Substitution Mechanism, and Formation Conditions"
Sam Broom-Fendley, Martin P. Smith, Marcelo B. Andrade, Santanu Ray, David A. Banks, Edward Loye, Daniel Atencio, Jonathan R. Pickles, Frances Wall

"Light Rare Earth Element Redistribution during Hydrothermal Alteration at the Okorusu Carbonatite Complex, Namibia"
Delia Cangelosi, Sam Broom-Fendley, David Banks, Daniel Morgan, Bruce Yardley

"The Role of Sulfate-Rich Fluids in Heavy Rare Earth Enrichment at the Dashigou Carbonatite Deposit, Huanglongpu, China"
Delia Cangelosi, Martin Smith, David Banks, Bruce Yardley

"Mineralogy and Genesis of Pyrochlore Apatite from the Good Hope Carbonatite, Ontario: A Potential Niobium Deposit"
Roger H. Mitchell, Rudy Wahl, Anthony Cohen

"Strain Partitioning in Host Rock Controls Light Rare Earth Element Release from Allanite-(Ce) in Subduction Zones"
Luca Corti, Davide Zanoni, G. Diego Gatta, Michele Zucali

METAMORPHIC STUDIES GROUP

In case you missed the Metamorphic Studies Group Virtual meeting, video recordings of the oral presentations are now available from https://www.minersoc.org/msg-rip-virtual-2020.html

Videos include the talk:

Not all kyanite is created equal – The petrogenesis of kyanite migmatites in Eastern Bhutan
S.E. Phillips, T.W. Argles, N.B.W. Harris, C.J. Warren, N.M.W. Roberts and B. Kunz which won best student oral presentation award for Stacy Philips.

The best student poster presentation went to Allie Nagurney for:

Microstructural Controls on the Crystallization of Garnet: An Example from the Meguma Terrane, Nova Scotia
Allie Nagurney and Mark Caddick

Mineralogical Association of Canada

www.mineralogicalassociation.ca

THE 2019 PINCH MEDAL AWARDED TO MR. GAIL E. DUNNING

The 2019 Pinch Medal of the Mineralogical Association of Canada has been awarded to Mr. Gail E. Dunning of Sunnyvale (California, USA). Through his detailed field studies and publications, Mr. Dunning has demonstrated a high degree of mineralogical expertise, primarily in the unusual primary and secondary minerals from the US (California and Nevada) and from northern Mexico. He has, to date, been involved in the discovery of 8 new minerals, with potentially more to come, and, in 2019, the new mercury mineral gaildunningite, from the Clear Creek Mine (California), was named in his honour.

Mr. Dunning (born 1937) is a physical chemistry graduate of the University of California, Los Angeles and a retiree from the General Electric Company, where he had worked since 1959 as a chemist of radioactive materials and, later, as a senior metallurgical engineer overseeing the materials testing laboratory. The latter afforded him the opportunity to become proficient in many of the techniques applicable to studying minerals, such as X-ray radiography, metallography, and scanning electron microscopy.

Gail Dunning and MAC past-president Andy McDonald at the March 2020 meeting of the Bay Area Mineralogists.

In 1955, he met J. Fenimore ('Fen') Cooper, a geology major who became a lifelong friend and collecting partner. From 1962 to 1976, Gail and Fen collected extensively, traveling throughout California and the western US, studying mining sites and collecting common, rare and unusual minerals. Their most active and rewarding field collecting was done at the Kalkar Quarry in Santa Cruz (California). It was here that they discovered their first new mineral, "tin benitoite", which was subsequently named 'pabstite' after Dr. Adolf Pabst of the University of California, Berkeley. Gail and Fen wrote extensively of their findings and the mines they visited, co-authoring more than 20 articles together.

Over his near 50 years collecting and studying minerals, Mr Dunning has been involved in ~50 papers pertaining to mineralogy. His main interests have been in Ba-silicates and Hg-bearing minerals; he also has a keen interest in ore microscopy, this being applied to the examination and characterization of sulfides and sulfosalts (including to terrestrial occurrences of the rare mineral troilite). Three of the recent notable studies Gail has been involved with include: 1) mercury at the Clear Creek mine in San Benito County, California (Dunning et al. 2005); 2) barium silicate mineralogy of the Western Margin of North America (Dunning et al. 2018); and 3) the McDermitt Caldera Complex in Nevada and Oregon (Dunning et al. 2019). Mr. Dunning has served as President of the Bay Area Mineralogists (1988–1989) and as its treasurer (1990–1994); he is currently the awards chairperson for the mineral group. Still quite active, he is currently working on a paper describing the paragenesis of Hg minerals from cavities at the McDermitt mine in Humboldt County, Nevada.

In a break with tradition, Gail was presented with his Pinch Medal at the March 2020 meeting of the Bay Area Mineralogists. This took place under a moon-lit, star-filled sky, owing to the building closures surrounding the COVID-19 pandemic. At least 20 members and well-wishers were in attendance (100+, if not for the pandemic situation), many of whom personally congratulated Gail on his medal.

The Mineralogical Association of Canada is proud to recognize the long-term dedication and efforts of members of the collecting community. Mr. Gail E. Dunning is an exceptional member and, in light of his contributions to the science of mineralogy, we are pleased to award him the 2019 Pinch Medal.

REFERENCES

Dunning GE, Hadley TA, Magnasco J, Christy A, Cooper JF (2005) The Clear Creek mine, San Benito County, California: a unique mercury locality. Mineralogical Record 36: 337-363

Dunning GE, Wahlstrom RE, Lechner W (2018) Barium silicate mineralogy of the western margin, North American continent, Part 1: geology, origin, paragenesis and mineral distribution from Baja California Norte, Mexico, western Canada and Alaska, USA. Baymin Journal 19: 1-70

Dunning GE, Cox M, Christy AG, Hadley TA, Marty J (2019) Geology, mining history, mineralogy and paragenesis of the McDermitt Caldera Complex, Opalite mining district, Humboldt County, Nevada, and Malheur County, Oregon. Baymin Journal 20: 1-165

IN MEMORY OF DR. MARK NEIL FEINGLOS, MD, CM (1948–2020)

It is with great sadness that we report the unexpected passing of Dr. Mark Neil Feinglos on 14 March 2020. He died in the home he loved in Durham (North Carolina, USA) where he had lived for over 40 years.

He was a professor of medicine at Duke University Medical Centre where he was Chief of the Endocrinology, Metabolism and Nutrition Division for more than a decade. Dr. Feinglos completed his BSc degree at McGill University (Canada) prior to pursuing a career in medicine.

Mark had one, central passion: mineral collecting. He began collecting minerals at the age of five when his aunt bought him a box set of minerals as a gift. Mark's passion for mineralogy grew over the course of his life, and he built up one of the most scientifically important private mineral collections in the world. Over the years, Mark identified many new minerals, as he was often sent specimens that could not be classified. Working within Duke's mineral collection, Mark discovered something that looked like a new mineral type, and worked to name the new mineral 'dukeite' in honor of Duke University and the Duke family. In 1997, Mark was honored to have a mineral named after him, 'feinglosite'. This was after he was the first to notice the unfamiliar specimen in the Natural History Museum of London (UK). And he felt privileged to be part of a project that led to the world's largest database of minerals, which became useful even to NASA in its analysis of moon rocks. Mark won the William Pinch Medal in 2003, its second recipient after its namesake, Mark's best friend Bill Pinch.

GEOCONVENTION 2020 JOINT MEETING in association with GAC–MAC Annual Conference is going virtual on 21–23 September 2020.

GeoConvention will be hosting the 2020 program completely virtual! We are excited to be exploring opportunities to bring nearly 800 presentations to your computer or mobile device through an interactive platform that will allow for learning, knowledge sharing and even networking! Content will be accessible wherever or whenever you are: no travel expenses, no commuting, sit back, relax and enjoy the show!

Registration rRates have been updated to reflect a virtual meeting. The Registration Portal will open soon. Stay up-to-date by visiting the GeoConvention 2020 website at https://geoconvention.com/.

MAC TRAVEL AND RESEARCH GRANT AWARDS IN 2019

The Mineralogical Association of Canada (MAC) awarded 23 Student Travel and Research Grants in 2019 that totaled $15,000: six went to undergraduate students, nine to MSc students, and eight to PhD students. Congratulations to these deserving individuals! Report excerpts from 6 of the recipients follow.

Andrew Wagner is an undergraduate student at Saint Mary's University (Canada) under the supervision of Dr. Erin Adlakha. The MAC Student Travel Grant mitigated his transportation costs to the University of Toronto (Canada) where he completed analytical work using their laser ablation inductively coupled plasma mass spectrometer. His project focuses on characterizing trace element concentrations of apatite-hosted silicate melt inclusions from the Mine Stock Pluton, which is associated with the Cantung tungsten skarn deposit, Northwest Territories (Canada). Through this work, he aims to understand the composition, metal content and origin of fertile magmas of tungsten skarns and evaluate the role of magma mixing in the production of mineralizing fluids.

Serhiy Buryak is a second-year MSc student at the University of Alberta (Canada) under the supervision of Dr. Alberto Reyes. His research project is titled "Geochronology and Characterization of the Wombat Kimberlite Pipe Post-Eruptive Maar Lake Sediment Fill, Subarctic Canada". The MAC Travel Grant provided a unique opportunity to showcase his research results at the European Geosciences Union (EGU) General Assembly 2019 in Vienna (Austria). He presented a poster at the "Limnogeology" session, which drew a lot of constructive feedback from the international research community. Furthermore, through discussions with European colleagues, he was brought up-to-date on multidisciplinary paleolake research, including how to apply geochronological, geochemical and mineralogical tools to characterize ancient lake records. Attending EGU 2019 was a very rewarding experience.

Chantal Norris-Julseth recently received her BSc (Honors) in geology from Brandon University (Canada), and is currently at the University of Toronto under the supervision of Prof. Melissa Anderson. She is studying active seafloor volcanism and the role structures play in the formation of volcanic massive sulfide (VMS) deposits. The award allowed Chantal to attend the 2019 GAC–MAC–IAH conference in Quebec City to present results from her MSc, which was titled "Structural Evolution of the NE Lau Back-Arc Basin: Links to Tectonic Regime and Magmatic–Hydrothermal Systems." She talked at the "Submarine Volcanism and Marine Minerals: Key Resources for the Future" session where she met many of the leading researchers in her field. Attending related sessions and taking part in the student networking event allowed her to expand her network of contacts before she graduates. In the future, she would like to work in the field of economic geology, ideally in exploring for VMS deposits within Manitoba's greenstone belts.

Teegan Ojala is a first-year MSc student at McGill University (Canada) under the supervision of Dr. Galen Halverson. She is studying the Barney Creek Formation within the McArthur Basin, as well as the Fraynes Formation of the Birrindudu Basin (both in Australia), in order to look at the geochemistry of the shales in the two formations, which are thought to be equivalent and to have been linked in the past into one larger basin, the Greater McArthur Basin. Her research project was based on drill-core samples provided by Dr. Marcus Kunzmann, a sedimentologist with CSIRO in Australia. The MAC research grant permitted her to expand the scope of her research to working directly with Dr. Kunzmann on rocks of the McArthur basin, both in the field and in the drill core library in Darwin. During her time in Australia she was able to visit a number of geologically interesting sites including the Flinders Ranges in Southern Australia and she was able to collect a large number of samples from the Fraynes Formation from a drill-core library in Darwin. The newly collected samples will be analyzed for carbon, oxygen, and neodymium isotopes and will provide very useful data for her master's thesis.

Catherine Crotty is a PhD student at McGill University under the supervision of Prof. Vincent van Hinsberg. She used the MAC Travel and Research Grant to present recent research findings at Goldschmidt 2019 in Barcelona (Spain). Her project aims to quantitatively reconstruct the trace metal composition of the hydrothermal fluids that were being emitted into the Archean oceans by "black smokers". She is doing this by experimentally determining the partition coefficients between hydrothermal fluids and antigorite, chlorite, and albite, which constitute dominant minerals in the main (ultra)mafic ocean crust lithologies. The partitioning data she obtained will be applied to natural samples from the 3.2 Ga Tartoq Group, a supracrustal belt for which the *P–T* history and rock compositions are known. This allows for easy identification of samples that have experienced the lowest metamorphic grades and ones most likely to retain prograde fluid signatures. At the conference, she presented the successful synthesis of chrysotile and antigorite, at 325 °C and 350 °C respectively, and their partition coefficients. Once partitioning data are extended to higher *P–T* conditions and applied to natural samples, it will be possible to indirectly constrain the composition of the Archean oceans by understanding the input of trace metals into the ocean by black smoker vents.

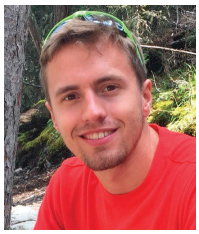

Jacob Forshaw is a second year PhD student at the University of Calgary (Canada) under the supervision of Prof. Dave Pattison. His research is concerned with a newly emerging, and fundamental, question in petrology: to what degree is the equilibrium model of metamorphism compromised by kinetic impediments to reaction? He used the MAC travel grant to attend the GAC–MAC–IAH 2019 meeting in Quebec City, where he presented the first findings of his PhD research on the interplay between equilibrium and kinetics in regional metamorphism. This work involved detailed petrographic, textural and chemical analysis to reveal the sequence, spacing, and nature of metamorphic reactions in two tectonic settings. Comparison of these observations with the reactions as predicted by equilibrium thermodynamics showed distinct differences between the two, which carries broad implications for the assessment of the pressure–temperature–time paths that underpin our understanding of tectonic processes. Attending this conference provided a fantastic opportunity for him to network with fellow metamorphic geologists from both the Canadian and international community, as well as receive critical feedback on his research.

Meteoritical Society

http://meteoriticalsociety.org

REPORT OF THE METEORITE NOMENCLATURE COMMITTEE

Audrey Bouvier

The Nomenclature Committee (NomCom) of the Meteoritical Society (MetSoc) continued its activities despite the major challenges we have all faced over the past few months. I would like to thank all the NomCom members for volunteering their time and effort, as well as Tasha Dunn (Colby College, Maine, USA) for her two terms on NomCom, and Devin Schrader (Arizona State University, USA) for joining us last January.

NomCom is currently composed of nine appointed members: Audrey Bouvier (Chair; Universität Bayreuth, Germany), Emma Bullock (Carnegie Institution of Washington, USA), Hasnaa Chennaoui Aoudjehane (Université Hassan II de Casablanca, Morocco), Vinciane Debaille (Université Libre de Bruxelles, Belgium), Massimo D'Orazio (Università di Pisa, Italy), Mutsumi Komatsu (Sōkendai, Japan), Francis McCubbin (Deputy Editor; NASA Johnson Space Center, USA), Bengkui Miao (Guilin University of Technology, China) and Devin Schrader (Arizona State University); and three ex-officio NomCom members: Jérôme Gattacceca (*Meteoritical Bulletin* Editor; CEREGE, France), Jeff Grossman (Database Editor; NASA, USA) and Brigitte Zanda (MetSoc Vice President; Muséum national d'Histoire naturelle, Paris).

The purpose of the NomCom is to approve new meteorite names, to establish guidelines, and to make decisions regarding the naming and classification of meteorites. New meteorites, dense collection areas, type-specimen repository collections, and revisions are published through the *Meteoritical Bulletin* and the Meteoritical Bulletin Database (MBDB) (https://www.lpi.usra.edu/meteor/).

Meteorites

The 2018 entries of the MBDB, totaling 2,714 meteorites, have been published by Gattacceca et al. (2020) in issue 107 of the *Meteorite Bulletin*. The full write ups of 1,145 non-Antarctic meteorites and supplementary tables can be found online as Supporting Information and in the MBDB Archive. The number of Northwest Africa (NWA) meteorites reached a new peak with 799 meteorites. Antarctic and NWA meteorites make up 58% and 29% of the total number of meteorites, respectively. Over 200 submissions from South America were also approved. Notable entries are 7 meteorites from fall events reported in 2018: Hamburg (H4, USA, 16 January), Ablaketka (H5, Kazakhstan, 16 February), Aba Panu (L3, Nigeria, 19 April), Mangui (L6, China, 1 June), Ozerki (L6, Russia, 21 June), Renchen (L5-6, Germany, 10 July), and Gueltat Zemmour (L4, Morocco, 21 August).

Meteoritical Bulletin No. 108, containing the 2019 entries, is in preparation. It will contain 2,141 meteorites, including 12 newly approved falls, from which 4 more are from 2018: Benenitra (L6, Madagascar, 27 July), Komaki (L6, Japan, 26 September), Ksar El Goraane (H5, Morocco, 28 October), Mhabes el Hamra (H4/5, Mauritania, 23 December). Notable 2019 reported falls are Viñales (L6, Cuba, 1 February), Aguas Zarcas (CM2, Costa Rica, 23 April), Oued Sfayat (H5, Algeria, 16 May), and Taqtaq-e Rasoul (H5, Iran, 10 August).

The total annual numbers of lunar and martian meteorites reached 45 and 23, respectively, last year. Most of these were found in NW Africa. Coordinates are known for several lunar meteorites (e.g., Errachidia in Morocco; Swayyah in Western Sahara), plus the largest lunar so far: 103 kg of lunar feldspathic breccia designated as NWA 12691. New Martian meteorites are mostly shergottites, but two new nakhlites (Caleta el Cobre 022, first nakhlite from Chile; and NWA 12542) and five polymict breccias (including Rabt Sbayta 010 and 012 with coordinates) paired with NWA 7034 were reported. Martian meteorites that are likely paired with NWA 7034 are now classified as "Martian (polymict breccia)."

Dense Collection Areas (DCAs)

There are currently over 340 named dense collection areas (DCAs).

Thirteen new DCAs were defined last year in Chad (Bardaï), China (Dunlike, Hongshagang, Huangtuya, Korla, Shanshan, Tamusubulage, Wubao), Libya (Hamadat Zegher), Morocco (Hassi Arsane), United States of America (Sunfair, Daveytown), and Western Sahara (Swayyah).

Type-Specimen Repositories

Nine new type-specimen repositories were approved from 8 countries:

- BGI – Botswana Geoscience Institute, Lobatse (Botswana)
- CUG – Planetary Science Institute, China University of Geosciences, Wuhan (China)
- LeMans – Musée Vert, Muséum d'histoire naturelle du Mans, Le Mans (France)
- Wits – University of the Witwatersrand, Johannesburg (South Africa)
- MCNB – Museu de Ciències Naturals de Barcelona (Spain)
- KirkU – Faculty of Aeronautics and Space Sciences, Kirklareli University (Turkey)
- NASU – National Museum of Natural History, National Academy of Sciences, Kyiv (Ukraine)
- LVNHM – Las Vegas Natural History Museum, Las Vegas (Navada, USA)
- Marietta – Marietta College, Marietta (Ohio, USA)

Procedures

Write-up instructions for the three most common groups of meteorites (ordinary chondrites, eucrites, and ureilites) are now available. These guidelines enable the editor and deputy editor to review and approve meteorites (ordinary chondrites, eucrites, and ureilites) from dense collection areas. Any submission not meeting these criteria will be reviewed by the committee as usual.

Guidelines to Authors

Following the *Meteoritics & Planetary Science* article "Best Practices for the Use of Meteorite Names in Publications" by Heck et al. (2019), the guidelines to authors were updated in both the *Meteoritics & Planetary Science* and *Geochimica et Cosmochimica Acta* journals. Please use these guidelines when preparing your manuscripts for publication.

Meteorite Naming

Remember to send your write-ups for new and provisional names to the *Meteoritical Bulletin* Editor at least three weeks before submitting your conference abstract or manuscript to journals to avoid potential issues with naming and classification and delays in publication. The release of the write-up to the database may be held on request if there is an embargo from publishers.

Finally, please do not hesitate to contact us with questions or concerns about the NomCom, especially with suggestions for improvement.

Audrey Bouvier
Chair of the Nomenclature Committee
Universität Bayreuth

REFERENCES

Gattacceca J, McCubbin FM, Bouvier A, Grossmann J (2020) The Meteoritical Bulletin, No. 107. Meteoritics & Planetary Science 55: 460-462

Heck PR and 29 coauthors (2019) Best practices for the use of meteorite names in publications. Meteoritics & Planetary Science 54: 1397-1400

IN MEMORIAM: WILLIAM A. CASSIDY (1928–2020)

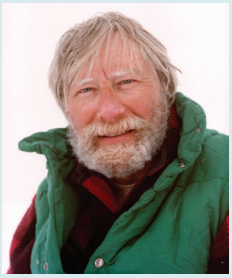

William A. (Bill) Cassidy, emeritus professor in the Department of Geology and Planetary Science at the University of Pittsburgh (Pennsylvania, USA), quietly passed away on 25 March 2020 aged 92 at his home in Monroeville. Bill leaves behind a deep legacy of contributions to the fields of impact crater studies and meteoritics.

While pursuing a BS in geology at the University of New Mexico (USA) in the early 1950s, Bill was made aware of Campo del Cielo and the lost Meson de Fierro iron of Argentina during a class taught by Lincoln LaPaz. A Fulbright Scholarship in Australia and a PhD from Penn State University (Pennsylvania, USA) followed, leading to a research scientist position at the Lamont–Doherty Earth Observatory (New York, USA) from where Bill would mount the first of many expeditions to the Campo del Cielo crater field. Bill's studies of the site proved of historic importance. It was relatively young (4,000 years old) and consisted of over two dozen individual craters, most small enough to be fully excavated to reveal their original geometry and impactor trajectories. Meteorites were recovered from most of these craters, providing an early indisputable link between these two planetary phenomena. Bill's research on the Campo del Cielo site continued into his eighties, and he was loved throughout the region for his consistent efforts to include Argentine scientists, technicians, artists and laypeople in the work. Bill was involved in other seminal crater studies, including investigations of the Aouelloul and Tenoumer craters in Mauritania and the Monturaqui impact site in Chile. He also conducted pioneering research on Australasian microtektites (especially the very interesting but poorly studied "bottle green" variety), Muong Nong–type tektites, and lunar samples.

Another enduring part of Bill Cassidy's legacy is as founder of the US-led Antarctic Search for Meteorites (ANSMET) program. Bill was one of the first outside of Japan to recognize that nine meteorites recovered in 1969 from the Yamato Mountains of Antarctica were the vanguard of a huge number of specimens. He persistently submitted proposals to the US Antarctic Research Program until he finally achieved funding for the 1976–1977 field season, the first of several conducted jointly with Japanese collaborators. Since that time, the ANSMET program has operated without interruption, sending field parties to Antarctica annually and recovering over 24,000 meteorite specimens. These include several paradigm-shifting specimens, such as EET 79001 (the first meteorite determined to be Martian in origin), ALH 81005 (the first Lunar meteorite), and many samples from rare, scientifically valuable, and previously unknown classifications. The inherent altruism of the US Antarctic meteorite program, which provides samples of all recovered specimens to scientists from around the world, is a direct result of Bill's decision to give up privileged access to the meteorites in favor of a program (partnering with NASA and the Smithsonian Institution) that allows other scientists to make their own discoveries. The results have been extraordinary: a program that has lasted for generations, whose long-term impact on science easily rivals that of Apollo. Ultimately, Bill led fourteen ANSMET expeditions, the last in 1994. He returned to Antarctica again in the late 1990s as a part of a NASA-funded Carnegie Mellon University (Pennsylvania, USA) project to develop robotic meteorite search technologies.

Multiple honors have been bestowed upon Bill in recognition of his contributions to planetary science. He was awarded the Barringer Medal of the Meteoritical Society in 1995 for his lifelong work on impact craters and their debris. The mineral *cassidyite* [$Ca_2Ni(PO_4)_2 \cdot 2H_2O$], a rare mineral from Wolf Creek Crater (found in cracks and cavities in weathered meteorites), was named in his honor. Bill was awarded the Antarctic Service Medal in 1977, and also had a glacier named after him: the Cassidy Glacier, a tributary of the Taylor Glacier in the Dry Valleys region of Antarctica, which places his legacy firmly on the map. Asteroid 3382 Cassidy also places his legacy firmly in the heavens. And in 2015, a hall of the Parque Campo del Cielo Museum (Argentina) was named in his honor.

Bill will be long remembered for his dry sense of humor, his humility, and his generosity. His legacy extends far beyond the craters he explored and the tens of thousands of meteorites his projects recovered. Hundreds of scientists forged bonds of friendship, respect, and trust as a direct result of Bill's efforts during six decades of field work, both in Antarctica and elsewhere, learning to put aside personal gain or comfort in the pursuit of science.

Ralph P. Harvey, **John W. Schutt**
Case Western Reserve University (Ohio, USA)
Christian Koeberl, University of Vienna (Austria)

GIFTS AND GRANTS GUIDELINES

The stated mission of the Meteoritical Society is "to promote research and education in planetary science with emphasis on studies of meteorites and other extraterrestrial materials that further our understanding of the origin and history of the solar system." Besides the society's publications, the annual scientific meetings, establishing official names for newly found meteorites, and the awards sponsored by the society, there are other ways by which we work toward furthering our mission. These include supporting student travel to conferences and workshops; supporting student research; assisting scientists from economically disadvantaged countries; supporting classes or field schools, especially those that bring meteoritics and planetary science to developing countries; compiling oral histories from prominent members of the society; and supporting outreach to the broader public community on meteoritics and planetary science.

To support these activities, the society has created an endowment fund. The majority of the endowment consists of the General Fund which can support one-time activities that are not part of normal society business. The endowment fund also has named funds: the Nier Fund, the McKay Fund, and the Travel for International Members Fund. Details about activities supported by all of these funds are given under Activities Supported on the society's website.

For those who wish to assist in this mission, donations can be made to the General Fund or to any of the specific funds (see Ways to Contribute on the society's website).

ANNUAL MEETING SCHEDULE

Due to the worldwide restrictions caused by the Covid-19 pandemic, the 2020 Meteoritical Society meeting has been postponed. The schedule will be as follows: Chicago remains the meeting location for 2021, with Glasgow moving to 2022. The meetings for Perth (Australia) and Brussels (Belgium) have each been pushed back by one year to 2023 and 2024, respectively. We thank our members for their understanding, and our meeting hosts for their flexibility during this time of uncertainty.

2020	Glasgow (Scotland), 9–14 August [POSTPONED]
2021	Chicago, Illinois (USA), 14–21 August
2022	Glasgow (Scotland), dates TBD
2023	Perth, Western Australia (Australia) dates TBD
2024	Brussels (Belgium), dates TBD

RENEW YOUR MEMBERSHIP NOW!

Please don't forget to renew your membership for 2020. Students—this is particularly important if you are interested in applying for one of our student presentation awards, as you must be a member to be eligible. You can renew online at: http://metsoc.meteoriticalsociety.net.

Société Française de Minéralogie et de Cristallographie

www.sfmc-fr.org

23rd INTERNATIONAL MINERALOGICAL ASSOCIATION MEETING

IMA 2022
MINERALOGY AND SPACE
Lyon, 18-22 July

Following the tradition of the quadrennial general meetings of the International Mineralogical Association (IMA), which is organized by national societies, the French Society of Mineralogy and Crystallography will host the 23rd General Meeting of the IMA in Lyon (France) from the 18th to the 22nd July 2022.

The year 2022 is one to celebrate mineralogy. It marks the bicentennial of the death of René Just Haüy (born 1743), the father of modern mineralogy and crystallography. Two centuries ago is also when Haüy's *Traité de minéralogie* and *Traité de cristallographie* were published. Back to 2022, and the last two main Mars exploration programs, Mars 2020 and Huoxing 1, will have had just enough time to return some science and for the analysis to begin. And with the return of *Hayabusa 2*, fragments of a primitive carbonaceous asteroid will be analysed for the first time.

The 23rd meeting of the IMA will mark these celebrations. In Lyon, we want to paint IMA 2022 with the colours of space exploration. Alongside the more traditional mineralogy, we want to inspire the new generation and take a step closer toward that final frontier. The meeting will bring together all the new facets of modern mineralogy; it will be the playground where mineralogy will meet exploration planetology, all to celebrate two centuries of mineralogy.

The overarching themes of IMA2022 are as follows:

- Mineral Systematics
- Physics and Chemistry of Minerals
- Ores and Ore Mineralogy
- Mineralogy and Petrology
- Planetary Mineralogy
- Planetary Interiors
- The Dynamical World of Minerals

To keep up-to-date, regularly visit the official conference website www.ima2022.fr and follow us on Facebook and Twitter. The venue is the Lyon Convention Centre, a state-of-the-art convention centre featuring 25,000 m² of innovative architecture that is situated between the River Rhône and the Tête d'Or park.

The organizing committee, on behalf of the French Society of Mineralogy and Crystallography, will be Razvan Caracas, Hervé Cardon, and Cathy Quantin-Nataf.

We are looking forward to seeing you in Lyon in 2022!

4th EARTH MANTLE WORKSHOP

4th EMAW TOULOUSE 2021
Earth Mantle Workshop
Toulouse, 2021

30 June–2 July 2021, Toulouse (France)

The European Mantle Workshop (EMAW) has changed its name to the Earth Mantle Workshop (EMAW) – with no change in acronym. The workshop will be held from Wednesday 30th June 2021 until Friday 2nd of July 2021 in Toulouse (France).

Program Topics

- Mineralogical, petrological and geochemical studies of mantle xenoliths, orogenic peridotites, abyssal peridotites and the mantle section of ophiolites
- Inferences on mantle composition and evolution from the study of volcanic rocks
- The role of volatile components in mantle processes
- Experimental studies on the production, migration and emplacement of mantle melts and fluids, as well as fluid/melt–rock interaction
- Mass transfer in convergent and divergent plate margins
- Geophysical studies of Earth's mantle
- Numerical models of the Earth's mantle and crust–mantle interaction
- Alteration, serpentinisation and carbonation of peridotite and associated rocks

The main themes will be approached from theoretical, experimental, analytical and/or numerical standpoints.

Pre-workshop field trip to Pyrenean peridotite massifs, including Lherz (28–29 June 2021)

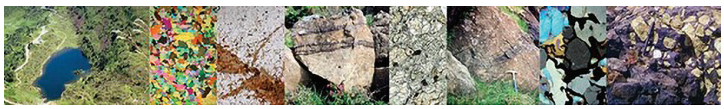

Web site: https://emaw2021.sciencesconf.org

Contact: emaw2021@sciencesconf.org

See second EMAW circular for more information.

EMU NOTES IN MINERALOGY

Information about the series at
www.minersoc.org/emu-notes.html

Mineralogical Society

Order online at **www.minersoc.org**

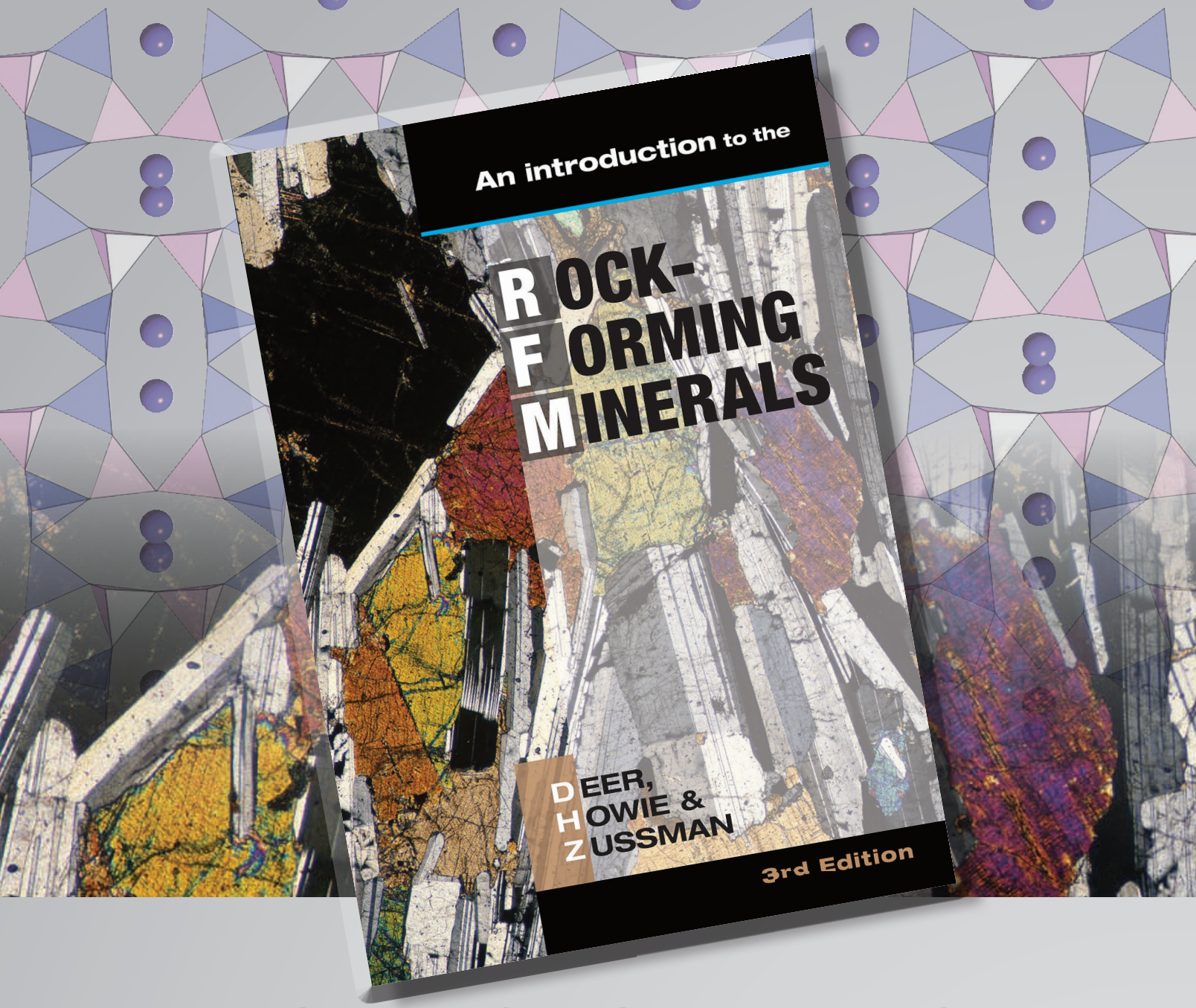

Introduction to the Rock-Forming Minerals III

by Deer, Howie and Zussman

The third edition of this iconic textbook was published by the Mineralogical Society in May 2013 and is now available for sale. This volume has been completely updated, is printed in full colour at A4 size and includes >200 colour images, including those from the *Atlas of Rock-Forming Minerals* (with the permission of Pearson UK) and from *CrystalMaker*. A CD including interactive images of crystal structures of many of the minerals listed in the book is also included.

Pricing

- List price (for libraries and other institutions): **£55**
- Non-member price: **£45**
- Mineralogical Society Member price: **£35**

For Postage add £7.95 per book for UK, £12.95 for Europe (airmail), and £20.95 for Rest of the world (airmail). For surface rates please contact the Society (info@minersoc.org).

Order the book online at **www.minersoc.org**

SPECIAL DEAL FOR STUDENTS!

Students, join the Society today (free of charge for one year) at www.minersoc.org and save £10 on the cost of this book.

Mineralogical Society

THERMODYNAMICS IN EARTH AND PLANETARY SCIENCES[1]

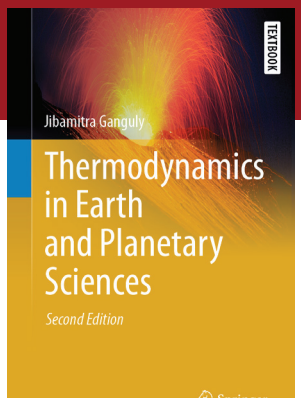

Thermodynamics is a vast subject with a long and complex history. It is now about two hundred years since the general acceptance of the ideal gas equation of state ($PV = nRT$) (e.g., Biot 1816) and the discovery of limiting behaviour in the high temperature heat capacity of elemental solids (Petit and Dulong 1819). Since then, empirical thermodynamic laws and statistical thermodynamic models have revolutionised our understanding of a myriad of physical and chemical processes and material properties. Thermodynamics underpins much of our modern lifestyle and our understanding of the natural world. It plays, in the words of Russian Nobel laureate in chemistry Ilya Prigogine, "a fundamental role far beyond its original scope" (Prigogine 1977).

Without a doubt, the geological sciences have been one of the greatest beneficiaries of the field of thermodynamics. Thermodynamics provides us with a theoretical framework with which we can understand subjects as disparate as the formation and evolution of the planets, the minerals in the rocks around us, the development of ore deposits, volcanism and the composition and stratification of our atmosphere.

The development of thermodynamic concepts as it pertains to the geosciences is the subject of Jibamitra Ganguly's *Thermodynamics in Earth and Planetary Sciences*. Now in its second edition, this book is a treasure trove of information on thermodynamic concepts and the often surprising and fascinating geoscience applications. Ganguly has gathered together topics that would otherwise not be found in a single text. Thermodynamic aspects of the deep Earth and planetary physics, aqueous geochemistry, and surface effects all have their own chapters, in addition to the more standard fare of the thermodynamic laws, equations of state, and mixing models. The second edition is also graced with a new chapter on statistical thermodynamics and stable isotope geochemistry. Several new examples and updated references have also been added to the text, reflecting the continued advances in the field since the publication of the first edition in 2008.

Ganguly's style is refreshingly down-to-earth. Throughout the book, he introduces important thermodynamic concepts while interweaving them with necessary mathematical derivations. These derivations do require some concentration to work through, but Ganguly takes care to explain each step in the derivation, and students will surely appreciate that he does not omit steps, something all-too-common in other texts. Example problems are scattered through the text to give the reader confidence that they have understood the material. The second edition has a new appendix, which contains worked answers to many of these problems.

For me, where this book really shone was in the geological applications, which are supplied after the elucidation of each major concept. These are both fascinating and varied. One of my favourite examples comes in the middle of the chapter on reactions between solid solutions and gas mixtures, and is taken from Mueller and Saxena (1977). It outlines how observations of the CO_2-rich atmosphere of Venus can be used to constrain the mineralogy of its surface by assuming thermodynamic equilibrium at its hot surface.

In another section, Ganguly discusses the origins of osmotic pressure generated across semi-permeable membranes by gradients in chemical potential. He then highlights several recent studies which have investigated how osmotic pressure generated by natural salinity gradients could be used to provide a source of clean electrical energy. Whether or not this method will ever be economically viable (probably not), the example was such a pleasant surprise that it fully deserves a mention here. Taken together, the collected examples in the book succeed in demonstrating just how powerful having a knowledge of thermodynamics can be. Perhaps even more importantly, Ganguly's choices reveal that thermodynamics in the geosciences remains very much a living subject, driven by the need to explain new observations of the natural world. In this respect, and in its ambitious scope, it distinguishes itself from other works, such as G.M. Anderson's also excellent, and easy-going, *Thermodynamics of Natural Systems* (3rd Edition, 2018).

For the budding practitioner, the appendices are particularly useful. In addition to the worked examples (Appendix D), there are three other appendices. Appendix A is on entropy production and kinetics and serves as a gateway to the field of nonequilibrium/irreversible thermodynamics, a challenging subject which is currently experiencing renewed interest from a number of Earth science fields. Appendix B covers a few important mathematical methods for those who need to consolidate their knowledge of calculus, Taylor Series and Sterling's Approximation. Finally, Appendix C is an extremely useful resource on how to estimate the thermodynamic properties of solids. For those working at the cutting edge of petrology, there is never quite enough experimental data, and so it is common practise to use heuristics to fill in the gaps in our knowledge. This appendix enlists experimental data to provide empirical heuristics, and also briefly introduces modern ab initio techniques which allow us to move beyond such empiricism.

I have only two quibbles with this impressive text. The first is that a couple of important topics, such as short-range order and disequilibrium in solid-dominated systems, could have been extended to give uninitiated readers an understanding of their origins, consequences, and broad relevance to geological systems. However, prospective readers should be assured that even the short sections come with recommended texts for further reading. These are well chosen, as indeed are the vast majority of references in the book.

My second quibble is that the ordering of information within the book feels unnatural at times. For example, electronic orbitals and crystal field theory are introduced very briefly in Chapter 1, but only fleshed out in Appendix C. Additionally, the emphasis on the macroscopic view of thermodynamics has forced the new and much-appreciated chapter on statistical thermodynamics to the end of the book. I strongly recommend buying the print copy rather than the digital version: this will allow you to easily flick between sections.

This revised edition of *Thermodynamics in Earth and Planetary Sciences* succeeds in its goal of providing both the background and the tools required to make useful thermodynamic models of the natural world. It will serve as an excellent resource for senior geoscience students looking to gain a broad understanding of thermodynamics and its applications. It should also become a useful reference text for petrologists, planetary scientists, and other researchers seeking to understand aspects of thermodynamics outside their primary field.

Robert Myhill, University of Bristol

REFERENCES

Anderson G (2017) Thermodynamics of Natural Systems: Theory and Applications in Geochemistry and Environmental Science. 3rd edition. Cambridge University Press, Cambridge, 428 pp

Biot J-B (1816) Mesure de la dilatation des gaz par la chaleur. Chapitre IX, Traité de Physique Expérimentale et Mathématique, Tome I. Deterville, Paris, pp 182-190 (in French)

Mueller RF, Saxena SK (1977) Chemical Petrology. Springer, Berlin, 394 pp

Petit AT, Dulong P-L (1819) Recherches sur quelques points importants de la théorie de la chaleur. Annales de Chimie et de Physique, 10: 395-413 (in French)

Progogine I (1977) Time, Structure and Fluctuations. Nobel Lecture, 8 December 1977. In: Forsén S (ed) Nobel Lectures, Including Presentation Speeches and Laureate's Biographies. Chemistry, 1971–1980. World Scientific, New York, pp 263-285

1 Ganguly J (2020) *Thermodynamics in Earth and Planetary Sciences*. 2nd Edition. Springer. 610 pp, ISBN 978-3-030-20878-3 (print), €89.99 | £79.99 | US$109.99

Elements

An International Magazine of Mineralogy, Geochemistry, and Petrology

Thematic Issues
2005–2020

Join a participating Society to receive *Elements*!

Elements is available online at **elementsmagazine.org**
and **pubs.geoscienceworld.org/elements**
To order back issues: **msa.minsocam.org/backissues**

Thematic Issues 2005-2020

Available online at elementsmagazine.org

2005 – Volume 1

January | Fluids in Planetary Systems
March | Diamonds
June | Genesis: Rocks, Minerals, and the Geochemical Origin of Life
September | Toxic Metals in the Environment: The Role of Surfaces
December | Large Igneous Provinces: Origin and Environmental Consequences

2006 – Volume 2

February User Research Facilities in the Earth Sciences
April | Arsenic
June | Water on Mars
August | Early Earth
October | Glasses and Melts: Linking Geochemistry and Materials Science
December | The Nuclear Fuel Cycle: Environmental Aspects

2007 – Volume 3

February | Zircon: Tiny but Timely
April | On the Cutting Edge: Teaching Mineralogy, Petrology, and Geochemistry
June | Energy: A Geoscience Perspective
August | Frontiers in Textural and Microgeochemical Analysis
October | The Critical Zone: Where Rock Meets Life
December | Medical Mineralogy and Geochemistry

2008 – Volume 4

February | Supervolcanoes
April | Phosphates and Global Sustainability
June | Deep Earth and Mineral Physics
August | Platinum-Group Elements
October | Carbon Dioxide Sequestration
December | Nanogeoscience

2009 – Volume 5

February | Scientific Exploration of the Moon
April | Bentonites: Versatile Clays
June | Gems
August | Mineral Magnetism: From Microbes to Meteorites
October | Gold
December | Metal Stable Isotopes: Signals in the Environment

2010 – Volume 6

February | Mineral Evolution
April | Sulfur
June | Fluids in Metamorphism
August | Atmospheric Particles
October | Thermodynamics of Earth Systems
December | Sustainable Remediation of Soils

2011 – Volume 7

February | Cosmochemistry
April | Iron in Earth Surface Systems
June | Global Water Sustainability
August | When the Continental Crust Melts
October | Tourmaline
December | Mine Wastes

2012 – Volume 8

February | Impact!
April | Minerals, Microbes, and Remediation
June | Fukushima Daiichi
August | Granitic Pegmatites
October | Rare Earth Elements
December | Urban Geochemistry

2013 – Volume 9

February | One Hundred Years of Isotope Geochronology
April | Serpentinites
June | The Mineral-Water Interface
August | Continental Crust at Mantle Depths
October | Nitrogen and Its (Biogeocosmo) Chemical Cycling
December | Garnet: Common Mineral, Uncommonly Useful

2014 – Volume 10

February | Asteroids: Linking Meteorites and Planets
April | Ophiolites
June | Kaolin: From Ancient Porcelains to Nanocomposites
August | Unconventional Hydrocarbons
October | Cosmogenic Nuclides: Earth's Surface Clock
December | Graphitic Carbons

2015 – Volume 11

February | Mineralogy of Mars
April | Arc Magmatic Tempos
June | Apatite: A Mineral for All Seasons
August | Social and Economic Impact of Geochemistry
October | Supergene Metal Deposits
December | Geomicrobiology and Microbial Geochemistry

2016 – Volume 12

February | Earth Sciences for Cultural Heritage
April | Enigmatic Relationship Between Silicic Plutonic and Volcanic Rocks
June | Cosmic Dust
August | Geologic Disposal of Radioactive Waste
October | Studying the Earth using LA-ICPMS
December | Origins of Life: Transition from Geochemistry to Bio(geo)chemistry

2017 – Volume 13

February | Volcanoes: From Mantle to Surface
April | Sulfides
June | Rock and Mineral Coatings
August | Boron: Light and Lively
October | Mineral Resources
December | Layered Intrusions

2018 – Volume 14

February | Luminescence Dating: Reconstructing Earth's Recent History
April | Comets
June | Terroir – Science Related to Grape and Wine
August | Central Andes: Mountains, Magmas, and Ore Deposits
October | Deep-Ocean Mineral Deposits
December | Marine Biogeochemistry of Trace Elements and Their Isotopes

2019 – Volume 15

February | Planet Mercury
April | Reactive Transport Modeling
June | The South Aegean Volcanic Arc
August | Weathering
October | Catastrophic Events in Earth's History and Their Impact on the Carbon Cycle

NEW ISSUES IN 2020 – Volume 16

February | Abiotic Hydrogen and Hydrocarbons in Planetary Lithospheres
April | Raman Spectroscopy in the Earth and Planetary Sciences
June | Redox Engine of Earth
August | Lithium: Less is More
October | Noble Gas Thermochronology
December | Hydrothermal Fluids

12TH INTERNATIONAL KIMBERLITE CONFERENCE

12 IKC

30 YEARS OF DIAMONDS IN CANADA

15–19 August 2022 • Yellowknife

Ekati, Canada's first diamond mine, Northwest Territories (NWT). Copyright © Dominion Diamond Mines

SCIENTIFIC THEMES

1. Diamonds
2. Emplacement and Economic Geology of Kimberlites and Related Magmas
3. The Origin and Evolution of Kimberlites and Related Magmas
4. Diamond Deposits – Exploration and Mining
5. Cratonic Mantle – Petrology, Geochemistry and Geophysics

FIELD TRIPS

1. Northwest Territories Diamond Mines
2. Kimberlites Across Canada
3. Slave Craton Geology
4. Northwest Territories Kimberlite Drill Core Collection
5. Advances in Drift Prospecting for Kimberlite in Canada

SHORT COURSES

1. Geology of Diamonds: Reviews in Mineralogy and Geochemistry
2. The G-Cubed Toolbox: Capturing Full Value from Public-Domain Kimberlitic Indicator Mineral and Microdiamond Data
3. Introduction to Kimberlites: Geology, Terminology, Emplacement and Economics
4. Principles of Rough Diamond Valuation
5. Advances in Drift Prospecting for Diamonds: Using Glacial Processes to Unravel Dispersal Paths

www.12ikc.ca

Follow 12 IKC

instagram.com/ikcacconference/

facebook.com/InternationalKimberliteConference/

linkedin.com/company/international-kimberlite-conference/

Conference Secretariat:
Venue West Conference Services Ltd.
Tel: +1 604 681 5226
(Mon–Fri: 9:00 am - 5:00 pm PST;
Mon–Sat: 5:00 pm - 1:00 am GMT)
Email: secretariat@12ikc.ca

International response to COVID-19 has resulted in scientific meetings to be canceled and/or postponed. Check meeting web pages for ongoing updates.

2020

June 6–7 **DMG Annual Sections Meeting: Geochemistry and Petrology & Petrophysics**, Frankfurt, Germany. Web page: www.uni-frankfurt.de/48936053/How_to_get_to_the__Institut_für_Geowissenschaften **POSTPONED**

June 14–19 **Asteroids, Comets, Meteors Conference**, Flagstaff, AZ, USA. Web page: www.hou.usra.edu/meetings/acm2020/ **CANCELED**

June 21–26 **Goldschmidt2020 Virtual Conference**. Web page: goldschmidt.info/2020/

June 28–July 3 **Exploring Fluxes, Forms and Origins of Deep Carbon in Earth and Other Terrestrial Planets**, Lewiston, ME, USA. Web page: www.grc.org/deep-carbon-science-conference/2020/ **CANCELED**

July 12–16 **Virtual JpGU–AGU Joint Meeting, For a Borderless World of Geoscience**. Web page: www.jpgu.org/meeting_e2020v/

July 28–30 **14th International Nickel–Copper–PGE Symposium**, Marquette, MI, USA. Web page: www.nmu.edu/eegs/symposium-2020

August 2–6 **Virtual Microscopy & Microanalysis 2020**. Web page: www.microscopy.org/MandM/2020/

August 9–14 **Meteoritical Society Annual Meeting**, Glasgow, UK. Web page: meteoriticalsociety.org/?page_id=18 **POSTPONED**

August 11–13 **Experimental Analysis of the Outer Solar System II**, Fayetteville, AR, USA. Web page: www.hou.usra.edu/meetings/exoss2020/ **POSTPONED**

August 14 **Virtual 2020 COMPRES Annual Meeting**. Web page: compres.us/events/annualmeeting/2020/2020-compres-annualmeeting-general-information

August 16–20 **260th ACS National Meeting & Exposition**, San Francisco, CA, USA. Web page: www.acs.org

August 16–21 **12th International Symposium on the Geochemistry of the Earth's Surface (GES-12)**, Zurich, Switzerland. Web page: ges12.com **CANCELED**

August 29–September 2 **EMC2021 3rd European Mineralogical Conference**, Cracow, Poland. Web page: www.emc2020.ptmin.eu/ **POSTPONED**

August 31–September 5 **Magmatism of the Earth and Related Strategic Metal Deposits**, Apatity, Russia. Web page: www.ksc.ru/en/90years/magmatism/ **POSTPONED**

September 1–5 **GEOHEALTH 2020, International Network of GeoHealth Scientists Meeting**, Bari, Italy. Web page: geohealth-scientists.org/

September 6–10 **EMC2020 3rd European Mineralogical Conference**, Cracow, Poland. Web page: www.emc2020.ptmin.eu/ **POSTPONED**

September 14–17 **8th International Clumped Isotopes Workshop**, Jerusalem, Israel. Web page: iciw2020.org **POSTPONED**

September 21–23 **GeoConvention 2020 Virtual Event**, Calgary, Canada. Web page: www.geoconvention.com

September 21–24 **5th International Serpentine Days Workshop**, Sestri Levante (Genova), Italy. Web page: serpentinedays2020.it/ **POSTPONED**

September 24–28 **Short Course: Cosmochemistry, Meteorites, and the Origin of the Planetary Systems**, Cologne, Germany. Web page: https://metbase.org/

September 25–30 **Cities on Volcanoes 11**, Heraklion, Greece. Web page: pcoconvin.eventsair.com/volcanoes11

September 28–October 2 **DMG Short Course: Application of Diffusion Studies to the Determination of Timescales in Geochemistry and Petrology**, Bochum, Germany. Web page: www.gmg.rub.de/petrologie/

October 4–8 **Materials Science & Technology 2020, combined with ACerS 122nd Annual Meeting (MS&T20)**, Pittsburgh, PA, USA. Web page: www.matscitech.org/MST20

October 5–8 **Martian Geological Enigmas: From the Late Noachian Epoch to the Present Day**, Houston, TX, USA. Web page: www.hou.usra.edu/meetings/martianenigmas2020

October 5–9 **DMG Short Course: In situ Analysis of Isotopes and Trace Elements by Femtosecond Laser Ablation ICPMS**, Hannover, Germany. E-mail: s.weyer@mineralogie.uni-hannover.de

October 6–9 **Third Conference on European Rare Earth Resources**, Delphi, Greece. Web page: eres2020.eres-conference.eu

October 23 **New Topics Meeting: Diffusion in Minerals, Rocks and Melts: Potential and Pitfalls**, London UK. Web page: www.minersoc.org/diffusion.html

October 23–29 **57th Annual Meeting of the Clay Minerals Society**, Richland, WA, USA. Web page: pnnl.cvent.com/events/clay-minerals-society-57th-annual-meeting/event-summary-74c571c7cbc-d4100b517a40662d0ff9b.aspx

October 25–28 **Geological Society of America National Meeting**, Montreal, Canada. Web page: community.geosociety.org/gsa2020/home

November 9–13 **Astrobiology 2020**, Vredefort Dome, South Africa. Web page: astrobiology.uj.ac.za

November 9–14 **36th International Geological Congress**, Delhi, India. Web page: www.36igc.org

November 16–20 **Introduction to Secondary Ion Mass Spectrometry in the Earth Sciences**, Potsdam, Germany. Web page: sims.gfz-potsdam.de/short-course/

November 29–December 4 **2020 MRS Fall Meeting**, Boston, MA, USA. Web page: www.mrs.org/fall2020

December 1–3 **8th Asian Current Research on Fluid Inclusions**, Townsville, Australia. Web page: www.jcu.edu.au/economic-geology-research-centre-egru/conferences-acrofi-viii

December 7–11 **2020 AGU Fall Meeting**, San Francisco, CA, USA. Web page: www.agu.org/fall-meeting

2021

January 24–29 **45th International Conference and Expo on Advanced Ceramics and Composites (ICACC2021)**, Daytona Beach, FL, USA. Web page: ceramics.org/event/45th-international-conference-and-expo-on-advanced-ceramics-and-composites

February 15–19 **IAVCEI 2021 Scientific Assembly**, Rotorua, New Zealand. Web page: confer.eventsair.com/iavcei2021/

February 28–March 3 **EMPG-XVII, 17th International Symposium on Experimental Mineralogy, Petrology and Geochemistry**, Potsdam, Germany. Web page: www.17empg2020.de/

March 21–25 **Spring ACS National Meeting & Exposition**, San Antonio, TX, USA. Web page: www.acs.org/

April 19–23 **MRS Spring Meeting & Exhibit**, Seattle WA, USA. Web page: www.mrs.org/spring2021

May 17–19 **2021 GAC–MAC Annual Conference**, London, ONT, Canada. Web page: gac.ca/gac-mac-london-2021/

June 6–11 **International Symposium on Quartz (QUARTZ2021)**, Tønsberg, Norway. Web page: www.nhm.uio.no/english/research/events/conferences/quartz2020/

June 9–11 **2nd International Conference on Contaminated Sediments**, Bern, Switzerland. Web page: www.oeschger.unibe.ch/services/events/conferences/contased_2021/announcement/index_eng.html

July 4–9 **2021 Goldschmidt Conference**, Lyon, France. Web page forthcoming.

July 7–10 **Extractive Industry Geology (EIG) Meeting**, Exeter, UK. Web page: www.eigconferences.com

July 12–16 **17th International Clay Conference**, Istanbul, Turkey. Web page: icc.aipea.org

July 12–17 **2021 Summer School: Metamorphosis of Metamorphism**, Pavia, Italy. Web page: www.mineralogylab.com/event/schoolmetamorphism2020/

July 21–23 **International Archean Symposium**, Perth, WA, Australia. Web page: 6ias.org

August 1–5 **Microscopy & Microanalysis 2021**, Pittsburgh, PA, USA. Web page forthcoming

August 1–6 **GEOANALYSIS 2021, 11th International Conference on the Analysis of Geological and Environmental Materials**, Freiberg, Germany. Web page: www.geoanalysis2021.de

August 14–21 **84th Annual Meeting of the Meteoritical Society**, Chicago, IL, USA. Web page: www.metsoc2021-chicago.com

August 22–26 **Fall ACS National Meeting & Exposition**, Atlanta, GA, USA. Web page: www.acs.org

August 24–26 **9th International Conference on Mineralogy and Museums**, Sofia, Bulgaria. Web page: www.bgminsoc.bg

August 29–September 2 **EMC2021 3rd European Mineralogical Conference**, Cracow, Poland. Web page: www.emc2020.ptmin.eu/

October 10–13 **Geological Society of America National Meeting**, Portland, OR, USA. Web page: forthcoming.

October 24–29 **29th International Applied Geochemistry Symposium (IAGS)**, Viña del Mar, Chile. Web page: iags2021.cl

November 28–December 3 **2021 MRS Fall Meeting**, Boston, MA, USA. Web page: www.mrs.org/fall2021

December 13–17 **AGU Fall Meeting**, New Orleans, LA, USA. Details forthcoming

2022

August 15–19 **12th International Kimberlite Conference**, Yellowknife, NT, Canada. Web page: www.12ikc.ca

The meetings convened by the societies participating in *Elements* are highlighted in yellow. This meetings calendar was compiled by Andrea Koziol (more meetings are listed on the calendar she maintains at https://sites.google.com/a/udayton.edu/akoziol1/home/mineralogy-and-petrology-meetings). To get meeting information listed, please contact her at akoziol1@udayton.edu

Primitive Meteorite Contains Cometary Surprise

Rhonda Stroud[1]

DOI: 10.2138/gselements.16.3.220

Comets, and some primitive asteroids, preserve the microscopic remnants of the basic building blocks of rocky bodies in our solar system. Analyzing these building blocks can provide important clues both to the source of the water for Earths' oceans and to the inventory of organic matter delivered to the early Earth. In general, samples from comets preserve a greater abundance of organic matter and primordial presolar dust grains from the protosolar molecular cloud, and generations of stars older than the sun, than do samples from asteroids. Meteorites, which come from asteroids, generally have less organic matter and preserve fewer presolar grains. This is because asteroids and comets formed at different places in the solar nebula, and, thus, sampled different distributions of organic and mineral components. Furthermore, the warmer conditions on asteroids allowed for liquid water and greater subsequent physical and chemical alteration of the accreted material.

The recent publication "A Cometary Building Block in a Primitive Asteroidal Meteorite" in *Nature Astronomy* (Nittler et al. 2019) revealed that despite the tens of astronomical units of physical separation between where Kuiper Belt comets formed and where carbonaceous (C-type) asteroids formed, the parent asteroid of the primitive meteorite LaPaz Icefield 02342 captured and preserved a fragment of material that was typically accreted to the more distant comets (Fig. 1).

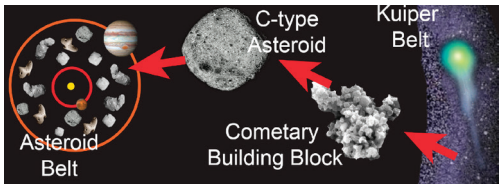

Figure 1 Schematic to show the migration of a cometary building block from the Kuiper Belt inward to the accretion zone for the carbonaceous (C-type) asteroids outside the orbit of Jupiter, and, thus, the eventual location of primitive meteorite LaPaz Icefield 02342's parent body in the main Asteroid Main Belt.

LaPaz Icefield 02342 was found in Antarctica in 2002 and belongs to a class of primitive meteorites known as Renazzo-type carbonaceous (CR) chondrites. The first indication to the research team that there was something very unusual in their polished thin section of this meteorite came from scanning electron microscope images that showed a poppy-seed–sized (~100 µm) inclusion (Fig. 2). This inclusion was extremely carbon rich, ~70% C by area, but full of submicrometer mineral grains and readily distinguished from the epoxy used to stabilize the thin section. Team members Carlos Moyano-Cambero and Jemma Davidson identified this inclusion, or carbon-rich clast (CRC), as an important region for isotopic characterization, in addition to nearby regions with features more typical of CR chondrite meteorite matrix. Using the NanoSIMS 50L ion microprobe at the Carnegie Institution of Washington (USA), Moyano-Cambero, Davidson, and Larry Nittler were able to find large differences in the O, H and N isotopic compositions of material in the carbon-rich clast compared to the surrounding matrix. The clast contained a much greater concentration of O-rich grains with isotopic compositions indicative of a presolar origin, unusual Na-rich sulfate grains with unusual O isotopes, and organic matter with H and N isotopic compositions similar to that found in ultracarbonaceous Antarctic micrometeorites that are thought to derive from comets.

Additional evidence for the origin of the inclusion as a bit of cometary building-block material came from scanning transmission electron microscope (STEM) and X-ray absorption spectroscope (XAS) data.

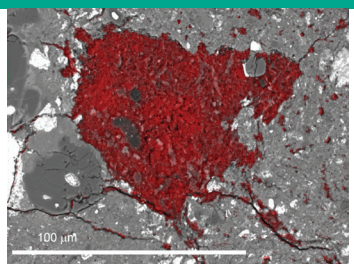

Figure 2 False color (red) backscatter secondary scanning electron microscope image of the cometary building block incorporated into the matrix of LaPaz Icefield 02342.

Scientists Bradley De Gregorio and Rhonda Stroud (United States Naval Research Laboratory, Washington DC, USA) extracted cross-sections from the carbon-rich clast and the matrix outside the clast to better understand the fine-grained mineralogy and the organic functional chemistry distributions. The STEM images of the clast cross-sections strongly resembled those from ultracarbonaceous Antarctic micrometeorites, and were reminiscent of images from chondritic porous interplanetary dust particles (IDPs) collected in the stratosphere, our main source of presumed cometary material (Fig. 3). Organic carbon in the clast-enveloped assemblages of amorphous Mg-rich silicates with embedded metal and sulfide grains, similar to the GEMS (glass with embedded metal and sulfides) found in IDPs (which have yet to be definitively identified as individual matrix components in any meteorite). This carbon likely served to protect the presolar silicates in the clast against alteration by liquid water on the host asteroid. In contrast, the STEM images from the LaPaz matrix were consistent with prior observations of matrix from other primitive CR chondrites: namely, abundant silicates and sulfides, isolated nanoscale-blebs of organic matter, and low degrees of porosity. The XAS results supported the conclusion that infiltration of asteroidal water was more pervasive in the matrix than in the clast, in that the organic matter in the interior of the clast was less oxidized than the organic matter in the nearby matrix.

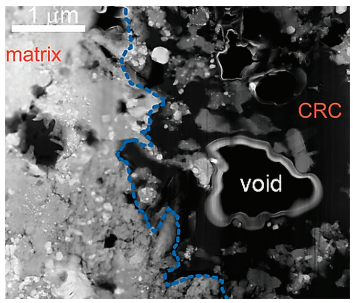

Figure 3 Annular dark field scanning transmission electron microscope image of a cross-section that spans the boundary between the matrix and the carbon-rich clast (CRC) cometary building block. The matrix is dominated by fine-grained silicates and Fe–Ni sulfides, whereas the clast is porous and is dominated by organic carbon with discrete silicate–metal and sulfide assemblages, indistinguishable from the GEMS (glass with embedded metal and sulfides) that are found in cometary interplanetary dust particles.

This first-of-its-kind find of cometary materials embedded in a bit of asteroid tells us that the ingredients of C-type asteroids include microscopic assemblages that formed in the Kuiper Belt and then migrated inward to the vicinity of Jupiter. Based on oxygen and hydrogen isotope measurements, such materials may also have contributed to the surface carbon and ocean water of the early Earth. Because the incorporation of the cometary material into the meteorite provides a thermal barrier to ensure a safe journey through the Earth's atmosphere, additional discoveries of such clasts in other primitive meteorites in the future may provide some of the best-preserved cometary components available for laboratory study until sample return from a comet surface is achieved. In the near term, sample return from the C-type asteroids Ryugu, by the Hayabusa2 mission, and Bennu, by the OSIRIS-REx mission, could provide an abundance of similar materials through which to track the early history of the solar system.

REFERENCE

Nittler LR and 7 coauthors (2019) A cometary building block in a primitive asteroidal meteorite. Nature Astronomy 3: 659-666

1 US Naval Research Laboratory
Washington DC, USA
E-mail: stroud@nrl.navy.mil

VC Ultra

Acid Vapor Cleaning System

Savillex's VC Ultra Acid Vapor Cleaning System offers labs performing microwave sample preparation a safe, efficient and user-friendly alternative for cleaning microwave digestion vessels and other labware.

- Large, fluoropolymer cleaning chamber can accommodate up to 40 microwave digestion vessels and covers
- Customized digestion vessel cleaning racks minimize handling and acid exposure
- Pre-programmed cleaning cycles eliminate method development

Clean your general labware.

Clean your microwave digestion vessels.

Learn More at
www.savillex.com